



**HAL**  
open science

## Contributions to the understanding of hydrothermal processes : application to black liquor

Hélène Boucard

► **To cite this version:**

Hélène Boucard. Contributions to the understanding of hydrothermal processes : application to black liquor. Chemical and Process Engineering. Ecole des Mines d'Albi-Carmaux, 2014. English. NNT : 2014EMAC0018 . tel-01178183

**HAL Id: tel-01178183**

**<https://theses.hal.science/tel-01178183>**

Submitted on 17 Jul 2015

**HAL** is a multi-disciplinary open access archive for the deposit and dissemination of scientific research documents, whether they are published or not. The documents may come from teaching and research institutions in France or abroad, or from public or private research centers.

L'archive ouverte pluridisciplinaire **HAL**, est destinée au dépôt et à la diffusion de documents scientifiques de niveau recherche, publiés ou non, émanant des établissements d'enseignement et de recherche français ou étrangers, des laboratoires publics ou privés.

Université Fédérale



Toulouse Midi-Pyrénées

# THÈSE

En vue de l'obtention du

## DOCTORAT DE L'UNIVERSITÉ DE TOULOUSE

Délivré par :

École Nationale Supérieure des Mines d'Albi-Carmaux conjointement avec l'INP Toulouse

---

**Présentée et soutenue par :**

**Hélène BOUCARD**

**le** vendredi 12 décembre 2014

**Titre :**

Contributions to the understanding of hydrothermal processes :  
application to black liquor

---

**École doctorale et discipline ou spécialité :**

ED MEGEP : Génie des procédés et de l'Environnement

**Unité de recherche :**

Centre Rapsodee, CNRS - UMR 5302, École des Mines d'Albi-Carmaux

**Directeur/trice(s) de Thèse :**

Radu BARNA

**Jury :**

Maria José COCERO, Professeur, Universidad de Valladolid, Espagne, Rapporteur

Pierre CEZAC, Professeur, Université de Pau et des Pays de l'Adour, Rapporteur

Tadafumi ADSCHIRI, Professeur, Tohoku University, Japon, Examineur

Denilson DA SILVA PEREZ, Docteur, FCBA Grenoble, Examineur

Olivier BOUTIN, Professeur, Université Aix-Marseille, Examineur

Jacques FAGES, Professeur, École des Mines d'Albi-Carmaux, Président

Elsa WEISS-HORTALA, Maître assistant, École des Mines d'Albi-Carmaux, Co-encadrante

Radu BARNA, Professeur, École des mines d'Albi-Carmaux, Directeur



*“Il faut regarder toute la vie avec des yeux d’enfants”*

-- Par Henri Matisse (1953)

*“Il n’est qu’une chose horrible en ce monde, un seul péché irrémissible,  
l’ennui”*

*“Les folies sont les seules choses qu'on ne regrettent jamais”*

-- Oscar Wilde

*A Timothée  
A ma famille  
Aux amis*



Nous y voilà! Le temps des remerciements est arrivé. Au-delà du fait qu'il sonne le glas du doctorat, et que mine de rien ce n'est pas rien; c'est toujours difficile de savoir par où commencer...

\*\*\*il y a ceux qui m'ont fait l'honneur de s'impliquer dans cette thèse, et à qui je dois aujourd'hui de pouvoir écrire mes remerciements dans ce manuscrit: les membres du jury.

Ce fut un honneur et un plaisir de pouvoir discuter avec vous de mes travaux. Merci aux rapporteurs, **Maria José Cocéro** et **Pierre Cézac**, vos commentaires m'ont permis d'élever notre travail, j'espère qu'ils trouveront écho dans les quelques compléments apportés au manuscrit. Ensuite, je tiens à remercier messieurs **Da Silva Perez** et **Moindrot** pour leurs connaissances sur la lignine et le procédé Kraft; il était important pour nous de garder ce lien avec l'industrie au delà du fait que la thèse soit "académique". Je souhaiterais remercier **Olivier Boutin** d'avoir accepté de faire parti de ce jury et d'avoir contribué à l'amélioration de nos travaux. Je tiens enfin à remercier **Jacques Fages: Jacques**, ce fut un honneur que vous présidiez mon jury de thèse. Je profite de ces quelques lignes pour vous remercier pour vos encouragements et votre bienveillance durant ces trois ans. Je remercie ensuite les professeurs japonais qui ont fait le déplacement jusqu'à Abli pour assister à ma soutenance et pas que: **Professeur Adschiri**, je vous remercie de m'avoir accueillie et intégrée dans votre laboratoire comme si j'en avais toujours fait partie, je vous remercie d'avoir pris le temps de m'expliquer tant de choses et d'avoir apporté votre expérience et expertise à mes travaux. J'ai appris énormément grâce à vous et à ceux que j'ai pu rencontrer grâce à vous. **Professeur Watanabe**, je vous remercie de m'avoir ouvert les portes de votre laboratoire et de m'avoir facilité l'accès à certaines techniques d'analyses, dont les logiciels en japonais me donnaient l'impression d'être une poule devant une clé à molette...merci également pour votre contribution et aide à mes travaux.

\*\*\*Ensuite, il y a ceux qui ont choisi de s'impliquer dans cette thèse, et à qui je dois "tout simplement" d'avoir pu faire et mener à bien mes travaux: le laboratoire RAPSODEE et ses occupants.

Puisque la plume progresse en ce sens, j'en viens à remercier mes encadrants, "mes chefs". Je ne savais pas où vous mettre dans les remerciements: en premier... parce que sans vous, tout ça n'existerait pas; ou en dernier... parce que sans vous tout ça n'existerait pas; mais finalement je vais vous mettre là: **Elsa**, je me souviens de la première fois que je t'ai vu quand je suis arrivée aux Mines, tu "fumais la clope" et puis hop à peine finie tu m'as embarquée, et ça y est c'était parti, la thèse commençait et les enseignements aussi. Ensuite, on a (bien!!) bossé, discuté, échangé, co-chambré... Merci d'avoir toujours répondu présente y compris pour des corrections et avis de dernières minutes. Merci pour ton dynamisme à toute épreuve, ta bonne humeur et ton aide.

**Radu**, je vous remercie pour votre confiance et votre bienveillance, j'espère avoir été à la hauteur. Merci pour votre disponibilité, vos conseils avisés, votre écoute, votre soutien, vos explications diverses... tout au long de cette thèse. Je vous remercie pour tout ce que j'ai appris scientifiquement, personnellement et humainement grâce à vous. Je vous remercie également d'avoir dirigé, guidé, cette thèse tout en me laissant y mettre ma couleur. On a tous des vieux démons, merci d'avoir entendu les miens.

Je remercie ensuite toute l'équipe du laboratoire RAPSODEE de m'avoir accueillie et permis de mener à bien cette thèse. Chacun d'entre vous y est quelque part pour quelque chose...

Il y a certes quelques mentions particulières: **Céline, Philippe, Séverine, Sylvie, Jean-Marie** merci de m'avoir apporté votre expertise pour m'aider à comprendre le comportement de la liqueur noire et de ses produits au travers des analyses. **L'équipe technique** au complet, pour vos aides plus ponctuelles mais pas moins indispensables. **Christine**, le mécanisme des "petites billes" du chapitre 4 n'est que la résultante de nos innombrables discussions, ton "oeil" (associé à celui du MEBE) n'a pas son pareil, merci pour tout ça et pour tout le reste! **Fabienne**, je te remercie pour ton soutien et ton aide. **Valérie, Chrystel et Anne-Marie**, merci pour tout !!! Merci également à mes stagiaires **Fatou et Jessica** qui ont contribué à l'avancée de mes travaux.

Dans notre "bas étage", au RDC, il y a ceux qu'on croise et qui font qu'on passe une bonne journée en dépit du reste: **Marion D, Marta, Alex, Doan, Dung, Nat, Marion B, Mathieu, Fenglin, Rabab, Augustina, Andréa, Chams, Seb, Bruna, Marwa, Germain, Victor, Christophe, Matthieu, Guillaume, Chaima, Abdou, Brieu, Haroun, Ingrid, Moussa, Jocelyn, Christophe C, Max, Raph, Anaïs et les nouveaux**. Une pensée particulière pour mes "co-bureau" **Pierrot et Bat** : on y était bien quand meme ;-)). A tous: merci pour les discussions, les débats, les incompréhensions, les coups de gueule, les indignations, les fous rires, les rêves, les manips qui marchent, les avancées scientifiques révolutionnaires, celles qui le sont moins et tous les autres bons moments.

\*\*\*Il y a aussi ceux qui n'ont pas choisi de s'impliquer dans cette thèse mais s'y sont retrouvés contraints et forcés, et à qui je dois d'avoir gardé la tête sur les épaules et les pieds sur terre: la famille et les amis. En fait tous ceux qui au bout de 3 ans ne connaissent toujours pas mon sujet de thèse et se demandent encore à quoi ça sert (au fond ce n'est qu'un détail), mais ils sont là (c'est ça qui est important).

Je remercie donc ma famille de m'avoir soutenue, tout particulièrement mon frère et mes parents qui montrent un soutien et une écoute sans faille. Merci d'être là! Merci d'avoir compris que c'était important pour moi et que faire une thèse, parfois, ça (pré)occupe.

Les amis, ceux d'avant la thèse et de toujours (ils se reconnaîtront), ceux du Japon (ils se reconnaîtront aussi): Merci!!!!

\*\*\*Enfin il y a celui qui est là, qu'a choisi, mais pas trop non plus, de s'impliquer dans cette thèse, et à qui je dois d'avoir gardé en tête certaines réalités : Timothée

Merci de me comprendre, de me supporter (bel effort pendant la rédaction de thèse, c'est peu dire), de savoir me faire prendre du recul comme personne, de me dire, parfois, ce que je n'ai pas envie d'entendre mais qu'il est bien que j'entende, et de me poser les questions que j'évite de me poser... Merci pour tout ça et pour le reste.

\*\*\*Une dernière pensée pour mon acolyte de thèse: la liqueur noire.

En y repensant c'était une belle aventure!

During these three years, results obtained have been exposed and explained on several occasions:

### ***Publications***

H. Boucard, M. Watanabe; S. Takami; E. Weiss-Hortala, R. Barna, T. Adschiri, “Beneficial use of CeO<sub>2</sub> nanocatalyst for black liquor conversion under sub and supercritical conditions”, Journal of supercritical fluids, 2014, (in press).

Q. Wu, E. Weiss-Hortala, R. Barna, H. Boucard, S. Bulza, "Glycerol and bioglycerol conversion in supercritical water for hydrogen production", Environmental Technology, vol. 33, 2012, p.2245-2255

### ***Communications with review comity and proceedings***

H. Boucard, S. Takami, E. Weiss-Hortala, R. Barna, T. Adschiri; catalytic conversion of black liquor under supercritical conditions for H<sub>2</sub> production; 5th International symposium on energy from biomass and waste - Venise, **Oral**, 2014

H. Boucard, M. Watanabe, S. Takami, E. Weiss-Hortala, R. Barna, T. Adschiri; “Catalytic Conversion of Black Liquor under Sub-/Supercritical Conditions”, 14<sup>th</sup> European meeting of supercritical fluids – Marseille, **Oral**, 2014

H. Boucard, E. Weiss-Hortala, R. Barna; “Generation of carbon microparticules by hydrothermal conversion of black liquor”, 14<sup>th</sup> European meeting of supercritical fluids – Marseille, **Poster**, 2014

H. Boucard, E. Weiss-Hortala, R. Barna; “Valorization of Black Liquor under Sub-/Supercritical Water”, 14<sup>th</sup> European meeting of supercritical fluids – Marseille, **Poster**, 2014

H. Boucard, E. Weiss-Hortala, R. Barna; Conversion hydrothermale de la liqueur noire en conditions supercritiques ou proche supercritique ; SFGP-2013 - XIVe congrès de la Société Française de Génie des Procédés, **Poster**, 2013

H. Boucard, M. Ducouso, E. Weiss-Hortala and R. Barna; Hydrothermal conversion of poplar wood, 4th International Conference on Engineering for Waste and Biomass Valorisation, Porto, **Oral**, 2012

H. Boucard, Q. Wu, E. Weiss-Hortala, R. Barna, Hydrothermal conversion of black liquor in supercritical water, 5th international symposium on supercritical fluids, san Francisco, **Poster**



***Communications without proceeding***

H. Boucard, E. Weiss-Hortala, and R. Barna; Conversion hydrothermale de la liqueur noire en voie supercritique, Journées des fluides supercritiques, Albi, **Oral**, 2012

H. Boucard, E. Weiss-Hortala, and R. Barna; Valorization of black liquor in supercritical water; seminaire Water; New Deli, **Oral**, 2012

# Contents

---

Contents.....	9
General introduction.....	13
Introduction générale.....	19
Chapter 1: Context and objectives of the study.....	27
I.    Hydrothermal processes .....	33
I.1.    Definition of supercritical water .....	34
I.2.    Macroscopic and microscopic properties of supercritical water.....	35
I.3.    Hydrothermal treatment of wet biomass.....	43
I.4.    Implementation of hydrothermal processes: progress and limitations.....	49
II.   Black liquor and the paper industry .....	50
II.1.   Cooking and leaching steps: black liquor origin and composition .....	50
II.2.   Current valorization of black liquor.....	57
II.3.   Industrial issue .....	60
II.4.   Conclusion .....	61
II.5.   State-of-the-art on hydrothermal conversion of black liquor and its associated model compounds .....	63
III.  Objectives of the thesis.....	69
Chapter 2: Materials & Methods.....	71
I.    Raw material: .....	75
I.1.   Black liquor.....	75
I.2.   Cerium oxide.....	77
II.   Reactors.....	77
II.1.  Batch reactors used for experiments .....	77
II.2.  Experimental procedure .....	83
III.  Outflow materials: Phases characterization.....	85
III.1.  Gas analysis .....	85
III.2.  Liquid analysis .....	86
III.3.  Solid analysis .....	87
III.4.  Conclusions.....	89

Chapter 3: Overview of hydrothermal conversion of black liquor through parametric study in batch reactor .....	91
I. Batch reactors .....	97
I.1. Batch process description .....	97
I.2. Reactor design.....	98
II. Influence of operating conditions on phases distribution and kinetics .....	101
II.1. Influence of reaction time .....	101
II.2. Influence of concentration .....	108
II.3. Influence of temperature .....	111
II.4. Conclusion .....	113
III. Changing in phases composition as a function of temperature .....	114
III.1. Hydrothermal gasification .....	114
III.2. Hydrothermal liquefaction .....	117
III.3. Hydrothermal carbonization .....	121
IV. Conclusion & Prospects.....	123
IV.1. Conclusion .....	123
IV.2. Prospects .....	125
V. To remember the chapter.....	126
Chapter 4: Study of particles generation .....	127
I. Theory of coke generation.....	133
I.1. Carbonaceous solid generation: reactions involved.....	134
I.2. Particles generation: phase equilibrium .....	134
II. Summary of operating conditions selected and methods .....	138
III. Effect of reaction time on the solid formation.....	139
IV. Explanation of the phenomena identified .....	144
IV.1. Liquid analysis .....	144
IV.2. Chemical analysis of solid .....	146
IV.3. Mechanism of solid formation - Discussions.....	155
IV.4. Conclusions.....	160
V. Influence of heating and cooling rate .....	163
V.1. Influence of heating rate .....	163
V.2. Influence of cooling rate .....	165

V.3. General conclusion on heating and cooling rates: .....	167
VI. Summary of chapter.....	168
VI.1. Phenomena involved during particles generation .....	168
VI.2. Applications of carbonaceous materials .....	170
Chapter 5: Catalytic hydrothermal conversion using CeO <sub>2</sub> nanocatalyst for H <sub>2</sub> production and coke suppression .....	173
I. Catalyst characterization & its expected action .....	179
I.1. Characteristic of cubic CeO <sub>2</sub> nanocatalyst.....	179
I.2. Expected action of CeO <sub>2</sub> .....	180
II. Understanding of the phenomena involved during the hydrothermal conversion of black liquor.....	181
II.1. Catalytic conversion of black liquor under supercritical conditions.....	181
II.2. Catalytic conversion of black liquor under subcritical conditions.....	187
II.3. Comparison between the catalytic conversion of Black Liquor under sub and supercritical conditions. ....	192
II.4. Conclusion .....	196
III. Preliminary study for technical industrial feasibility .....	198
III.1. Batch process .....	198
III.2. Continuous process .....	203
IV. Study of catalytic conversion of black liquor model molecules.....	205
IV.1. Study of the conversion of lignin.....	206
IV.2. Study of the conversion of GGGE .....	212
V. Summary of chapter .....	229
General conclusion & Prospects.....	231
I. Conclusion.....	233
II. Prospects.....	235
Conclusion générale et perspectives.....	239
I. Conclusions .....	241
II. Perspectives.....	244
Annexes.....	247
I. Annex 1: Industrial issues in Kraft process.....	249

II. Annex 2: Phases characterization.....	253
III. Annex 3: Carbon and texture characterizations obtained by carbonization from Inagaki .....	261
IV. Annex 4: Preliminary study on hydrothermal carbonization of black liquor (Proceeding for SFGP congress) .....	263
V. Annex 5: XRD of CT series – carbonization study.....	271
VI. Annex 6: Influence of heating rate NT/CT.....	273
VII. Annex 7: Influence of cooling rate – CL/CT.....	275
VIII. Annex 8: GC-MS results for liquid recovered after black liquor conversion under sub (350°C) and supercritical (450°C) conditions with and without CeO <sub>2</sub> catalyst.....	277
Bibliography.....	279
Figures list.....	293
Table list.....	303

## General introduction

---



After World War II, many industrial and civil sectors needed to be rebuilt. During the « glorious thirty period », an important economic and societal development was initiated and was accompanied by an increase of the population. For many years the keyword was “development”, however considering the demographic explosion, some people wonder about the limits of our resources: consciousness awakens. We realize, over the years, that our growth cannot depend only on the economy, and must take into account other criteria such as the society and the environment. The presages of “sustainable development” were initiated. From that moment, the society, the economy and the environment must be reconciled.

Given the current environmental degradation (global warming, depletion of natural resources and energy, pollution ...), politicians gradually introduce new rules in view to ensure the sustainability of our "societies". International conferences are arranged according to this vision (Earth Summits: Stockholm, Rio, Johannesburg ..; Protocols of Montreal, Kyoto ...). France is included in this approach and, formed several groups of experts working on the choices to be made in terms of sustainable development. The syntheses of these meetings are the bases for the Grenelle laws (I and II). These laws stipulate especially in terms of energy the respects of the rule of 3 X 20 until 2020:

- "20% reduction in emissions of Greenhouse Gases
- reducing of 20 % the energy consumption,
- 20% part of renewable energy in the total energy. "

Our society currently faces three challenges: resource depletion, waste accumulation and environmental degradation. Indeed, the activity of our industrialized societies generates a significant amount of waste or by-products, and at the same time the application of environmental rules is more and more stringent. Thus, waste treatment and reuse (circular economy) is becoming one of the main challenges of our society.

Waste or by-products treatments depend on their properties (humidity, organic and inorganic contents, viscosity, and so on). Biological, physico-chemical and thermo-chemical processes are gaining attention as they are used to destroy or valorize materials. Among these processes, thermo-chemical treatments are identified especially for waste and biomass valorization into useful materials and/or energy. In addition, thermo-chemical processes are offering dry and wet routes. For wet matter (high water content), wet routes namely hydrothermal processes are usually employed. Depending on degradation or valorization objectives, oxidation or conversion would be selected respectively. Indeed, hydrothermal processes use the properties of water, as reactant, solvent and catalyst; under high pressure ( $P > 15$  MPa) and high



temperature ( $T > 250^{\circ}\text{C}$ ), to degrade wet biomass (80 wt% of water content). Under oxidative and supercritical conditions ( $T > 374^{\circ}\text{C}$ ;  $P > 22.1 \text{ MPa}$ ), the organic matter is completely destroyed leading to minerals dissolved in clean water, and carbon dioxide. Under sub or supercritical water conditions without oxidant addition, organics are converted into useful products, such as hydrogen, building blocks molecules, or carbonaceous solids, which give a second life to the wastewater and wet by-product.

Industrially, hydrothermal conversion raises many technical, technological and scientific challenges. In order to contribute to optimize the process, hydrothermal conversion in batch reactor is the subject of this work. Indeed, the understanding of the phenomena taking place during hydrothermal conversion is essential to control and optimize the process. For this study black liquor was used as real biomass, due to its high content in water, organics and minerals. Black liquor is an alkaline by-product coming from the step of wood cooking in Kraft process; its composition is very complex.

Black liquor is currently used in the paper industry to recycle white liquor (salts mixture for cooking step), and generate energy by burning organics. Although energy recovery allows quite energy self-sufficiency, extra volumes, limitations in this process and complete destruction of organic matter (lignin), prompt the paper industry to investigate alternative processes. Valorization of black liquor is not the objective of the thesis, but some prospects for its alternative valorization will be mentioned along the manuscript. Black liquor is used as tool study for the understanding of hydrothermal processes, which is our main objective.

For that, the point of view of reaction pathway and the point of view of process are adopted with the following focus:

- One of the hydrothermal processes issues is the solid formation which plugs partially or completely pipes in continuous reactor or modifies physico-chemical equilibrium in batch reactor. Based on these observations, solid formation (coke formation and salts precipitation) has to be understood. A focus will be made on the mechanism of solid formation. A batch approach with a rapid heating and rapid cooling will allow approaching the conditions of continuous reactors.

- The conversion of a complex organic matter under hydrothermal conversion leads to useful products. As hydrothermal gasification into hydrogen is concerned, high temperatures ( $500\text{-}700^{\circ}\text{C}$ ) and thus expensive technology is required. One of the new challenges is to consider catalytic hydrothermal gasification in order to decrease the reactor temperature.

Focus will be made on the catalyst action for the hydrothermal conversion of residues for H<sub>2</sub> production. As previously, a rapid heating and cooling will approach the conditions of continuous reactor.

Regarding literature data on model molecules and black liquor (chapter 1), a preliminary parametric study is made (chapter 3) to apprehend the black liquor hydrothermal conversion into gas, liquid and solid phases and thus to guide the next studies.

Hydrothermal conversion generates solid formation but as solid phase is considered as undesired phase, the understanding of its formation (chapter 4) could be used to optimize the control of hydrothermal processes. What are the best operating conditions to study solid formation? What parameter is predominant? What are the phenomena involved?

If solid phase inhibition is desired, the addition of material is necessary such as CeO<sub>2</sub> catalyst. CeO<sub>2</sub> is known to avoid solid formation and to favor hydrogen production. The consequences of its addition on the reactivity during hydrothermal conversion of black liquor will be studied (chapter 5).

#### More specifically:

The first chapter is devoted to the context of the study. Firstly, properties of supercritical water are described following their evolutions as a function of temperature and pressure. Reactions identified during hydrothermal processes are also summarized. A part of this chapter will be focused on the technical, technological and scientific issues of hydrothermal processes as regards to industrial applications. A presentation of the raw black liquor is then exposed, through origin, composition and its current use in paper industry. Then, a detailed review is made on hydrothermal conversion of black liquor and its model molecules from literature. In conclusion the goals of the work are presented.

The second chapter describes materials and methods used along the studied. Reagents (black liquor, model molecules, catalyst), and reactors used for experiments are presented. The experimental procedures applied are also detailed. The last section exposes the analysis tools to characterize solid, liquid and gaseous phases.

A preliminary study is exposed along Chapter 3 in order to evaluate the influence of operating conditions during hydrothermal conversion. Reaction time under sub and supercritical conditions, concentration and temperature are investigated considering carbon balance between the phases recovered. Then the focus is made on the influence of temperature as regards to solid formation and gasification. Nevertheless the liquid phase analysis is

systematically carried out as the black liquor is originally a liquid by-product. In addition, the valorization aspect of black liquor is implicit in the results and it is therefore a scientific basis for further studies. The conclusions of this chapter figure out the background of the operating conditions selected towards solid generation and catalytic gasification, which are detailed in following chapters.

Chapter 4 is focused on the contributions to knowledge about mechanism of solid formation in batch reactor during hydrothermal conversion at 350°C. After a quick theoretical basis on carbonaceous solid formation theories and their limits, solid formation is investigated over reaction time. Trends in solid and liquid phase properties are the optimal indicators of solid generation. Solid generation is mainly followed toward its chemical composition, its morphology and its yield. Liquid composition is characterized using global parameters and concentration of some key compounds. The influence of heating and cooling rate is also investigated as regards to solid morphology and salts precipitation. Carbonaceous solids are mainly recovered in this study, while minerals are still dissolved in the aqueous phase. A mechanism for carbon-based solid generation at 350°C is finally proposed.

Chapter 5 deals with catalytic hydrothermal gasification in order to remove coke formation and to favor hydrogen production at moderate temperatures using CeO<sub>2</sub> nanocatalyst. Firstly, a comparative study of black liquor hydrothermal gasification is conducted under sub and supercritical conditions. Hydrogen production efficiency is then integrated in a short overview of energy balance regarding the catalytic and non-catalytic process. Secondly, in order to better understand phenomena involved during black liquor hydrothermal conversion, lignin and guaiacylglycerol- $\beta$ -guaiacyl ether (GGGE) are used as model compounds. Reactions involved during GGGE conversion are figured out and a mechanism pathway of black liquor conversion has been proposed.

The main results of the work are finally summarized in the conclusion and some prospects concerning hydrothermal conversion and its applicative possibilities to the black liquor problematics are mentioned.

# Introduction générale

---



Après la Deuxième Guerre Mondiale, de nombreux secteurs industriels tout comme civils ont dû être reconstruits. Pendant la période des « Trente Glorieuses », un important développement économique et sociétal a été initié et accompagné par un accroissement de la population. De ce fait, depuis de nombreuses années le maître mot est devenu développement. Cependant, en considérant l'explosion démographique, de nombreuses personnes se sont souciées des limites de nos ressources faisant naître une conscience de ce sujet. En effet, l'économie n'est pas le seul élément du développement, elle doit s'accompagner de considérations liées à la société et à l'environnement. Les présages du développement durable ont alors été initiés, mêlant plus intimement les aspects société, économie et environnement.

Etant donné la dégradation environnementale actuelle (réchauffement climatique, raréfaction des ressources naturelles et énergétiques, pollution...), les politiques ont introduit progressivement de nouvelles régulations afin d'assurer la durabilité de nos « sociétés ». des conférences internationales ont été dédiées à cette vision des choses (sommets mondiaux : Stockholm, Rio, Johannesburg... ; les protocoles de Montréal, Kyoto...). La France s'est insérée dans cette approche pour faire émerger une politique de développement durable. Les lois Grenelle de l'environnement (I et II) sont le résultat de ce travail et stipulent les règles du 3 X 20 concernant l'énergie à l'horizon 2020 :

- réduction de 20% des émissions des gaz à effet de serre
- réduction de 20% de l'énergie consommée
- introduction de 20% d'énergie renouvelable dans la demande globale en énergie.

Notre société doit actuellement faire face à 3 challenges : la raréfaction des ressources, l'accumulation de déchets et la dégradation de l'environnement. En effet, l'activité de nos sociétés industrialisées génère une quantité significative de déchets et sous-produits, alors que dans le même temps l'application des réglementations environnementales deviennent de plus en plus astringentes. En définitive, le traitement des déchets et leur réutilisation (économie circulaire) apparaît comme l'un des principaux challenges de notre société.

Le traitement des déchets et sous-produits dépend de leurs propriétés (humidité, contenu organique et minéral, viscosité,...). Les procédés biologiques, physico-chimiques et thermo-chimiques sont de plus en plus mis en avant pour détruire ou valoriser ces déchets spéciaux. Parmi ces procédés, le traitement thermo-chimique est particulièrement identifié pour la valorisation matière et énergie de biomasse et de déchets. De plus, la voie thermo-chimique offre la possibilité de travailler en milieu sec ou humide. Tout naturellement, les eaux usées se tournent vers un traitement en voie humide, plus communément appelés

procédés hydrothermaux. En fonction de l'objectif, dégradation ou valorisation, les procédés d'oxydation ou de conversion seront sélectionnés. En effet, les procédés hydrothermaux reposent sur les propriétés simultanées de solvant, réactif et catalyseur qu'atteint l'eau à haute pression ( $P > 15$  MPa) et haute température ( $T > 250^{\circ}\text{C}$ ) ; lui permettant de dégrader la biomasse humide (environ 80% massique d'eau). Sous des conditions oxydantes et supercritiques ( $T > 374^{\circ}\text{C}$ ;  $P > 22,1$  MPa), la matière organique est complètement détruite et résulte en la production d'une eau « propre » contenant des sels dissous et du  $\text{CO}_2$ . Pour des conditions sous ou supercritique, mais sans addition d'oxydant, les composés organiques sont convertis en produits à haute valeur ajoutée tels que l'hydrogène, les molécules plateforme ou des solides carbonés, offrant une « seconde vie » au résidu.

Industriellement, la conversion hydrothermale soulève de nombreux défis scientifiques, techniques et technologiques. Afin de contribuer à optimiser le procédé, ce travail concerne la conversion hydrothermale en réacteur batch. En effet, la compréhension des phénomènes impliqués est essentielle pour le contrôle et l'optimisation de ces procédés de conversion hydrothermale. Pour cette étude, la liqueur noire est utilisée en tant que biomasse réelle, en raison de son important contenu en eau et de sa haute concentration en composés organiques et minéraux. La liqueur noire est un sous-produit alcalin de composition complexe, qui provient de l'étape de cuisson du bois dans le procédé Kraft.

La liqueur noire est actuellement utilisée dans l'industrie papetière pour recycler la liqueur de cuisson (liqueur blanche) et générer de l'énergie par combustion de la matière organique. Bien que l'énergie récupérée permette une quasi autosuffisance, les surplus en volumes, les limites du procédé Kraft et la destruction complète de la matière organique (lignine) orientent les industriels papetiers vers de nouveaux procédés alternatifs. La valorisation de la liqueur noire n'est pas l'objectif de la thèse, mais quelques perspectives seront énoncées dans ce sens tout au long du manuscrit. La liqueur noire est utilisée en tant qu'outil d'étude pour la compréhension des procédés hydrothermaux, ce qui est notre principal objectif.

Pour cela, les points de vue adoptés seront ceux des mécanismes réactionnels et des procédés ; avec les objectifs précis suivants :

- L'un des verrous de développement des procédés hydrothermaux est la formation de solide, car celui-ci peut obstruer les réacteurs continus ou modifier les équilibres physico-chimiques en réacteur batch. La formation de solide devient un enjeu majeur (formation de coke et précipitation des sels) de développement et doit être mieux appréhendée. Une

attention particulière sera mise sur l'établissement du mécanisme de formation du solide. L'approche en réacteur batch avec une chauffe et un refroidissement rapides permet d'approcher autant que possible les conditions du réacteur continu.

- la conversion d'une matière organique complexe en conditions hydrothermale donne lieu à des produits à haute valeur ajoutée comme par exemple l'hydrogène. Dans ce contexte, les hautes températures généralement nécessaires (500-700°C) à la gazéification impliquent de manière sous-jacente des matériaux de construction onéreux. De ce fait, un défi nouveau est de catalyser la réaction afin d'abaisser la température de réaction. Cette fois l'attention sera portée sur l'action du catalyseur lors de la conversion hydrothermale pour la production de H<sub>2</sub>. De même que précédemment, la chauffe et le refroidissement permettront d'approcher les conditions du réacteur continu.

Au vue des données proposées par la littérature sur les molécules modèles et sur la liqueur noire (chapitre 1), une étude paramétrique préliminaire est réalisée (chapitre 3) afin d'appréhender les potentialités de la conversion hydrothermale de la liqueur noire en gaz, liquide et solide, afin de guider les futures voies d'études.

La conversion hydrothermale engendre la formation de solide. Cette phase est considérée comme indésirable ; ainsi la compréhension de sa formation (chapitre 4) peut être utilisée pour optimiser le contrôle des procédés hydrothermaux. Quelles sont les meilleures conditions opératoires pour l'étude du solide ? Quel paramètre opératoire est le prédominant ? Quels sont les phénomènes mis en jeux ?

Si l'inhibition de la phase solide est désirée, un réactif supplémentaire doit être ajouté comme par exemple le catalyseur CeO<sub>2</sub>. Ce dernier est en effet connu pour empêcher la formation de solide et favoriser la production d'hydrogène. Les conséquences des ont addition sur la réactivité lors de la conversion hydrothermale de la liqueur noire seront étudiées (chapitre 5).

#### Plus précisément :

Le premier chapitre est dédié au contexte de l'étude. Tout d'abord, les propriétés de l'eau sont décrites en suivant leurs évolutions en fonction de la température et de la pression. Les réactions identifiées au cours des procédés hydrothermaux sont aussi résumées. Une partie de ce chapitre se concentre sur les verrous scientifiques, techniques et technologiques de ces procédés par rapport aux applications industrielles. Une présentation du résidu, la liqueur noire, est développée depuis son origine et sa composition jusqu'à sa réutilisation actuelle dans l'industrie papetière. Ensuite, la conversion hydrothermale de la liqueur noire et de ses



composés modèles est présentée à partir des données bibliographiques. En conclusion, les objectifs du travail sont exposés.

Le deuxième chapitre détaille les matériaux et les méthodes utilisés tout au long du manuscrit. Les réactifs (liqueur noire, molécules modèles, catalyseur) et les réacteurs utilisés pour les expériences sont présentés et les procédures détaillées. La dernière partie expose les outils analytiques permettant la caractérisation des phases solides, liquides et gazeuses.

Une étude préliminaire est proposée au chapitre 3 dans le but d'évaluer l'influence des conditions opératoires lors de la conversion hydrothermale. Le temps de réaction, en conditions sous et super critiques, la concentration et la température ont été investigués en regard du bilan du carbone entre les phases. Ensuite l'influence de la température a été approfondie vis-à-vis de la formation du solide et de la gazéification. Néanmoins, l'analyse de la phase liquide a été systématiquement réalisée étant donné que la liqueur noire est un déchet aqueux. De plus, l'aspect valorisation de la liqueur noire se retrouve de manière implicite dans les résultats et constitue une base scientifique pour des expérimentations complémentaires. Les conclusions de ce chapitre permettent de préciser les conditions opératoires sélectionnées pour les deux études approfondies suivantes qui concernent la génération de solide et la gazéification catalytique.

Le chapitre 4 s'attache à apporter une contribution au mécanisme de formation du solide en conditions hydrothermales à 350°C dans un réacteur batch. Après une brève introduction des théories, et leurs limites, de formation des solides carbonés, la formation du solide est étudiée en fonction du temps de réaction. Les évolutions des propriétés des phases solides et liquides apparaissent comme des indicateurs optimaux de la génération du solide. La formation de solide est principalement suivie en regard de sa composition chimique, sa morphologie et son taux de conversion. La composition du liquide est caractérisée par des paramètres globaux ainsi que par le suivi de la composition de quelques composants clés. L'influence des vitesses de chauffe et de refroidissement sur la morphologie du solide et la précipitation des sels a aussi fait l'objet de l'étude. Ces travaux ont montré que le solide récupéré est essentiellement carboné tandis que les minéraux restent dissous dans la phase aqueuse. Une proposition de mécanisme de génération du solide carboné à 350°C conclut cette partie de la thèse.

Le chapitre 5 traite de la gazéification catalytique en conditions hydrothermales en vue de produire de l'hydrogène et de diminuer la formation de coke, en utilisant un nanocatalyseur d'oxyde de cérium. Premièrement, une étude comparative entre les conditions sous et super critiques a été réalisée en utilisant le catalyseur pour la gazéification de la liqueur noire.

L'efficacité de production d'hydrogène est ensuite intégrée dans une étude succincte de bilan énergétique mettant en balance le bénéfice d'utilisation du catalyseur. Deuxièmement, le mécanisme de conversion de la liqueur noire étant complexe, des molécules modèles ont été utilisées pour approcher quelques clés de ce mécanisme. Bien que la lignine soit un bon modèle de la liqueur noire, la molécule guaiacylglycerol- $\beta$ -guaiacyl ether (GGGE) a permis de dessiner les traits d'un mécanisme de conversion hydrothermale de la liqueur noire.

Les principaux résultats de ce travail ont été résumés dans la conclusion et quelques perspectives concernant la conversion hydrothermale ont été énoncées, de même que quelques pistes pour son intégration dans la problématique industrielle.



# Chapter 1: Context and objectives of the study

---



**Résumé du chapitre 1 :** Ce chapitre a pour objectif premier de poser les bases de notre raisonnement, ainsi en faisant appel aux références théoriques et bibliographiques nous pourrons développer nos discussions (chapitres 3, 4 et 5). La vocation de cette thèse est de contribuer à la compréhension des procédés hydrothermaux ; pour cela nous avons utilisé comme outil d'étude la liqueur noire, sous-produit de l'industrie papetière. Ce chapitre se divise en 3 parties, chaque partie est résumée ci-après.

#### Les procédés hydrothermaux :

Les procédés hydrothermaux utilisent l'eau à haute température et haute pression pour convertir tout ou partie de la matière organique qui lui est mélangée, ils apparaissent comme des traitements adéquats de la biomasse humique (quantité d'eau >70% en masse). Dans ces conditions, l'eau atteint des conditions subcritiques ou supercritiques ( $T > 374^{\circ}\text{C}$  et  $P > 22,1 \text{ MPa}$ ) ; alors, l'eau agit comme solvant, catalyseur et/ou réactif. En conditions sous-critiques ( $T < 374^{\circ}\text{C}$  et  $P > 22,1 \text{ MPa}$ ), l'eau est un solvant polaire dans lequel les sels sont solubles à l'inverse des molécules organiques, la solvataion des ions favorise les réactions ioniques. À l'état supercritique ( $T > 374^{\circ}\text{C}$  et  $P > 22,1 \text{ MPa}$ ), les propriétés de l'eau changent radicalement l'eau est un solvant apolaire permettant la solubilisation des molécules organiques, le produit ionique de l'eau diminue drastiquement impliquant la précipitation des sels et favorisant les réactions radicalaires. La solubilisation des molécules organiques avec l'eau autorise bon nombre de réactions chimiques telles que des réactions acides/bases, des réactions organométalliques, des réactions d'oxydation et des réactions de réductions... ces réactions sont aussi bien des réactions de dégradation que des réactions de synthèses organiques. De ce fait, le choix des conditions opératoires permet d'orienter les réactions vers des produits à valeur ajoutée et ainsi de donner une seconde vie à la biomasse ou aux sous-produits humides. Les procédés hydrothermaux sont envisagés en réacteurs batchs ou continus, chacun présentant des avantages et des inconvénients. Un inconvénient des procédés hydrothermaux commun aux deux types de réacteurs est la formation de solide lors de la conversion hydrothermale résultant des réactions de condensation, dont l'origine est organique et inorganique. Nous nous sommes concentrés sur cet inconvénient majeur, ainsi notre objectif global pour cette thèse est la formation de solide (dans quelles conditions est-elle favorisée ? Dans quelles conditions est-elle évitée ?...). Pour cela, nous avons choisi comme outil d'étude la liqueur noire, sous-produit de l'industrie papetière hautement chargé en matière organique et inorganique.

### La liqueur noire et l'industrie papetière :

La liqueur noire provient de l'étape de cuisson du bois par la liqueur blanche ( $\text{NaOH} + \text{Na}_2\text{S}$ ) lors du procédé Kraft. Cette étape permet de déstructurer la lignine contenue dans les copeaux de bois et d'en dissoudre une partie dans la liqueur blanche, ainsi à l'issue de la cuisson la partie non dissoute du bois est dirigée vers la ligne de production de papier et la partie liquide aqueuse, appelée la liqueur noire, est traitée. Elle est majoritairement composée d'eau et de matière sèche dont une partie organique (lignine dissoute, fragment de cellulose et hémicelluloses) et une partie inorganique (sels constituant la liqueur blanche et sels du bois). Le contenu détaillé de la liqueur noire utilisée lors de nos expériences se trouve dans la partie 1 du chapitre 2, cependant une composition type est déjà présentée à ce niveau du manuscrit (partie 2 chapitre 1). Cette partie développe, étape par étape, le devenir et la valorisation de la liqueur noire actuellement appliqués dans le procédé Kraft au sein de la papeterie.

Après la cuisson du bois par la liqueur blanche, la liqueur noire est récupérée (23% en masse de matière sèche) puis évaporée (70% en masse de matière sèche) et brûlée dans une chaudière à liqueur noire. A l'issue de cette étape, la matière organique est complètement convertie en  $\text{CO}_2$  et la partie inorganique est récupérée sous forme de sels fondus qui sont ensuite mélangés à de l'eau pour former la liqueur verte. De la chaux est ensuite ajoutée à la liqueur verte (étape de caustification) afin de réagir avec le carbonate de sodium et reconstituer les éléments de la liqueur blanche, qui sera réinjectée en entrée du procédé Kraft pour cuire le bois. Lors de cette étape du carbonate de calcium est formé, et est dirigé vers l'ultime étape : la calcination. La calcination du carbonate de calcium produit du  $\text{CO}_2$  et régénère la chaux qui est ensuite réutilisée pour la caustification. Le procédé Kraft permet à la papeterie d'être quasi autonome énergétiquement et présente l'avantage de régénérer 95 % de ses besoins en composés inorganiques (liqueur blanche). Cependant, deux inconvénients majeurs poussent les papetiers à chercher une autre voie de valorisation de la liqueur noire : l'étape d'évaporation est très énergivore et l'étape de combustion n'offre pas de valorisation intéressante de la partie organique de la liqueur noire principalement constituée de lignine. En effet, de nombreux intermédiaires réactionnels peuvent être envisagés si une conversion partielle de cette molécule est considérée. La première partie de ce chapitre soutient cette hypothèse en considérant les propriétés de l'eau mises en jeu par la conversion hydrothermale. Un premier état de l'art sur la conversion hydrothermale de la liqueur noire et de ses molécules modèles (guaiacol, catéchol, GGGE...) montre que de nombreux produits solides, liquides et gazeux peuvent être obtenus par des mécanismes réactionnels complexes.

Les objectifs de la thèse :

Tel que mentionné dans l'introduction, le principal objectif de cette thèse est de mieux comprendre les procédés hydrothermaux d'un point de vue mécanisme réactionnel et d'un point de vue procédé, avec un intérêt particulier sur les points suivants :

- Le problème de formation du solide lors de la conversion hydrothermale : un mécanisme de formation du solide sera proposé en chapitre 4
- La production d'hydrogène avec un focus mis sur la conversion catalytique, le choix du catalyseur est fait en vue d'éviter la formation de solide : L'impact du catalyseur sur les réactions mises en jeu lors de la conversion hydrothermale sera expliqué compte tenu des produits obtenus
- Dans chaque chapitre le réacteur continu sera approché autant que possible par le choix des conditions de fonctionnement du réacteur batch : une chauffe aussi rapide que possible précédera la réaction, un refroidissement par trempe la suivra.

**\*\*\*Fin du résumé**





Wastewater and by-product management is one of the major points of the sustainable approach, implemented in the development of industrial processes. The general objective is to “close” industrial processes by promoting a circular flow of matter and energy, reducing in- and out-flows and therefore, the environmental footprint of industry. Several treatments, such as biochemical, physico-chemical, thermochemical ..., are currently used in order to clean wastewater or by-product and valorize their content as energy or useful materials.

Along thermochemical treatment, dry and wet routes are offered. Depending on the content of water, organic and inorganic in the by-product, one treatment will be preferred over the other. For aqueous by-product (80 wt% of water), hydrothermal processes are appropriate. They use the properties of water at high temperature and for high pressure to degrade the organic matter, avoiding evaporation. During several decades, hydrothermal process was particularly used for oxidation to destroy completely organic matter, transforming into CO<sub>2</sub>, and let the water almost clean [1]. However, without pushing the degradation of organic matter to its maximum it is possible to form intermediate molecules that can be valuable after separation. In this consideration, by-product finds a second utility. Degradation mechanisms are complex and raises technical, technological and scientific issues. To evaluate the hydrothermal conversion modalities, a raw biomass has been chosen in our study: black liquor. Black liquor is an alkaline by-product coming from the step of wood cooking in Kraft process.

This chapter lays the foundations for understanding the hydrothermal conversion of black liquor, firstly, exposing the properties of water and reactions related to hydrothermal conversion, then with a description of the black liquor and a state of the art of its hydrothermal conversion.

## **I. Hydrothermal processes**

Hydrothermal processes use water, as reactant, solvent and catalyst, at high temperatures and pressures, to convert biomass. Biomass is defined as organic matter having vegetable or animal origin. Hydrothermal processes, particularly supercritical water oxidation and gasification were applied from several decades due to its solvent and reactant properties [2], [3], [4]. In this section, the properties of water at high temperatures and pressures are presented prior to detail the hydrothermal processes.

### I.1. Definition of supercritical water

Supercritical conditions of water are reached when temperature is higher than 374°C and pressure is higher than 22.1 MPa (blue square on Figure 1).

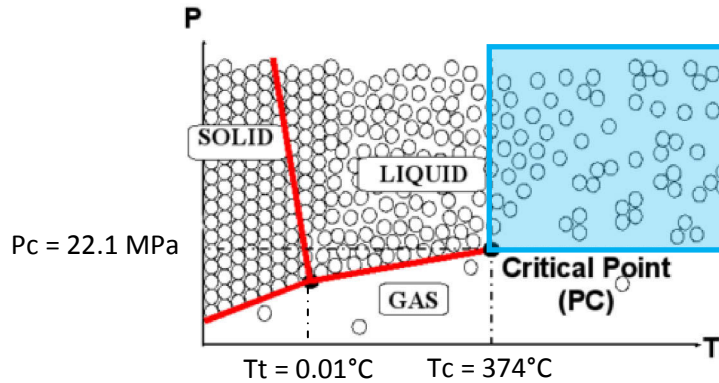


Figure 1: Phase diagram of water<sup>1</sup>.

Equilibrium between liquid and gas is possible for a temperature between triple temperature ( $T_t = 0.01^\circ\text{C}$ ) and critical temperature ( $T_c = 374^\circ\text{C}$ ). After critical point ( $P_c = 22.1\text{ MPa}$  and  $T_c = 374^\circ\text{C}$ ) only one phase is observed. Indeed, progressively following this equilibrium curve from triple point to the critical point, differences between liquid and gas properties decrease to reach specific properties of a homogeneous phase: the supercritical phase. Supercritical water has physico-chemical properties from gas and liquid, which are detailed in the next section.

Water is basically found under 3 phases: liquid, solid and gaseous phases; a fourth phase called supercritical phase is detailed when  $T \geq 374^\circ\text{C}$  and  $P \geq 22.1\text{ MPa}$  are simultaneously reached. An experiment conducted in space by CNES, in the DECLIC program has shown that supercritical water looks like fog between liquid and gas (Figure 2).

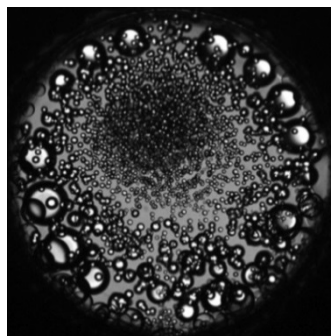


Figure 2: Supercritical water observation in DECLIC (from CNES).

<sup>1</sup> <http://neel.cnrs.fr/spip.php?article992>

## I.2. Macroscopic and microscopic properties of supercritical water

Macroscopic and microscopic properties of water at high temperature and high pressure are able to explain the specific behavior of this “magic solvent”.

### I.2.1. Sub and supercritical water: a solvent as well as a reactant

#### *Macroscopic aspect: density and dielectric constant*

##### Density:

Density of water at atmospheric pressure decreases significantly from liquid phase to vapor phase, going from  $997.048 \text{ kg.m}^{-3}$  at  $20^\circ\text{C}$  to  $0.597 \text{ kg.m}^{-3}$  at  $100^\circ\text{C}$ . The density of water at  $400^\circ\text{C}$ , 25 MPa is close to  $170 \text{ kg.m}^{-3}$  that is included between liquid and gas values. For  $P = 15 \text{ MPa}$ , a drastic change occurs around the critical temperature. Density evolves from a liquid mixture directly to a vapor mixture. For higher pressure, the evolution is softer, suggesting the pressure controls temperature effects on density and phases mixture, favoring dense phase. Thus, even under supercritical conditions, water remains a good solvent for molecules and a media where gases have a great miscibility.

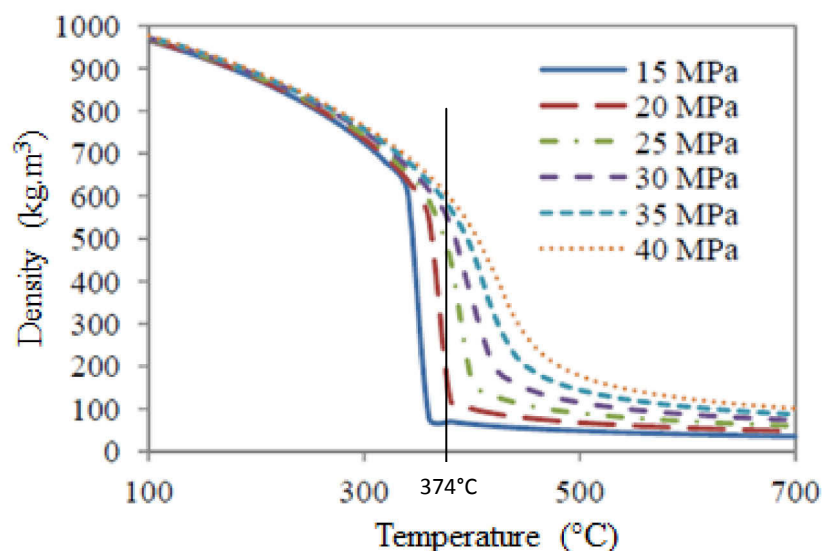


Figure 3: Density evolution with temperature ( $100^\circ\text{C}$  to  $700^\circ\text{C}$ ) and pressure (15 MPa to 40 MPa).

##### Dielectric constant

The dielectric constant is defined as the ratio of its permittivity to the permittivity of free space. The dielectric constant characterized the bonds between solute and solvent, like hydrogen or ionic bonds. A solvent with a high dielectric constant like water at conditions of ambient temperature and pressure (78.5) is able to solubilize salts. Water at ambient

conditions is a polar solvent able to dissolve salts. On the contrary, non polar organics are immiscible. Besides, it is known that the dielectric constant of a fluid is directly related to its density. As the density of water differs greatly in subcritical and supercritical states, important dielectric constant evolution is expected (Figure 4) as well as changes in salts solubilization and organics miscibility.

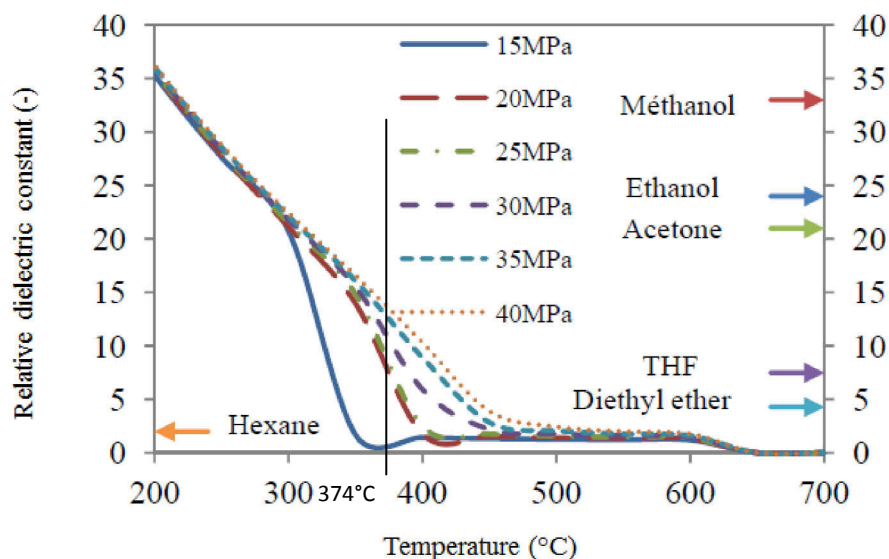


Figure 4: Dielectric constant evolution with temperature (200°C to 700°C) and pressure (15 MPa to 40 MPa).

Others dielectric constants of typical organic solvent are indicated on figure 4, as reference. Thereby, in subcritical conditions, dielectric constant of water is close to that of acetone, an organic polar solvent; and under supercritical conditions it is close to hexane, an organic non polar solvent. Depending on the couple temperature/pressure, supercritical water is able to gain properties of non polar solvent and so become a good solvent for organic matter. In these conditions, water is reactive. However, as water is non polar, salts are immiscible and processes limited by interphase transfer are not more operating.

Moreover, Gibbs energy depends on dielectric constant and affect kinetics [5].

Depending on its pressure and temperature; considering only the dielectric constant, water properties are different:

**- In subcritical conditions: water is a poor polar solvent; salts are less soluble and organics more miscible compare to ambient conditions.**

**- In supercritical conditions: water is a non polar solvent, miscible with organics components. The salts are not soluble and precipitate. Ionization is not favored in supercritical phase.**

**- Kinetics reactions are changed by decreasing the dielectric constant.**

Besides, water reactivity is explained regarding its microscopic properties.

*Microscopic aspect: collisions frequency and dipole moment*

Water ( $H^+$  or  $HO^-$ ) becomes a reactant close to the supercritical point, as follow through the microscopic properties.

Collision frequency:

Chemical reactions in gas phase are subjected to the efficiency of molecules collisions. Collision frequency depends on distance between molecules, their movement, their steric configuration, their concentration. Higher this frequency is, more reactions are efficient.

As seen previously, density of supercritical water is comprised between steam and liquid water ones. Among diffusion, convection and migration phenomena, the first one is predominant. Therefore collisions frequency is comprised between liquid and gas ones, consequently the diffusion is faster than in liquid and less efficient than in gas.

Considering the water as solvent (high concentration), the reaction temperature ( $T \geq 374^\circ C$ ) and the media diffusivity (low density), the kinetics of reactions will be higher.

Non-polarity of supercritical water:

Water molecules preserve the same structure whatever the conditions of temperature and pressure. However, under supercritical conditions, water molecules are paired and form dimers or clusters. Taken together, these kinds of combinations (Figure 5) form a non-polar structure.

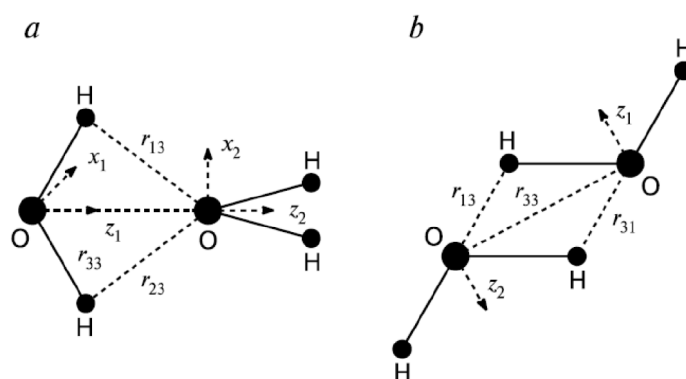


Figure 5: Water dimers: in bifurcated form (a) and reverse form (b) (from [6]).

Bushuev et Davletbaeva [13] showed that under supercritical conditions reverse dimers are predominant [7], so water appears as a non polar solvent. In these conditions, ions are less dissolved in the media.

## I.2.2. Salts precipitation

### *Macroscopic aspect: ionic product*

Ionic product ( $K_w$ ) characterized the ionization ability of water. Figure 6 shows the evolution of  $pK_w$  with the temperature and the pressure. The  $pK_w$  decreases continuously to the region of critical point, reaching a minimum of about 11 closely before the supercritical conditions. Continuing the heating in isobar condition,  $pK_w$  increases to much higher volumes (20-26) in the supercritical region.

Higher the  $pK_w$  is, less ionized species can be produced. Subcritical ionizing power of water is higher than in normal conditions, supercritical ionizing form of water is much lower than for water in standard conditions. When the temperature rises near to the critical temperature,  $pK_w$  decreases reflecting the fact that water ionizes better salts but as soon as  $T_c$  is overshoot, the ionizing power falls drastically. This is due to the coupled action of a low density and a low dielectric constant. Consequently solubilization and stabilization of ions decrease dramatically in supercritical state.

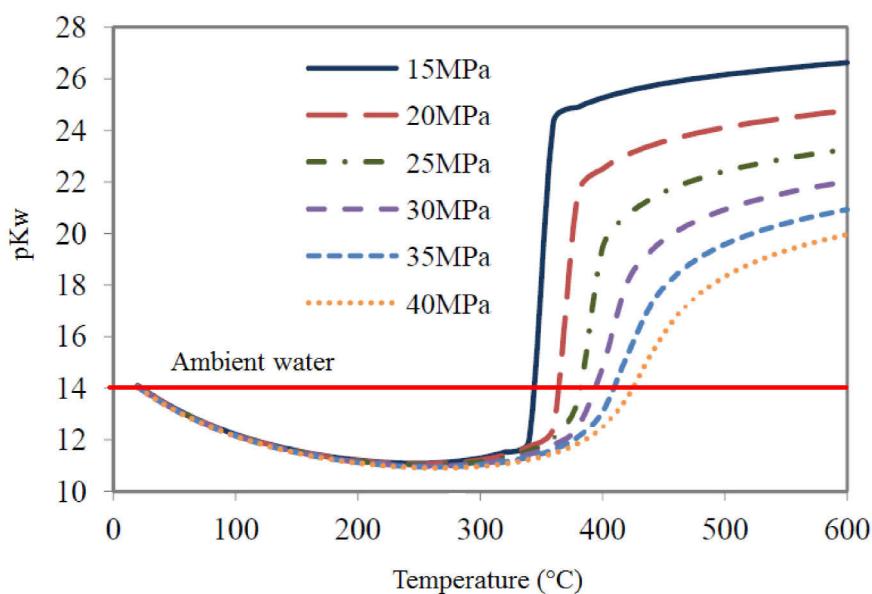


Figure 6: Evolution of ionic product as a function of temperature (from 20°C to 600°C) and pressure (15 MPa to 40 MPa).

Water close to the critical point is more ionized and is able to be acid or basic catalyst. Thus ionic reactions are favored at subcritical conditions, while radical reactions are promoted at supercritical ones.

*Microscopic aspect: hydrogen bonds and ions solvation*

Hydrogen bonds:

The frequency of hydrogen bonds has an effect on diffusion phenomenon in the supercritical phase, [8], [9], [10].

In liquid phase, as the phase is dense, molecules are closer to each other and so many hydrogen bonds are established. Kinetics of formation/destruction of these bonds is extremely fast but the balance is in favor of formation, consequently many hydrogen bonds exist.

On the contrary, under supercritical conditions hydrogen bond number is small. Indeed, thermal agitation, as well as the density decrease affects the distance between water molecules.

Ions solvation:

As seen previously, ionic product decreases drastically at supercritical conditions.

The solvation of ions takes place using superimposed solvation spheres surrounding ions ([11], [12], [13]). The first one is relatively stable and exists in all conditions. At ambient conditions, many others “layers” are grafted over the first solvation sphere, contributing to the stable ions solvation. It has been shown ([14], [15]) that less solvation spheres or layers are found at high temperature. However, its low density is not able to ensure the cluster solvation and salts precipitate.

This section deals with chemical properties as regards to the reactivity. The next part presents physico-chemical properties that impact the process design.

**I.2.3. Water properties related to process design**

*Macroscopic aspect: Dynamic viscosity*

The dynamic viscosity reflects the resistance of fluid to the flow. At atmospheric conditions, dynamic viscosity is  $10^{-3}$  Pa.s then decrease to  $20 \cdot 10^{-6}$  Pa.s at  $T_c$  and finally increases again slightly up  $25 \cdot 10^{-6}$  Pa.s.



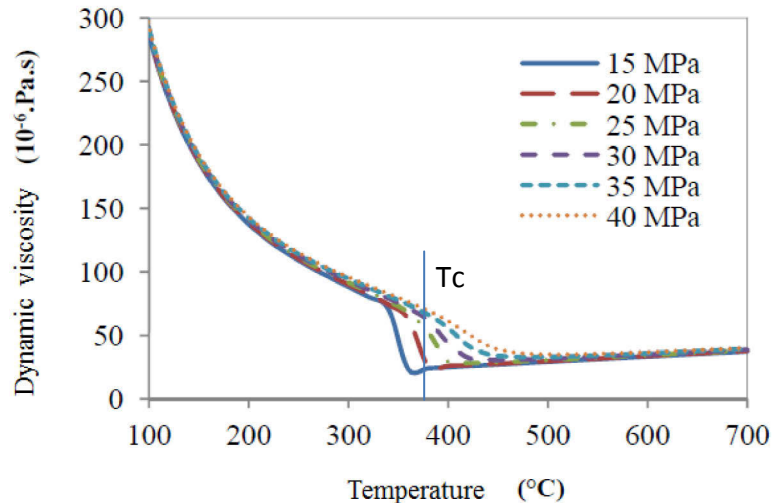


Figure 7: Evolution of dynamic viscosity as a function of temperature (100°C to 700°C) and pressure (15 MPa to 40 MPa).

**The resistance of supercritical water is lower under supercritical conditions than at ambient conditions and is similar to gas resistance (air:  $18 \cdot 10^{-6}$  Pa.s). So a weak flow resistance has to be considered during process design.**

In addition, energetic aspects have to be also considered.

*Macroscopic aspect: enthalpy, heat capacity and thermal conductivity*

### Enthalpy

The enthalpy reflects the amount of energy required to cross the critical temperature.

Figure 8 shows that enthalpy increased sharply around  $T_c$ . However, higher the pressure is, lower the energy required to reach the supercritical state is.

A balance has to be found in process technology between a “low” pressure requiring a high amount of energy but a more common technology; and high pressure requiring less amount of energy but a special and expensive technology.

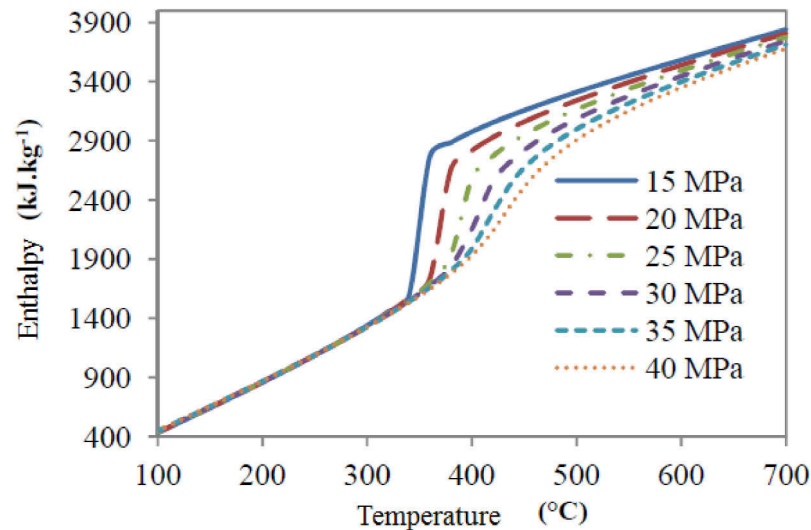


Figure 8: Evolution of enthalpy as a function of temperature (100°C to 700°C) and pressure (15 MPa to 40 MPa).

### Heat capacity

The water heat capacity ( $C_p$ ) is the energy required to increase 1kg of water of 1°C. Up to around 300°C, the  $C_p$  is almost stable but a peak is then observed for each pressure. Higher the pressure is, higher the peak temperature is. According to the simulation Figure 9, peaks at 25 and 30 MPa are the highest.

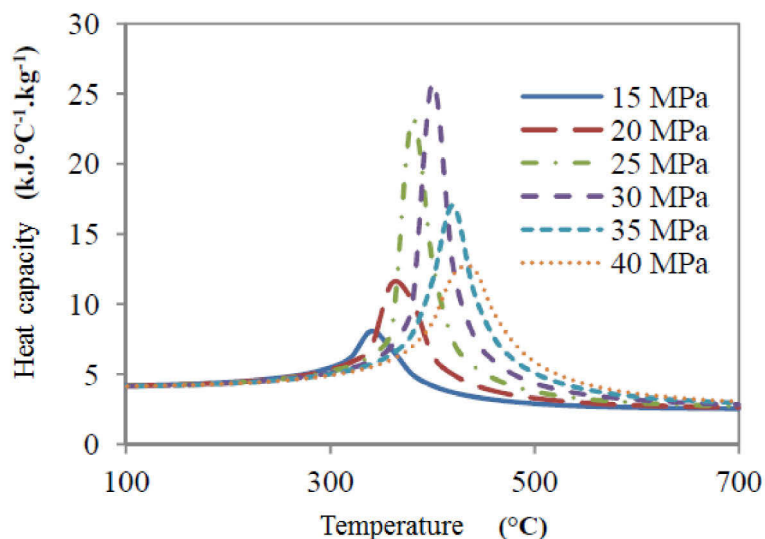


Figure 9: Evolution of heat capacity as a function of temperature (100°C to 700°C) and pressure (15 MPa to 40 MPa).

**A pressure around 25 MPa corresponds to heat capacity optimum and constitutes a good compromise regarding technology cost.**

Thermal conductivity

This parameter is related to the heat transfer. Figure 10 shows that thermal conductivity tumbles down until 350°C; then, close to the critical point, lower the pressure is, greater the curve falling is. In this area, the value of thermal conductivity is intermediate between liquid water ( $0.6 \text{ W.m}^{-1}.\text{K}^{-1}$ ) and steam ( $0.025 \text{ W.m}^{-1}.\text{K}^{-1}$ ). After 500°C, thermal conductivity increases slightly.

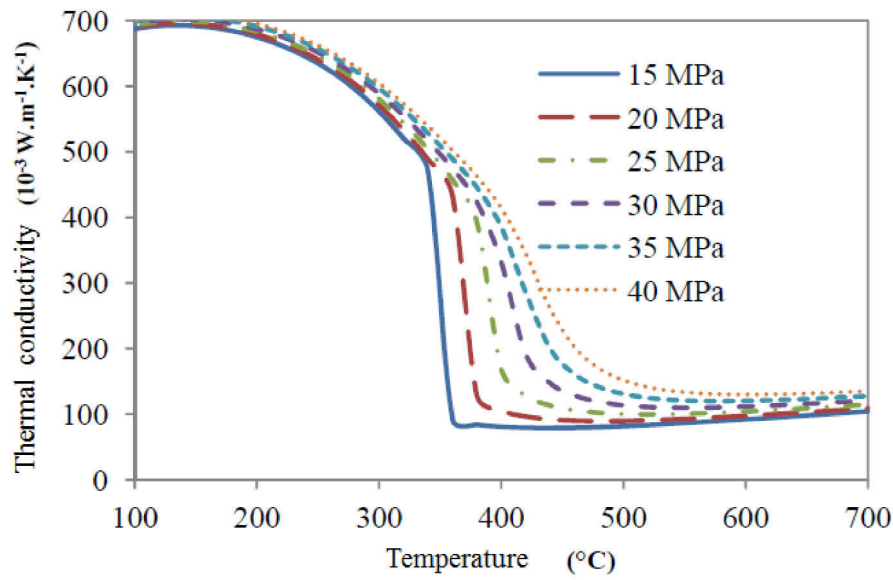


Figure 10: Evolution of thermal conductivity as a function of temperature (100°C to 700°C) and pressure (15 MPa to 40 MPa).

**In supercritical conditions, heat exchanges are worse than in subcritical conditions.**

#### I.2.4. To conclude: sub and supercritical water properties

Sub and supercritical water show following properties ([16], [17]) presented in Table 1.

Table 1: Synthesis of water properties at subcritical and supercritical conditions.

	Subcritical conditions	supercritical conditions
<b>Phase</b>	L / G / S	supercritical / S
<b>miscibility</b>	salts	gases / organics
<b>[H<sup>+</sup>], [HO<sup>-</sup>]</b>	high / ionic reactions	Low / Radical reactions
<b>kinetics</b>	fast	very fast
<b>heat</b>	low energy required / energy transfer high	high amount of energy required / energy transfer low
<b>fluid resistance</b>	high	low

The combination of supercritical water properties gives it a significant interest as reactive media for biomass treatment. Indeed, as the water is solvent, catalyst, reactant ... a plurality of reactions occurs during hydrothermal process leading to the formation of gas, liquid and solid. However, instruments and technologies are limiting industrial applications of supercritical water processes.

### I.3. Hydrothermal treatment of wet biomass

As seen previously, water under supercritical conditions or close to supercritical conditions has reactive properties which combined, give it interesting applications based on chemical reactions ([18], [19], [20], [21], [22], [23]) such as waste treatment ([24], [25], [1], [26], [3]), biomass conversion ([27], [28], [29], [30], [31], [32]), nanoparticles synthesis ([33], [34], [35], [36], [37], [38], [39]).

Chemical reactions and mechanism pathways are guided by operating conditions. Indeed, as shown by Kruse et al., the modification of temperature process acts on the product obtained during hydrothermal conversion, by favoring certain reactions to other. Thus supercritical conditions favors radical reactions while subcritical water enhance ionic reactions.

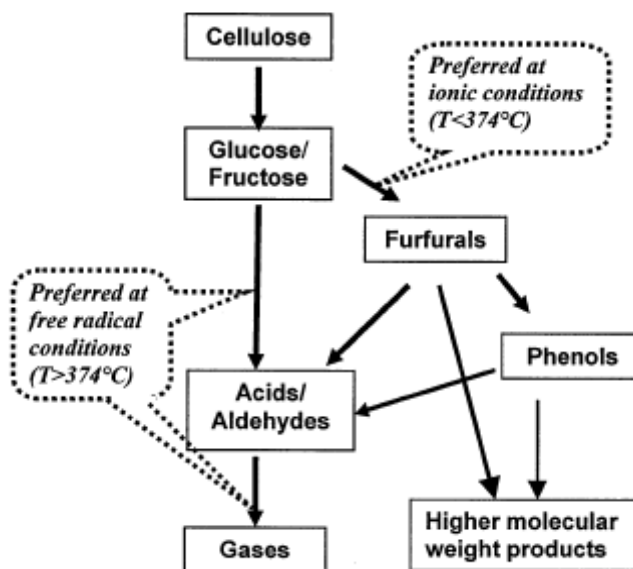


Figure 11: Preferred reaction pathway following process temperature [4].

Combining water properties and operating conditions, the applications are possible (Figure 12):

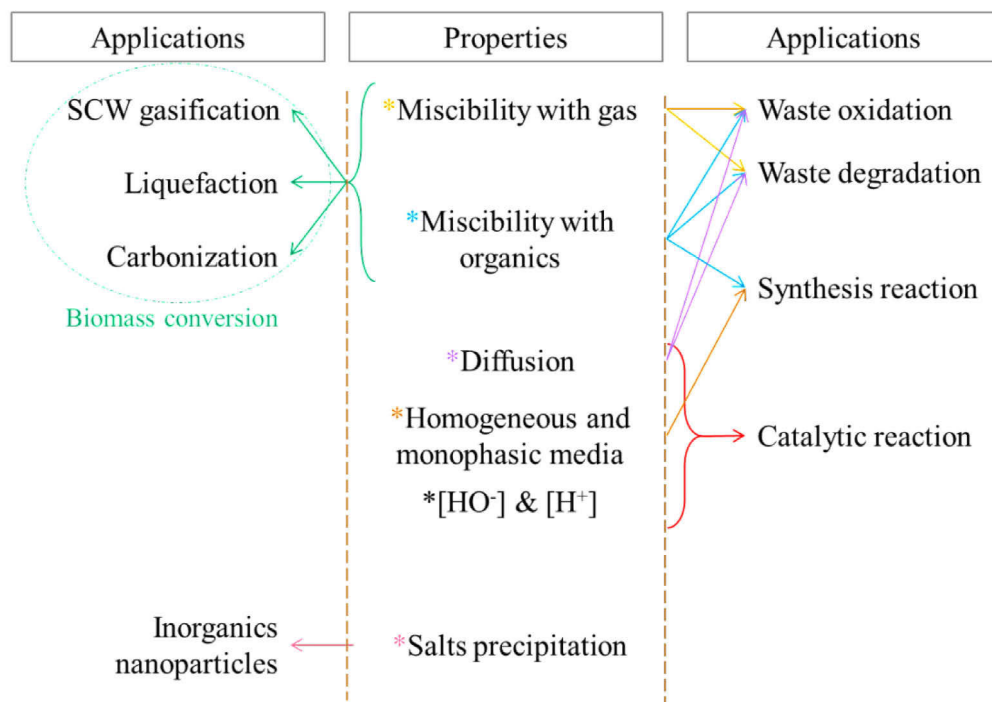


Figure 12: Applications of supercritical water properties.

Water properties promote certain reactions, as indicated on Figure 13.

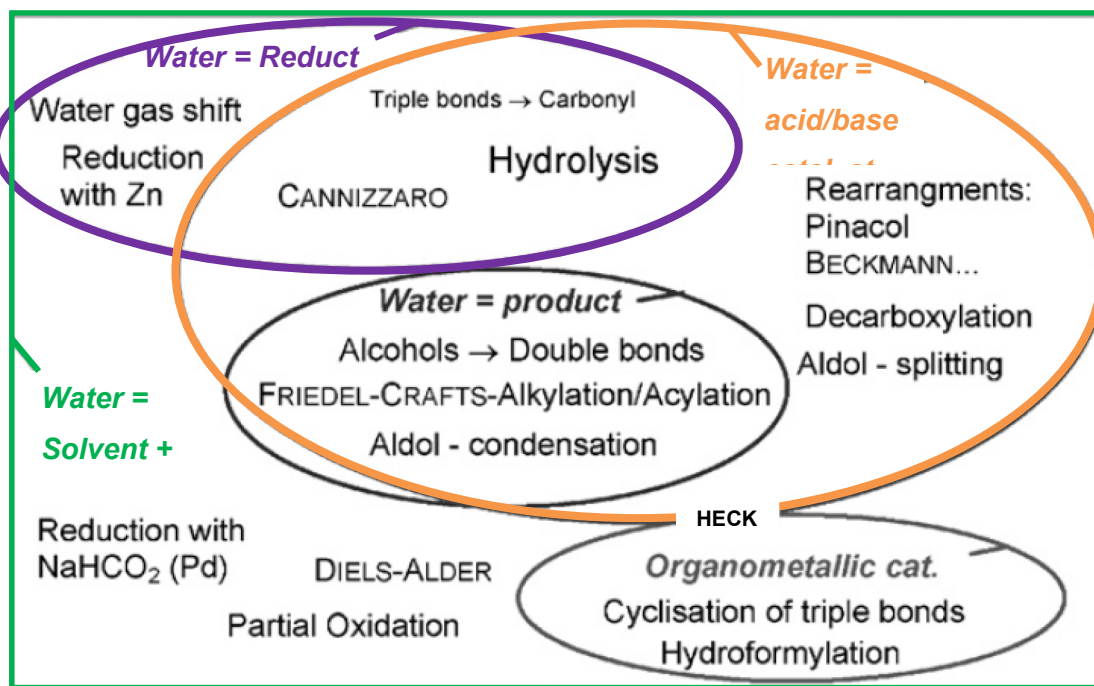


Figure 13: Synthesis reactions considering water properties [5].

Main reactions occurring in liquid phase are detailed after; equations are schematically presented without stoichiometry:

**Hydrolysis:** For example, studies on hydrolysis of esters show different mechanisms under sub and supercritical conditions ([5]). Reactions lead to corresponding alcohols and decarboxylation of the acids formed.

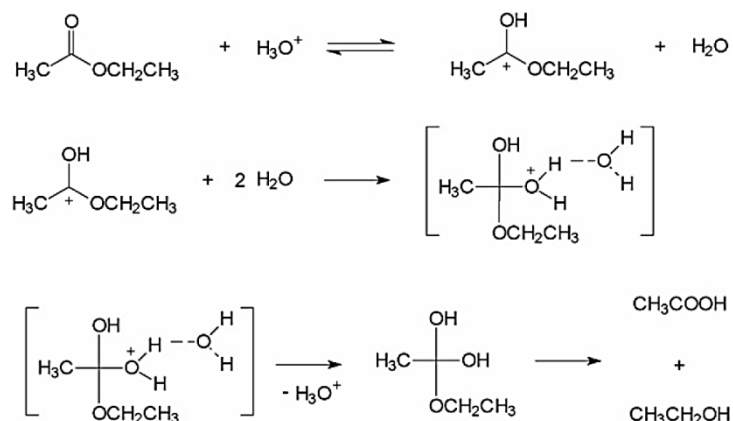


Figure 14: Hydrolysis of esters from [5].

**Condensation:** In these reactions water is considered as acid catalyst (source of  $\text{H}^+$  ions). They lead to water elimination from alcohols forming double bonds (dehydration). Another type of condensation occurring during hydrothermal conversion is the Friedel-Craft alkylation (Figure 15) and acylation (Figure 16), especially under subcritical conditions where  $\text{pK}_w$  is the lower ([40], [41]).

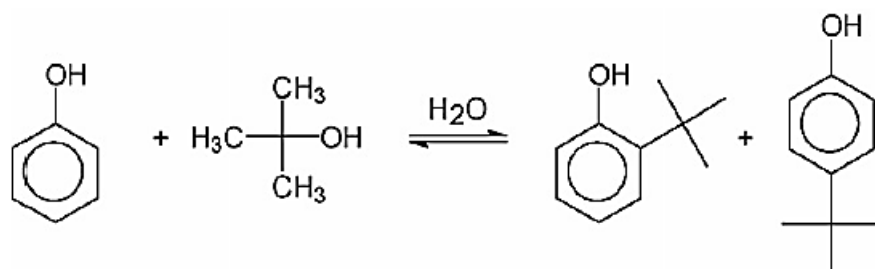


Figure 15: Friedel-Craft alkylation ([5])

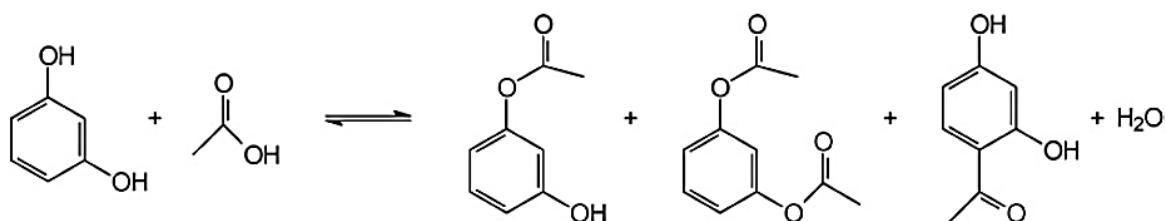


Figure 16: Friedel- Craft acylation ([5]).

Water is also basic catalyst and lead for example to intramolecular Claisen condensation or Dieckmann condensation ([42]). Under supercritical conditions, water has sufficient basicity to allow aldol condensation or Cannizzaro reaction (Figure 18).

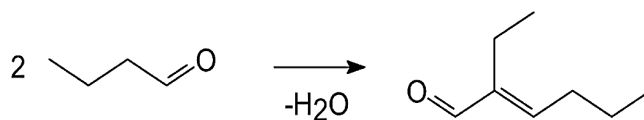


Figure 17: Aldol condensation ([5]).

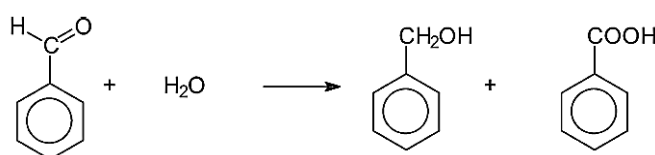


Figure 18: Cannizzaro reaction.

In addition, the reactivity of molecules under these conditions (temperature and pressure) makes the Diels-Alder reaction possible [5].

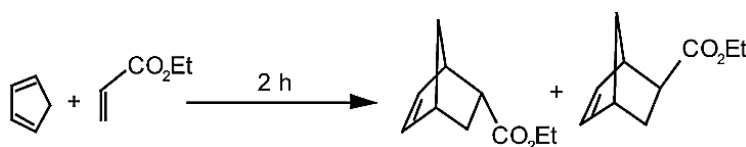


Figure 19: Diels-alder reaction.

**Oxidations:** Oxidations occur during hydrothermal conversion, such as formation of methanol from methane or aldehyde oxidations, ketones and acids from alkylarenes oxidations ([43], [44]). However the balance between kinetic reactions of their formation/disappearance is not in favor of their formation so their yields are often very low. To promote the formation of their compounds, the addition of catalyst, transitions-metal compounds especially, or addition of oxidizing species such as  $O_2$  is required.

**Reductions:** Reduction reactions are possible with addition of reducing agents under subcritical conditions. Usually a catalyst like platinum is needed for the reduction of alkynes and alkenes in alkanes with  $NaHCO_2$  as reducing agent ([45]). Under supercritical conditions, the presence of  $H_2$ , produced by water-gas-shift reaction, is used as reducing agent ([46], [47], [48]). The water reactivity, under supercritical conditions, creates a good media for hydrogenation reactions.

Organometallic reactions: Under supercritical conditions organometallics reactions (Heck coupling, Glaser coupling reactions, cyclotrimerization of alkynes), have been considered [49], [50] in presence of catalyst.

The gas phase is created by the gasification of small molecules like formaldehyde or formic acid, which gives  $\text{CH}_4$ ,  $\text{CO}_2$ ,  $\text{CO}$  and  $\text{H}_2$  by decarboxylation ((1), (2) and (3)). Gases produced by this first gasification react with water according to water-gas-shift reaction (4),  $\text{CO}_2$  methanation (5) and  $\text{CO}$  methanation (6) [51].



After reaction, products are distributed in three phases at normal conditions: gas phase [29], liquid phase [5] and solid phase [52], [37] (Figure 20). Reactions are as follow:

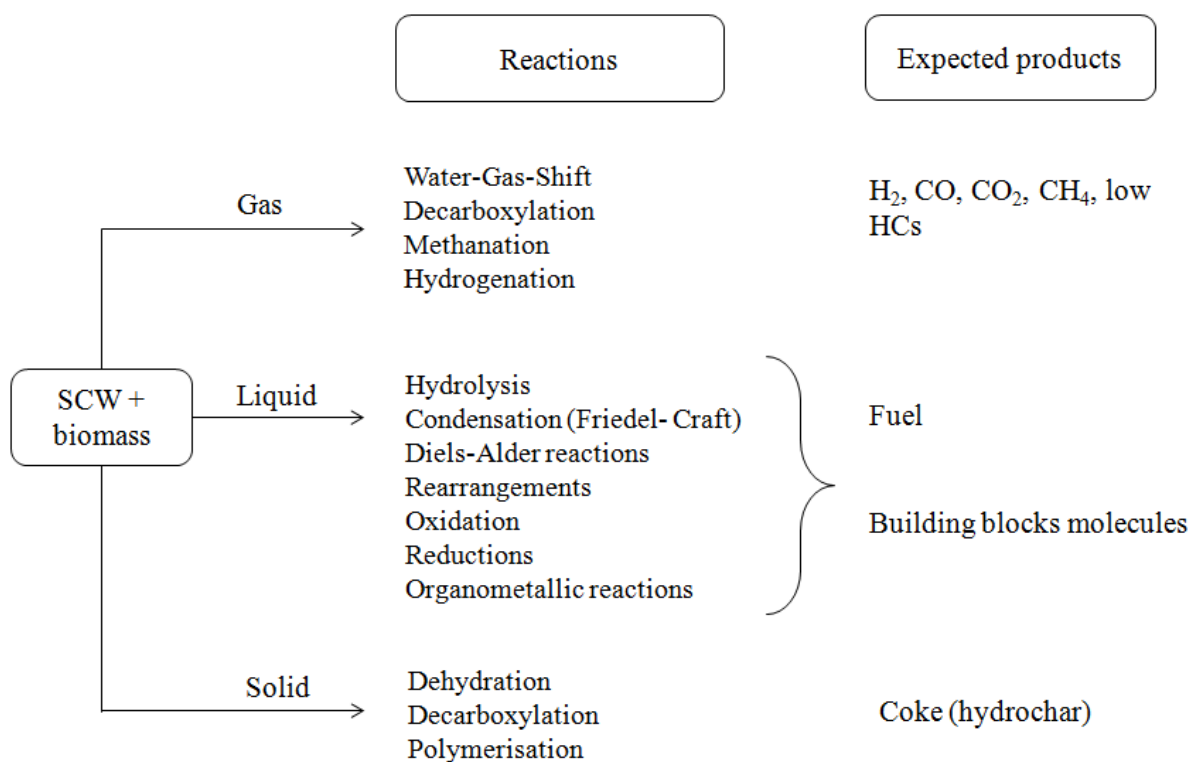


Figure 20: Reactions occurring during hydrothermal conversion of biomass.



Catalytic activity of alkali salts has to be considered also because of the alkali content of black liquor. Alkali components are usually used as catalyst. They break C-C bond during the hydrothermal conversion which increases gas formation. The water-gas-shift reaction is promoted while CO and CO<sub>2</sub> methanation reactions are inhibited. A reactivity order of catalyst has been reported by Wu ([51]) as K<sub>2</sub>CO<sub>3</sub> > KOH > Na<sub>2</sub>CO<sub>3</sub> > NaOH. As gasification is improved, the proportion of carbon remaining into liquid and solid phase should be lower.

Depending on operating conditions (T, P, reaction time, concentration...), and reagents (biomass, oxidant, catalyst...), products are different. Increasing the temperature, predominant phase evolves from solid phase to the gaseous one. Figure 21 shows added-value products recovered as energy carrier or molecules from each phase (gas [53], [54], [55], [56]; liquid [57], [58], [59]; solid [60], [61], [62], [63]). In figure 21, green color is used for energy recovery and orange color for chemicals recovery. Hydrochar can be considered as product forming energy and chemicals recovery.

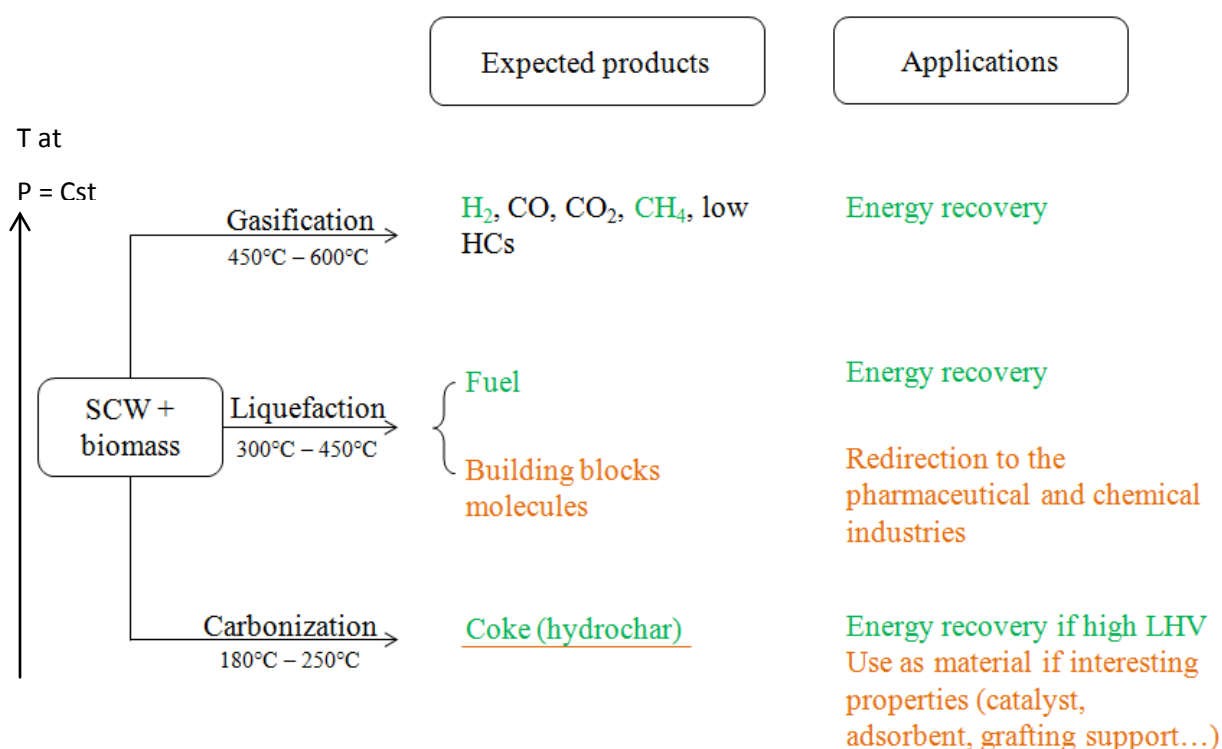


Figure 21: Products obtained by SCW and their applications.

Hydrothermal conversion in supercritical conditions has three purposes:

- Energy production (or energy carriers)
- Waste Treatment (i.e. by oxidation)
- Production/fractionation/extraction of building blocks molecules

Theoretically hydrothermal processes allow considering a lot of reactions but the industrial implementation of these processes is difficult.

#### **I.4. Implementation of hydrothermal processes: progress and limitations**

The first consideration is on reactor type: batch or continuous? Usually, reactors implemented in industry are continuous reactor for production reasons and facilities for monitoring parameters such as temperature, pressure, products quality, etc. Batch reactors are usually not implanted because of volume capacity and the difficulties to monitor the reactions. However, considering hydrothermal processes, applications with continuous processes are limited for safety reasons, thus several locks are yet to be solved formation of solid being one of the most important.

During hydrothermal process, solid is formed from inorganic and organic matters. To palliate inorganic solid, coming from salts precipitation, several technologies have been developed such as fluidized bed reactors, reverse flow reactors, cooled-wall reactor, transpiring-wall reactor and conversely tubular reactors. However to palliate completely organic solid formation, no technologies exist. The only solution to avoid organic solid formation is oxidation under supercritical water which degrades the whole organic matter in CO<sub>2</sub>. Otherwise, plugging reactor is inevitable.

In addition, the reactor materials must be corrosion resistant, withstand high pressures and high temperatures, and which is very expensive. Furthermore, it is often impossible to find the material that satisfies all constraints.

So, hydrothermal processes raise the following issues:

- Formation of organic solid
- Formation of inorganic solid
- Gasification requires high temperature and consequently expensive materials.

In order to study the complexity of hydrothermal processes, a perfect “study tool” is a biomass with high water, organic and inorganic contents. Thus, black liquor has been chosen. Black liquor is alkaline by-product, coming directly from the paper industry using Kraft process. Its inorganic and organic content allow us to investigate solid formation in hydrothermal process, one of the major drawbacks. Due to its alkalinity, salts would act as catalyst to improve hydrogen production.

## II. Black liquor and the paper industry

Paper is mainly made from the fibrous part of the wood. Wood is composed of three polymers: cellulose and hemicelluloses constituting the fibers of the wood and lignin giving wood's rigidity. To isolate and recover fibers, lignin must be altered. The most widely used process for lignin fragmentation is the Kraft process detailed in Figure 22. Lignin is damaged during cooking step.

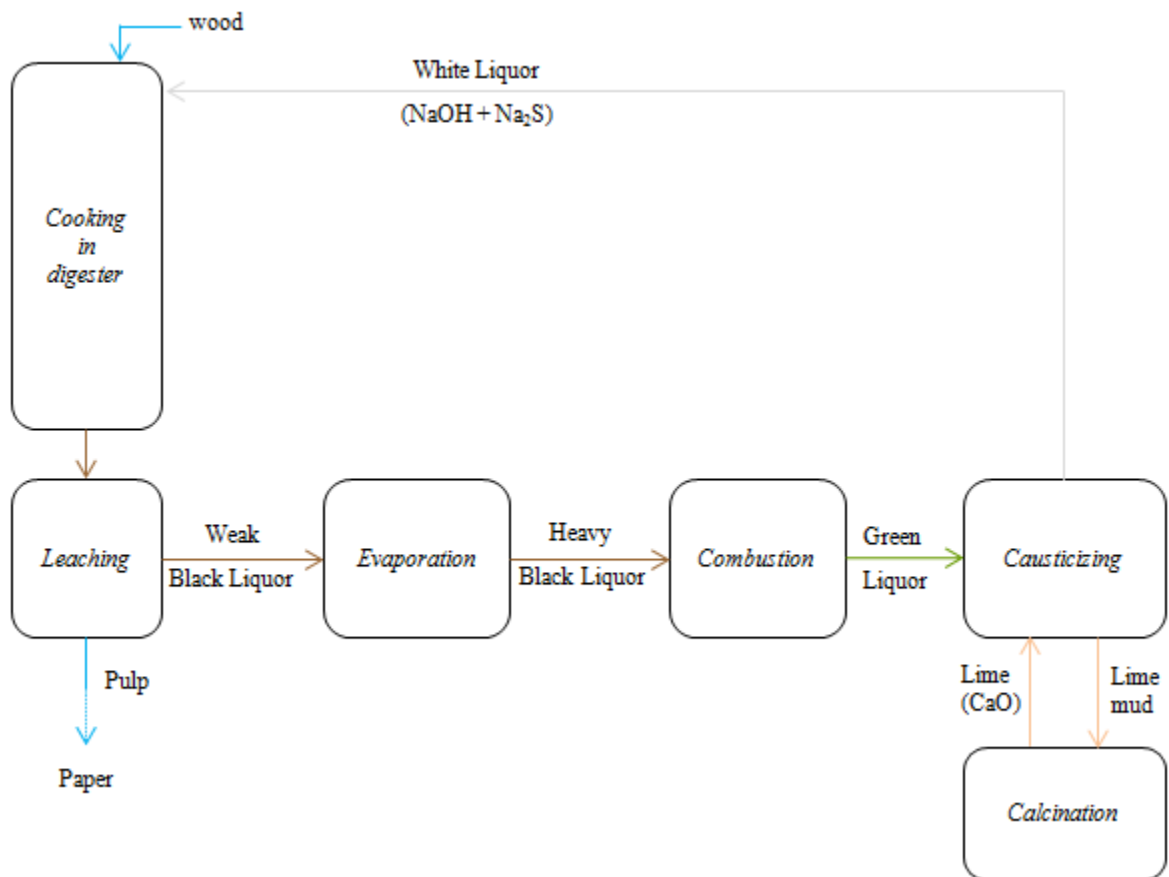


Figure 22: Kraft process.

Based on the simplified flow sheet from Figure 22, each step is more detailed in next sections.

### II.1. Cooking and leaching steps: black liquor origin and composition

#### II.1.1. Cooking step

Kraft process is characterized by the use of white liquor (mainly composed of NaOH, Na<sub>2</sub>S with a pH between 13 and 14) as cooking liquor to extract lignin. During the cooking step, wood chips are mixed with white liquor at 165°C during 8 hours with a pressure of ~0.75 MPa into a batch reactor called digester.

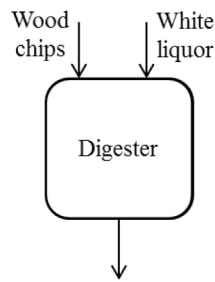


Figure 23: Cooking step.

Inside the digester, white liquor attacks wood. Mechanism of the digestion is proposed and summarize Figure 24 [64]:

-The first and main important step is the **diffusion of ions** ( $\text{HO}^-$ ,  $\text{HS}^-$  and  $\text{S}^{2-}$ ) within the chips. It results the fragmentation of cellulose fibers from wood.

-The second step consists in the **reaction between ions and wood polymers**: cellulose, hemicelluloses and lignin; during this stage delignification and partial hydrolysis of hemicelluloses and cellulose occur. Thus, lignin is fragmented into smaller molecules or ions by ionic reaction.

-The third and last step is the **diffusion of extracted compounds** (Kraft lignin and sugars) from the wood.

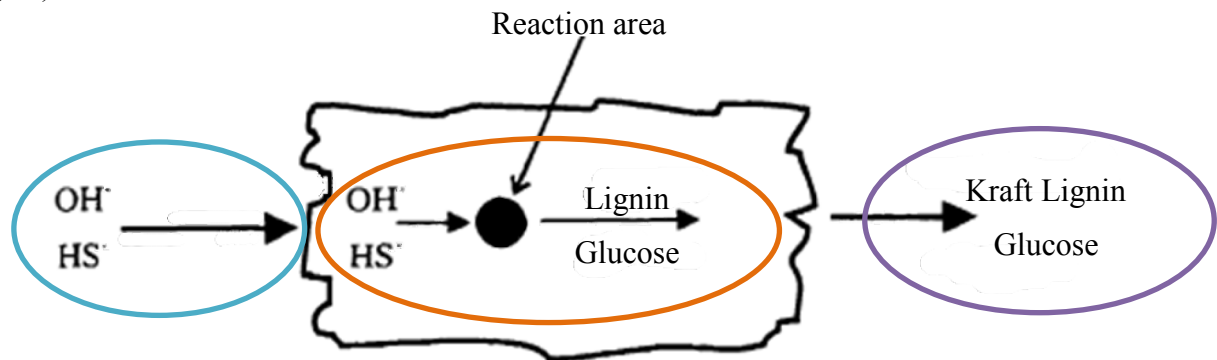


Figure 24: Process of Kraft pulping (adapted from [64]).

### II.1.2. Kraft lignin

Lignin represents between 25 to 30 wt% of wood components [65].

It is an aromatic natural polymer with a very complex structure which is different for each wood species. It is therefore impossible to draw a single molecule. However, it is recognized that the lignin is made by the uncontrolled polymerization of 3 sub-units of

monolignols [66] different in degree of methoxylation: *p*-coumarylic, coniferyl and sinapylic; called respectively H, G and S units.

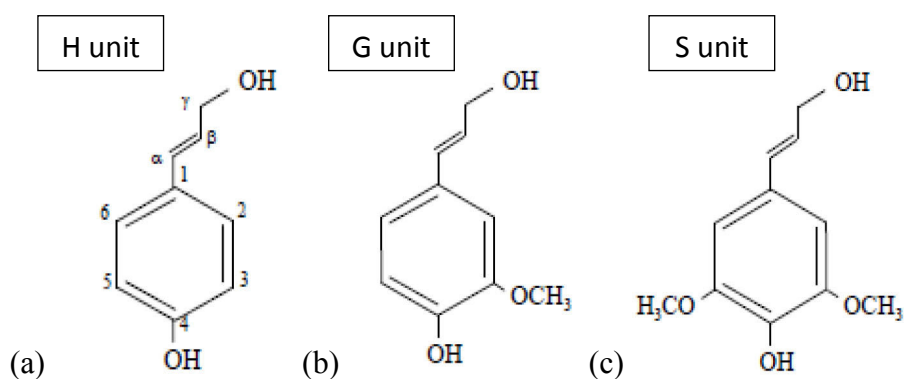


Figure 25: (a) *p*-coumarylic Alcohol, (b) coniferyl alcohol and (c) sinapylic alcohol.

Given what we know, once polymerized, lignin structure could be as follow:

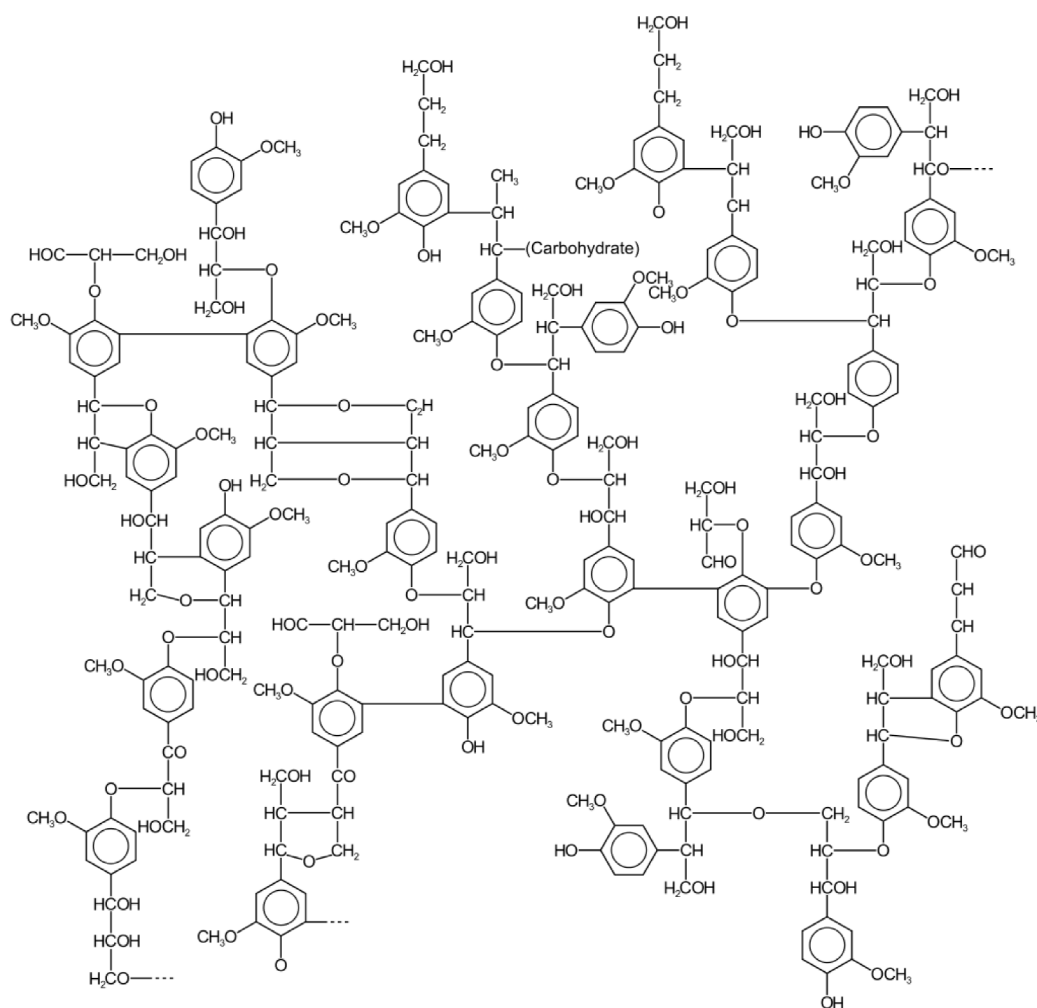


Figure 26: Possible structure of lignin [67].

Lignin formation results from two types of bonds, each of the sub-units association made a single lignin, [65], [66]:

-  $\beta$ -O-4 bond between G and G units and G and S units: “labile” bonds. These bonds are broken during Kraft process.

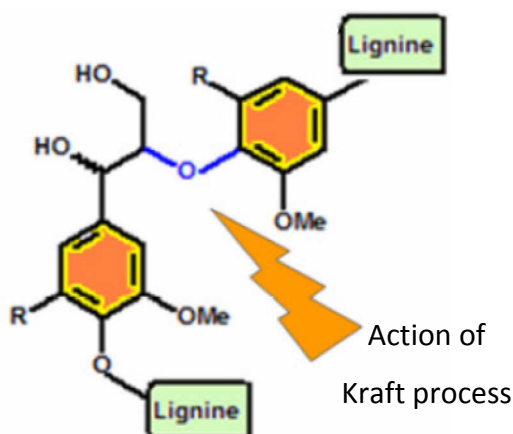


Figure 27: Labile bond of lignin: liaisons  $\beta$ -O-4.

-Biphenyl bond mainly between G and G units: « Strong » bonds

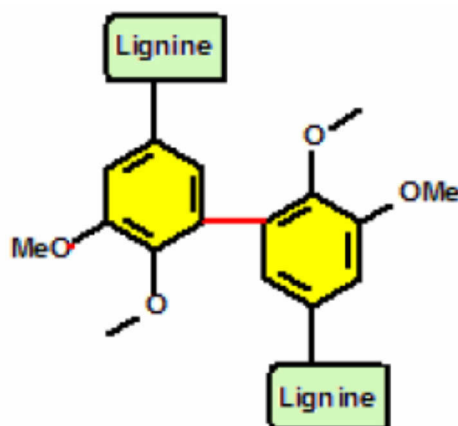


Figure 28: Strong bond of lignin.

Lignin in hardwood is mainly composed by G and S units while lignin in softwood, like maritime pine, is mainly composed by G units. Lignin reactivity (i.e. degradation) is due to its hydroxyl and ether functions.

During the cooking step,  $\beta$ -O-4 bonds are broken with the action of hydroxyl ions that reduce the molecular weight of molecules. The cleavage of ether bond with alkali releases

phenolate functional group in the reaction medium that improves lignin dissolving in the cooking juice (liquid phase). Thus reticulation reaction would be expected [68], then hydrosulphide ions react to form thiolignin or Kraft lignin as described in Figure 29.

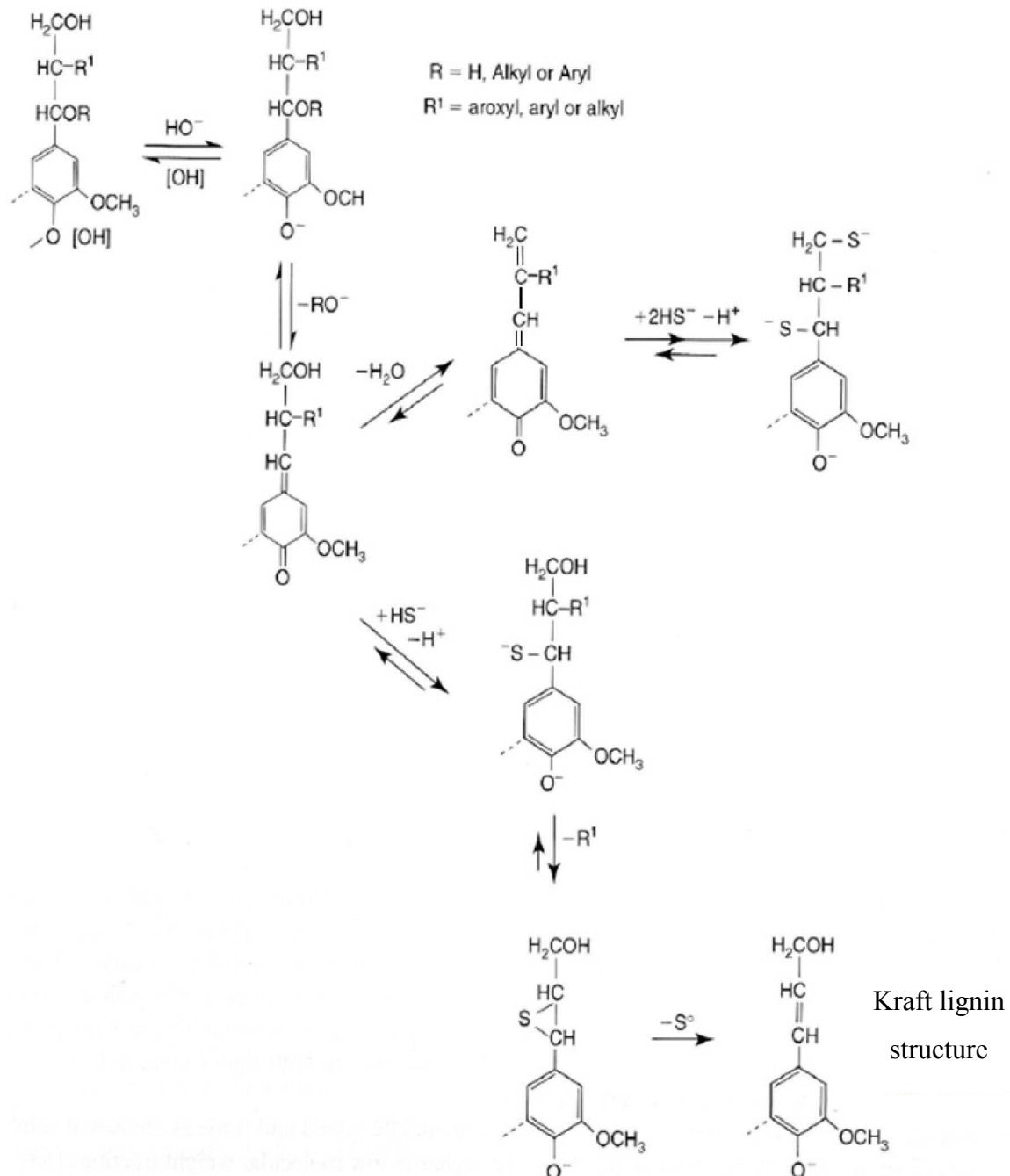


Figure 29: Lignin degradation mechanism during Kraft process (adapted from [68]).

Furthermore as cooking liquid of wood, black liquor content is a very complex mixture of organics and inorganics.

### II.1.3. Typical composition of black liquor

Black liquor is a highly alkaline solution with a very complex composition. It is a combustible, toxic and corrosive material. In addition to a substantial amount of water (~ 80%), following families of compounds have been identified:

- Inorganic compounds: Liquors circuit is closed in the Kraft process, so it is quite possible to find some unwanted inorganic compounds, moving along the recycling process. The main part of inorganic salts are sodium salts (NaOH, Na<sub>2</sub>S, Na<sub>2</sub>CO<sub>3</sub>, Na<sub>2</sub>SO<sub>4</sub>, NaCl, Na<sub>2</sub>S<sub>2</sub>O<sub>3</sub>, Na<sub>2</sub>SO<sub>3</sub>), a small amount is due to potassium salts contained in the raw wood and the other part corresponds to the calcium salts such as CaCO<sub>3</sub>. Some free ions are also identified: Na<sup>+</sup> and K<sup>+</sup>.

- Organic acids: They are the second largest family. They mainly come from the degradation of cellulose and hemicelluloses; and they are in ionic form. Most important acids are acetic acid and formic acid.

- Fatty acids and resin acids: they are the third largest family of compounds and are commonly called “tall oil” (II.1.4). The main part of the fatty acids (~ 95%) consists of oleic and linoleic acids. The distribution of the compounds in tall oil is:

- 45% of fatty acids
- 35% of resin acid
- 20% other acids not listed

- Carbohydrates: During wood cooking, a part of the cellulose and hemicellulose are degraded by the white liquor. This reaction is called "peeling-reaction" and produces hydroxy acid whose the main is glucose.

- Lignin: This is the major constituent of black liquor. In the Kraft process, lignin is called “Kraft lignin” or thiolignin. Lignin is a compound with high added value. Of all the components of the black liquor, lignin mainly provides organic matter, so it will be mostly from it that valuable molecules will be created.

- Methanol, produced by the demethylation of methoxyl groups in the lignin structure, is also identified in the composition of black liquor

In industry, black liquor is recovered and directly recycled, as described in the next section.



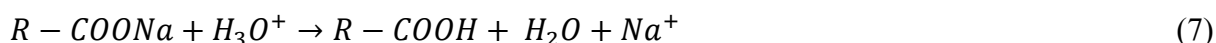
### II.1.4. Leaching step

Once the cooking is completed, the pulp (fibrous part) is separated from the cooking liquid by washing (leaching) and goes to paper process. The recovered juice contains Kraft lignin, depolymerized cellulose and hemicelluloses (hydrolyzed during cooking by hydroxide ions action), unused white liquor, minerals from wood. Its black color and its sweet appearance refers to the name of "black liquor".

In cooking step, approximately 160 million of tons of chemical pulp are produced per year and 50 million tons of lignin are dissolved and treated.

Leaching step is followed by the pre-evaporation to concentrate black liquor to 23 wt% of total dry matter. Then a first by-product, called also "soap", is extracted from this black liquor.

Soap is washed, acidified and then decanted to obtain tall oil [69]. Tall oil is currently the only valuable product recovered from black liquor. During the leaching step, soap is extracted from black liquor. It is then acidified with sulfuric acid to produce "crude tall oil":



Crude tall oil is mainly composed of: fatty acid (oleic acid, linoleic acid...), resin acid (abietic acid, pimaric acid) and unsaponifiables (hydrocarbons, sterols...)[69]. Unsaponifiables are not used in the industry so this part is considered as unwanted. The valuable components (green boxes in Figure 30) of crude tall oil are shown in Figure 30, the process is not detailed:

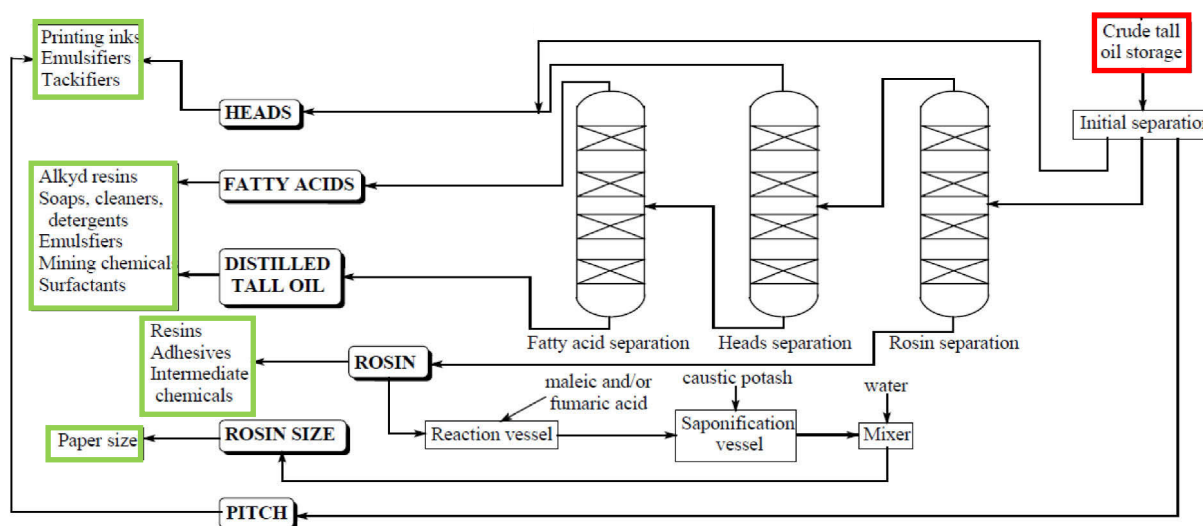


Figure 30: Tall oil process (extracted from [69]).

Actually, black liquor is directly recycled in the plant for white liquor and energy recovery. The steps and the technical issue encountered are detailed in the next section.

## II.2. Current valorization of black liquor

### II.2.1. Treatment of black liquor

Once soap extracted, the black liquor is processed in the plant following four steps (evaporation, combustion, causticizing and calcination) to convert it into white liquor.

#### *Evaporation*

Black liquor is industrially evaporated thanks to vapor at 0.3 MPa, in multiple effect and counter-current evaporators. The final outflow of black liquor is 70 wt% of dry matter. After evaporation, black liquor is stored and then burnt by combustion.

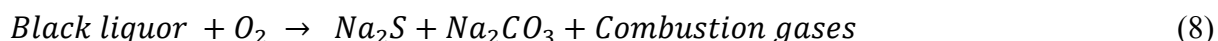
#### *Combustion*

The combustion of black liquor (70 wt%) is one of the most important process units. It allows recovering energy by burning the organic matter of the black liquor and simultaneously, to recycle the inorganic matter for the white liquor as melting salts.

It takes place in a specific reactor divided into three sections: reduction, drying and oxidation zones and detailed in figure 31.

In the boiler, black liquor (thick liquor) is sprayed into the secondary air. Organics are pyrolysed and pyrolysis products are oxidized in the oxidation zone by a tertiary air. Pyrolysis and combustion gases rise to the top of the boiler. The temperature is therefore higher on the top. All combustion gases are washed for environmental reasons and routed to the heat recovery steam generator. Produced steam is used subsequently in the plant for different steps.

The unbalanced equation for the combustion of black liquor may be written:



The combustion gases contain:  $N_2$ ,  $O_2$ ,  $NO_x$ ,  $CO_2$ ,  $H_2O$ ,  $SO_x$  and a low amount of  $CO$  and  $H_2S$ . The  $NO_x$ ,  $SO_x$  and  $H_2S$  contents are drastically reduced in the extracted gases after washing.

The inorganic compounds, in form of molten residue, fall to the bottom of the boiler, and are further processed as molten salts: mainly  $Na_2S$  and  $Na_2CO_3$  (saline).

Thus, the organic part of the black liquor generates steam by burning and 65 % of its energy is recovered.

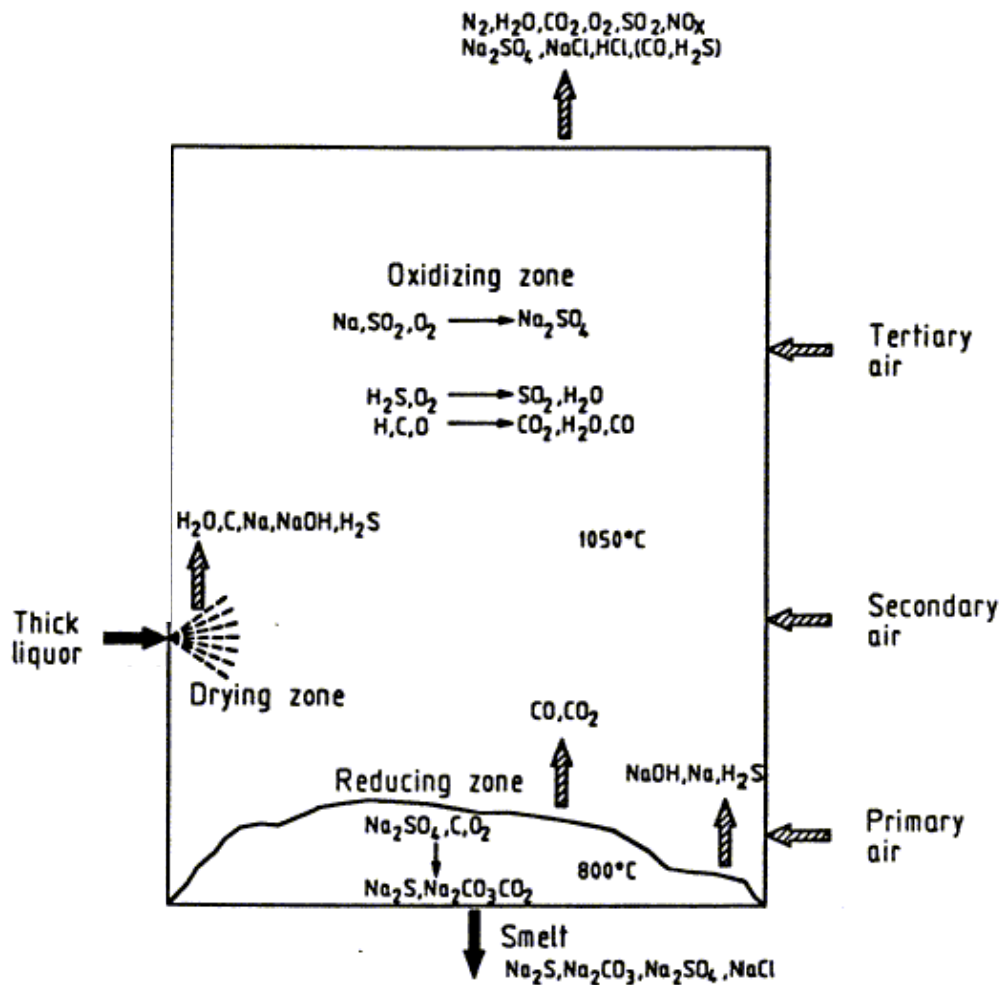


Figure 31: Reactions into black liquor boiler<sup>2</sup>.

The storage and combustion of the liquor is a bottleneck in the pulp production because of sprayed black liquor flow limitation. In addition, the combustion of the black liquor has numerous disadvantages such as:

- Size of elements and amount of fume treated
- Potential issue with operating equipment
- Environmental footprint ( $\text{CO}_2$ ,  $\text{NO}_x$ ,  $\text{SO}_x$ ...) and human risks (ATEX area)

<sup>2</sup> [http://www.ineris.fr/ippc/sites/default/interactive/brefpap/bref\\_pap/francais/bref\\_fr\\_kraft\\_niveau.htm](http://www.ineris.fr/ippc/sites/default/interactive/brefpap/bref_pap/francais/bref_fr_kraft_niveau.htm) (july 2014)

### Causticizing

After combustion, saline flow (melted salts, mainly  $\text{Na}_2\text{S}$  and  $\text{Na}_2\text{CO}_3$ ) is recovered and dissolved in water. This mixture, giving to the water a greenish color, is called "green liquor". The aim of causticizing step is to complete the regeneration of white liquor ( $\text{Na}_2\text{S}$  +  $\text{NaOH}$ ) from the saline flow as sodium sulphide ( $\text{Na}_2\text{S}$ ) is already in the desired form. Green liquor is transferred into causticizers where quick lime is added. Green liquor is transferred into causticizers where quick lime is added.

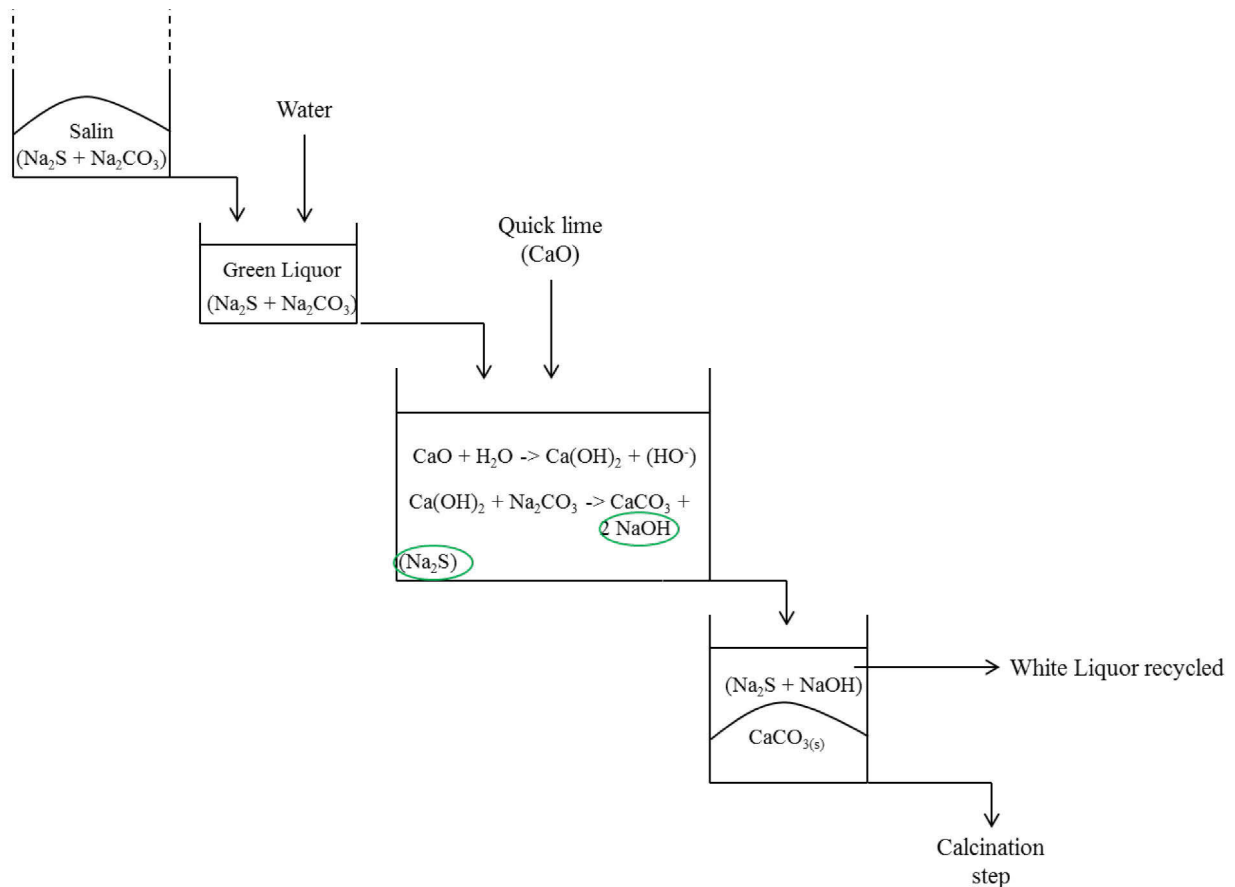


Figure 32: Causticizing step.

The reaction between quicklime ( $\text{CaO}$ ) and water of green liquor forms calcium hydroxide ( $\text{Ca(OH)}_2$ ) which reacts with sodium carbonate ( $\text{Na}_2\text{CO}_3$ ) to produce calcium carbonate ( $\text{CaCO}_3$ ) and to reform sodium hydroxide ( $\text{NaOH}$ ). The sodium hydroxide ( $\text{NaOH}$ ) and sodium sulphide ( $\text{Na}_2\text{S}$ ) are soluble (white liquor is recovered) in contrast to the calcium carbonate ( $\text{CaCO}_3$ ) which precipitate. In causticizers outlet, the solid-liquid mixture is transferred to a settling tank in order to separate white liquor from  $\text{CaCO}_3$  precipitate.

The recycled white liquor represents 97 % of the initial white liquor [70] introduced into the process for cooking step. Regarding the calcium carbonate slurries, they are conveyed to the final part of the recycling zone, namely calcination.

### *Calcination*

Calcium carbonate recovered by filtration is calcinated in a rotary kiln into lime (CaO) and CO<sub>2</sub> (9). The enthalpy of this reaction is equal to +1786 kJ/kg<sub>CaCO<sub>3</sub></sub> at normal temperature and pressure. Temperature of this step is around 850°C. The necessary energy is obtained from the gases of the combustion of black liquor.



Then lime obtained is reintroduced in the causticizing step while CO<sub>2</sub> is released to atmosphere. Gas flow, for this step, is about 1000 Nm<sup>3</sup>/ton of pulp and energy consumption is about 1.5 to 1.8 GJ/ton of pulp.

#### **II.2.2. Mass and heat balance**

Pulps production by Kraft process has a yield between 45 to 55 wt%. For each ton of pulp produced [70], about 10 tons of weak black liquor (15 wt %) is recovered; about 1.5 ton of black liquor dry matter is burned in the boiler to recover about 375 kg of cooking chemicals and to produce more than 5 tons of high pressure steam. During cooking step the ratio liquor/wood is between 3-5 L of white liquor/kg of wood chips [71].

Energy recovery comes from the boiler where organic content of black liquor is oxidized to produce steam at high pressure (11 bars). Then steam is partially used to generate electricity [70]. 13 000 to 15 000 kJ can be recovered per kg of black liquor. Typically, about 3.8 kg of steam/kg of dry black liquor are produced. The resulting high pressure steam goes through a turbine to generate electricity. The burning of 1500 tons of solid black liquor per day generates 25 to 35 MW of electricity [70].

### **II.3. Industrial issue**

Despite Kraft process provides optimization (white liquor recycling, heat recovery, added-value products valorization), but many industrial issues can occur and decrease its efficiency. This aspect is detailed in annex 1.

#### **II.3.1. Technical and technological issues**

Technical and technological issues [70] concern both mechanical and process problems mainly due to black and white liquors composition. Each unit of the process, presented previously, is the seat of potential problems such as fouling, tube corrosion, leakage, cracking. These issues lead to higher energy demand and lower efficiency of the process. They are associated to gases emissions.

### **II.3.2. Environmental issue**

Considering black liquor composition, gases emissions are mostly due to sulfur emissions as methyl mercaptans, dimethyl disulfide, sulfur dioxide, and above all hydrogen sulfide which is very toxic. However, H<sub>2</sub>S is not considered has a main issue, it is used for white liquor recycling.

NO<sub>x</sub>, particles and CO<sub>2</sub> emissions from the process contributes also to its whole environmental impact. CO<sub>2</sub> emissions come from the combustion of organics in black liquor. The non-valorization of this organic carbon into useful material is a problem for the paper industry.

### **II.4. Conclusion**

Black liquor has a high organic and inorganic content. Its recycling is a looped industrial process, based on the burning of the organic matter and inorganic recycling. Throughout this process, the added-value products extracted are the tall oil, the white liquor and the heat recovered for production process uses. Kraft process has the ability to handle both softwood and hardwood, and to recover almost 97% of white liquor. However, compositions of black and white liquors lead to technical and technological issues. With environmental restrictions, significant improvements have been made to respect air emissions, effluent discharge [70], noise, etc. Figure 33 shows a synthesis of it flowsheet.

In addition to the cost, operational problems and environmental issues, some disadvantages of Kraft process push the paper industry to look for new technologies:

- Evaporation steps need a high amount of energy; it is the area with the highest energy demand.

- On the one hand, to respect the environmental standards boiler limits the flow rate of incoming black liquor, and on the other hand, to respect the imposed flow of pulp paper for paper production, black liquor could necessarily stored after evaporation.

In reason of its high organic, inorganic and water content, black liquor is a good subject for hydrothermal conversion study. In reason of its alkalinity and its lignin contents, black liquor could have a high potential of alternative valorization as currently. The following section is devoted to the state of art of hydrothermal conversion of black liquor and its model compounds.

Green is used for advantages and red is used for drawbacks of Kraft process.

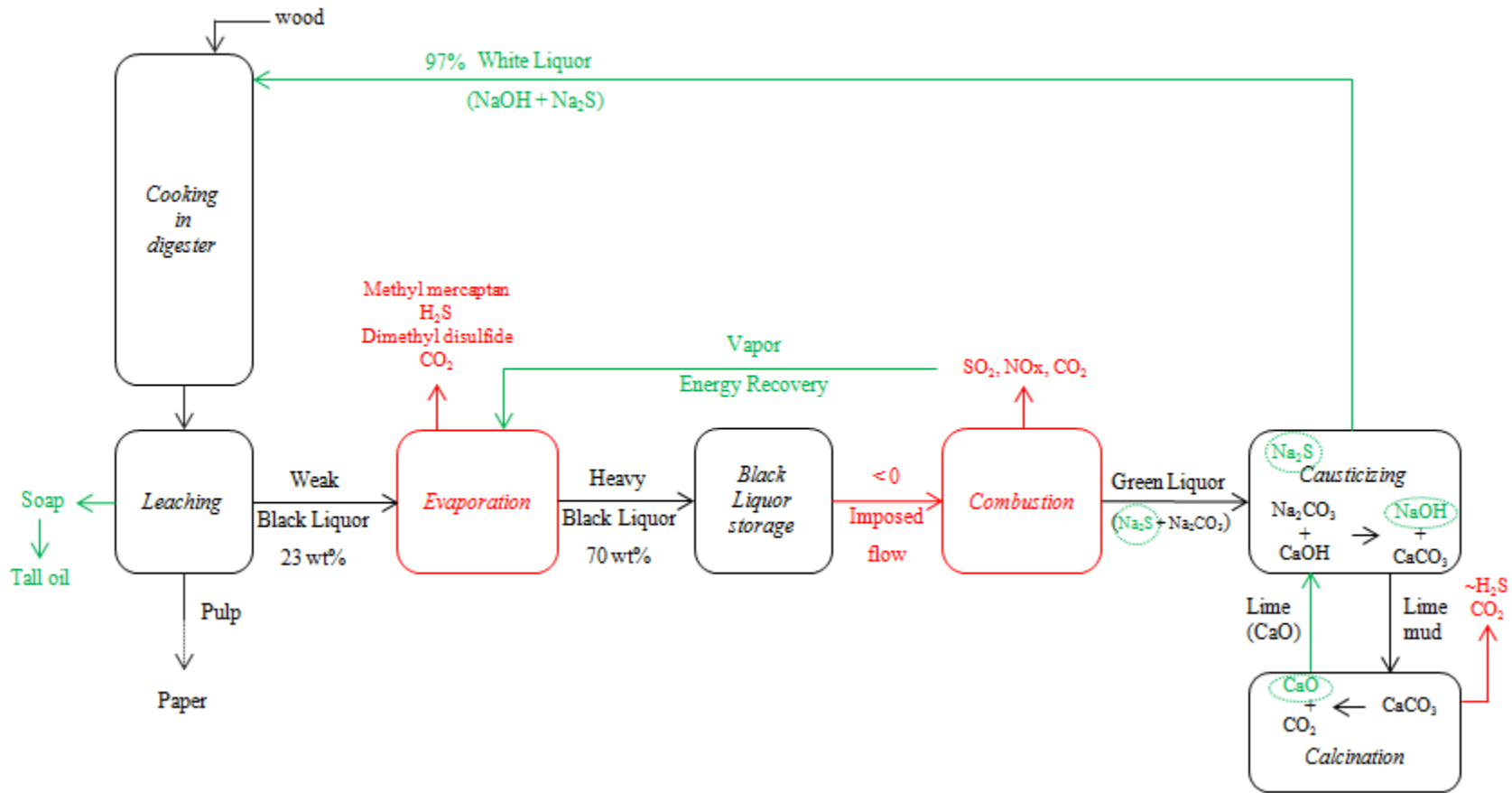


Figure 33: Synthesis of black liquor treatment in paper industry.

## II.5. State-of-the-art on hydrothermal conversion of black liquor and its associated model compounds

In contrast to model molecules, a real waste has a complex composition which is not exactly known. Literature shows a lack of knowledge considering the industrial black liquor hydrothermal conversion. Oxidation and gasification of black liquor have been studied [53], [72]. However, composition varies from the different authors as well as the process design. It was noticed that Kang et al. [73] studied the hydrothermal carbonization of black liquor powder (acidified black liquor), coming from a chemical industry. They suggested that the carbonization of dried black liquor is due to either the polymerization of aldehyde with powder of black liquor non dissolved or phenolic compounds. However, no significant contributions of raw liquid black liquor liquefaction or carbonization have been yet published.

On the contrary, numerous research teams work on hydrothermal conversion of model compounds, with and without oxidant or catalyst, and suggest reaction pathways [74], [75] which will be used as baseline of reasoning. Thus, a first state to understand the hydrothermal conversion of black liquor is to consider its associated model molecules. It means lignins such as alkali lignin, organosolv lignin and others types of lignin. However, hydrothermal conversion of model lignins is also too complicated. Thus smaller model molecules of lignins such as guaiacol (Figure 34), catechol (Figure 35), guaiacylglycerol- $\beta$ -guaiacyl ether known as GGGE (Figure 36) are needed.

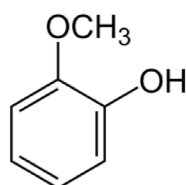


Figure 34: Guaiacol formula.

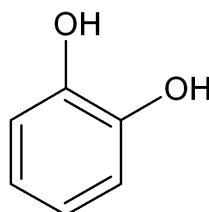


Figure 35: Catechol formula.



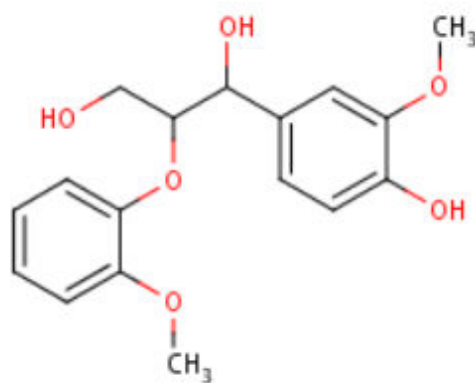


Figure 36: GGGE formula.

The best way to understand the hydrothermal conversion of black liquor is to consider hydrothermal conversion of lignin and its smallest model molecules.

### II.5.1. Model compounds: mechanism of hydrothermal treatment

Kang et al. ([76]), suggested reactions pathways for hydrothermal liquefaction and gasification of lignin, as follow:

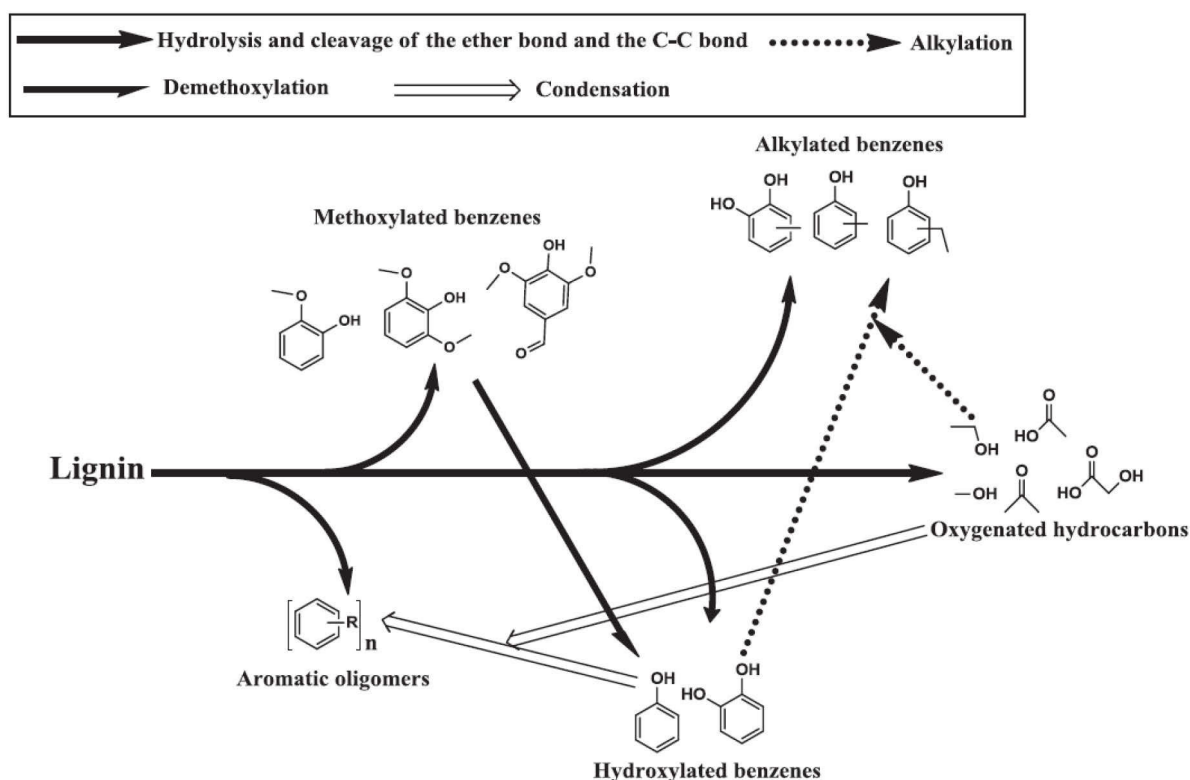


Figure 37: Mechanisms suggested by Kang et al. for the hydrothermal liquefaction of lignin [76].

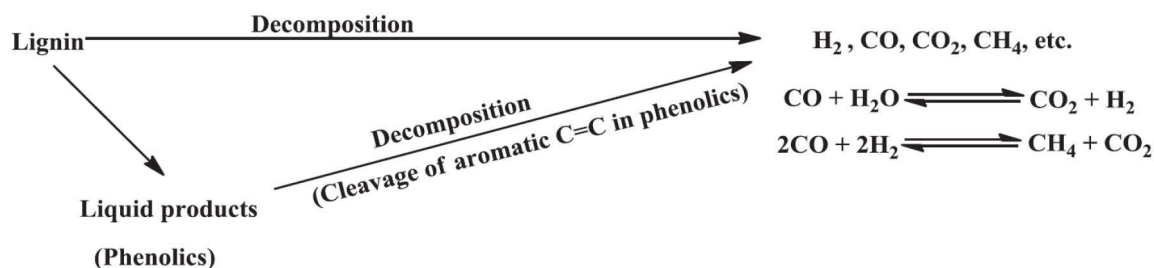


Figure 38: Reactions pathways suggested by Kang et al. for the hydrothermal gasification of lignin [76].

Liquefaction and gasification have been performed at various temperature conditions. Probably, aromatics and others smaller molecules produced by liquefaction should be converted to gas at higher temperature.

Fang et al. [23] suggest the following reaction pathways for hydrothermal conversion of lignin:

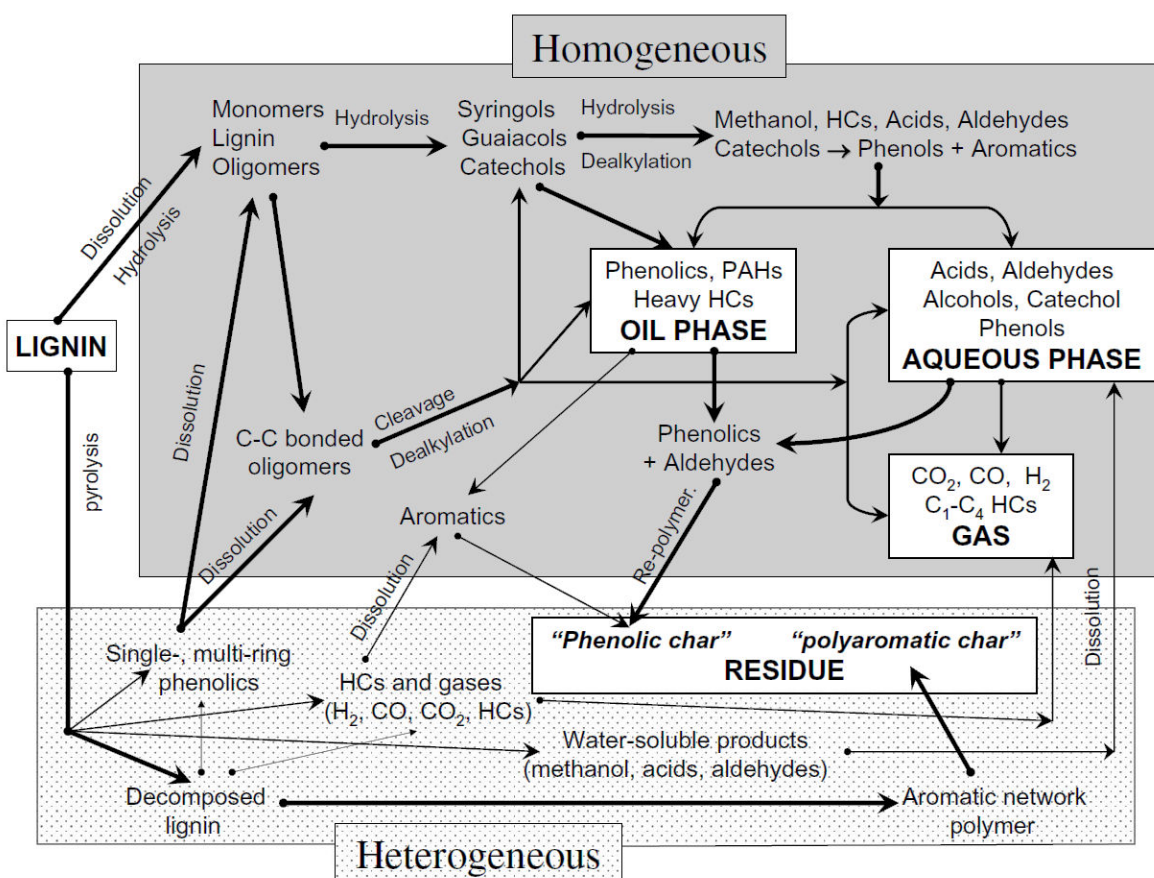


Figure 39: Reactions paths for hydrothermal conversion of lignin suggested by Fang et al. ([23]).

As shown by Fang et al., hydrothermal conversion of lignin model compound is extremely complex. A plurality of typical reactions intermediates has been identified. After reaction, at normal conditions, three phases are expected as gas phase, solid phase and liquid phase (divided into aqueous and oily phases), each one resulting of series of reactions.

The main products obtained by the degradation of black liquor model compounds (lignin, alkali lignin, guaiacol, GGGE...) are referenced in the Table 1 and confirm the mechanism pathways of degradation seen previously (Figures 37, 38 and 39). Even if different lignins exist (organosolv, Kraft...), they are usually used to recover phenolic compounds in liquid phase. Some studies (Table 2) show a catalytic effect of alkali salts on specific reactions, and the formation of solid residue by repolymerization. In these papers, incoming lignin is solid and mixed with a solvent; products recovered are mainly in liquid phase. In the following table, “HT” means “hydrothermal”, “HTC” means hydrothermal conversion and “A-L” means “Alkali Lignin”.

Table 2: Main products expected by conversion of black liquor model compounds

Ref	Process/ incoming material	Reactor type	Products	Objectives	Comments
Peng et al. [77]	Pyrolysis/ Lignin	Fixed bed reactor	Phenolic molecules	Material	- Alkaline additive promote the degradation of decarboxylation and decarbonylation. – Removal of unsaturated alkyl branch
Gosselink et al. [78]	SCF/ Lignin	Batch	Aromatic molecules	Material	CO <sub>2</sub> /acetone/H <sub>2</sub> O
Kang et al. [76]	Wet oxidation/ Lignin	Batch	Aromatics aldehydes	Material	Ether bond cleavage and oxidation on $\alpha$ -carbon during conversion
	HT gasification/ Lignin	Batch	Fuel Gas	Energy	Cleavage of bonds: Ether, aliphatic C-C, aliphatic C=C, fragmentation reaction; interaction between gas formed and liquid products
Azadi et al. [57]	HT liquefaction/ Lignin	Batch	-Phenolic molecules -Bio-oil	- Material -Energy	Cleavage of bonds: ether, aliphatic C-C; reactions of demethoxylation, alkylation
Okuda et al. [74]	HT liquefaction/ Guaiacol, GGGE	Batch	Phenolic molecules	Material	Solvent: water/p-cresol Less coke formed
Okuda et al. [58]	HT liquefaction/ Lignin	Batch	Phenolic molecules	Material	Solvent: water/ Phenol - the presence of phenol inhibits coke formation (=solid residue)
Pinkowska et al. [79]	HT liquefaction/ AL	batch	Phenolic molecules	Material	Cleavage of C-O bond and C-C bond
	HT carbonization/ AL	Batch	Biochar	Material	Repolymerization of liquid products and formation of solid residue
Guo et al. [80]	Pyrolysis/ Gasification	Batch	Biofuel Chemicals	Energy Material	Catalytic action of NaOH and Na <sub>2</sub> CO <sub>3</sub> on gasification and pyrolysis reactions
Guo et al. [81]	HT Gasification/ AL	Batch	Gas		Catalytic effects of existing form of Na: Organic bound Na or inorganic bound Na => organic Na improve amount of H <sub>2</sub>

Addition of alkali salts promotes degradation forming especially H<sub>2</sub>; reactions favored are decarboxylation and decarbonylation. Degradation of lignin leads to aromatic phenolic compounds in liquid phase by cleavage of bonds (ether, C-C, C-O...), these molecules polymerize easily forming a solid residue. Similar products would be expected after hydrothermal conversion of black liquor despites its complexity.

## II.5.2. Hydrothermal treatment of Black Liquor conversion

A similar table (Table 3) presents an overview of the processes used for black liquor treatment.

Table 3: Principal products expected by black liquor (BL) conversion

Ref	Process/ incoming	Reactor type	Products	Objectives	Comments
<b>Sricharoen- chaikul [82]</b>	Gasification/ BL	Continuous reactor	H <sub>2</sub> , CO, CO <sub>2</sub> , low hydrocarbons	Energy	-When black liquor is diluted, the conversion rate is higher -The amount of H <sub>2</sub> is high and the amount of CO <sub>2</sub> is low -catalytic effects of salts -at 400°C (40% of H <sub>2</sub> ) and at 600°C (60% of H <sub>2</sub> )
<b>Cao et al. [53]</b>	Gasification/ BL	Continuous reactor	H <sub>2</sub> , CO, CO <sub>2</sub> , low hydrocarbons	Energy	-salts precipitation in reactor (redissolution at ~360°C) -pH of liquid product is lower than incoming black liquor
<b>Naqvi et al. [83]</b>	Gasification/ dry BL	Fluidized bed	H <sub>2</sub> , CO, CO <sub>2</sub> , low hydrocarbons	Energy	Comparison between air or oxygen supply => higher synthetic natural gas with O <sub>2</sub> supply
<b>Nong et al. [84]</b>	Gasification/ BL	Gas turbine	H <sub>2</sub> S, CH <sub>4</sub>	Matter	Kinetics of reaction between (CH <sub>3</sub> ) <sub>2</sub> S and H <sub>2</sub> with ZnO => H <sub>2</sub> S is absorbed by alkali solution
<b>Kang et al. [73]</b>	HT carbonization/ BL	batch	Solid fuel	Energy	Formaldehyde use to polymerize phenols compounds
<b>Wiinikka et al. [85]</b>	Gasification/ BL	gasifier		Energy	Cooling has effect on gas composition => low cooling rate: higher amount of H <sub>2</sub> and lower amount of CO <sub>2</sub>
<b>Haggstrom et al. [86]</b>	Gasification/ BL	Combined process	Methanol from syngas	Matter	Use of syngas to produce methanol by catalytic synthesis
<b>Xiao et al. [87]</b>	Pyrolysis/ BL	Gas turbine	Pyrolysis and sulfide gases	Gas treatment	Gaseous sulfides are produced from black liquor pyrolysis
<b>Zhao et al.[88]</b>	Carbonization	Batch	Solid	Energy or matter	polymerization of aldehyde with BL non dissolved or products of HTC

Black liquor could be used particularly to produce gas by supercritical water gasification, with a low amount of CO<sub>2</sub> and hydrocarbons, and an interesting amount of H<sub>2</sub>; sulfur is also noticed in the gas phase as H<sub>2</sub>S. Comparing processes, hydrogen production is higher with supercritical water gasification than regular gasification. Solid formed from the

conversion is due to the polymerization of phenolic compounds with aldehydes. Gasification has been studied in continuous and batch reactors while carbonization has been studied exclusively in batch reactor. Hydrothermal liquefaction of black liquor is not particularly investigated.

### **III. Objectives of the thesis**

As mentioned in the introduction, the main objective of my thesis is to better understand the hydrothermal processes from the point of view of the reaction mechanism and from the point of view of process with the following focus:

- Problem of solid formation: mechanism of its formation
- Hydrogen production with a focus on catalytic conversion: impact of the catalyst on the different reactions
- Batch versus continuous reactor: by fast heating and cooling rate, batch process approaches continuous process.



## Chapter 2: Materials & Methods

---





## **Résumé du chapitre 2 : Matériel & Méthodes**

Dans ce chapitre les procédures expérimentales sont décrites ainsi que les entrants, les réacteurs batchs utilisés et les techniques d'analyse employées pour caractériser les phases obtenues après réaction (après ouverture du réacteur). Ce chapitre se divise en 3 parties.

### Les entrants :

La liqueur noire est une solution aqueuse basique, corrosive et toxique pour l'environnement, elle contient 23 % massique de matière sèche dont 7% de matière inorganique et 16% de matière organique. Elle est considérée comme un sous produit de l'industrie papetière et non comme un déchet ; pour nous elle est considérée comme une biomasse humide à haute teneur en matières organique et inorganique. Elle nous est fournie directement par le papetier après récupération du tall oil (unique valorisation matière de la liqueur noire dans le procédé Kraft). Afin de constituer les solutions qui nous serviront lors de nos expériences, nous mélangeons de l'eau pure à cette liqueur noire afin d'obtenir des solutions à 10 % massique en liqueur noire. Pour les expériences réalisées dans le cadre de l'étude catalytique relatée dans le chapitre 5, de l'oxyde de cérium ( $\text{CeO}_2$ ) est utilisé en tant que nanocatalyseur. Ce catalyseur est de structure cubique et tient son action catalytique de son activité redox qui lui permet de capter et relâcher l'oxygène des molécules d'eau présentes. Cette action sera décrite plus en détails dans le chapitre consacré à cette étude (chapitre 5). L'oxyde de cérium cubique est synthétisé au sein du laboratoire du Professeur Adschiri, à l'université de Tohoku au Japon. L'utilisation de ce nanocatalyseur a également été mise en œuvre au sein du laboratoire du professeur Adschiri.

### Les réacteurs :

Dans cette thèse les réacteurs utilisés sont des réacteurs batchs exclusivement. Trois réacteurs différents ont été utilisés : 2 réacteurs de 5 mL et 1 réacteur de 500 mL. Ils diffèrent principalement par leur système de chauffe. Toute la partie 2 de ce chapitre est consacrée à leur description, le tableau 4 compare les conditions de fonctionnement de ces réacteurs.

### Les sortants : caractérisations des phases obtenues après réaction.

Après réaction, les réacteurs sont refroidis puis ouverts. Trois phases sont généralement obtenues : une phase gazeuse, une phase liquide et une phase solide. Chaque phase est récupérée et analysée.

La quantité de la phase gazeuse est mesurée puis les composés sont quantifiés par  $\mu$ -GC. La phase liquide est analysée au travers de la mesure de paramètres globaux COT (carbone organique total), DCO (demande chimique en oxygène), GPC chromatographie de perméation de gaz), mais aussi en identifiant et quantifiant des composés organiques (formaldéhyde, phénols, GC-MS pour identifications plus précises) et minéraux (ICP-OES). La phase solide est analysée d'un point de vue de sa composition (analyse élémentaire, thermogravimétrie, cristallographie, fonctions chimiques par IRTF et spectroscopie RAMAN) mais aussi de sa morphologie, sa texture et de ses propriétés de surface (MEBE, BET, Pycnomètre, granulométrie laser et MET).

Toutes ces analyses nous permettent de caractériser autant que possible les phases afin de comprendre les réactions mises en jeu lors de la conversion hydrothermale.

**\*\*\* Fin du résumé**

In this chapter experimental procedures are described as well as reactors, raw materials and outflow characterizations.

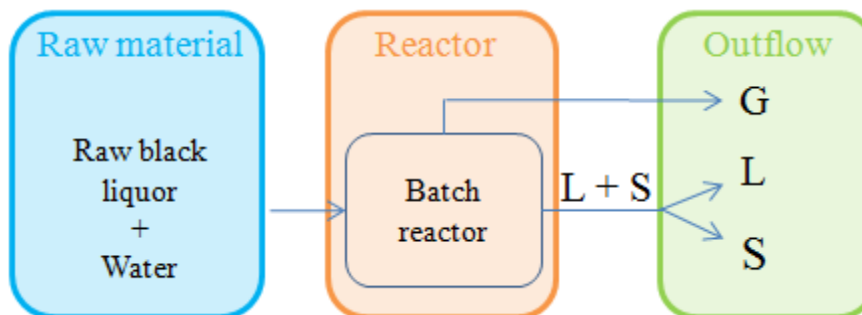


Figure 40: Experimental procedures for hydrothermal conversion of black liquor.

In the previous chapter, properties of supercritical water and general presentation of black liquor have been introduced. The first part of this chapter is devoted to the characterization of our black liquor.

The second part of the chapter presents the description of the three kinds of batch reactors used. They differ in their volume, shape and processing.

The third part of the chapter inventories the characterizations of the outflowing phases. Some of them have been carried out in RAPSODEE Center and other in Professor's Adschiri and Watanabe laboratories, at the Tohoku University, Sendai, Japan. Therefore, the Japanese laboratories will be mentioned when necessary.

## I. Raw material:

### I.1. Black liquor

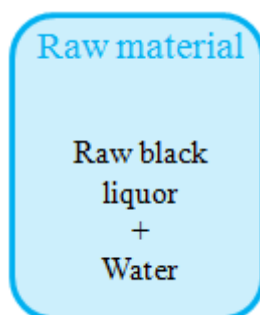


Figure 41: Reagents in hydrothermal process.

Black liquor is used as such, obtained after tall oil recovering, and pure water are introduced to obtain a 10 wt% black liquor solution.

To understand and explain as well as possible reactions that occur during the hydrothermal conversion, the most complete possible characterization of the black liquor is required. A typical composition of black liquor has been given by the industrial furnisher Smurfit Kappa, Cellulose du Pin (paper plant) and is reported hereafter:

<b>pH</b>		<b>13.2</b>
<b>Dry matter</b>		<b>23 wt. %</b>
Organic content		16 wt. %
Inorganic content		7 wt. %

Sodium	Na	19.2 wt. %
Potassium	K	13.8 wt. %
Sulfur	S	3.4 wt. %
Carbonates	CO <sub>3</sub> <sup>2-</sup>	5.7 wt. %
Sulfate	SO <sub>4</sub> <sup>2-</sup>	1.1 wt. %
Sulfide	S <sup>2-</sup>	2.3 wt. %
Residual alkali	NaOH	5.2 wt. %

Lignin content	36.2 wt. %
Polysaccharides	2.5 wt. %
Sum of hydroxy acids	73.0 g/kg
Acetic acid	19.0 g/kg
Formic acid	21.0 g/kg

Figure 42: Black liquor composition given by Smurfit Kappa cellulose du Pin, France.

This analysis confirms that black liquor is a complex mixture, highly charged in organic and inorganic matter. Black liquor is an alkaline aqueous media (pH = 13.2) containing 23 wt% of dry matter, with a density of 1.12 kg.L<sup>-1</sup>. The ratio inorganic/organic content is equal to 0.44; this ratio means that inorganic and organic represent respectively 30 wt% and 70 wt% of the dry matter. The proportion of lignin in the black liquor is ~36 wt %; being considered as the main part of its organic content. RMN analysis confirms that aliphatic and phenolic compounds exist in black liquor.

Details about the procedures used to characterize the black liquor are presented in the section III.

Considering CHNOS elemental analysis (RAPSODEE), the black liquor has the following composition: C (22.50 wt%), H (5.30 wt%), N (0.14 wt%), O (37.34 wt%), S (2.50 wt%). Looking at the composition given by Smurfit Kappa, the remaining percentages are mostly due to sodium, Na. Thus, by difference the amount of sodium is calculated (10):

$$\%_{Na} = 100 \% - \sum_i^{C,H,N,O,S} \%_i = 32.22 \text{ wt}\% \quad (10)$$

Converted in atomic percentage, the composition is: C (17%), H (48%), N (0%), O (21%), S (0.7%), Na (15%).

For the experiences, raw black liquor has been diluted to obtain a solution at 10 wt% of black liquor. Its carbon repartition into organic and inorganic carbon, obtained by total organic carbon measurements, gives: 10.7 g.L<sup>-1</sup> of organic carbon and 0.6 g.L<sup>-1</sup> of inorganic carbon. However, the organic matter contains only 0.104 g.L<sup>-1</sup> of phenolic compounds and 0.0557 g.L<sup>-1</sup> of formaldehyde. The chemical oxygen demand of black liquor is 20.75 g.L<sup>-1</sup>.

## **I.2. Cerium oxide**

We used in some experiments a specific nano catalyst, the CeO<sub>2</sub>. It is synthesized in Professor's Adschiri laboratory by hydrothermal synthesis and provided for our experiments by his research team. After reaction, solid phase (coke and catalyst) are recovered by filtration and dried at 60°C under vacuum. Then solid is weighted and calcinated at 450°C to remove coke and to recover CeO<sub>2</sub> catalyst.

## **II. Reactors**

Hydrothermal conversion has been carried out using several kind of batch reactors which are described in this part.

### **II.1. Batch reactors used for experiments**

A part of this PhD has been made in France at RAPSODEE center, the other one has been made in Japan in Professor Adschiri's Laboratory, Tohoku University. Reactors used for hydrothermal conversion are different in volume and design. Three different kinds of reactors have been used, two in France (5 and 500 mL) and one in Japan (5 mL).

#### **II.1.1. 5 mL batch reactor – RAPSODEE center**

We dispose of a serie of 30 industrial minireactor (5 mL). The 5 mL reactor allows reaching a couple (T, P) of (600°C, 30 MPa). Each mini-autoclave (Figure 43) is a hollow cylinder made of stainless steel (316 Ti). The reactor consists of two parts: a body and a cap. They are screwed together and the sealing is maintained with a joint in copper between the two parts. The inner volume is 5 mL and a hole has been made to release the gas during the opening procedure of the reactor (Figure 44). This reactor is unstirred and the direct monitoring of

temperature and pressure is impossible. Pressure is induced by the volume of solution initially introduced (II.2).

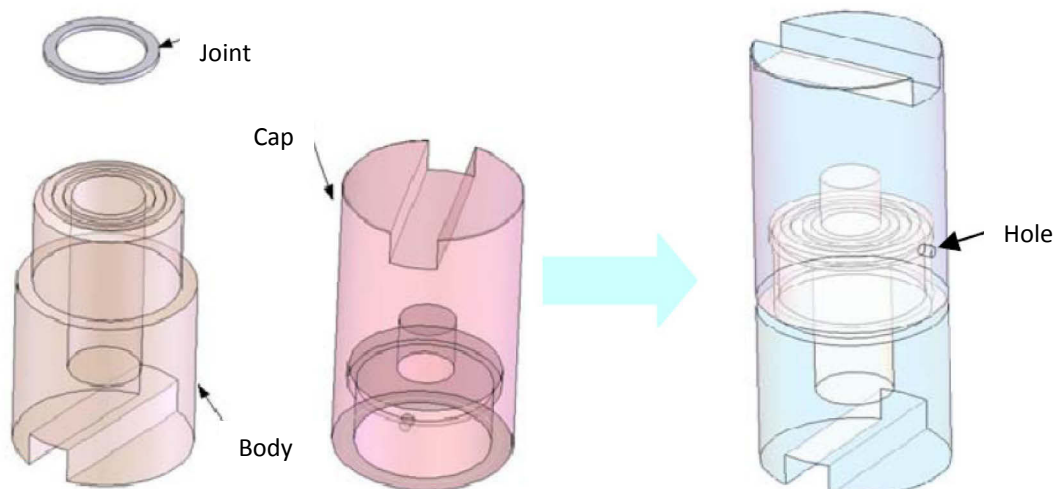


Figure 43: 5 mL batch reactor: mini-autoclave.

Once the autoclave is closed, the system is placed in the opening-closing system (Figure 44).

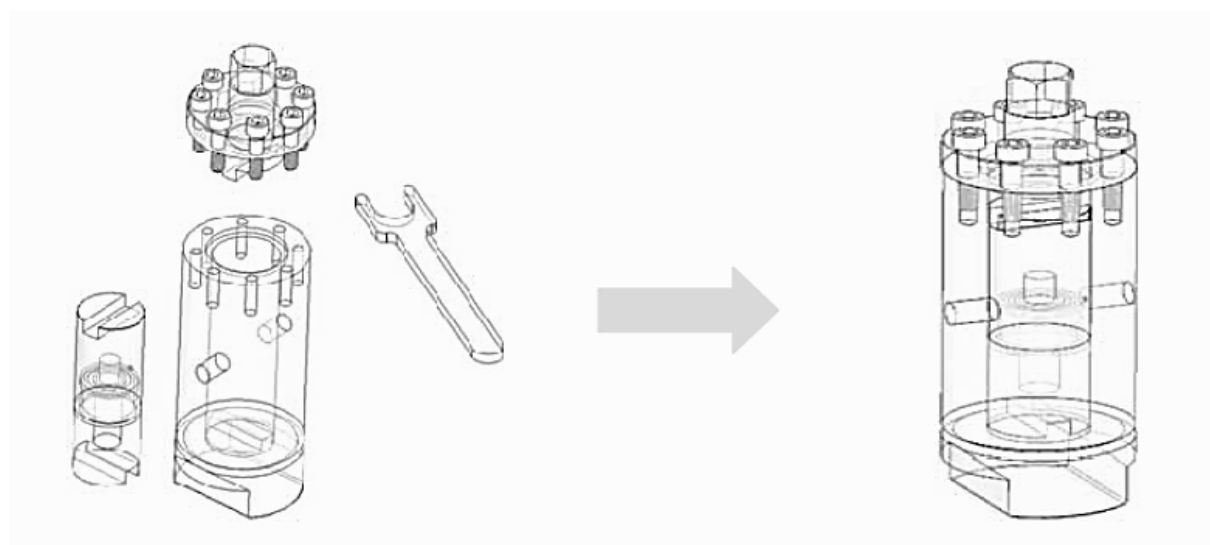


Figure 44: Opening / closing apparatus.

The clamping is operated by applying a torque of 100 Nm to ensure pressure resistance. Then, the hermetically sealed autoclaves are placed in an oven (external heating). Two ovens have been used, the first one is Nabertherm L5/11/P320 oven with a heating rate of  $20^{\circ}\text{C}\cdot\text{min}^{-1}$ , the second one is a gas chromatography oven with a heating rate of  $40^{\circ}\text{C}\cdot\text{min}^{-1}$ .

When the target temperature in the oven is reached, reaction time started. At the end of the desired reaction time, reactors are removed from the oven and cooled down.

Two cooling methods have been applied. The first one is a slow cooling: at the end of reaction time, warm reactors are cooled under air circulation to bring them to ambient temperature. For this method, cooling time is around 30 min.

The second method is a quenching cooling: at the end of experiments, warm reactors are placed in a bath of ice and water to bring them to ambient conditions. For this method, cooling time is less than one minute and it could be considered as “instantaneous”.

Reactors, at ambient temperature, are opened. The opening system is linked to a sampling system to collect gases (Figure 45).

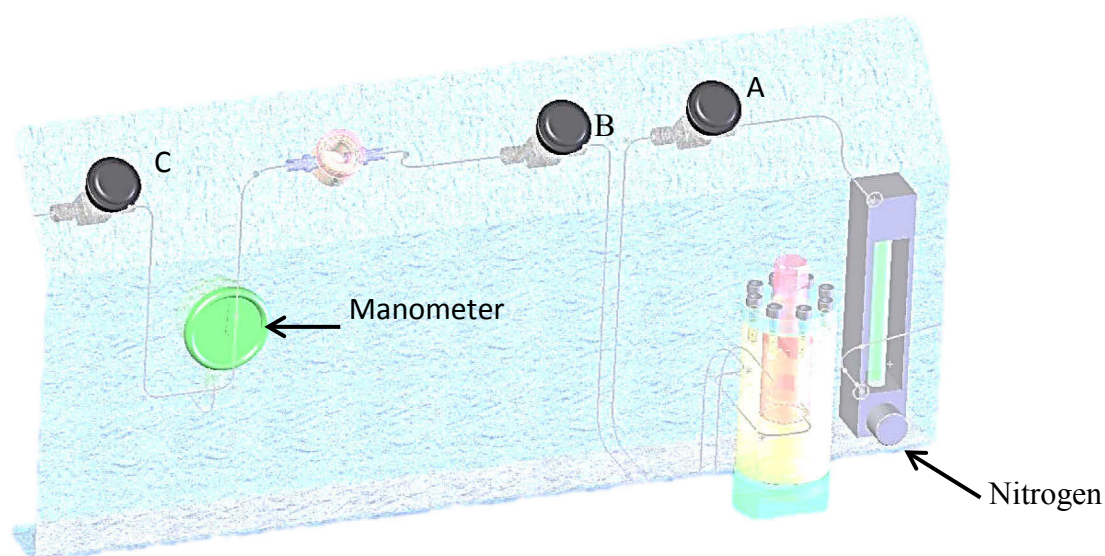


Figure 45: Sampling for collect gas for 5 mL batch reactor.

The autoclave is placed into the system, at room temperature, and covered by a cap to seal the opening-closing system. The system is closed, and regulated by valves (A, B and C);  $N_2$  is then injected in continuous through the system to eliminate the air contained in the tubes, ( $P_{N_2 system} \approx P_{atm}$ ). For gas sampling, valves are closed and reactor is then opened; gas escapes through the hole in the cap of the reactor (Figure 42). Gas generates an overpressure  $P_s$ , measured by the manometer (2.5 MPa – WIKA EN 837-1) after the opening of the autoclave. Taking into account the loop volume ( $V_{mini}^0 = 29.32 \text{ mL}$ ) in which the gas has spread [51], the total moles of gas is calculated. The gas sampling system is flushed with  $N_2$  and gas collected in a sampling bag to be analyzed using the overpressure and volume of the system as follows. The volume of liquid ( $V_{autoclave}^{liq}$ ) is assumed to be constant before and after the reaction since the water is in large excess relatively to the biomass.  $V_{autoclave}^{empty}$  is the unoccupied inner volume of the reactor with:



$$V_{autoclave}^{in} = V_{autoclave}^{liq} + V_{autoclave}^{empty}$$

Equation 11: Volumes considered in the reactor

$$n = n_{total}^{gas} - n_{system}^{N_2} - n_{autoclave}^{N_2}$$

Equation 12: Calculation of the number of moles of gas produced

With:

$$n_{total}^{gas} = \frac{(V_{mini}^0 + V_{autoclave}^{empty}) \times (P_{atm} + P_S)}{R \times T}$$

Equation 13: Calculation of the number of total moles in the gas

$$n_{system}^{N_2} = \frac{V_{mini}^0 \times P_{system}^{N_2}}{R \times T}$$

Equation 14: Calculation of the number of moles of  $N_2$  in the system

$$n_{system}^{N_2} = \frac{V_{autoclave}^{empty} \times X_{air}^{N_2} \times P_{atm}}{R \times T}$$

Equation 15: Calculation of the number of moles of  $N_2$  in the system

### II.1.2. 5 mL batch reactor – Professor ADSCHIRI’s laboratory

At Tohoku University, another serie of 5 mL batch reactor has been used to performed experiments. These reactors allow a couple (T, P) of (500°C, 30 MPa). They are non stirred; pressure and temperature are neither monitored. Pressure is induced by initial volume of black liquor and temperature indication (external temperature) is given by the oven. However, in the Japanese laboratory, heating system is different; reactors are heated thanks to heating blocks as described in Figure 46.

Reactors used in Japan are slipped inside the heating block with a quasi “instantaneous” heating of the media.

Reactors were cooled by quenching in a mixture of ice and water as quenching fluid (temperature 0°C).

The opening system is similar to the system used at RAPSODEE Center, without manometer neither system to collect gas. Therefore, the volume of gas produced cannot be directly known. For that, a specific cap is placed on the top of the reactor to connect it directly to the gas analyzer ( $\mu$ -GC). Thus, thanks to a calibration curve the volume of gas can be known; in addition to obtain the gas composition.

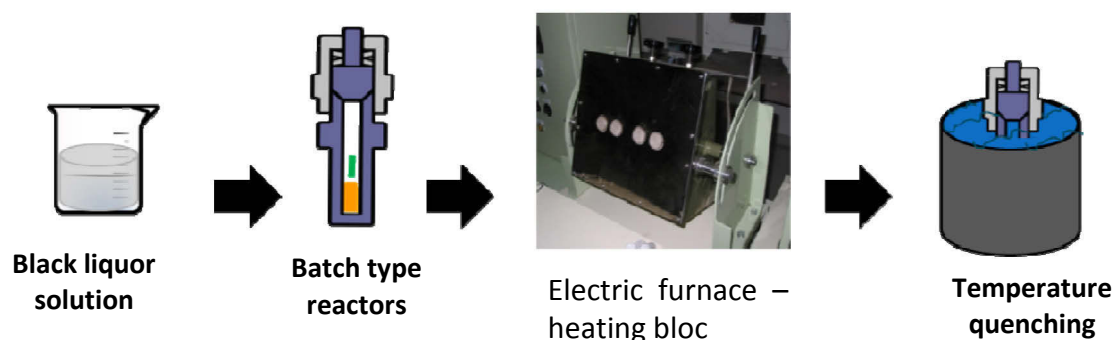


Figure 46: 5 mL batch reactor (Adschiri Laboratory).

### II.1.3. 500 mL batch reactor – RAPSODEE center

This reactor has been used a couple of times to study the influence of temperature rate on hydrothermal conversion. The 500 mL reactor, Figure 47, allows reaching a couple (T, P) of (500°C, 30 MPa). The specific volume is equal to 553 mL. Reaction pressure is induced by the initial volume of black liquor solution and the controlled temperature in the reactor. The system is monitored by a control unit which regulates and displays the stirring rate, temperature and pressure during the experiment.

The reactor consists of a stainless steel body with an inner diameter of 6.5 cm and a jacket made in Inconel 718 where a stainless steel beaker (316 Ti) is placed to prevent the corrosion and holds the pressure. The thickness of the beaker is 1 mm. The thickness of the jacket is 6 mm and allows on the one hand resisting to corrosion of supercritical water and on the other hand improving the heat transfer (316 Ti thermal conductivity at 500°C is 21.4 W.m<sup>-1</sup>.K<sup>-1</sup> and Inconel 718 at 538°C is 19.4 W.m<sup>-1</sup>.K<sup>-1</sup>). This reactor is stirred (agitator blades) that improves the heating and homogenizes the media.

Heating is provided by a heating collar disposed on the body of the reactor and also by heating rods put on the cap which allow a heating rate of 7°C.min<sup>-1</sup>. The maximum power delivered by the device is 2000 W for heating the body and of 200 W for the four heating rods on the cap.

Cooling is achieved by injecting cold air into the stainless steel body of the autoclave. The cooling is not instantaneous.

When the system is at room temperature, the final pressure in the reactor is measured (P<sub>S</sub>) by the unit control. When gas is noticed, gaseous products are recovered at the cooled outlet of the system in a gas collector to measure the volume and then in a sampling bag. The gas

collector is a cylinder filled with water, and graduated. Gas is finally pumped in a gas bag and analyzed if necessary. Reactions made with this reactor were performed at 350°C; the gas phase was too low to be collected, so the system to collect gas was not used.

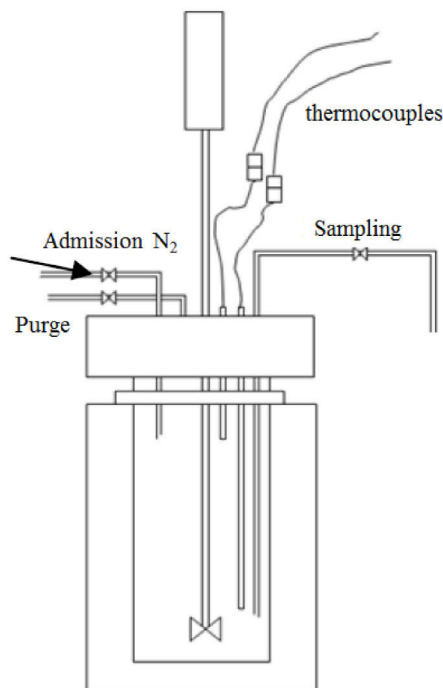


Figure 47: 500 mL batch reactor.

Table 4 summarizes reactor conditions.

Table 4: Comparison of reactor conditions.

	France		Japan
<b>Volume(mL)</b>	500	5	5
<b>Temperature range (°C)</b>	T < 500°C	T < 600°C	T < 500°C
<b>Pressure range(MPa)</b>	P < 30 MPa	P < 30 MPa	P < 30 MPa
<b>Dimensions (inner diameter/ height)</b>	6.5 cm / 12 cm	1.5 cm / 4 cm	1 cm / 10 cm
<b>Material</b>	Inconel	Stainless steel 316	Stainless steel 316
<b>Stirring/ Stirring speed</b>	Yes / 1000 tr.min <sup>-1</sup>	No	No
<b>Heating system</b>	heating blocks	heated air	heating blocks
<b>Temperature rate</b>	7°C.min <sup>-1</sup>	20°C.min <sup>-1</sup> 40°C.min <sup>-1</sup>	Instantaneously

After the reactor opening, phases are recovered and analyzed. Characterization tools are detailed in the following part.

## II.2. Experimental procedure

The experimental procedure can be divided into five steps described as following.

### II.2.1. Reactors filling

Temperature is fixed and controlled by the heating system but pressure is induced by the mass introduced in the batch reactor at ambient conditions. The calculation of the introduced mass is based on the density of the media at the experimental temperature and pressure of reaction and the total volume of the reactor. The introduced mass is calculated as follows.

The density of black liquor solution ( $\rho_{\text{solution}}$ ) was calibrated previously (chapter 2-II.1.1); it is slightly different from that of pure water ( $\rho_{\text{eau}}$ ). The ratio  $f$  (16) between the two densities at ambient conditions ( $T_{\text{amb}}$ ,  $P_{\text{atm}}$ ) is assumed to be constant regardless of the operating conditions.

$$f = \frac{\rho_{\text{solution}}(T_{\text{amb}}, P_{\text{atm}})}{\rho_{\text{eau}}(T_{\text{amb}}, P_{\text{atm}})} \quad (16)$$

With the software “Water & Steam” provided by Springer, using the temperature and pressure fixed for the experiment, the density of pure water is calculated. Using the ratio  $f$ , the density of the solution under experimental conditions is estimated. Then, from the internal volume of the reactor and the density at experimental conditions, the total mass of the solution ( $m_{\text{Solution}}$ ) is obtained (17).

$$m_{\text{Solution}} = \rho_{\text{solution}}(T_{\text{exp}}, P_{\text{exp}}) \times V_{\text{autoclave}}^{\text{in}} \quad (17)$$

The initial volume of solution ( $V_{\text{solution}}$ ) is finally estimated (18).

$$V_{\text{Solution}} = \frac{m_{\text{Solution}}}{\rho_{\text{solution}}(T_{\text{amb}}, P_{\text{atm}})} \quad (18)$$

The mass of solution ( $m_{\text{Solution}}$ ) is introduced using a micropipette, the mass is controlled by an analytical balance. Reactors are then closed and heated.

### II.2.2. Heating system and heating rate

Each type of reactor has a specific heating system, detailed previously for each type of reactor.

### II.2.3. Temperature profile and reaction time

One of the experimental difficulties comes from the difference between the temperature indicated by the furnace and the effective temperature in the reactor. A simulation performed using Comsol showed that for a reactor initially taken at ambient temperature and placed in preheated oven at 400°C, temperature of 371°C is reached in the autoclave in 20 min; while the oven reaches these temperature 5 minutes faster.

Because of the different experimental conditions (mass of liquid, final temperature, differences in the heating rate...), it is difficult to estimate precisely the temperature profile during the heating. Therefore, we consider as heating time, for all systems, the time required for the heating system to reach the setting temperature. Thus, to compare experiments, reaction time starts when oven temperature is stable.

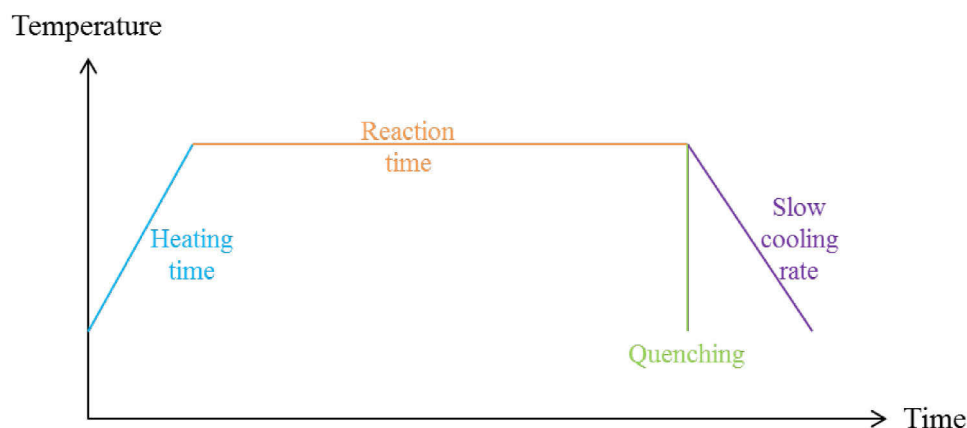


Figure 48: Temperature profiles.

### II.2.4. Cooling

Two cooling methods have been used for the mini reactors (5 mL). The first one is a slow cooling (cooling under air circulation) and the second one by quenching (cooling in ice water mixture). Slow cooling is 30 min and quenching is considered as instantaneous ( $t < 1$  min).

After cooling, reactors are placed in the opening system to be opened, to separate gas, liquid and solid phases produced by reactions and collect them.

### II.2.5. Opening reactor

As reactors were sealed, they are replaced in the opening / closing system to be opened.

Each reactor has a particular opening system detailed in the Chapter 2 II.1.

Given the quantities introduced into the reactors and recovered after reaction, it is impossible to estimate errors due to experience. However, it is possible to take into account errors due to analysis techniques. Errors have been taken into account when it showed an interest.

### III. Outflow materials: Phases characterization

Thereafter the methods employed to qualify and quantify black liquor and respectively the phases produced by hydrothermal conversion are listed. Principles of following analysis are detailed in annexes (annex 2).

Once the hydrothermal process finished, gas phase is analyzed directly after reactor opening. The mixture liquid and solid is recovered then filtered to separate the two phases.

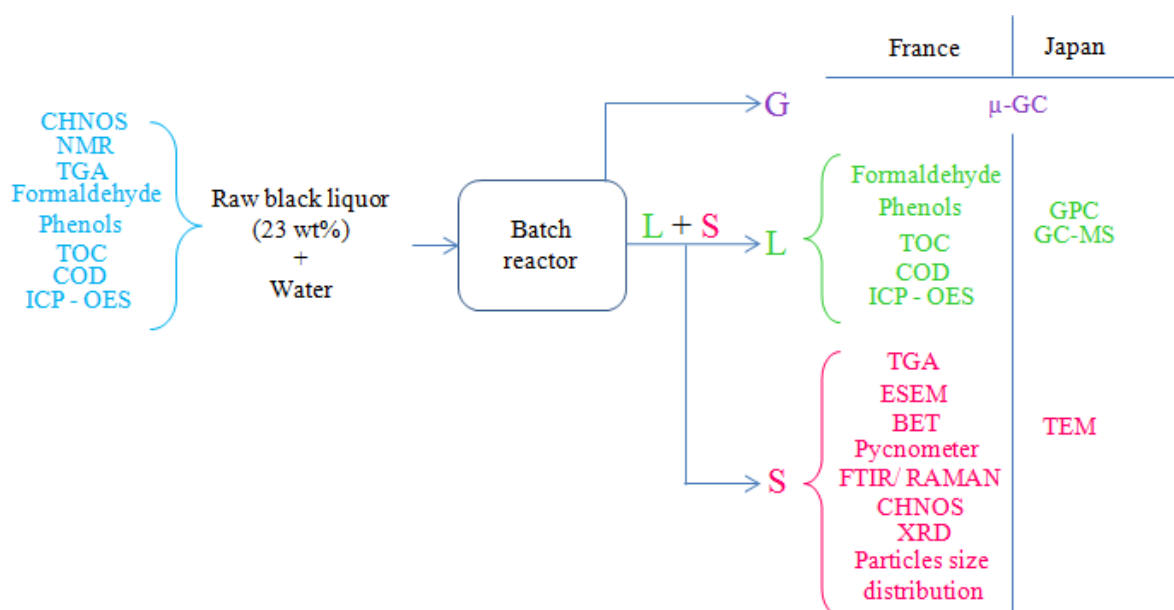


Figure 49: Scheme of characterizations tools.

#### III.1. Gas analysis

Gaseous phases were exclusively analyzed by micro-gas chromatography with a micro-GC – Agilent 3000 but the modules of analysis are different in France and Japan. This technique is used to separate, identify and quantify the components. For both columns the length is 10 meters. Each module is composed of an injector, a column, a flow control system and a thermal conductivity detector (TCD), able to do analyses in few seconds.

France: Four modules are used. Gases detected are:

-A module (column: molecular sieve): H<sub>2</sub>, CH<sub>4</sub>, CO.

-B module (column: PLOT U): CO<sub>2</sub>, C<sub>2</sub>H<sub>2</sub>, C<sub>2</sub>H<sub>4</sub> and C<sub>2</sub>H<sub>6</sub>.

-C module (column: Alumine): C<sub>3</sub>H<sub>8</sub>.

-D module (column: OV-1): C<sub>6</sub>H<sub>6</sub>.

For A module, carrier gas is Argon while for B, C and D modules, carrier gas is Helium.

Japan: Two modules are used. Carrier gas is Argon. Gases detected are:

-A module (column: Molesieve 5A): H<sub>2</sub>, N<sub>2</sub>, O<sub>2</sub>, CH<sub>4</sub>, CO.

-B module (column: PoraPLOT Q): channel A, CO<sub>2</sub>, C<sub>2</sub>H<sub>2</sub>, C<sub>2</sub>H<sub>4</sub>, C<sub>2</sub>H<sub>6</sub> and all others low hydrocarbons.

μ-GC allows identifying and quantifying the proportion of initial carbon converted into gas phase:

$$\%Carbon\ converted = \frac{m_{carbon\ in\ gas\ phase}}{m_{initial\ carbon}} * 100 \quad (19)$$

### III.2. Liquid analysis

Liquid phase is analyzed using several techniques hereafter presented.

Total Organic Carbon (TOC): The results given by the Shimadzu COT-meter (COT-5050) are the amounts of total carbon (TC) and inorganic carbon (IC). The difference between these two values is the total organic carbon (TOC). The values of TOC contents in the liquid phase before reaction and after reaction allow assessing the conversion of organic carbon from the liquid phase. Error due to TOC measurement is 2%.

$$\%TOC\ removal = \frac{TOC_i - TOC_t}{TOC_i} * 100 \quad (20)$$

Chemical oxygen demand: COD (Hach Lange): COD indicates the mass of oxygen (O<sub>2</sub>) consumed by compounds per liter of solution. It is expressed in mg/L or ppm. This parameter gives information on the oxidation degree of molecules in the aqueous media. Indeed, COD measures the amount of O<sub>2</sub> required to achieve oxidation. This analysis is carried out under acid conditions in a solution with sulfuric acid and potassium dichromate with cuvette test (LCK014, LCK514). After reaction, the sample is analyzed at the wavelength 605 nm for ranges 100-2000 mg.L<sup>-1</sup> (LCK514) and 1000-10000 mg.L<sup>-1</sup> (LCK014).

Phenols and formaldehydes measurement: Phenols and formaldehyde are measured using cuvette tests. Tubes contain specific solution reacting with the molecules to be measured. Several ranges of concentration are available.

Ultra-violet spectroscopy measurement: Spectroscopy UV HP8452 with diode array. This technique was used to measure chromophorous concentration evolution in liquid phase.

Molecules containing  $n$  or  $\pi$ -electrons absorb the energy of UV light. The method to create the spectrogram is based on Beer-Lambert law considering attenuation of intensity by the liquid.

Inductively Couple Plasma Optical Emission-spectrometry (ICP-OES): ICP JOBIN YVON-ULTIMA 2. This analysis instrument is composed of a sample introduction system, a plasma torch, a high frequency generator, optical transfer equipment, a spectrometer and a computer interface.

Gel Permeation chromatography (GPC): (HP1100). This chromatography is a part of size exclusion chromatography which separates molecules towards their size. GPC separates compounds using molecular weight of molecules.

Gas chromatography coupled with mass spectroscopy (GC-MS): (GC: Agilent 7890A; MS:Agilent 5975C) This analysis combined features of gas chromatography and mass spectrometry. The features of the GC-MS used in Japan are the following:

**Column:** HP-5MS (OD: 250  $\mu\text{m}$ , film thickness: 0.25  $\mu\text{m}$ , length: 30 m; Column pressure: 48.7 kPa)

**Inject type:** Splitless

**Injection temperature:** 300°C

**Column oven temperature program:** 5 min at 40°C, raised at the rate of 10°C/min up to 300°C, 5 min at 300°C

**Ion chamber temperature:** 230°C

### III.3. Solid analysis

Solid obtained from hydrothermal carbonization and presented in chapter 4 is characterized using particles size distribution, elemental analysis, microscopy (transmission electron microscopy and environmental scanning electron microscopy), total surface and specific surface measurements with BET, density (helium pycnometer), thermogravimetric analysis, Fourier Transform infrared spectroscopy, RAMAN spectroscopy, X-ray diffraction.

Particles size distribution: Mastersizer 3000 Malvern. The size of the analyzed particles can vary from a few nanometers to several millimeters. An in-situ analysis gives the particles size distributions in the reaction media. Repartition distribution is made following volume represented by each class.



CHNOS: elemental analysis (Thermo NA 2100). The weight fraction of C, H, N, S and O is estimated. The analyses of C, H, N, S and O are separated. On the one hand C, H, N, S and on the other hand O, are estimated. Oxygen is calculated by difference or by analysis.

Electronic microscopy: In France, Environmental scanning electron microscopy (ESEM, Philips XL 30 FEG) has been used and in Japan, transmission electron microscopy (TEM, Hitachi H7650). TEM measurements have been made with an acceleration voltage of 100 kV to see the morphology of the solid residue and to analyze chemically the sample.

BET: Tristar II 3020. This technique allows measuring the surface area of the material. Equations are detailed in annexes part

Pycnometer: ACCUPYC 1330 Micromeritics. This analysis is used to know the relative density of a sample at  $P = 1.4$  bars and  $T = 20^{\circ}\text{C}$  with gas displacement. Gas used is helium.

Thermogravimetric analysis (TGA): TG-ATD 92, Setaram. This technique measures the mass loss of a sample depending on the temperature. TGA analyses are used for solid characterization:

- Isotherm of 10 min. at  $30^{\circ}\text{C}$
- Slope from  $30^{\circ}\text{C}$  to  $260^{\circ}\text{C}$  with  $5^{\circ}\text{C}/\text{min}$
- Isotherm of 1h at  $260^{\circ}\text{C}$
- Slope from  $260^{\circ}\text{C}$  to  $360^{\circ}\text{C}$  at  $5^{\circ}\text{C}/\text{min}$
- Isotherm of 1h at  $360^{\circ}\text{C}$
- Slope from  $360^{\circ}\text{C}$  to  $1100^{\circ}\text{C}$  at  $5^{\circ}\text{C}/\text{min}$
- Cooling to  $30^{\circ}\text{C}$

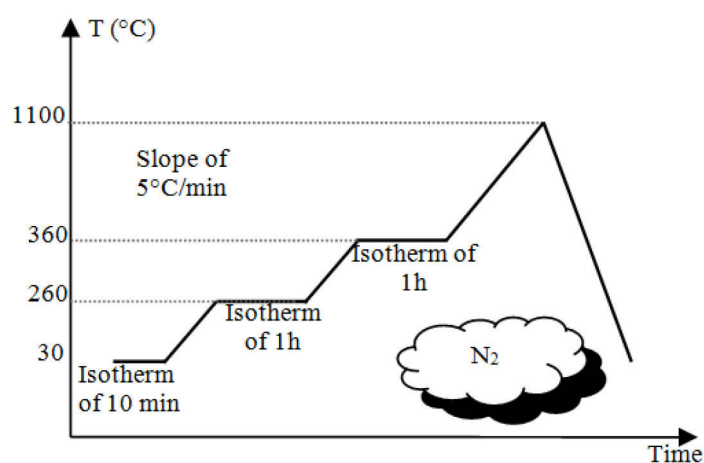


Figure 50: Procedures for solid thermogravimetric analysis.

Fourier Transformed Infrared Spectroscopy: FTIR (PERKIN ELMER 200 FTIR). This is an analysis for solid, liquid and gas. In our work, it has been used for solid analysis. FTIR is an easy way to identify the presence of such functional group in a molecule.

RAMAN spectrometry: RAMAN – AFM: Alpha 300R, WITec RAMAN spectroscopy is a vibrational spectroscopy like infrared spectroscopy, based on inelastic scattering of a monochromatic source laser at 514 nm.

X-ray diffraction (XRD): (PANalytical X'Pert MPD diffractometer)

An X-ray diffractometer is used to identify the crystallinity/amorphism of a solid. Indeed, each crystalline phase has a single diffractometer with specific fine peaks. On the contrary if the structure is amorphous, this indicates that it is composed by not organized atoms. X-rays are then diffracted in all directions, pattern are then obtained with large peaks.

Parameters used for XRD analysis are: Cu K $\alpha$  (1.543 Å) radiation source at 45 kV and 40 mA of intensity. The reflections were collected in the 2\*theta ranges from 9° to 80° with a step size of 0.017°, a scan step time of 29.89 s. The irradiated length is 5 mm. The phase identification was carried out with the JCPDS database.

#### **III.4. Conclusions**

Phase's characterization allows us to analyze properly the phases obtained and thus increase our understanding on batch hydrothermal conversion. The different phases are characterized to get data either on efficiency (H<sub>2</sub> production, TOC removal...) or solid formation (particle size, chemical composition...).



## Chapter 3: Overview of hydrothermal conversion of black liquor through parametric study in batch reactor

---



### **Résumé du chapitre 3 : Potentialités de la conversion hydrothermale de la liqueur noire au travers d'une étude paramétrique en réacteur batch.**

L'objectif de ce chapitre est, au travers d'une étude paramétrique, de mettre en évidence les conditions opératoires permettant de répondre à nos objectifs : l'étude de la formation de solide, celle de son annihilation... (cf introduction)

#### Les réacteurs batchs :

Compte tenu de nos objectifs pour cette thèse et des objectifs de cette étude (présentée dans ce chapitre 3), les réacteurs batch sont bien adaptés. En effet, ils permettent de récupérer les phases gaz, liquide et solide, et ils offrent une grande flexibilité d'utilisation et une bonne robustesse ; ils permettent ainsi de balayer une large gamme de conditions opératoires pour identifier les voies d'études intéressantes (chapitres 4 et 5). Cependant les désavantages liés aux réacteurs batchs ne permettent pas d'obtenir des résultats fiables quantitativement à l'issue de chaque expériences, il est donc nécessaire de multiplier les expériences pour obtenir des résultats statistiquement pertinents. Le mode opératoire des réacteurs batchs se divise en 5 étapes : le remplissage des réacteurs aux conditions ambiantes, l'atteinte des conditions de température et pression souhaitées, le temps de réaction aux conditions souhaitées, le retour aux conditions ambiantes.

La conversion hydrothermale de la liqueur noire est un processus complexe de gazéification, liquéfaction et carbonisation. L'étude paramétrique se concentre sur l'effet de paramètres choisis sur les phases sortantes.

#### Influence des conditions opératoires sur la proportion des phases obtenues :

Les paramètres d'étude sont le temps de réaction, la concentration et la température.

L'influence du temps de réaction a été étudiée en conditions sub (350°C) et supercritiques (500°C). Cette étude montre que ce paramètre a une forte influence sur la conversion du carbone de la phase liquide initiale à la phase gazeuse dans les conditions supercritiques. La réactivité (ou la dégradation) est clairement mise en évidence par les spectres UV-Visible et la production de gaz. Au contraire, la conversion du carbone de la phase liquide initiale est moins affectée par le temps de réaction en conditions subcritiques. La conversion de carbone de la phase liquide initiale à la phase solide augmente avec le temps de réaction quelque soit les conditions opératoires (sub et supercritiques)

L'influence de la concentration n'est pas significative sur la conversion du carbone lors de la conversion hydrothermale de la liqueur noire dans la gamme opératoire considérée.

La température est le paramètre opératoire le plus influant. En fonction de la température du procédé, 3 régions de températures sont délimitées pour orienter la gazéification, la liquéfaction ou la carbonisation ; en fonction des produits souhaités, la température guide la conversion.

#### Influence de la température sur la composition des phases obtenues :

La gasification hydrothermale de la liqueur noire (entre 450°C et 600°C) montre une intéressante proportion d'hydrogène dans le gaz formé et une faible proportion de CO<sub>2</sub> (due à l'alcalinité de la solution aqueuse). A partir de 500°C, de l'hydrogène sulfuré est identifié, ce qui pose des problèmes au niveau laboratoire pour l'analyse des gaz en  $\mu$ -GC (gaz corrosif nécessitant des colonnes d'analyses adaptées et coûteuses) mais ne posant pas de problèmes au niveau industriel notamment pour les papetiers qui utilisent ce gaz pour reformer la liqueur blanche. En parallèle d'une phase gazeuse intéressante, une phase solide est systématiquement produite. Ce solide est d'origine organique et inorganique.

La liquéfaction hydrothermale est étudiée entre 400°C et 500°C, l'intérêt se concentre au niveau de la phase liquide qui présente une composition complexe de composés phénoliques ayant un intérêt industriel fort. Cependant, leur séparation présente un challenge important.

La carbonisation hydrothermale est prépondérante en dessous de 400°C. A ces températures, la phase gazeuse est quasiment inexistante alors que la phase solide est prépondérante. A ces températures, la polymérisation des composés phénoliques avec le formaldéhyde est une des réactions favorables. Vers 350°C, le solide est constitué de microparticules de carbone sphériques présentant un fort intérêt.

Ainsi, la conversion hydrothermale révèle la formation de 3 phases dont la proportion et l'intérêt sont guidés par la température. La phase solide est systématiquement formée, sa morphologie évolue d'une structure microparticulaire sphérique à une structure informe pour des conditions plus sévères.

A l'issue de ces conclusions, 2 voies d'étude se dessinent :

- La première en conditions subcritique à 350°C afin d'étudier la formation et l'évolution de la phase solide formée de microparticules de carbone (chapitre 4).
- La deuxième portant sur la formation d'hydrogène à basse température, permettant ainsi de travailler sans hydrogène sulfuré. L'ajout d'un catalyseur ( $\text{CeO}_2$ ) est étudié afin d'augmenter la production d'hydrogène et d'éviter la formation de solide lors de la réaction.

**\*\*\* Fin du résumé**





Hydrothermal conversion processes are used to convert wet biomass or wastes, under pressure and temperature. This conversion is more or less complete and depends strongly on the operating conditions which impact its efficiency and thus the chemical composition of the phases. Indeed, the operating conditions could favor gasification, liquefaction or carbonization processes as mentioned in the first chapter.

According to the literature, black liquor is essentially converted by hydrothermal gasification to produce hydrogen [53] by virtue of its alkalinity. As hydrogen is actually produced at high temperatures; liquid fuels would be recovered at lower temperature following the concept of bio-refinery [89]. Liquefaction of lignin, main component of black liquor, lead to a promising full range of phenolic compounds [90], [76] which could be also expected during black liquor liquefaction. Always, lignin conversion leads more or less to coke formation, due to polymerization [91], [92], [58]. As mentioned previously, solid formation is a technological issue of continuous reactor developments. The same process would be observed during black liquor carbonization.

Hydrothermal conversion process can be performed in continuous or batch reactors. Because of the precipitation of alkali salts contained in black liquor, we choose to do experiments in batch reactor to prevent irregular performance of the system (blocking of the tubular reactors). In fact, operating of batch reactor in the conditions of our experiments is easier than continuous processes.

## **I. Batch reactors**

### **I.1. Batch process description**

Batch reactors are considered as the simplest type of reactors existing in term of operating process [93]. They are usually easy to use and allow testing very quickly the influence of operating conditions on reactions. Literature presents different types of batch reactors (quartz capillary, diamond anvil cell...) employed in supercritical water processes, and different heating systems. For high pressure processes, batch reactors are called autoclaves.

The advantages and drawbacks of autoclaves for hydrothermal treatment are presented hereafter (Table 5):

Table 5: Advantages and drawbacks of batch reactor

Advantages	Disadvantages
Adapted to gas, liquid, solid and paste [94]	Low volume
High concentration of biomass and inorganic matter	Pressure induced by mass of material and process temperature
Flexibility to use [94]	Inconstant final quantity[94]
High feedstock concentration	Analysis are usually made after reaction
Robust	Catalytic effect of the reactor walls
Reduce of reaction volume, that increase collision frequency and so accelerate reaction	Low total yield
	Mixture by convection for unstirred reactors

Batch operation can be separated into 5 steps:

- Loading reagents, at ambient conditions
- Setting conditions of temperature and pressure,
- Setting reaction time (contact time in the fixed parametric conditions),
- Return to ambient conditions of temperature and pressure,
- Reactor discharge.

## I.2. Reactor design

### I.2.1. Stirred or unstirred reactor

Stirred reactor has a guaranty of homogeneity of temperature and concentration (homogeneous mixture) during reaction.

### I.2.2. Heating system

The performance of heating system is measured by:

- Its response time to modify the temperature (heating rate),
- The uniformity of the temperature in the reactor,
- The stability of the temperature (temperature control).

These points are crucial in case of crystallization processes and operations with temperature dependent products. Heating system is also the crucial point to reach and maintain the pressure in the reactor. Because of the general low heating conduction in the batch reactor, the quality and performance of heating system are very important for the supercritical water equipment.

### **I.2.3. Operating conditions: temperature, pressure, concentration, reaction time and catalyst**

As seen previously, hydrothermal conversion is influenced by operating conditions.

Temperature and pressure: in batch process, pressure is governed by the reaction temperature and by the initial loading of the vessel; so temperature and pressure have to be considered connecting one to the other. Many studies [32] have shown that temperature is the most important parameter for biomass hydrothermal conversion when pressure is high ( $P > 20$  MPa). Temperature guides reactions, to form mainly solid, liquid (oily and aqueous phase) or gas. Higher the temperature is; faster reactions will be. First solvolysis of biomass begins at 190°C to finish at 220°C. During solvolysis, hemicellulose and lignin are dissolved in water [32]. For low temperature ( $T < 300^\circ\text{C}$  and a self-generated pressure) carbonization is favored and solid phase is mainly obtained. At higher temperature ( $T \sim 300^\circ\text{C}$ ) and  $P < P_{\text{critique}}$ , degradation of raw material occurs with reactions such as dehydration, decarboxylation, fragmentation, rearrangement, condensation, polymerization... At middle temperature ( $300^\circ\text{C} < T < 450^\circ\text{C}$ ) and high pressure ( $P > P_c$ ) liquefaction is promoted and liquid phase is quantitatively the major obtained phase. Very high temperature ( $>500^\circ\text{C}$ ) and high pressure ( $P > P_c$ ) promotes gasification process and influences the yield of each gas formed [95] because of the endothermicity of the reaction [76].

Concentration: Concentration of organic matter is an important parameter for the hydrothermal conversion. Indeed, the efficiency of gasification is better considering a low concentration ( $\sim 10$  wt%) of initial biomass. In contrast, for obtaining liquid phase, a high concentration of biomass increases the content of products in liquid and solid phase. An optimization of the content of water has to be performed in relation to the objective of the process: to produce more liquid, solid or gas phase in the experimental conditions (fixed T, P)

Reaction time: The yield of the different conversions changes with reaction time. For example, char production yield decreases with reaction time whereas, gas production yield increases for experiments performed in same conditions of pressure and temperature. However, Kang et al. [76] has reported that hydrogen percentage of gaseous product is favored by short reaction time with metal catalyst like copper, iron.... Considering complete degradation (oxidation), a good balance between reaction time, temperature and oxidant has to be found. Considering a conversion and not a complete degradation, if reaction time is too

short, decomposition of black liquor will not be enough and if the reaction time is too long, undesirable products such as coke would be produced in large quantity.

Catalyst: Alkali salts, metal oxide, activated carbon.... are catalysts used to obtain higher yields at lower temperature, improving the process efficiency and/or promoting some reactions (hydrogenation, oxidation, water-gas-shift reaction...).

Hydrothermal conversion of black liquor under supercritical conditions, or close to these conditions, is a complex process of gasification, liquefaction and carbonization. The parametric study that will be developed in this chapter investigates their response:

- How temperature impacts the distribution of the three phases rather than the other parameters?
- What is the effect of the reaction time on the global kinetics of conversion?
- Effect of organic and mineral concentrations (black liquor concentration) on the kinetics of conversion?
- The effect of temperature on solid formation and thus on mineral recovery?
- An hydrogen production efficiency as regards to the temperature range?

## II. Influence of operating conditions on phases distribution and kinetics

Carbon or mass balances are basically used to evaluate the distribution of products in the three phases. In the literature, temperature appears as the most important parameter to be considered. However, reaction time and concentration of raw material have also been studied to confirm this assumption.

The operating conditions used in this section are summarized in Table 6. Reactors used are 5 mL reactors in RAPSODEE center.

Table 6: Range of operating conditions studied under constant reaction pressure of 25 MPa under supercritical conditions and under self generated pressure for subcritical conditions.

		Parametric study											
		Reaction time				Concentration		Temperature					
Operating conditions	Temperature (°C)	350 and 500				500		350	400	450	500	550	600
	Reaction time (min)	0	8	15	30	15		15					
	Pressure (MPa)	25 or 16.4 ( at 350°C)											
	Concentration (wt %)	10				5	10	20	30	10			

### II.1. Influence of reaction time

Reaction time has been studied at sub and supercritical conditions for solution of 10 wt% of raw black liquor. Indeed, the distribution of organics is related to the conversion efficiency, improved at high temperature. Thus the carbon distribution to the three phases is presented at 350°C and 500°C. The evaluation of the carbon in each phase is at least based on the measurement of the total organic carbon in the liquid phase.

### II.1.1. Subcritical conditions

Figure 50 presents the variation of normalized TOC concentration in the liquid phase at subcritical condition for reaction times in a short range (0-30 min).

At subcritical conditions, the conversion seems to be quickly “activated” during the heating of the media as 20% of the TOC was removed before reaching the reaction temperature. A stabilization of carbon conversion is observed during the first 8 min of reaction time then the carbon conversion decreases quite linearly ( $R^2 = 0.99$ ). The equation of this linear decrease is:

$$\text{normalized TOC concentration} = -0.013x + 0.9547 \quad 8 \text{ min} \leq x \leq 30 \text{ min} \quad (21)$$

This profile indicates that the TOC removal is a phenomenon with constant kinetics; either organic carbon has been transferred to gaseous, liquid or solid phases or mineralized. The error related to TOC measurement is 2% of the value indicated on graphs.

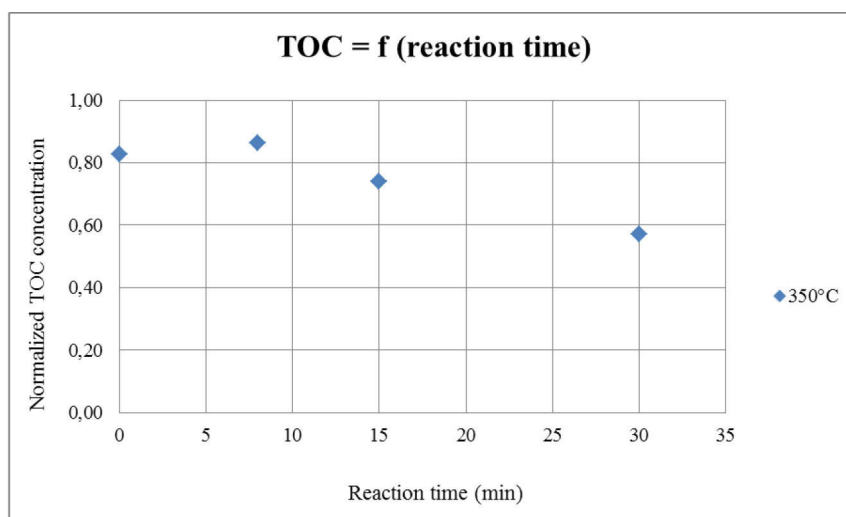


Figure 51: Normalized TOC concentration at 350°C depending on reaction time.

After 30 min of reaction time at subcritical conditions only 42% of the initial TOC was removed from the liquid phase. The color of the solutions is shown in Figure 52. The dark brown color is due to aromatics and conjugated systems such as  $\alpha$ -carbonyls groups and quinines. In Figure 52, the color variation is not appreciable versus reaction time. This result could be explained in two ways:

- 1) The color is not changing because the solution contains the same organic compounds. As the TOC removal kinetics is quite constant, it means that all molecules are just degraded for one step (removal of one carbon for example).
- 2) The color is not changing because the color is very intense even if the concentrations of the chromophore groups are low. In this assumption, some molecules are not degraded while another fraction is quite mineralized. As the TOC removal is varying linearly, it would suggest that the TOC removal has the same kinetics whatever the complexity of the molecule.

To discuss these two hypothesis, the UV-Vis spectrum of each solution was also plotted in Figure 53. The region between 254 nm and 280 nm is characteristic of aromatics.

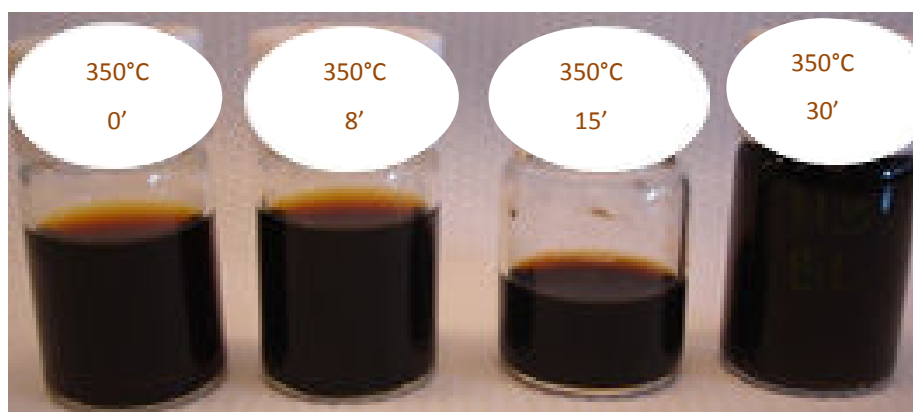


Figure 52: Collected liquids after treatment versus reaction time (black liquor solution is 10 wt%, self generated pressure, 350°C, batch reactor 5 mL)

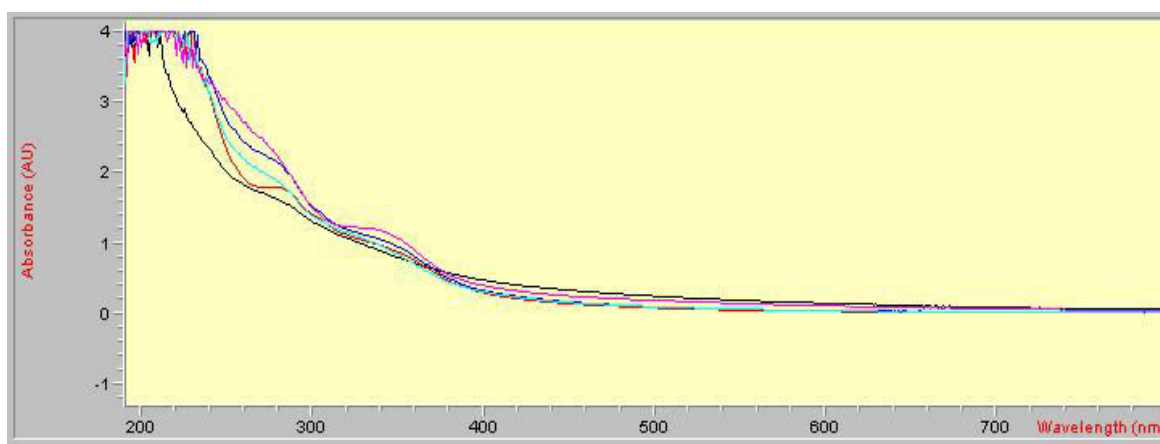


Figure 53: Influence of reaction time at 350°C (Black liquor, 0 min, 8 min, 15 min, 30 min)

From black liquor to the solution after hydrothermal treatment, the main differences are obtained at 270 nm and 340 nm in terms of absorbance. Surprisingly the values of absorbance



are increasing with reaction time. This suggests that aromatics concentration is increasing with time, due to the reaction: at 350°C, aromatization is promoted by reaction time, implicitly, gas production also. This analysis shows rapidly that the process has a weak influence on the chromophore groups that explains the deep brown color. Taking into account that 2 regions of the spectra are mainly affected by the reaction time, and the weak gas production, the TOC variation would be preferably explained by the second hypothesis.

Organic carbon is thus mainly recovered in liquid phase but its proportion in liquid phase decreases with reaction time at 350°C. The analysis of gaseous and solid phases, as well as the inorganic liquid carbon, informs us about the carbon distribution.

Given the volume introduced and uncertainties linked to the measurements, the Figure 54 represents approximatively the trend of carbon distribution following reaction time. The error related to carbon distribution is 1 %.

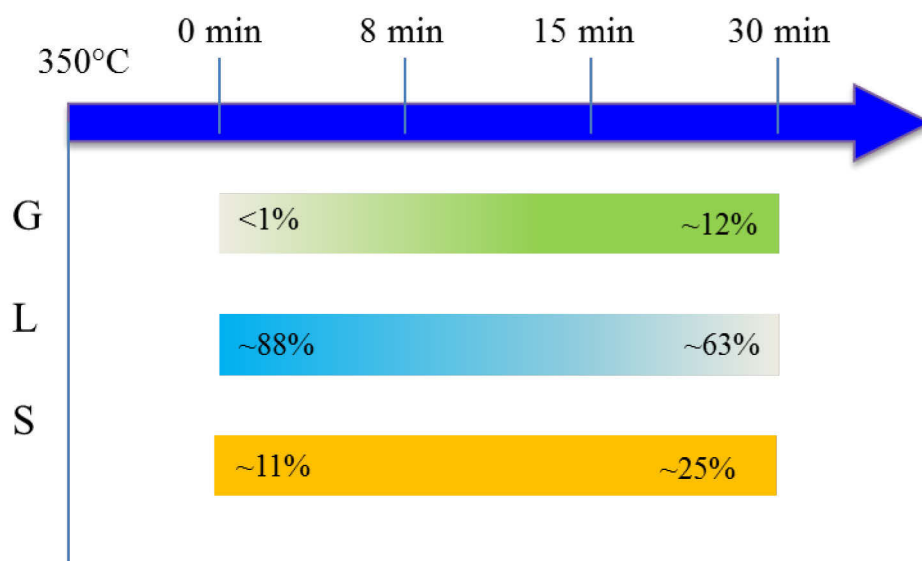


Figure 54: Carbon distribution at 350°C as a function of reaction time

### II.1.2. Supercritical conditions

At 500°C and 25 MPa, the normalized TOC concentration was also measured for different reaction time. Figure 55 shows that the TOC removal variation is quasi linear between 0 and 15 min and then was quite stabilized for 30 minutes of reaction time. The linear equation ( $R^2=0.97$ ) is:

$$\text{Normalized TOC concentration} = -0.0476 x + 0.8275 \quad 0 \leq x \leq 15 \text{ min} \quad (22)$$

At 500°C, the conversion is 3.7 times faster than that at 350°C. As mentioned at subcritical conditions, the linear TOC variation indicates that the organic carbon is removed from the solution with the same kinetics. Compared to subcritical conditions, reaction time influences more the degradation and so the conversion under supercritical conditions. For a temperature above 374°C, properties of water changes drastically as mentioned in the chapter 1 that upgrades the conversion due to its higher reactivity. After 30 min only 15% of the initial TOC is recovered in the liquid phase. As mentioned previously, the error related to TOC measurement is 2% of the value indicated on graphs.

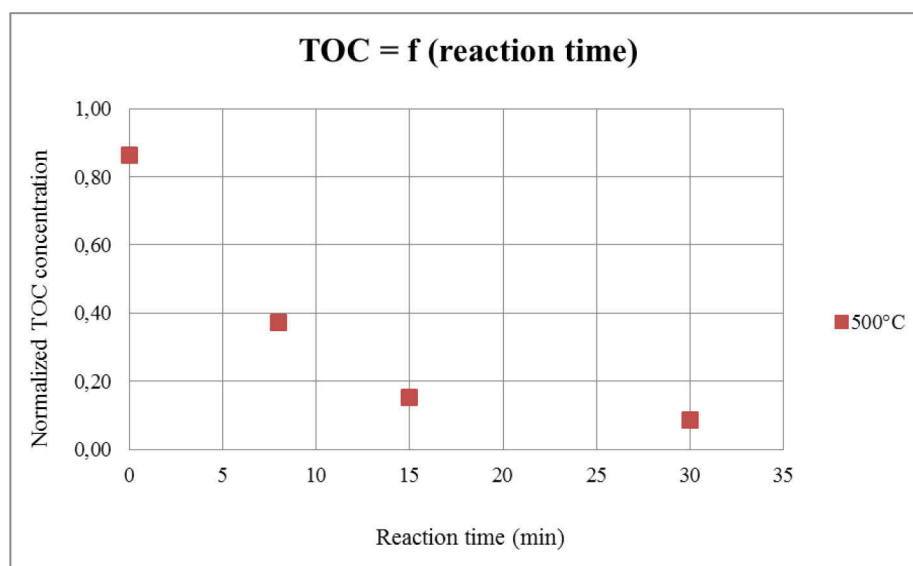


Figure 55: Normalized TOC concentration at 500°C depending on reaction time

Figure 56 shows the color variation of solutions obtained after various reaction times. The deep brown color disappears at 15 min reaction time leading to an orange color. After 30 min of reaction the solution is totally clear and uncolored. Under supercritical conditions, reaction time influences greatly the conversion.

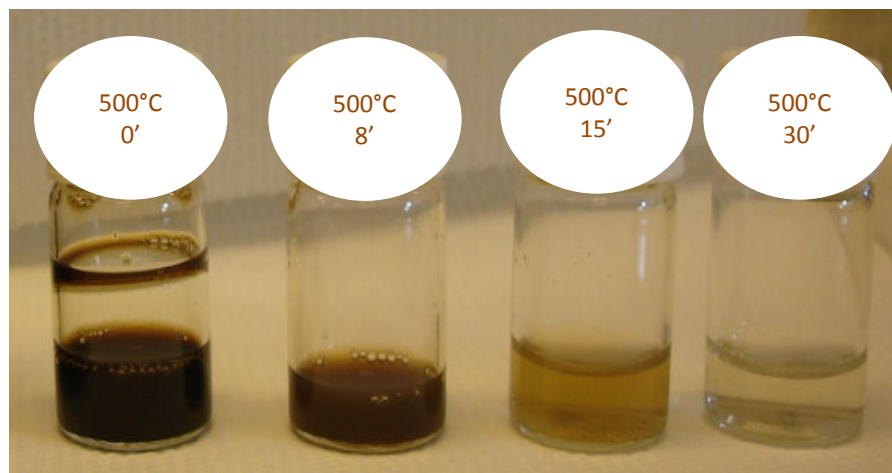


Figure 56: Collected liquids after treatment versus reaction time (black liquor solution is 10 wt%, 25 MPa, 500°C, batch reactor 5 mL)

As for subcritical conditions, UV-Vis spectra are presented in Figure 57. The lighting of the brown color is clearly related to a rapid consumption of aromatics that absorbs around 280 and 340 nm.

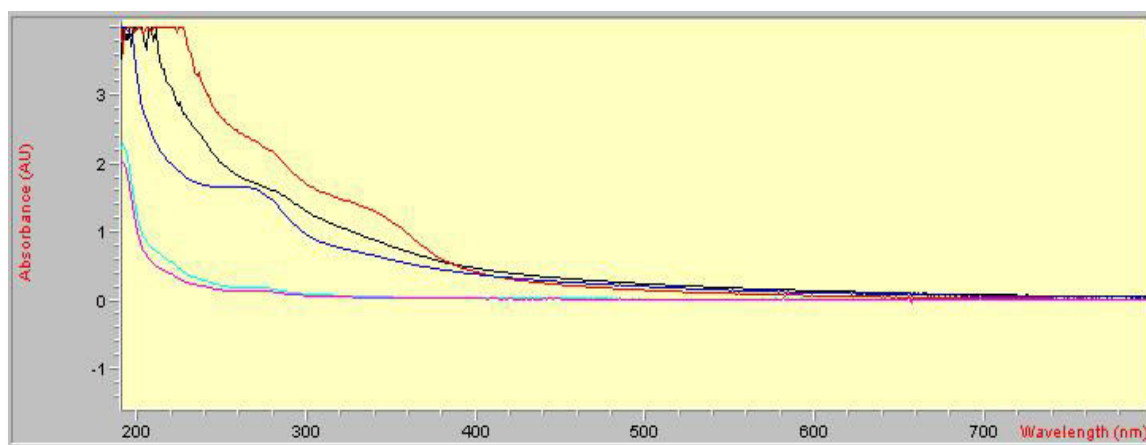


Figure 57: Influence of reaction time at 500°C (black liquor, 0 min, 8 min, 15 min, 30 min)

Once again, organic carbon is distributed to the three phases. Figure 8 represents approximately the trend of carbon distribution following reaction time. At 30 min reaction time and 500°C, the major part of carbon is observed in the gas phase, while in the solid and liquid phases its repartition is very similar. The error related to carbon distribution is 1 %.

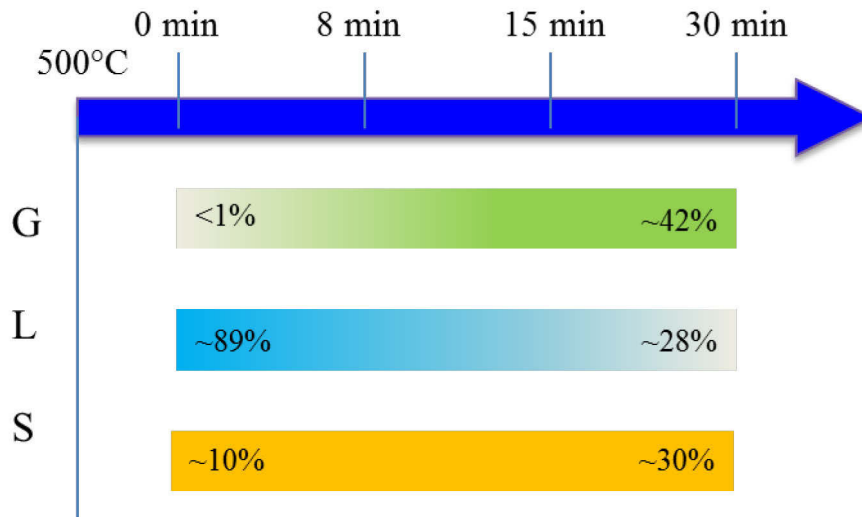


Figure 58: Carbon distribution at 500°C as a function of reaction time

### II.1.3. Inorganic carbon distribution

Figure 58 shows the evolution of pH at 350°C and 500°C in terms of reaction time. Initial black liquor solution has a pH of 12, with an inorganic contained of 7 wt%. After reaction pH is a little lower at ~10 and still basic, due to the liquid alkalinity. Reaction times do not influence the pH of the solutions as it was measured at atmospheric conditions. The error related to pH measurement is 0.1 ph unit.

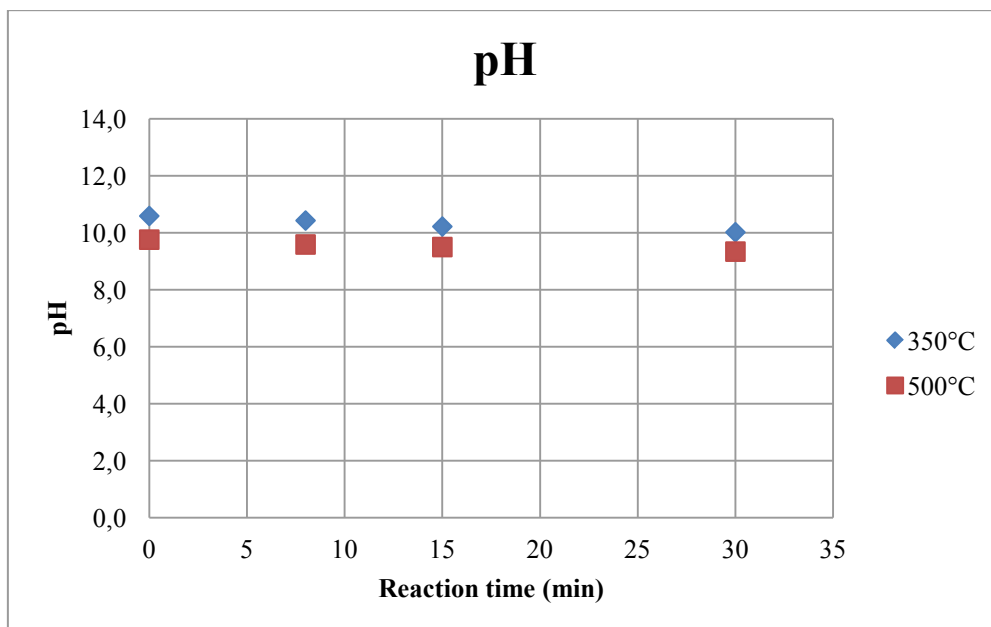


Figure 59: pH of the liquid obtained at 350°C and 500°C in term of reaction time.

To conclude, reaction time has a great influence on carbon conversion from liquid to gaseous phase in supercritical conditions. The reactivity (or degradation) is clearly highlighted through UV-Vis spectra and gas production. On the contrary, the conversion of carbon from liquid phase is less affected by reaction time in subcritical conditions. The carbon conversion from liquid to solid phase increases with reaction time and seems to follow the same trends (Figures 54 and 58). Thus, the amount of carbon recovered in solid is the same for both temperatures.

## II.2. Influence of concentration

The influence of the second parameter (Table 6) experimented is the concentration of raw material. Considering that water is more reactive at supercritical rather than at subcritical conditions, the influence of the concentration is investigated at 500°C. Figure 60 presents the fraction of TOC remaining in the solution after 15 min reaction time. The increase of black liquor concentration leads to a similar conversion of organic matter, as the remaining TOC stabilized at ~15 wt%. So the conversion efficiency is the same. This could be due to the “constant” catalytic action of minerals, which are increased in the same order of magnitude as the organic content. As mentioned previously, the error related to TOC measurement is 2% of the value indicated on graphs.

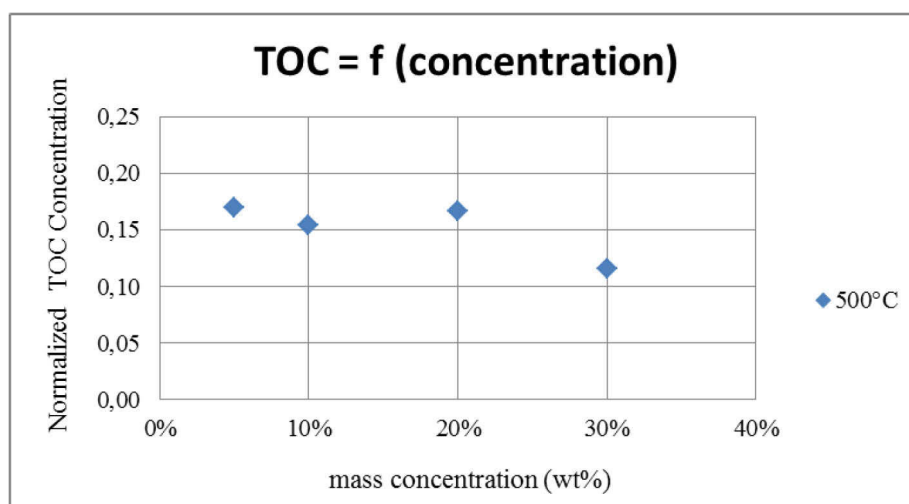


Figure 60: Normalized TOC concentration at 500°C depending on black liquor concentrations.

Pictures in the Figure 61 shows the color of the remaining liquids

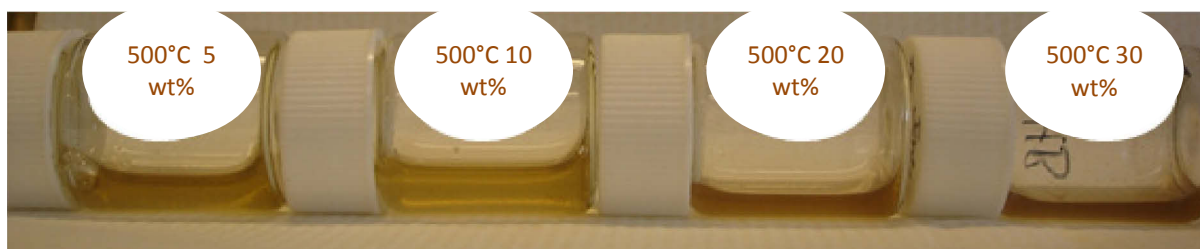


Figure 61: Liquid obtained after 15 min of reaction time at 500°C, for four different concentrations of raw black liquor: 5 wt%, 10 wt%, 20 wt% and 30 wt%.

Color changes from yellow, at low concentrations, to dark orange, for higher concentrations. As mentioned in the previous section, color is linked to the remaining organic and its distribution between the different classes, especially aromatic content: higher the concentration is, higher the remaining of aromatic amount will be.

In addition, whatever the concentration of the initial solution, pH of final liquid is around 10 at 5 wt% and 10 wt% then increase to 11, Figure 62 shows this result. The value of pH is essentially due to alkalinity of the salts contained in the liquid; higher their concentration is, higher the pH will be. Results in Figure 62 suggest that salts mostly remained in the liquid phase. The error related to pH measurement is 0.1 pH unit.

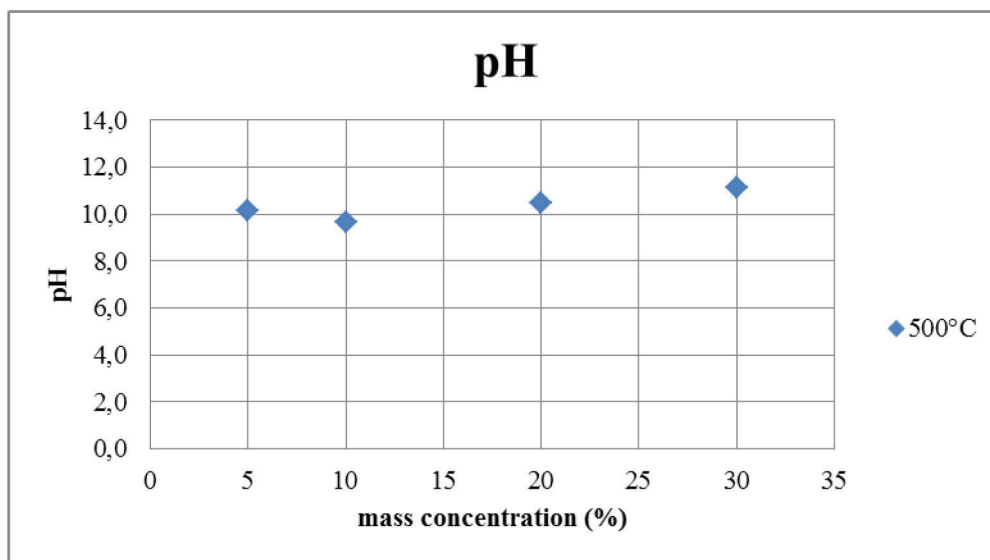


Figure 62: pH of the liquid obtained at 500°C, 15 min of reaction time, various initial concentrations.

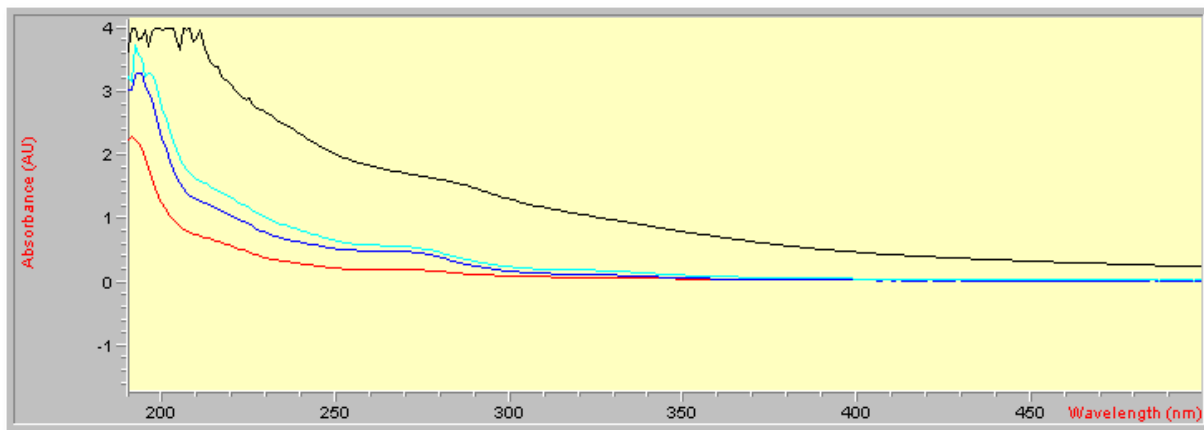


Figure 63: Influence of the concentration (Black liquor, 10 wt%, 20 wt%, 30 wt%) at 500°C.

As regards to the UV-Vis spectra (Figure 63), the profiles are similar, and the absorbance is increasing with the concentration. The relative composition of the solutions, especially their aromatic content, respects the initial black liquor concentration. Therefore, it seems that black liquor concentration has low influence on the aromatics degradation process at 500°C and 15 min reaction time. The increase in absorbance is due to a more intense color.

Total carbon is distributed in the same way independently of the concentration as shown in Figure 63. The overall results seem to indicate that concentration of black liquor is not a limitative factor for hydrothermal conversion efficiency in our experimental conditions. The alkali salts in the black liquor are assumed to catalyze the conversion its kinetics seems to be a linear function of organic and mineral concentrations. The error related to carbon distribution is 1 %.

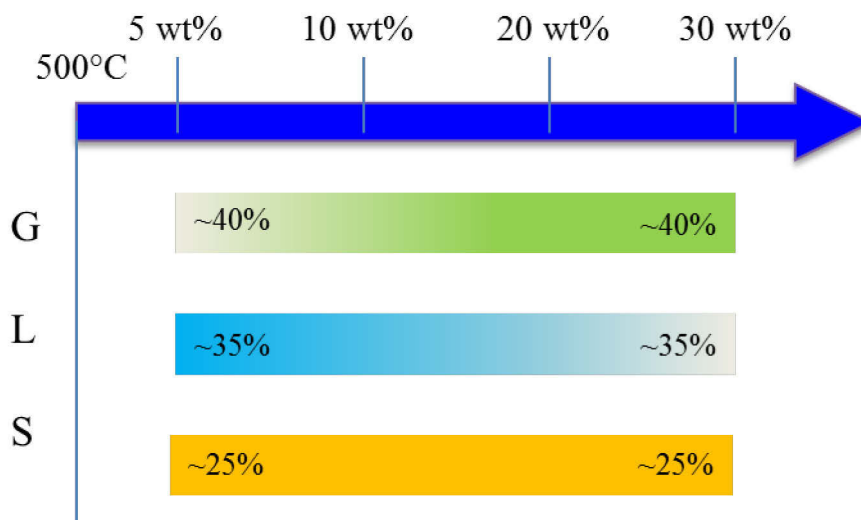


Figure 64: Carbon distribution at 500°C as a function of concentration

### II.3. Influence of temperature

Results obtained after the study of the influence of reaction time suggest that temperature is a determinant parameter in hydrothermal conversion. Thus, reaction temperature is studied from 350°C to 600°C, at 15 min of reaction time with raw black liquor solution at 10 wt%. Figure 65 presents the relative TOC concentration in the final liquid phase versus reaction temperature. TOC removal increases with temperature for the same reaction time. The profile is quite linear up to 500°C and then decreases slower (stabilization tendency). TOC evolution confirms that temperature is the most influencing parameter as regards to the carbon distribution in the three phases. As mentioned previously, the error related to TOC measurement is 2% of the value indicated on graphs.

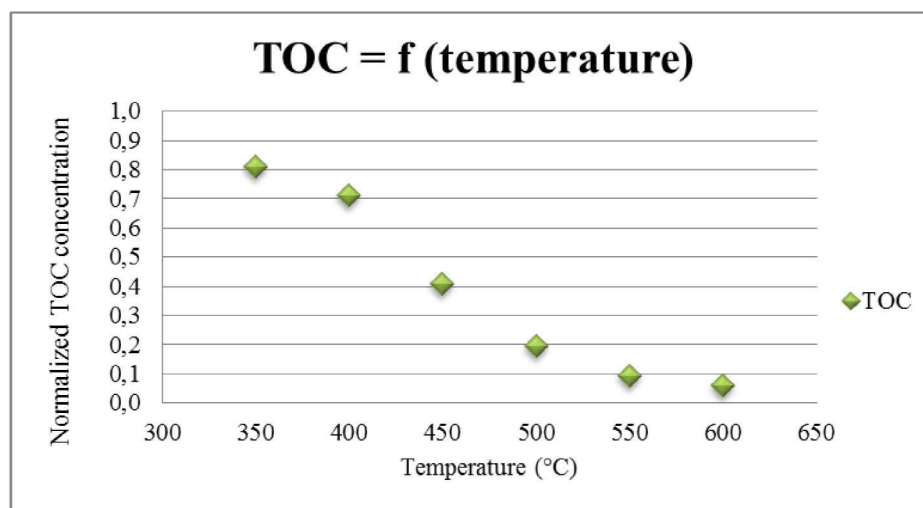


Figure 65: Normalized TOC concentration in liquids obtained after 15 min of reaction time, with initial black liquor at 10 wt%, for temperatures range from 350°C to 600°C.

Figure 66 presents the color of the obtained liquid. The color of the solutions at 350°C and 400°C are very similar, in accordance with a less TOC removal. Then the color decreases simultaneously with an increase of TOC removal. Similar colors have been observed by Cao et al. [53] during hydrothermal conversion of black liquor in continuous reactor.



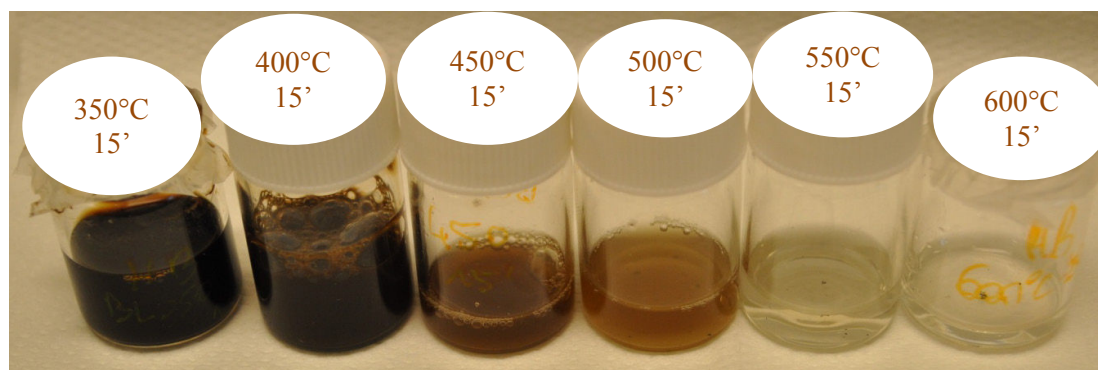


Figure 66: Liquid obtained after hydrothermal conversion conducted at temperature from 350°C to 600°C, at 15 min of reaction time with black liquor at 10 wt%

The deep color is clearly related to the composition of the solution which contains phenols and oligomers coming from lignin and its incomplete degradation [96], [97]. The increase of the temperature influences directly the aromatic content of the solution: higher the degradation is, lower the content of aromatics in the liquid will be and the black color disappear. As well as for the others parameters, temperature reaction does not change the pH value, it remains equal to 10.

The carbon balance is thus summarized in the Figure 67. The error related to carbon distribution is 1 %.

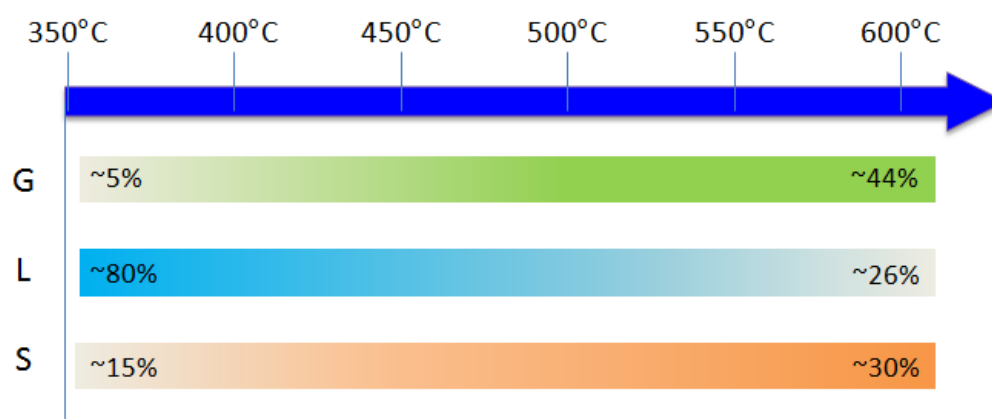


Figure 67: Carbon distribution after 15 min reaction time as a function of temperature.

In conclusion, three regions of temperature are determined to direct gasification, liquefaction or carbonization. According to literature Figure 69 summarizes the main ways to process hydrothermal conversion of biomass [53], [98], [76], [73], [97], [37].

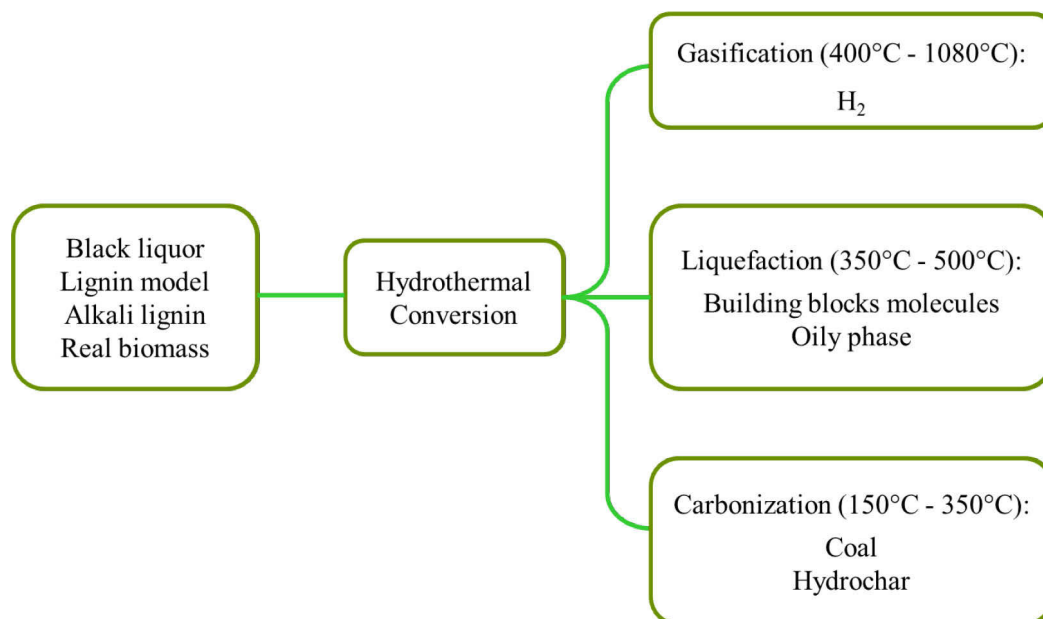


Figure 68: Summary of expected products from hydrothermal conversion of biomass

## II.4. Conclusion

According to the results, temperature is the most influencing parameter in the hydrothermal conversion of black liquor. Depending on the products desired, temperature can be used to guide the conversion. Reaction time increases the conversion initiated by temperature and concentration is an adjusting parameter to optimize the route.

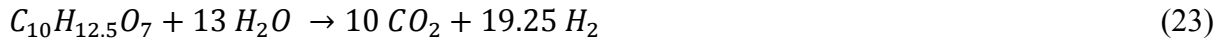
The next section is devoted to temperature influence on the black liquor conversion. In particular the composition of the three phases will be investigated.

### III. Changing in phases composition as a function of temperature

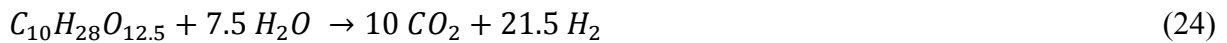
The hydrothermal conversion of black liquor to valuable products is mainly controlled by temperature reaction: Gaseous phase is favored at high temperature or under supercritical conditions; liquid phase containing building-block molecules has to be considered at moderate temperature or subcritical conditions; and solid phase is the desired phase obtain at low temperature. This section is focused on the three processes mentioned previously: gasification, liquefaction and carbonization.

#### III.1. Hydrothermal gasification

In general, the goal of gasification is to produce hydrogen. Taking into account a proximate molar composition of the liquid [2], the complete gasification can be expressed (23).



Equation 23 indicates that one equivalent mol of black liquor can produce about 20 mol of hydrogen. At high temperature, pressurized water is extremely reactive. Under these conditions, gasification reactions such as water gas-shift, decarboxylation, methanation and dehydrogenation are overriding. For this reason, researches are developed for the gasification process. The molar structure of our black liquor is  $C_{10}H_{28}O_{12.5}$  (chapter 2) so the hydrolysis (24) would lead to higher amounts of hydrogen.



The amount of gas obtained is too low to be collected and analyzed up to 400°C. The gases identified are listed in Table 7 from micro-GC analysis. The composition changes with the temperature: low hydrocarbons are detected at 450°C: CH<sub>4</sub>, C<sub>2</sub>H<sub>6</sub> which disappear at 600°C:

Table 7: Composition of gas obtained after 15 min reaction time, 25 MPa and a 10 wt% initial solution of black liquor.

	450°C	500°C	550°C	600°C
H <sub>2</sub>	H <sub>2</sub>	H <sub>2</sub>	H <sub>2</sub>	H <sub>2</sub>
CO <sub>2</sub>	CO <sub>2</sub>	CO <sub>2</sub>	CO <sub>2</sub>	CO <sub>2</sub>
		CO	CO	CO
CH <sub>4</sub>				
C <sub>2</sub> H <sub>6</sub>				
		H <sub>2</sub> S	H <sub>2</sub> S	H <sub>2</sub> S

H<sub>2</sub>S in the gas mixture is detected by mass spectroscopy analyzer but was not quantified. This gas has been also detected during hydrothermal conversion of black liquor in continuous process by Cao et al. [53]. H<sub>2</sub>S is only formed at high temperature. In addition to the usual reactions of gasification; equations given by (25), (26) and (27) could also occur [99].



H<sub>2</sub>S could also come from inorganic sulfur compounds abundant in the black liquor.

As the temperature increases, the total amount of gaseous phase increases. Table 8 illustrates gas compositions, excepting H<sub>2</sub>S not quantified. The production of hydrogen (23) and CO<sub>2</sub> would be the double. However, the basic pH of the solution increases the chemical absorption and fixing of CO<sub>2</sub> into carbonates in the liquid phase [82]. The capture of CO<sub>2</sub> is improved with reaction time. Carbon monoxide was also recovered into the gas phase. Its low part can be explained by the enhancement of the water gas shift reaction (which consumes CO) in presence of alkaline salts. This results is in accordance with the literature using either batch or continuous process [82], [53].

Table 8: Comparative molar composition of gas obtained for black liquor at 10 wt%, 25 MPa, 600°C, batch autoclave.

600°C, 15 min	600°C, 30 min
H <sub>2</sub> = 84,7 %	H <sub>2</sub> = 87,8 %
CO <sub>2</sub> = 14,2 %	CO <sub>2</sub> = 11,5 %
CO = 1,1 %	CO = 0,7 %

The error related to percentage calculated from μ-GC results is 0.1%. As H<sub>2</sub>S was not quantified, a molar ratio of hydrogen to carbon dioxide amounts was defined. This molar ratio is equal to 2.2 and 6 at 450°C and 600°C respectively. The literature data show an efficient production of hydrogen but with a lower ratio. Sricharoenchaikul et al [82] obtained in capillary reactor, a ratio H<sub>2</sub>/CO<sub>2</sub> equal to 3.1 at 375°C, 1.9 at 500°C and 0.9 at 650°C for a

<sup>3</sup> OSC : Organosulfur compounds (organic molecules which contains sulfur such as thiols, polysulfides, thiosulfonates, thioethers...)

reaction time of 60 sec. Rönnlund et al. [72] obtained in continuous reactor a ratio  $< 1$ ; Cao et al. [53] obtained in continuous reactor at 450°C a ratio  $H_2/CO_2$  equal to 1.12 and at 600°C a ratio equal to 0.8.

This high hydrogen production confirms the gasification efficiency of the batch process developed by our experiments.

At 450°C, TOC removal from the liquid (Figure 65) equals 60% whereas it equals 95% at 600°C. Indeed, GC-MS analysis of the liquid at 600°C (Figure 69) confirms the presence of only few types of molecules.

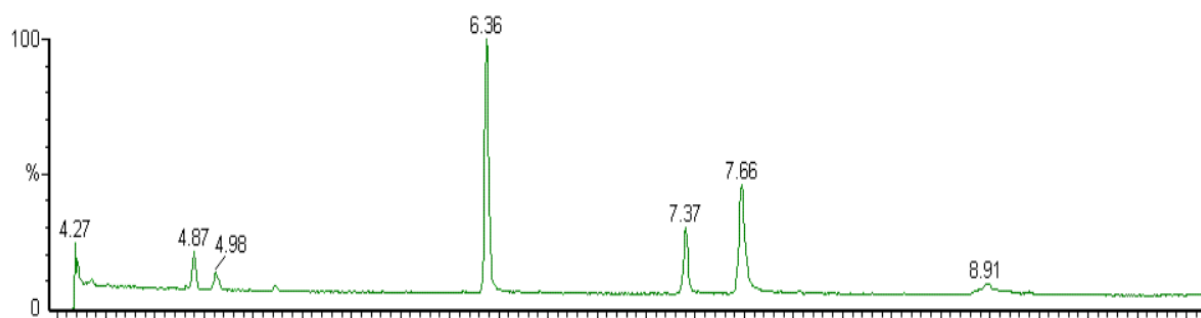


Figure 69: GC-MS of the liquid obtained at 600°C and 15 min of reaction time

The main molecules detected are: Phenol (6.36 min); 2-methyl-phenol (7.37 min) and 3-methyl-phenol (7.66 min). The composition of liquids after supercritical water gasification at 500°C, 600°C and 650°C was previously studied in the literature [100] and showed that phenol and derivatives are almost present in the solution above 500°C. Polymerization of phenolic compounds started immediately after production that conducts to the formation of a carbonaceous solid, namely hydrochar [58], [101]. The analysis of this solid phase was realized at high temperature (600°C). Figure 69 shows its surface as an example. The solid phase was mainly composed of carbon, oxygen and some minerals have been detected by EDX analysis. However, minerals do not play a role on the surface morphology [51].

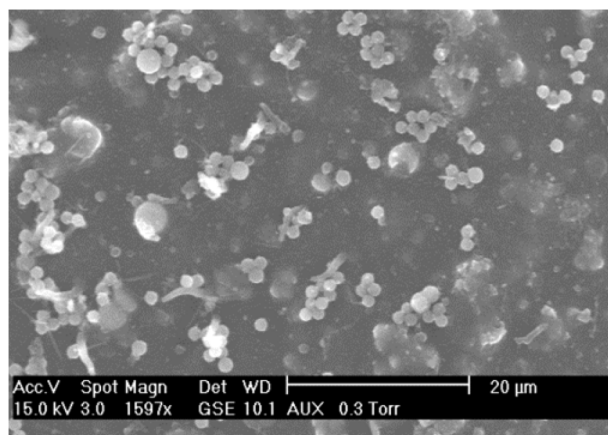


Figure 70: Solid obtained after 600°C 15 min of reaction time, 10 wt% of black liquor

In conclusion, efficient hydrothermal gasification is realized at high temperature range. In a short reaction time the amount of  $H_2$ , as well as its proportion in the gaseous phase, are of great interest. However, this high hydrogen content is simultaneously obtained with  $H_2S$ . This gas is toxic and the gaseous phase needs to be purified before subsequent use. Even at high temperature, the solid formation was not suppressed. The amount is low in the batch process but it is an issue to be considered. Salts, probably precipitated during the supercritical phase of the process, are redissolved in normal conditions (by cooling)

Considering medium temperatures, more organics should be recovered in liquid phase and  $H_2S$  production will be reduced or inhibited.

### III.2. Hydrothermal liquefaction

Hydrothermal liquefaction is basically carried out close to the critical temperature. Between 400°C and 500°C, TOC in the liquid falls from 80% to 20% of its initial value. By consequent, in this temperature region, organic content is expected to be particularly high. In the liquid, GC-MS analysis of the liquid obtained at 450°C, 15 min of reaction time is presented in Figure 70, and confirms a complex composition with a dominant presence of various phenolic compounds. Color of the liquid at 450°C is lighter (Figure 66). This attenuation is due to rings opening [72].

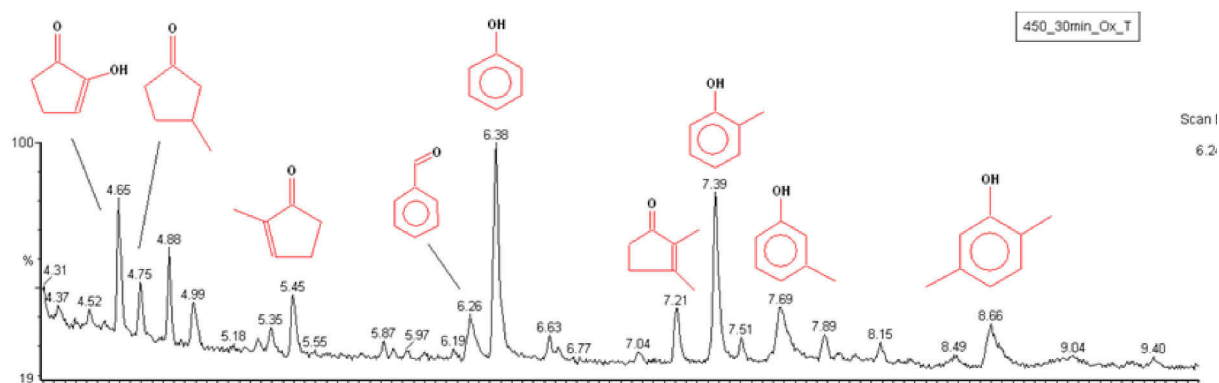


Figure 71: GC-MS analysis of the liquid obtained at 450°C, 15 min of reaction time

Main phenolic compounds represented in the Figure 71 are: (2-hydroxy-2-cyclopenten-1-one (4.65 min); (R)-(+)-3-methylcyclopentanone (4.75 min); 2-methyl-2-cyclopenten-1-one (5.45 min); phenol (6.38 min), 2-methyl-phenol (7.39 min) and so on). These molecules, despite of their diversity, are chemically interesting and are considered as building block molecules. A solution to recover the most interesting ones could be increase the selectivity of the process to increase their concentration, by modifying operating conditions. Indeed, as mentioned in chapter 1, water reactivity depends on temperature and pressure applied to the hydrothermal process. Then, use a membrane to separate the molecules.

The pH of the collected residual aqueous phase remains alkaline (pH>10). On the contrary, the pH of the outflow was measured in the neutral region in a continuous process [53]. The authors processed the pH measurement during the cooling step and showed that the pH was increasing. This phenomenon was due to the dissolving of alkaline salts which were deposited on reactor walls at supercritical conditions. In our batch reactor salts are dissolved during the cooling and thus before phase recovery. That could explain the alkaline pH measured in the final liquid after cooling.

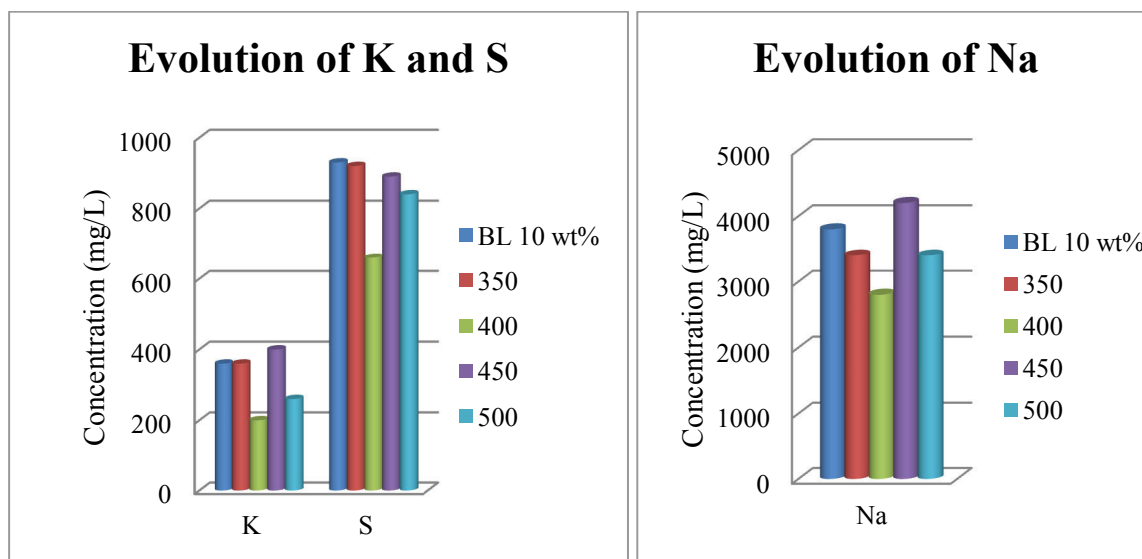
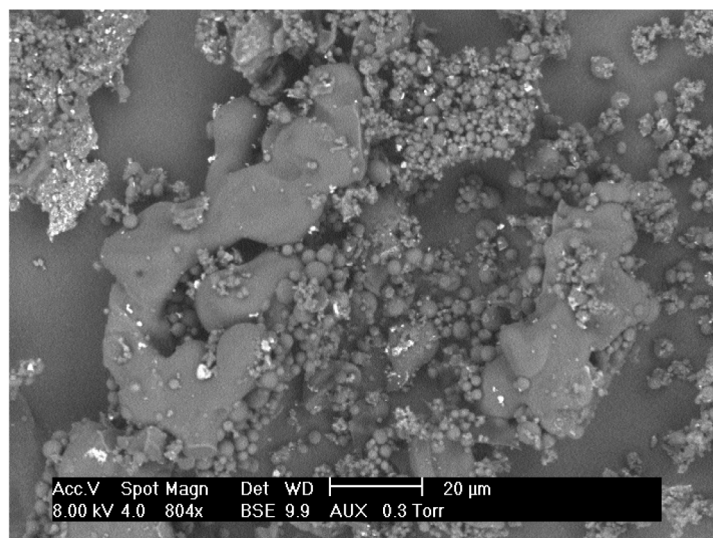


Figure 72: ICP measurements of the liquid obtained after hydrothermal conversion, 15 min of reaction time. The error related to ICP measurement is around 5 %.

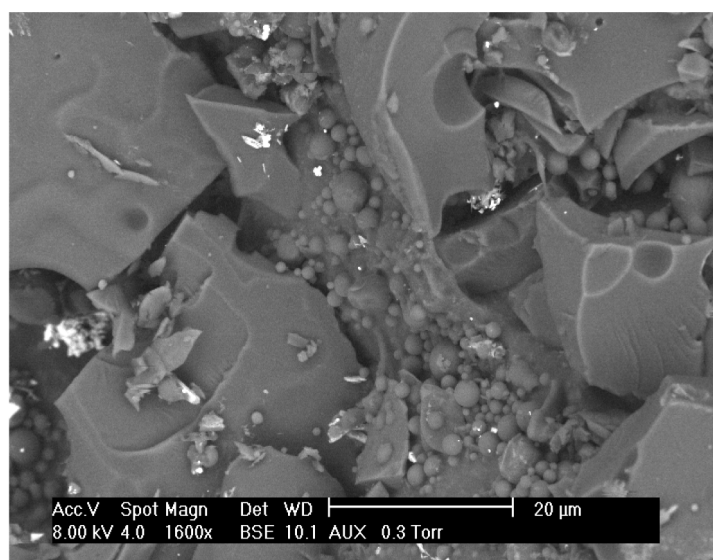
The salt concentrations were measured in the final liquid. Potassium, sulfur and sodium are the main inorganic components of black liquor, so their concentrations have been followed. Figure 73 presents the mass concentration of the salts in the liquid phase, compared to the initial solution of black liquor. Potassium, sulfur and sodium are not significantly transferred to other phases as the concentrations remain high in the liquid. Low diminutions observed in Figure 73 suggest a limited transfer of salts from the liquid to the solid phase as mentioned in the literature [100].

Figure 73 and Figure 74 show solids obtained at 450°C and 500°C, after 15 min of reaction time. Black parts of the pictures represent carbonaceous material while bright spots correspond to minerals. This result confirms the recovery of inorganic matter in solid phase.





*Figure 73: ESEM pictures for solid obtained at 450°C and 15 min of reaction time*



*Figure 74: ESEM pictures for solid obtained at 500°C and 15 min of reaction time*

Hydrothermal liquefaction is the objective of conversion at medium temperature range; the most part of organics is recovered in the liquid phase. The phenolic compounds are mainly recovered in an aqueous phase with the operating conditions investigated, and a complementary study is required to favor and increase selective building-block molecules. The separation of the different aromatic species from the collected liquid should be a challenge step. The formation of shapeless solid residue is not avoided using these operating conditions.

### III.3. Hydrothermal carbonization

Hydrothermal carbonization corresponds to processes performed at temperatures lower than 400°C. For this range of temperatures, no gas is quantitatively formed and hydrothermal carbonization reactions such as polymerization, demethanation, decarboxylation are favored [37]. During black liquor hydrothermal conversion, phenolic compounds polymerize together with aldehydes [58], [75], [23].

GC-MS analysis of the liquid obtained at 350°C and 15 min of reaction time, in Figure 75, shows two main peaks: 2-methoxy-phenol (7.88) mainly and 2-methoxy-4-methyl phenol (9.21). In addition to the high TOC measured, this result confirms that the degradation of black liquor has just started during this short reaction time.

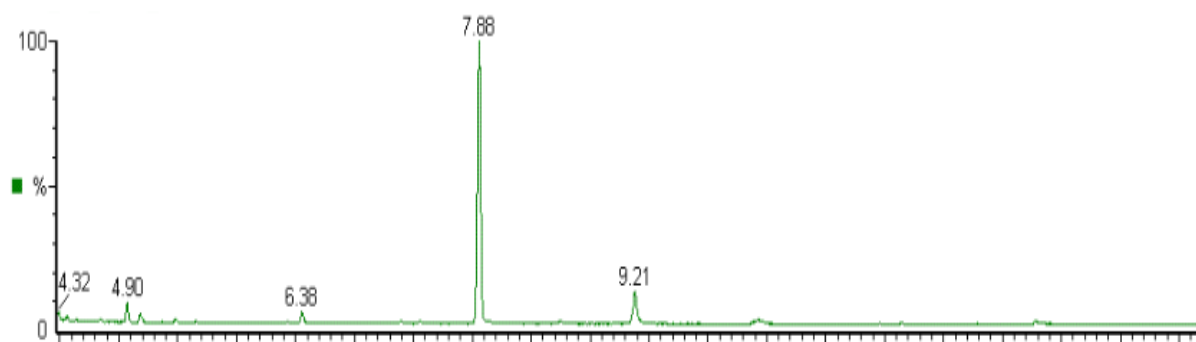
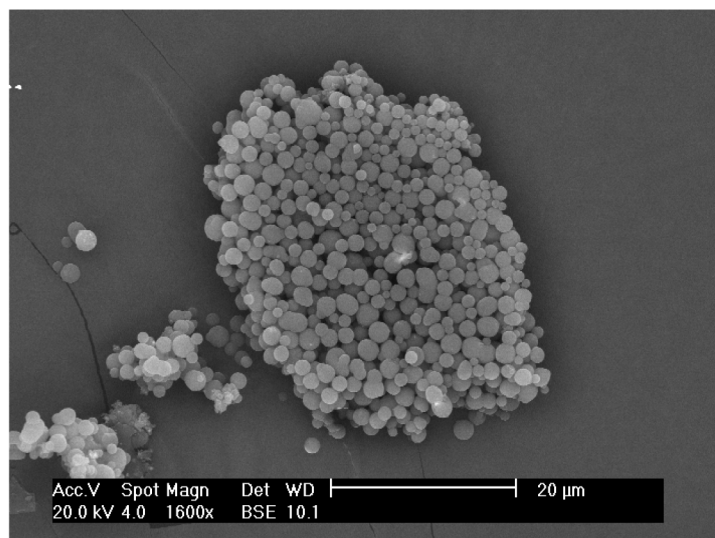


Figure 75: GC-MS analysis of liquid obtained at 350°C, 15 min of reaction time

At the end of experiments at 350°C, 15 min reaction time, two liquid phases are observed: a very low volume of oily phase and an aqueous phase. However only aqueous phase can be recovered and analyzed, the oily phase is too insufficient. Although the amount of oily phase is low, we suppose that it would contain high concentrations of organics such as phenolic compounds, furfurals etc, which are widely precursors of polymerization reactions [72]. After reaction, solid is recovered and filtered from liquid phase. Considering that TOC of the liquid is around 25% its initial value, the remaining carbon is recovered in the oily and in the solid phases.



*Figure 76: ESEM pictures for solid obtained at 350°C and 15 min of reaction time, 10 wt% of black liquor solution*

At 350°C, under subcritical conditions, the solid is composed of spherical microparticles as shown in Figure 76. The shape of the microparticles are supposed to come from the interfacial energies [72] of oil-in-water dispersion [39]. No minerals are observed on the solid using EDX detector.

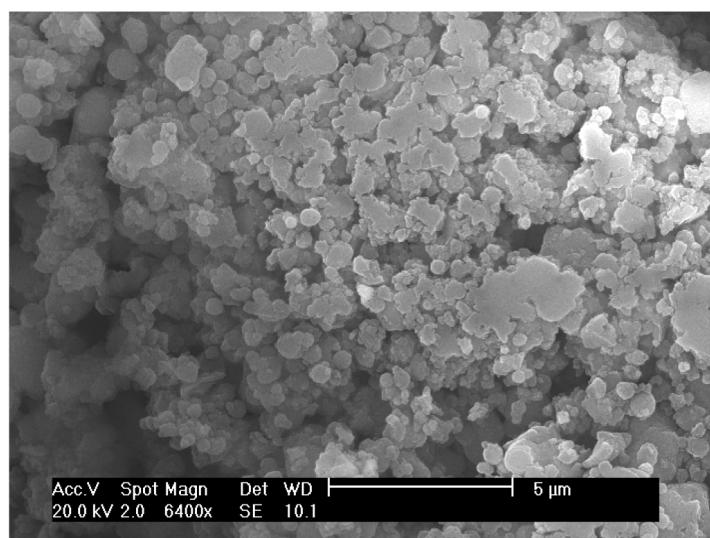


*Figure 77: ESEM pictures for solid obtained at 400°C and 15 min of reaction time with a 10 wt% black liquor solution*

Although the hydrothermal carbonization is not carried out to produce bio-oils, this phase seems to be required to obtain a specific shape, size and structure of the carbonaceous solid.

## IV. Conclusion & Prospects

### IV.1. Conclusion

Hydrothermal process revealed the formation of three phases. Among the different operating parameters investigated, the temperature controls the composition and distribution into the phases of the different species obtained by the hydrothermal conversion of black liquor (Figure 78).

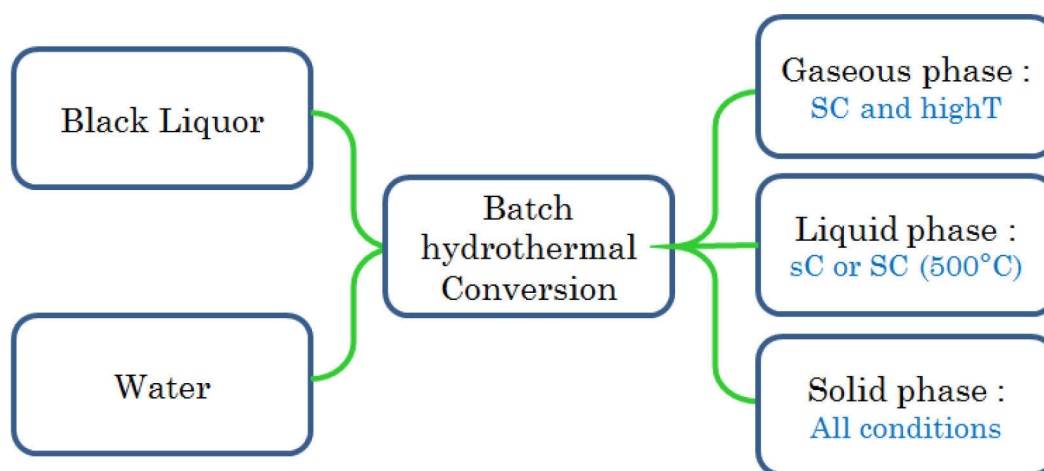


Figure 78: Summary on the presence of the phases

At high temperature a high proportion of hydrogen and a low proportion of CO<sub>2</sub> and the presence of H<sub>2</sub>S are revealed in the gaseous mixture.

At medium temperature, liquid-liquid conversion is favored and produced a mixture of interesting phenolic compounds such as phenol, 2-methyl-phenol (guaiacol), cresols. The proportion of carbon converted increased with temperature; meaning that a part of organic carbon was transferred to solid and/or gaseous phase. Minerals mostly remain in liquid phase while a slight amount covered the solid surface.

At low temperature, no quantitative gas formation is detected; liquid phase is still enriched in organics and black liquor begins to be degraded into lower phenolic compounds. These latter are automatically used to produce carbon microspheres in an oil-water emulsion. So, the solid recovered presents an interesting morphology, and would be valorize as useful material, according to the literature [102], [37], [103].

Whatever the reaction temperature, solid is always observed after reactions as shown in Figure 79. Carbon-based microparticles are only obtained at subcritical conditions as regards

to the range of reaction temperature. The morphology evolves from microparticles at 350°C to shapeless structure under severe conditions. The structure becomes denser and could be due to an evolution of microparticles by sintering or agglomeration of particles over the range of temperature.

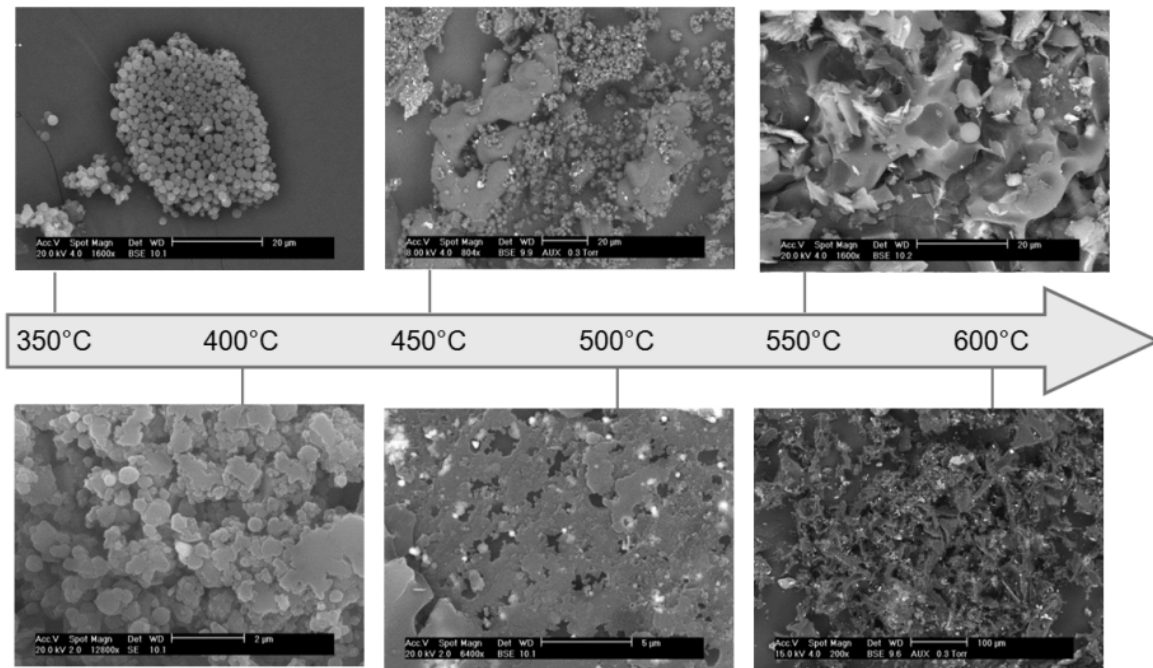


Figure 79: ESEM pictures of solid residue obtained after filtration of reaction media

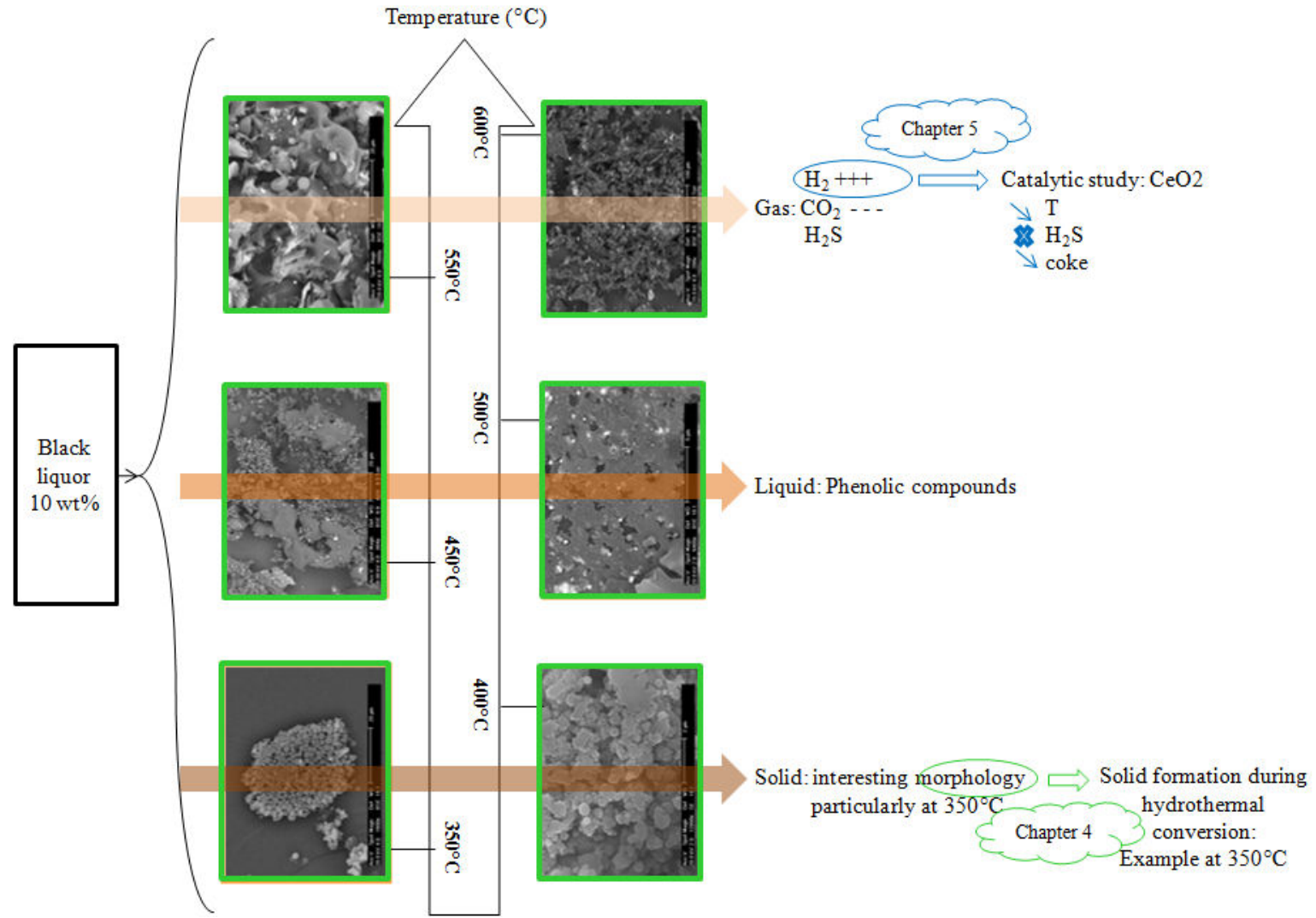
## IV.2. Prospects

These preliminary experiments, performed at small scale in stainless steel batch reactor, highlight that black liquor is converted into valuable compounds. However, two main observations have to be taken into account:

1) Solid is formed during hydrothermal conversion whatever the conditions, but proportions are changing. Coke formation is a huge problem in continuous as batch processes. In continuous process the formation of coke is responsible of partial or total plugging of pipes. In batch reactor, coke development alters reaction media. If coke is formed along the walls, the catalyst effect of these latters is diminished. If salts are quantitatively trapped inside coke, pH and chemical equilibria are modified and some reactions favored. Given that, a better understanding of the coke formation during hydrothermal conversion of black liquor is a good way to avoid and optimize the process. As presented in the chapter, the preliminary experiments confirm the interest of the black liquor as raw material to study coke formation as organic and mineral matter. The following chapter is dedicated to the solid formation under subcritical conditions at 350°C, regarding also valorization options of this material.

2) High amount of hydrogen is produced at 600°C and its ratio to CO<sub>2</sub> is significantly high. However, this temperature appears too high to develop an industrial process taking into account the corrosion and other technological difficulties, so it could be interesting to investigate quantitative hydrogen formation at lower temperature. In addition, if coke formation could be avoided, the black liquor conversion would be interesting for continuous process. Thus a catalytic study becomes interesting, especially using a nanocatalyst whose size is significantly lower than the diameter of continuous plug flow reactors. Chapter 5 will present these investigations using CeO<sub>2</sub> nanocatalyst.

### V. To remember the chapter



## Chapter 4: Study of particles generation





## **Résumé du chapitre 4 : Etude de la génération de particules**

L'objectif de ce chapitre est d'étudier la formation de solide, pour cela, nous nous sommes placés dans des conditions opératoires nous permettant de suivre au mieux l'évolution de sa formation ; c'est-à-dire nous placer dans des conditions pour lesquelles le solide est homogène et de morphologie connue : à 350°C, en conditions subcritiques pour des temps de réaction allant de 15 min à 24 h ; la pression en conditions subcritiques est auto générée et vaut 16,4 MPa. Dans ces conditions de température, la carbonisation hydrothermale est prépondérante par rapport aux autres processus (gazéification et liquéfaction). C'est un chapitre dense, la théorie s'y rattachant est placée en tête de chapitre.

Nous avons étudié dans ce chapitre l'effet du temps de réaction sur la morphologie du solide puis nous avons expliqué les phénomènes identifiés. Ce chapitre se divise en 5 grandes parties : une partie sur la théorie de la formation de solide et la carbonisation hydrothermale, une deuxième sur le choix des conditions opératoires, une troisième sur l'effet du temps de réaction puis une quatrième sur l'explication de ce qui est observé et enfin l'influence de la rampe de montée en température et le refroidissement sur la morphologie du solide en réacteur batch.

Pour ce chapitre un résumé global sera fait et non partie par partie.

La partie théorique révèle que la formation de solide peut se reposer sur 2 théories : celle de Brooks et Taylor et celle d'Inagaki. La bibliographie nous apprend également que le solide résulte de la polymérisation des composés phénoliques avec des molécules plus petites telles que le formaldéhyde, servant de connecteurs entre deux molécules phénoliques. Ainsi toutes les discussions se basent sur l'étude des phases liquides et solides.

Le liquide et le solide obtenus après réaction sont récupérés à pression et température atmosphérique. Même si le chauffage rapide et le refroidissement rapide sont utilisés pour avoir une meilleure représentation de l'influence du temps de réaction, il est très difficile de savoir précisément distinguer les phénomènes impliqués dans chaque étape.

Les informations apportées par l'analyse de la phase liquide et solide peuvent être résumées comme suit :

\*\*\* Trois étapes peuvent être identifiées au cours du processus de la formation solide :

De 15 min à 90 min : des particules isolées sont formées, ensuite la croissance des particules se produit et enfin la coalescence. Entre 2 h et 4 h : des blocs carbonés sont identifiés. Aucune

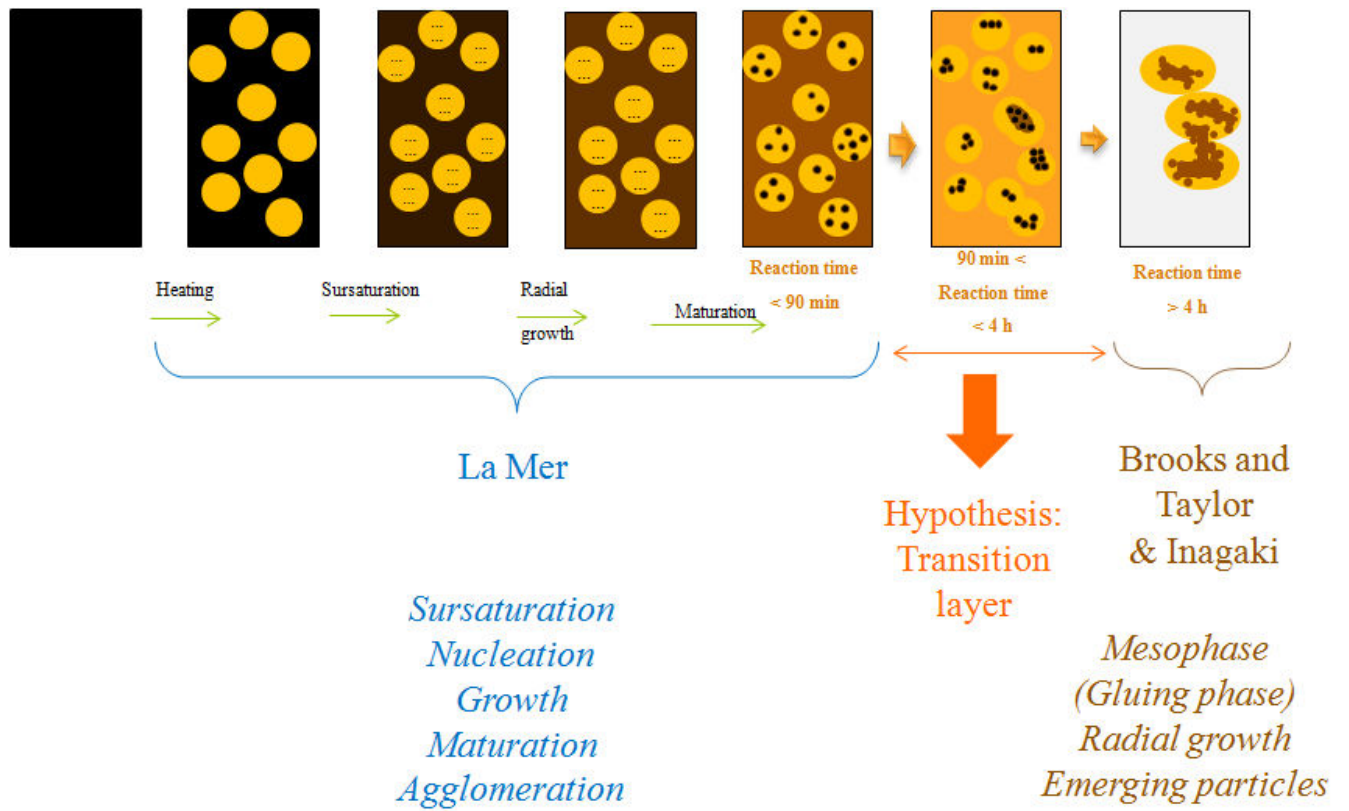
sphère n'est observée. Dès 6 h : les particules semblent émerger d'une couche. Cette couche semble être un support continu qui est solide à température et pression atmosphériques. Cette couche est donc probablement visqueuse pendant la réaction.

\*\*\* La composition élémentaire montre que le degré d'aromaticité augmente avec le temps de réaction. Ce point est confirmé par l'analyse ATG ce qui suggère que les solides ne présentent pas les mêmes fonctions chimiques ou organiques en fonction du temps de réaction appliqué. Les solides présentent de plus une coque hydrophile qui est observée.

\*\*\* La composition du liquide change rapidement et n'évolue plus significativement pour des temps de réaction longs, ce qui suggère que les modifications morphologiques de la phase solide sont dues à un réarrangement physique.

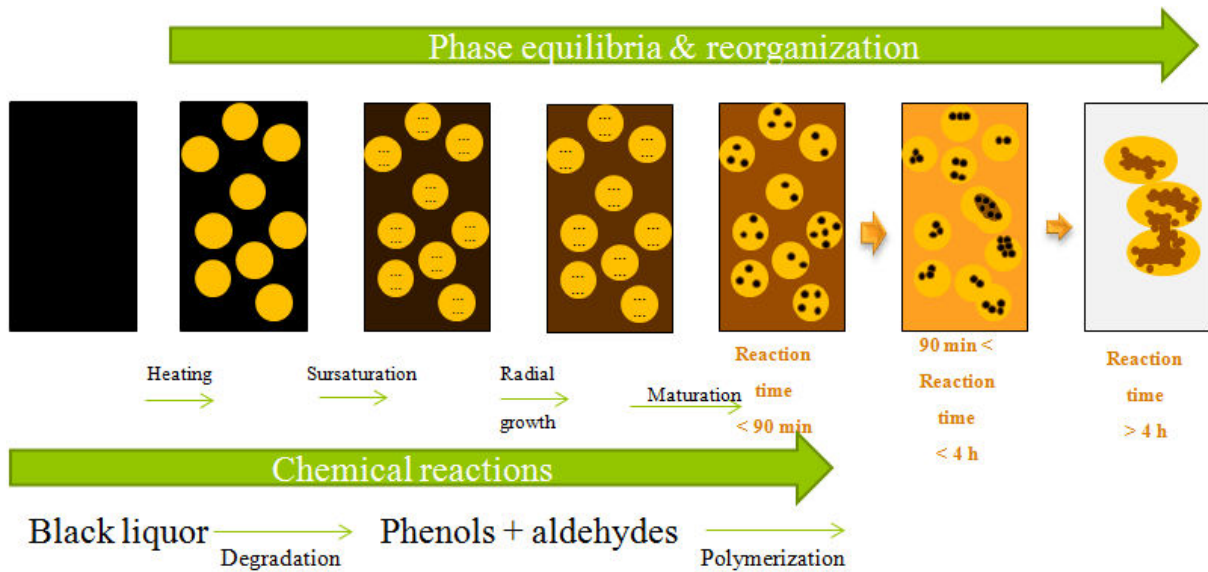
La confrontation avec la littérature suggère que dans un premier temps les composés organiques de la liqueur noire se décomposent en composés phénoliques et aldéhydes qui se regroupent puis polymérisent en une matière solide carbonée. Les particules obtenues à court temps de réaction dans nos expériences sont similaires à ceux obtenus par Titirici. Au contraire, certains auteurs, comme Ayache ou Inagaki et al. considèrent que les particules carbonées sont créées à partir d'un support continu en changeant d'aromaticité, ce qui traduit la morphologie du solide pour de longs temps de réaction. La notion de mésophase est introduite par Ayache et Inagaki pour traduire la phase « solide-liquide » dans laquelle se forment les particules. Ces deux théories suggèrent des mécanismes de formation différents mais les deux mécanismes semblent expliquer l'évolution de la morphologie solide dans nos expériences. En fait, les mécanismes chimiques et physiques impliqués dans la conversion hydrothermale de la solution de liqueur noire coexistent et fonctionnent avec des cinétiques différentes tout au long du temps de réaction. De plus, l'étape de refroidissement, quelque soit sa vitesse, a une influence inconnue sur les caractéristiques du solide. Une couche de transition est formée, au sein des gouttelettes de phase organique, entre la phase organique et les particules carbonées. Cette couche est à considérer comme un réservoir de sous-unités « phénols- formaldéhydes ».

On peut résumer toute la formation du solide avec les schémas suivants :

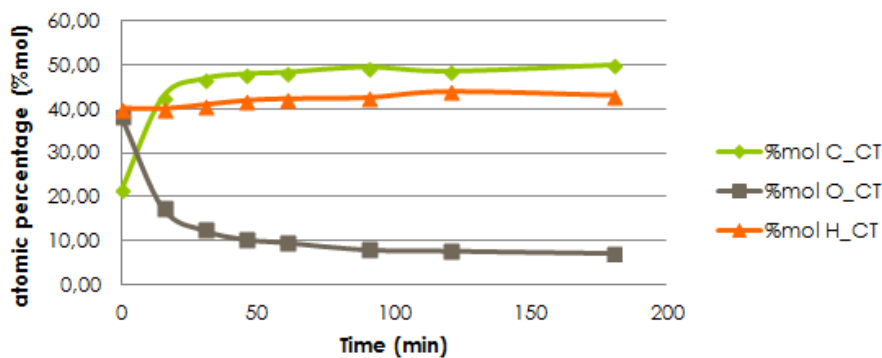
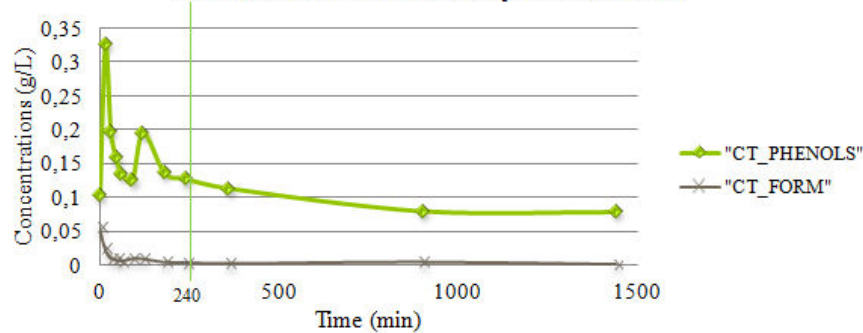


V.K. La Mer, *Ind. Eng. Chem*, vol. 44, 1952

M. Inagaki, et al., *New carbon matter*, 2010



**Phenols and Formaldehyde evolution**



La rampe de chauffe et le refroidissement n'influent que sur la taille des particules et n'agit pas les phénomènes mis en jeu.

Ces particules présentent un certain nombre d'applications présentées par le professeur Titirici et mentionnées dans la partie perspectives de ce chapitre.

**\*\*\* Fin du résumé**

As explained in Chapter I, the formation of solids has to be avoided in continuous hydrothermal processes of gasification or liquefaction. On the contrary, hydrothermal carbonization concerns the generation of solids with controlled properties. Therefore, the understanding of phenomena that occurred in solid formation under pressure is fundamental to optimize the hydrothermal conversion of raw materials. Alkali salts deposition and coke formation are the most important issues in hydrothermal processes at high pressure as it results in the corrosion of material and reduction of heat transfer efficiency [73].

Thus this chapter is focused on the solid formation during hydrothermal conversion of black liquor. Two points are discussed:

- Mechanism of solid formation in view to better understand phenomena involved in continuous processes: use of subcritical conditions to limit salts precipitation and study of the impact of heating and cooling rate
- Influence of operating conditions on solid carbonaceous properties (morphology, physico-chemical properties...) in subcritical processes to improve knowledge about hydrothermal carbonization research subject presenting more attention this last decade

Hydrothermal carbonization has common features with coalification, explanations of some phenomena can be found in the coalification theory [104].

### **I. Theory of coke generation**

The solid generated by hydrothermal processes, called hydrochar or coke, is formed by the polymerization of components from liquid phase [105], [75]. The characteristics of this solid are directly linked to the molecules formed during degradation of the initial raw material. Black liquor is a complex mixture of lignin-based molecules. Studies about lignin ([73], [58], [75]) have shown that under sub/supercritical conditions, the decomposition of lignin forms phenolic aromatics compounds and aldehydes. These two molecules are then involved in polymerization reactions, where aldehydes connect the aromatic structures. Generally a reactive mixture of aromatic and aliphatic hydrocarbons causes polymerization[106].

The first study made on carbon residue generation was conducted by Friedrich Bergius in 1911 [107]. He studied carbon gasification, at high temperature ( $T > 900^{\circ}\text{C}$ ) and high pressure ( $P > 20 \text{ MPa}$ ), without CO generation according to the reaction  $C + H_2O = CO_2 + H_2$  [103]. He discovered that the formation of solid residue from biomass agreed with coalification (natural process occurring over millions years). From these observations, he concluded that the best conditions to form solid were to create an intimate

link between biomass and water at low temperature ( $\sim 200^{\circ}\text{C}$ ) in a pressurized reactor to avoid the decomposition into gases.

From the first Bergius's experiments until 90's, numerous researches have been performed considering coal formation. The renewed interest in solid formation using hydrothermal conversion dates back to few decades ago with Qing Wang et al.'s works [108] on particles generation from glucose. The interest on this subject keeps growing nowadays.

Coke formation is due to physico-chemical processes involved, as well as phase equilibrium as discussed in the following paragraphs.

### **I.1. Carbonaceous solid generation: reactions involved**

During hydrothermal carbonization, solid formation occurs according to temperature and pressure conditions that involve degradation reactions. Reactions firstly occur in liquid phase and then in solid phase as follow [62], [109]: hydrolysis, dehydration, fragmentation, decarboxylation, polymerization and condensation, polymer aromatization, nucleation and then particles growth or disappearance. Reactions such as dehydration and decarboxylation lead to high degree of aromaticity in the solid residue, and explain its important amount of carbon content. A gaseous phase is also formed, especially obtained for long reaction time as a result of, inter alia, decarboxylation and demethanation reactions. However, depending on the feedstock and thus kinetics, the hydrothermal carbonization will follow a precise mechanism pathway [110]: if the components react quickly, at low temperature, fines spherules will precipitate; if the components react slowly, mesophase<sup>4</sup> spherules precipitate.

Effects of alkali salts of the black liquor in the solid formation have been studied ([111], [112]). Minerals are intercalated in the lattice of amorphous carbon during carbonization, which promotes the reaction of gasification and create porosity into the char particles.

Reactions involved are not only responsible of carbonization thus the phase equilibrium has to be taken into account. The following part is devoted to particles generated by hydrothermal carbonization.

### **I.2. Particles generation: phase equilibrium**

It is well known that hydrothermal carbonization, which reproduces the natural process of coal formation [103], [113], takes place at low temperature ( $130^{\circ}\text{C} - 250^{\circ}\text{C}$ ) and self-generated pressure. It typically generates micro particles which can have interesting textural,

---

<sup>4</sup> The term of "mesophase" is used to describe an intermediate media describes as "liquid-crystal" hydrocarbon

morphological or physico-chemical applications [103]. However, a lot of studies deal with model molecules such as glucose, starch but rarely with real material or wastewater.

Brooks and Taylor as explained in [106] worked on particles generated by hydrothermal carbonization and introduced the concept of mesophase particles formation during carbonization. Indeed, they have shown that the microsize solid particles obtained by carbonization came from the solidification of mesophase microspheres. This mesophase is an intermediary state between a liquid and a solid but it has liquid properties. Walker [110] considered that mesophase properties depend on:

- “The extent of planarity of intermediate molecules,
- Rates of carbonization,
- Fluidity of the phases and mesophase,
- Solid effect on mesophase formation and coalescence.”

Reactions occurring during thermal decomposition and carbonization processes depend on the interface between carbonaceous particles and the surrounding phase. This interface modifies the texture of the resulting particles. According to the annex 3, under pressure carbonaceous solid has a spherical shape because of liquid/liquid interface which minimizes interfacial energy between the two phases [114].

Based on the theory of Brooks and Taylor, other authors ([115], [116], [106], [117], [118]), completed the mesophase theory, considering that carbonaceous microspheres formed under pressure have a radius texture. It means that the aromatics based structure of the solid material is built following the radius of the particles. Then, the aggregation of particles to each other occurs due to a thin layer of plastic phase with the same constitution of aromatics structure. When spheres are covered by the plastic layer, a continuous media is formed and apparently only the viscous phase is seen. Then, new nucleation occurs as new spheres are coming from the demixing of drops from the plastic layer. The demixing is driven by a change in aromaticity degree of the carbonized precursor that suggests emergence of particles from the plastic layer [115]. Inagaki followed Brooks and Taylor’s theory and mentioned that carbonization mechanism and, as a result, carbonaceous structures, is based on its precursors and heat treatment conditions [118].

Inagaki introduced the importance of precursors in carbonization process and initiate the concept of BSU (Basic Structural Unit) for the creation of particles coming from the plastic layer. BSU is the first stable size of polymer (stable structure having the smallest number of monomers) that organizes carbonaceous particles by connecting together. Thus, once



organized, BSU, are able to build particles. The addition of BSU (growth of particle) under pressure is made following the radius of the particles [117], and increases the aromaticity of the particles. The size of particles is defined by the critical radius which allows a permanent existence of the particles. Particles with a smaller radius will disappear by evaporation or coalesce. Even for the particles with a large radius, the evolution in supercritical conditions is to evaporate or to coalesce.

To complete the “mesophase theory”, Azami et al.[119] have shown that the mesophase formation at the origin of spherical particles follows the Arrhenius equation. The mesophase formation is seen as an autocatalyzed process because its formation promotes the stacking of others molecules in the matrix. This mesophase is built as followed, assuming to the authors:

- “Generation of mesogen (precursor of mesophase) with aromatic molecules inside,
- Diffusion of mesogen to build the mesophase through an isotropic phase,
- Rearrangement into the mesophase, by condensation reactions, to build bigger molecules. These reactions lead to molecules with a distribution of molecular weight.”

Hydrothermal carbonization results in particle generation and a lot of researchers have tried to understand this general theory such as La Mer[120] which presents another viewpoint. His work synthesizes studies of others contributions (J. W. Gibbs, Ostwald, Farkas, Frenkel, Volmer, Becker and Doering) about the nucleation in phase transition [120]. Indeed, from La Mer, “nucleation is a process of generating within a metastable mother phase the initial fragments of a new and more stable phase capable of developing spontaneously, into gross fragments of the stable phase.”

From La Mer theory [120], solid particles are generated in the liquid phase from a nucleus created by local oversaturation in the liquid. It can be seen as molecules with an excess of surface energy sufficient to produce the aggregate as a new phase in the presence of the mother phase. Reactions lead to an incompatibility in the liquid phase resulting in a liquid separation and solid formation follows the formation of the new phase either by liquid-phase separation or by flocculation. This immiscibility leads to the formation of dispersed anisotropic droplets in the liquid phase. The interface between the two phases has to be seen as transition layer where properties of this layer evolve from liquid phase to solid phase progressively; and not as an abrupt surface. Some of the formed particles can disappear, other, on contrary will growth. From Kruse et al. microspheres particles formation starts at 180°C and the presence of lignin increases the homogeneity and the purity of microspheres [109].

In both theories, operating conditions such as temperature and reaction time are extremely important during hydrothermal carbonization. Fang et al. [121] have performed experiments at 410°C and 350°C in diamond anvil cell and studied the influence of heating rate. In particular, during slow heating at 350°C, they have shown that around 250°C, gas bubbles formed during the ebullition disappeared and a huge amount of particles precipitated. At 280°C the cell is entirely filled with black microparticles. After reaction, three phases are obtained: an oily orange film, and aqueous liquid phase and solid phase at the bottom of the cell. The same phases have been observed by Modell et al in the 1970's after their experiments on forest products [122].

Inagaki has exposed that during the cooling, non-condensed phase containing the dissociated units serves as gluing material linking particles together.

In conclusion, operating conditions are very important during batch hydrothermal carbonization, influencing the repartition of phases, as well as their chemical and physical characteristics. If general behavioral trends are expected, the real mechanism in batch reactor during reaction is more difficult to be identified. The mechanism is a compromise between physical considerations (creation of spheres) and chemistry (polymerization reaction).

Many parameters are of interest to study particles generation. in our project the influence of heating, cooling rate and reaction time in batch reactor has been chosen.

## II. Summary of operating conditions selected and methods

The previous chapter has shown that solid phase represents  $\sim 20$  wt% of the total initial carbon and has a morphology evolving from micrometer spherical particles, at  $350^\circ\text{C}$  and self-generated pressure, to shapeless structure under severe conditions. Carbonaceous microspheres are only obtained at subcritical conditions as regards to the range of reaction temperature. The formation of these microspheres is promising considering their possible applications (see section VI. 2 in this chapter).

As operating conditions influence solid morphology and, consequently, its applications, experiments have been performed for a better understanding of the solid formation.

To optimize the control parameters, a preliminary work has been performed [123] (annex 4) in our laboratory. As observed, the most influencing parameters are, for a fixed temperature: reaction time, heating and cooling rate.

This chapter is devoted to the study of the impact of these three parameters.

To sum up, 5 mL reactors are filled following the procedure explained in the chapter 2. The temperature of experiments is  $350^\circ\text{C}$ ; the pressure is self-generated and equal to 16.5 MPa, considering vapor-liquid equilibrium. The weight of 10 wt% black liquor solution introduced for experiments at  $350^\circ\text{C}$  is 3.1624 g. Studied parameters are summarize in Table 9.

Table 9: Summarize of operating conditions

Influencing parameter	Range of study
Reaction time	[15 min -24 h ]
Heating rate	$20^\circ\text{C}\cdot\text{min}^{-1}$ (C) $40^\circ\text{C}\cdot\text{min}^{-1}$ (N)
Cooling rate	Quench (T) : $\sim 1$ min Ambient air (L) : $\sim 30$ min

The abbreviations for the furnace operating conditions are written on the Figure 80 for memorizing: C or N describe the type of oven; T or L describe the type of cooling

C is noted to define the chromatography oven

N is for the brand of the other oven (Nabertherm)

T is for cooling by quench (“Trempe” in French)

L is for slow cooling (“Lent” in French)

The focus is made on CT experiments (rapid heating and rapid cooling) to approach continuous process in case of coke formation. Then the influence of heating rate and cooling

rate are investigated because hydrothermal carbonization is usually performed in batch reactor. To finish, solids are characterized. Investigated reaction times are 15 min, 30 min, 45 min, 60 min, 90 min and also 2 h, 3 h, 4 h, 6 h, 15 h, 18 h, and 24 h.

Eight reactors have been placed in parallel. Six were filtered after reaction to separated solid and liquid and two were immediately submitted to a granulometric analysis.

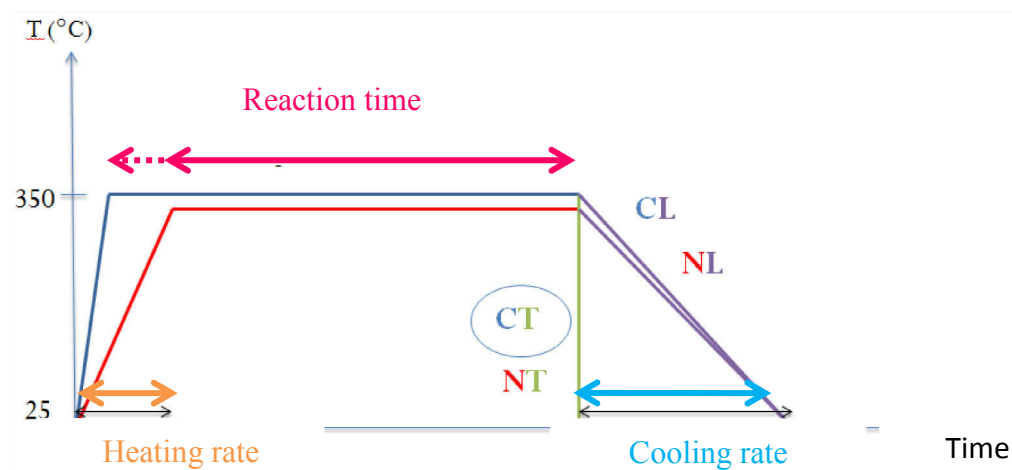


Figure 80: Temperature profile

### III. Effect of reaction time on the solid formation

This section is devoted to the influence of reaction time for the CT series (rapid heating and rapid cooling). These conditions would be suitable to recover particles size with morphology of solid as close as possible to the reaction, avoiding processes of shape change during cooling. Indeed, a very rapid cooling allows limiting the rearrangements of the particles (growing, disappearance, and so on). After cooling, solid and liquid are separated to be analyzed, solid is weighed. The Table 10 centralized solid mass for some reaction times.

Table 10: Masses introduced in 6 reactors, weight of solid recovered by filtration and overpressure measured during opening of reactors. The errors related to mass is 0.1 mg.

Reaction Time (min)	30	60	90	240 (4 h)	900 (15 h)	1440 (24 h)
Initial organic mass (mg)	305.5	305.5	305.5	305.5	305.5	305.5
Solid mass (mg)	46.4	39.3	55.7	40.7	31.3	26.8
Overpressure (bar)	0	0	0.04	0.08	0.1	0.125

The mass of recovered solids increases until 90 min and then decreases. Experimentally, the filtration of the solid obtained at long reaction time present technical problems. An oily phase appears during the reaction and its proportion increases with reaction time. This observation

has been also made in the literature [124]. Therefore the oil phase alters the complete recovery of the suspension in the reactor and the mass of solid recovered is underestimated.

The solid recovered was analyzed by ESEM and pictures are shown in Figure 81, for the same previous selected reaction times.

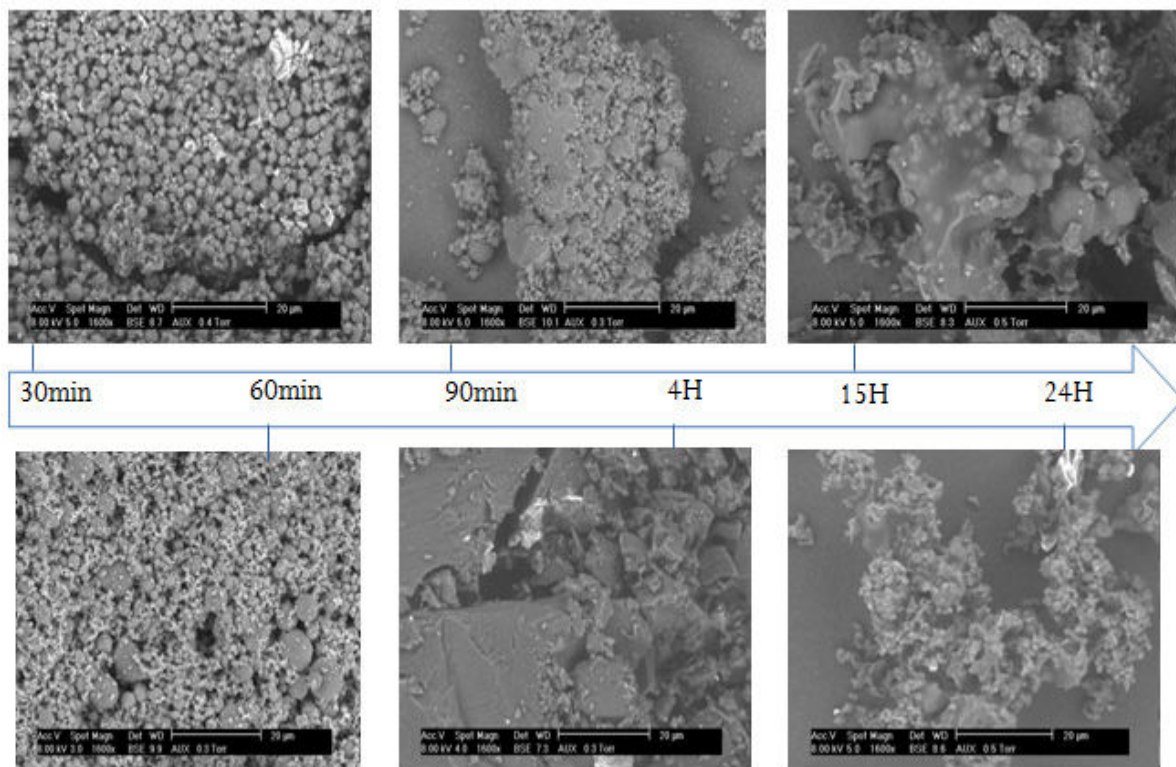
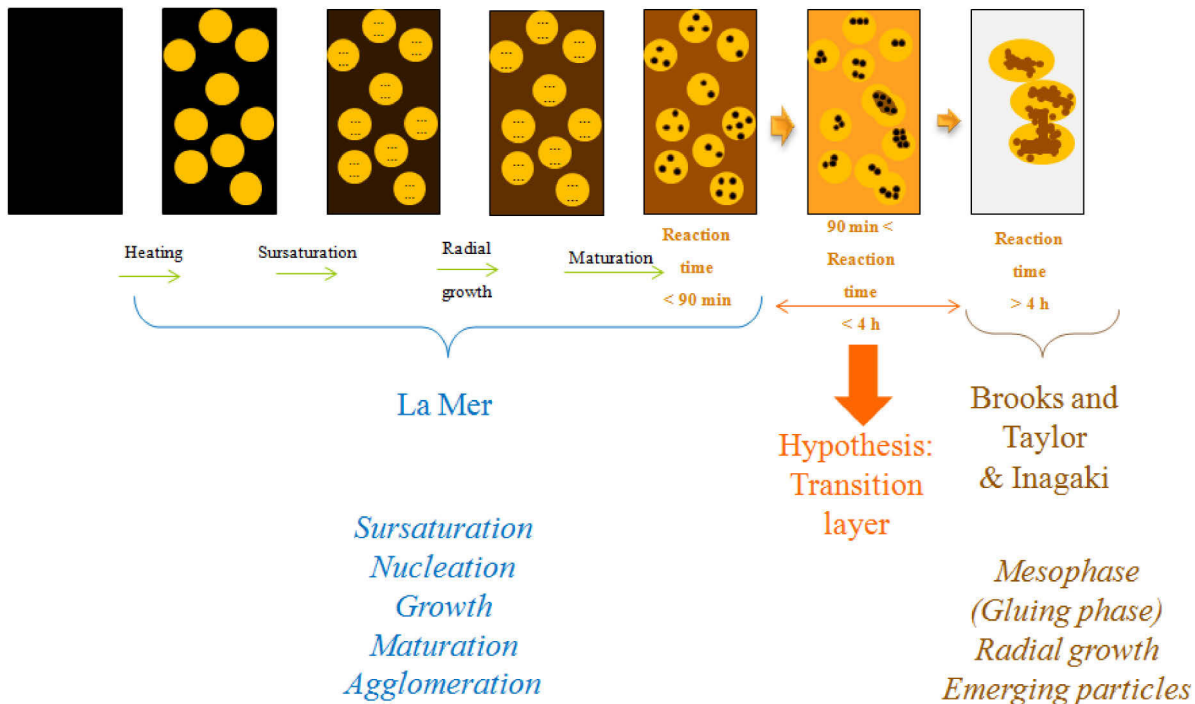


Figure 81: ESEM pictures of solids obtained by CT experiments, same magnification.

Particles obtained at 30 min are spherical with an average diameter size of 3  $\mu\text{m}$ . These particles grow with reaction time to reach the average diameter size of 7  $\mu\text{m}$  at 60 min. These particles are covered by others fine particles (average size of 250 nm). At 90 min, the particles continue to swell into agglomerates whose shape is not spherical. 90 min is the limit in reaction time where isolated particles are still noticed, then the accretion (or coalescence) of particles dominates. This deformation of morphology increases with longer reaction time. Between 2 h and 4 h, the solid appears as blocks. From 6 h to 24 h, the recovered solid is agglomerated and has no specific form. For long reaction time (from 15 h in the figure 2), spherical shapes are distinguished once again. These particles seem to emerge from a continuous media. This observation has also been made by Ayache et al. [115] and Inagaki et al. [117]. The solid obtained appears to be composed of fine particles coated with a "film". The confrontation between our solid evolution and carbonization theories is summarized in Figure 82; the yellow circle represents the oily phase droplet formed during reaction. To

ensure continuity between them, we propose a hypothesis. Part IV of this chapter is devoted to its justification:



*V.K. La Mer; Ind. Eng. Chem, vol. 44, 1952*

*M. Inagaki, et al., New carbon matter, 2010*

Figure 82: Confrontation between carbonization theories and our solids evolution.

To complete this observation and have global information about the suspension, particles size distribution has been obtained by laser granulometry and are presented Figure 83.

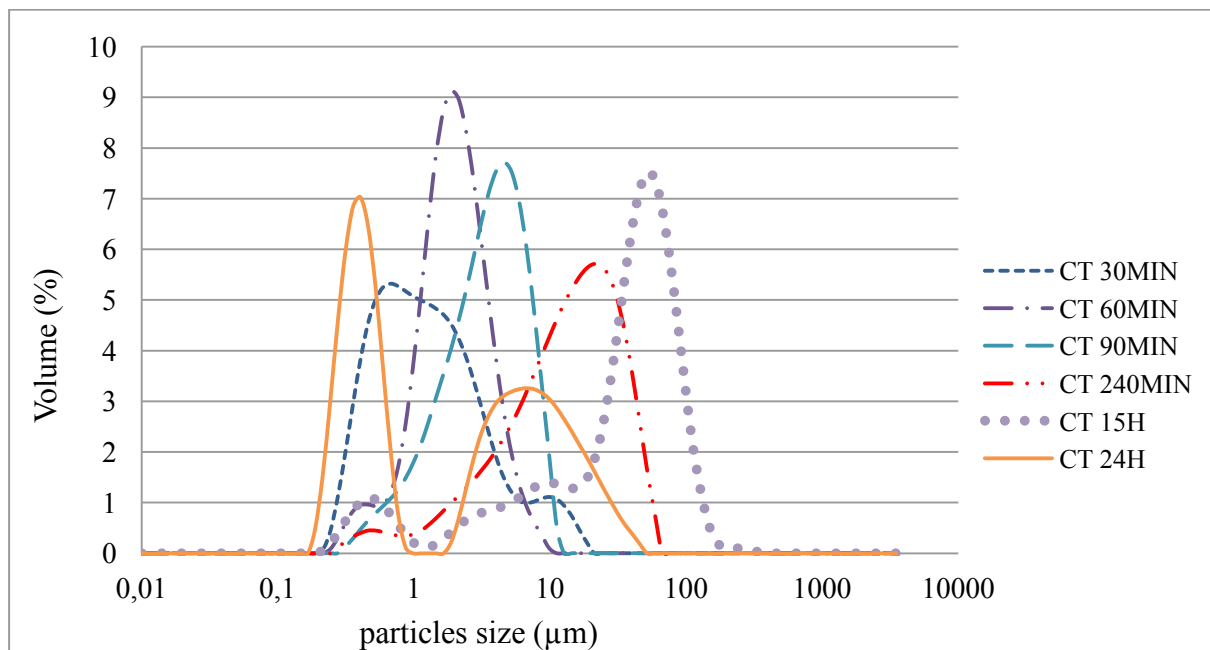


Figure 83: Size distribution for the solids obtained by CT experiments.

Between 30 min and 15 h, the average particle size increases from  $\sim 2 \mu\text{m}$  to  $\sim 80 \mu\text{m}$ . However, for 4 h (240 min) and 15 h of reaction time, in addition of the main peak, another class of particles has been identified at  $0.2 \mu\text{m}$  and  $10 \mu\text{m}$  average size. The class at  $0.2 \mu\text{m}$  was also identified at 4 h reaction time. Its corresponding volume, relative to the total volume, is low but increases over reaction time. On the contrary two medium sizes are clearly obtained at 24 h of reaction time. The volume of the very fine particles becomes predominant while the peak representing the largest particles is refined.

Until 90 min, this observation is consistent with ESEM pictures. However, for longer reaction time, a consideration has to be taken between the analysis of isolated particles and the analysis of agglomerated particles which are identified for particles size  $> 10 \mu\text{m}$ . In addition, the possibility of a new nucleation could explain the peak at  $0.2 \mu\text{m}$ .

#### Confrontation with literature:

ESEM observations and size measurements indicate that the particles and agglomerates sizes, as well as the solid morphology, are influenced by the reaction time. Particles are generated at short reaction time, then form patches at 4 h reaction time, when coalescence process becomes important. Then particles emerge from a continuous media at longer reaction times.

First of all, ESEM pictures were taken after reactor cooling and liquid filtration. So, we cannot absolutely avoid artifacts due to this procedure. However, observations resonate with literature.

According to the La Mer model [120], longer the process time is, bigger are the particles and more heterogeneous becomes their size distribution. These observations confirm that reaction time is an influencing parameter for particles generation and rearrangement of their distribution [103]. Similar morphology as for 15 h reaction time have been observed by Titirici et al. [125] for hydrothermal carbonization of C-maltose and C-sucrose.

An oily phase and an aqueous phase are observed in the experiments performed at  $350^\circ\text{C}$ , that agrees with the literature [109]. Under subcritical conditions, the oily phase is dispersed into the aqueous phase like oil-in-water emulsion, with a spherical shape to minimize interfacial energies. At this step of the study, one hypothesis considers microparticles generating inside the dispersed organic droplets and then become solid during cooling. The remaining organic phase is recovered at the top of the reactor after cooling. Consequently, organic phase contains precursor of polymerization reactions: phenol and formaldehyde that can generate nuclei of particles. However, Ayache et al. [126] have shown that during

carbonization, two organic phases are created simultaneously with a morphology depending on the reactor section: a thin layer phase and a spherical phase. Depending on the reactor section, a thin layer phase and/or a spherical phase are observed. When both phases are present, they are mixed and the solid residue looks like particles embedded into a plastic thin phase. In this case, the aggregation between two spheres is not due to the coalescence between them but due to the adhesion by a thin layer. Rahmani et al. [127] explained that during coalescence, active dispersion forces as well as Brownian, hydrodynamic and surface forces act as the driving forces for the droplets to merge. A high viscosity of the phase existing between droplets will inhibit the transition to a single spherical droplet.

As shown with the solid analyses, the morphology seems to be the most impacted property by the reaction time, as the mass of solid is experimentally underestimated. To understand the mechanism of solid formation, liquid analysis would give more data on the conversion of organics and phenomena involved.



## IV. Explanation of the phenomena identified

### IV.1. Liquid analysis

The analysis of the recovered liquid phase brings information on the black liquor decomposition and on the conversion from liquid to solid phase.

#### IV.1.1. TOC/COD

The organic phase is too low to be recovered; only the aqueous phase has been analyzed. In the aqueous phase total organic carbon (TOC), chemical oxygen demand (COD), then phenols and formaldehyde concentrations have been measured. Errors related to TOC and COD measurements are 2%, errors related to phenols and formaldehyde measurements are 5 mg/L.

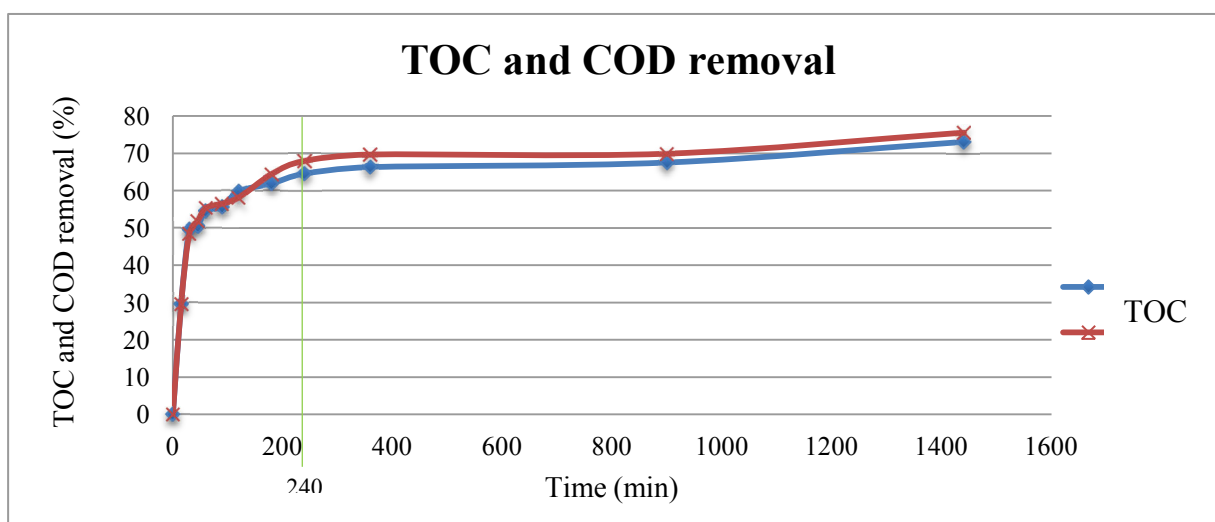


Figure 84: Evolution of TOC and COD removal with reaction time.

TOC and COD are global analyses of the solution giving data on organic carbon content and oxidation power. TOC and COD removal have similar evolution (Figure 4) versus reaction time. TOC and COD removal reached rapidly 50% in 30 min and then are almost stabilized around 70% after 4 h (240 min). This quasi plateau suggests that conversion reactions of black liquor have almost reached an equilibrium. Oxidation and mineralization, as well as carbonization reactions, are almost stabilized beyond 4 h reaction time. This would mean that the evolution of the solid morphology observed beyond 4 h is not due to chemical reactions occurring in the liquid to solid. From 240 min to the end of reaction time studied, TOC and COD do not evolve, so the degradation of black liquor seems to be stopped at this reaction temperature.

As mentioned previously, phenols and formaldehyde form solid by polymerization. Their concentrations have been monitored and are shown in Figure 85.

#### IV.1.2. Phenols and formaldehydes monitoring

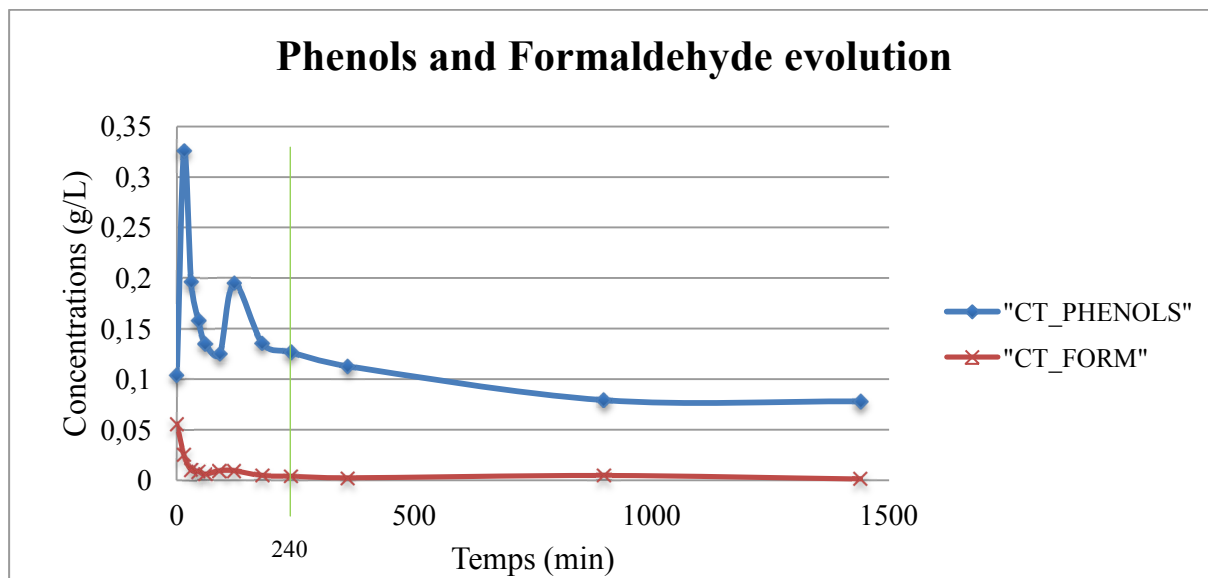


Figure 85: Evolution of phenols and formaldehyde concentrations over time

A peak of phenolic components is observed at 15 min, which means its rate of formation is higher than its consumption at the beginning of the reaction. Then it overall decreases as well as the formaldehyde content. The two reactants responsible of the solid formation have similar evolution with reaction time, corresponding in an increase of recovered solid until 4 h of reaction time. After 4 h reaction time, formaldehyde and phenols concentration appears to be stabilized, in accordance with the quasi plateau of TOC and COD values.

The decrease of TOC, COD, as well as phenols and formaldehyde concentrations, is accompanied by a color change of the recovered liquid (Figure 86). It becomes less and less dark with the increase of the reaction time, which is due to the decrease in the amount of chromophorous compounds (e.g. phenols, aromatic oligomers, and so on).

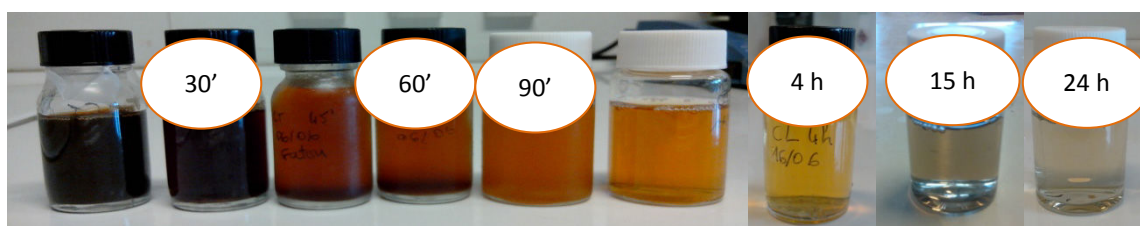


Figure 86: Liquids color evolution over time.

The composition and the evolution of the liquid phase seem to be significant until 4 h of reaction time. The morphology of the solid changed clearly at 3 h reaction time, by consequent, the liquid phase composition seems not to be the only parameter involved in solid formation and evolution. To better understand the evolution of the solid morphology its chemical properties have to be determined.

## IV.2. Chemical analysis of solid

Chemical analyzes, such as FTIR, TGA and C, H, N, O, S content contribute to better understand chemical structure and consequently the composition of the solid generated.

### IV.2.1. The elemental composition of the solids

Evolution of elemental analysis over time is plotted Figure 87. Errors related to ultimate composition are 0.1 %.

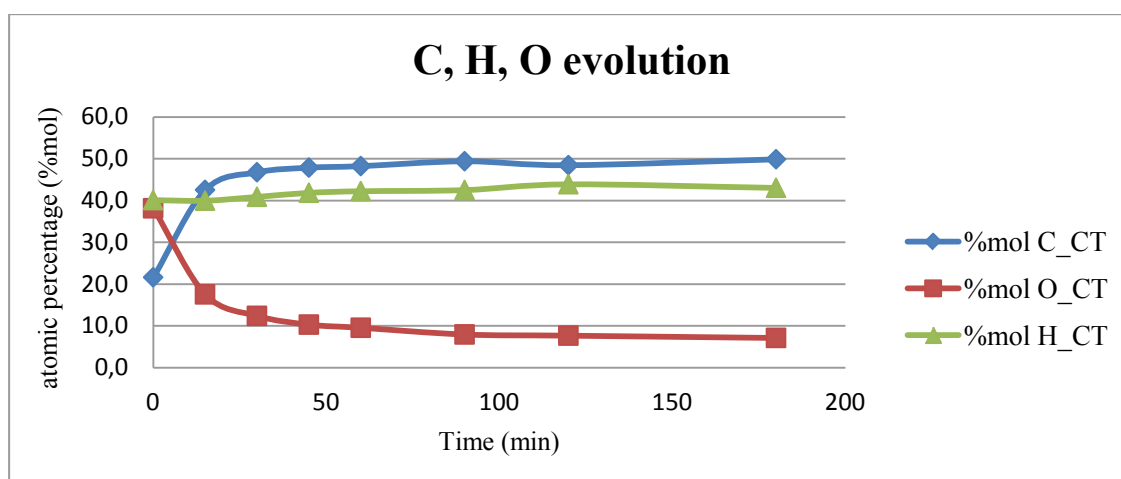


Figure 87: Evolution of C, H, and O in CT solids over reaction time

Figure 87 shows the evolution of carbon, hydrogen and oxygen compositions in the solid samples whereas sulfur and nitrogen are only detected as traces. The “0” point corresponds to the raw dried black liquor. The amounts of carbon and hydrogen increase over time, while the amount of oxygen decreases, in accordance with carbonization phenomena [128]. From 30 min of reaction, the amounts are quite stabilized. The proportions obtained over 30 min of reaction show an atomic distribution close to  $C_5H_4O$ . Titirici [103] has shown that more  $sp^2$  carbons (graphitic, aromatics) and less carbonyl groups (lower O content) are identified in the solid residue. This result suggests that high temperature ( $> 200^\circ C$ ) and long reaction time leads to more condensed matter, with less oxygen, coming from intramolecular

condensations, dehydration and decarboxylation reactions. She also suggests that above 280°C, demethanation reaction occurred during the process increasing aromatization.

Using ultimate composition, ratios H/C and O/C can be calculated and a Van Krevelen diagram can be drawn like Figure 88.

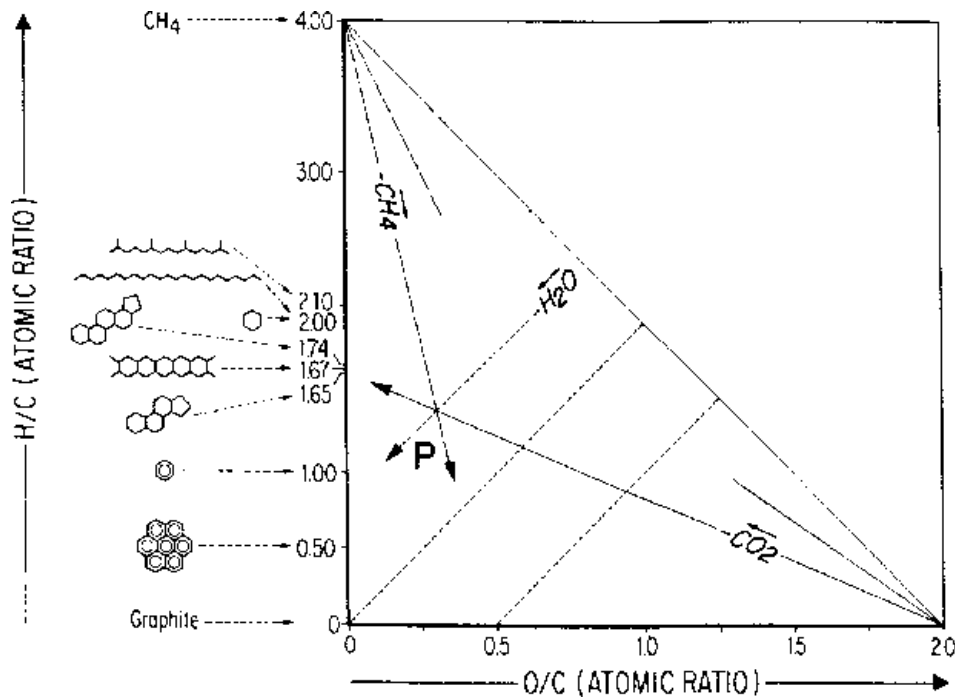


Figure 88: Reactions evolution on Van Krevelen diagram.

Van Krevelen diagram is also used to compare heating recovery from biomass (Figure 89).

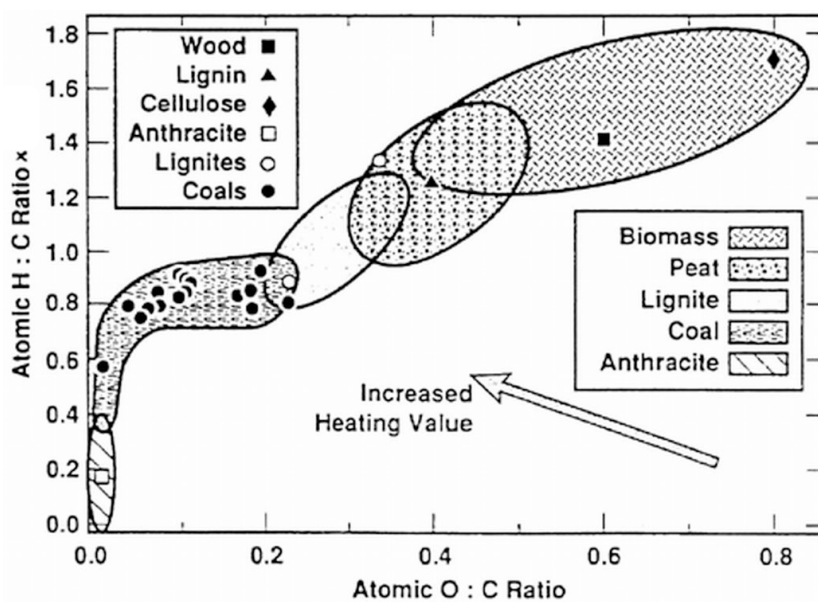


Figure 89: Biomass Van Krevelen diagram<sup>5</sup>.

<sup>5</sup> <http://www.handbook.ifrf.net/handbook/cf.html?id=23>

From our ultimate composition, a Van Krevelen has been drawn (Figure 90) to figure out the types of reactions (or rearrangements) occurring during hydrothermal carbonization process. This Van Krevelen diagram suggests that dehydration and decarboxylation reactions occurred in the solid phase during carbonization process over reaction time. On the contrary, demethanation does not seem to be involved at 350°C during carbonization process. Over reaction time solid approach “coals” region (cf. Figure 89).

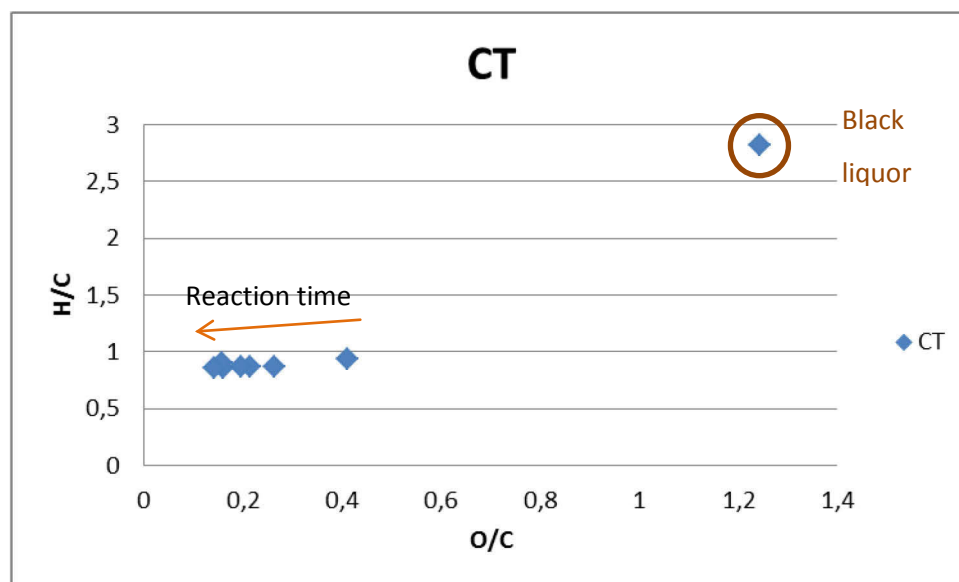


Figure 90: Van Krevelen diagram for CT solids compared to black liquor (atomic ratios).

Taking into account the global molar formula deduced previously, aromatization happened over reaction time with dehydration and decarboxylation reaction.

FTIR analysis brings information on the surface of the carbonaceous solid. All the spectrums were similar to this one presented in Figure 89.

The peaks observed close to  $3000\text{ cm}^{-1}$  correspond to CH stretching (in  $-\text{CH}_3$  and  $-\text{CH}_2-$ ) of saturated (under) and unsaturated molecules (above). The peaks around  $1600\text{ cm}^{-1}$  and  $1450\text{ cm}^{-1}$  correspond to the C=C bonds of the aromatic rings. The large peak around  $3300\text{ cm}^{-1}$  corresponds to the free -OH function and/or -OH intermolecular bonds (hydrogen bonding).

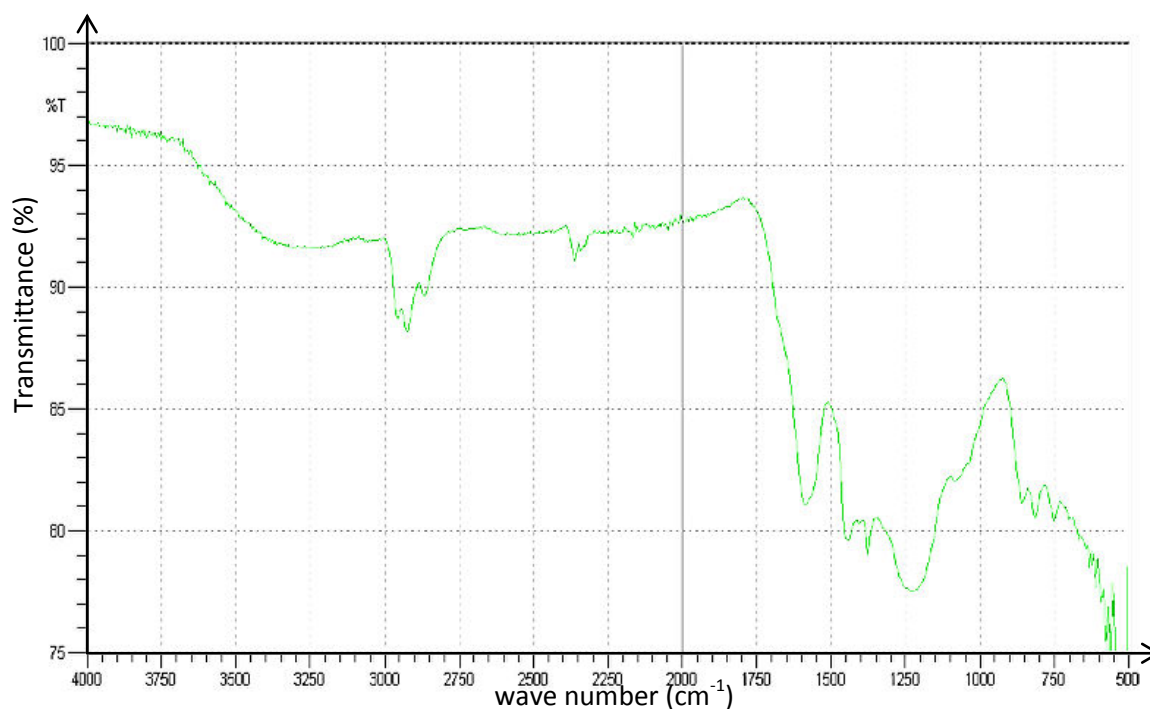


Figure 91: FTIR spectrum of solid residue obtained after reaction.

The combination of these peaks reveals the presence of alcohol function and aromatic rings which derived from phenolic compounds obtained by cleavage of the lignin; and their repolymerization. The profile obtained is in accordance with other hydrochars from biomass [129]. The other peaks are difficult to identify precisely:  $1350\text{ cm}^{-1}$  may correspond to a double bond S=O. That is in accordance with microanalysis realized with EDS detector that highlighted the presence of sulfur. The broad peak at  $1250\text{ cm}^{-1}$  may correspond to the vibration of the CO bond of acetate.

FTIR analysis suggests hydrophilic surface of the obtained carbonaceous solid. The literature confirms that hydrothermal carbonization is known to produce carbonaceous microparticles with a hydrophilic shell [130].

#### IV.2.2. Thermogravimetric analysis

The intensity of the peaks from FTIR is not suitable for quantifying the relative proportions of each organic function. Thermogravimetric analysis (TGA) was also carried out to analyze the thermal stability of hydrochars and to highlight differences in composition.

The derivative curves (DTG) of solids obtained after 15, 60 and 120 min reaction time are shown in Figure 92, comparing the influence of degradation temperatures. DTG curves present four main zones for each sample.

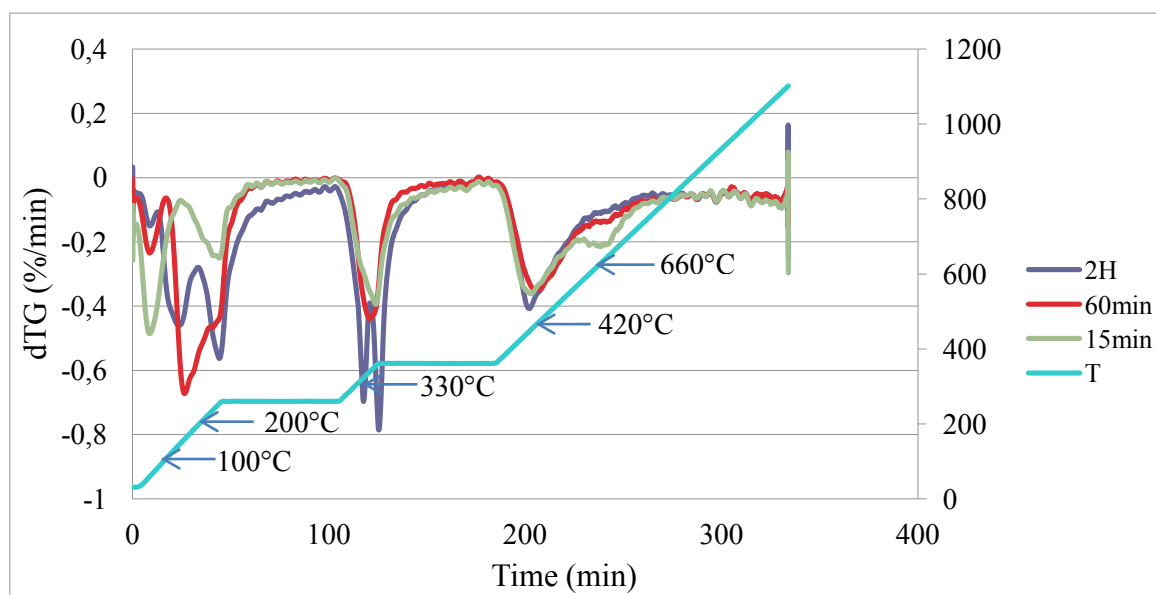


Figure 92: TGA of CT solids

The first peak (around 100°C) corresponds to the dehydration of the sample.

Two other peaks are observed between 100°C and 260°C and have different intensities for the three solids. These two families of compounds degraded in this region have different relative proportions. The peak at 260°C appears after 15 min of reaction time then the peak at 180°C appears from 60 min of reaction time.

The third series of peaks is obtained around 330°C, the curve for 2h shows two peaks (instead of one for the other curves). This means that two families of different compounds are present corresponding to different chemical composition of the solids.

From 400°C, the profiles are very similar. The peak at 600°C decreases by increasing reaction time. This means that this compound is gradually removed from the solid.

Analysis results show that solids do not present the same chemical structure and organics functions regarding to the operating conditions.

To complete the chemical analysis of solid phase and to understand the evolution distribution of chemical functions, XRD, Raman analysis, and then BET analysis have been made.

#### IV.2.3. XRD analysis & Raman spectroscopy

XRD spectra show a large peak, characteristic of amorphous carbon. The solid obtained is amorphous and its structure does not evolve over time (annex 5).

In addition, RAMAN analysis shows the molecular structure of the residue by measurement of lattice vibration that allows considering the degree of structure disorder or crystalline structure and also amorphous structure can be clearly identified [131][132].

The literature describes amorphous carbon Raman spectra as two peaks overlapped ([133], [134], [135]) with maxima observed at  $\sim 1300 \text{ cm}^{-1}$  and  $\sim 1600 \text{ cm}^{-1}$  so the range of Raman shift considering is  $[800 \text{ cm}^{-1} - 2000 \text{ cm}^{-1}]$ . A fast analysis attributes to the peak at  $1300 \text{ cm}^{-1}$ , the disordered carbon contribution (D band) and the contribution to the graphitic carbon (G band) at  $\sim 1600 \text{ cm}^{-1}$ , in the carbonaceous structure. A more precise data analysis is the peaks deconvolution. In our case, deconvolution in ten peaks is the best one since error is less than 3% (the highest error obtained is 5 %). Thus Raman spectra is a combination of the following carbonaceous chemical structure given by Keown et al. [134]:

$G_L$  band at  $1700 \text{ cm}^{-1}$ : Carbonyl group C=O

G band at  $1590 \text{ cm}^{-1}$ : Graphite  $E_{2g}^2$ ; aromatic ring quadrant breathing; alkene C=C

$G_R$  band at  $1540 \text{ cm}^{-1}$ : Aromatics with 3-5 rings; amorphous carbon structures

$V_L$  band at  $1465 \text{ cm}^{-1}$ : Methylene or methyl; semi-circle breathing of aromatic rings; amorphous carbon structures

$V_R$  band at  $1380 \text{ cm}^{-1}$ : Methyl group; semi-circle breathing of aromatic rings; amorphous carbon structures

D band at  $1300 \text{ cm}^{-1}$ : D band on highly ordered carbonaceous material; C-C between aromatic rings and aromatics with not less than 6 rings.

$S_L$  band at  $1230 \text{ cm}^{-1}$ : Aryl-Alkyl ether; para-aromatics

S band at  $1185 \text{ cm}^{-1}$ :  $C_{aromatics} - C_{alkyl}$ ; aromatics (aliphatic) ethers; C-C on hydroaromatic rings; hexagonal diamond carbon  $sp^3$ ; C-H on aromatics rings

$S_R$  band at  $1060 \text{ cm}^{-1}$ : C-H on aromatics rings; benzene (ortho-di-substituted) ring

R band between  $960$  and  $800 \text{ cm}^{-1}$ : C-C on alkanes and cyclic alkanes; C-H on aromatic rings

The deconvolution of Raman spectra has been performed with a Matlab program. The Raman spectra is fitting considering the least square minimization equation between the calculated signal  $I_i^{cal}$  and the Raman one  $I_i^{exp}$  [136]:

$$OF = \sum_{i=1}^{i=n} (I_i^{cal} - I_i^{exp})^2 \quad (28)$$

The ratio of  $I_{(GR+VL+VR)}/I_D$  indicates the ratio of small to large aromatics ring systems. If this ratio is  $<1$ , it means that the degree of graphitic carbon is less than amorphous carbons.



For our particles, three spectra have been observed, for a solid obtained after 60 min of reaction is Figure 93:

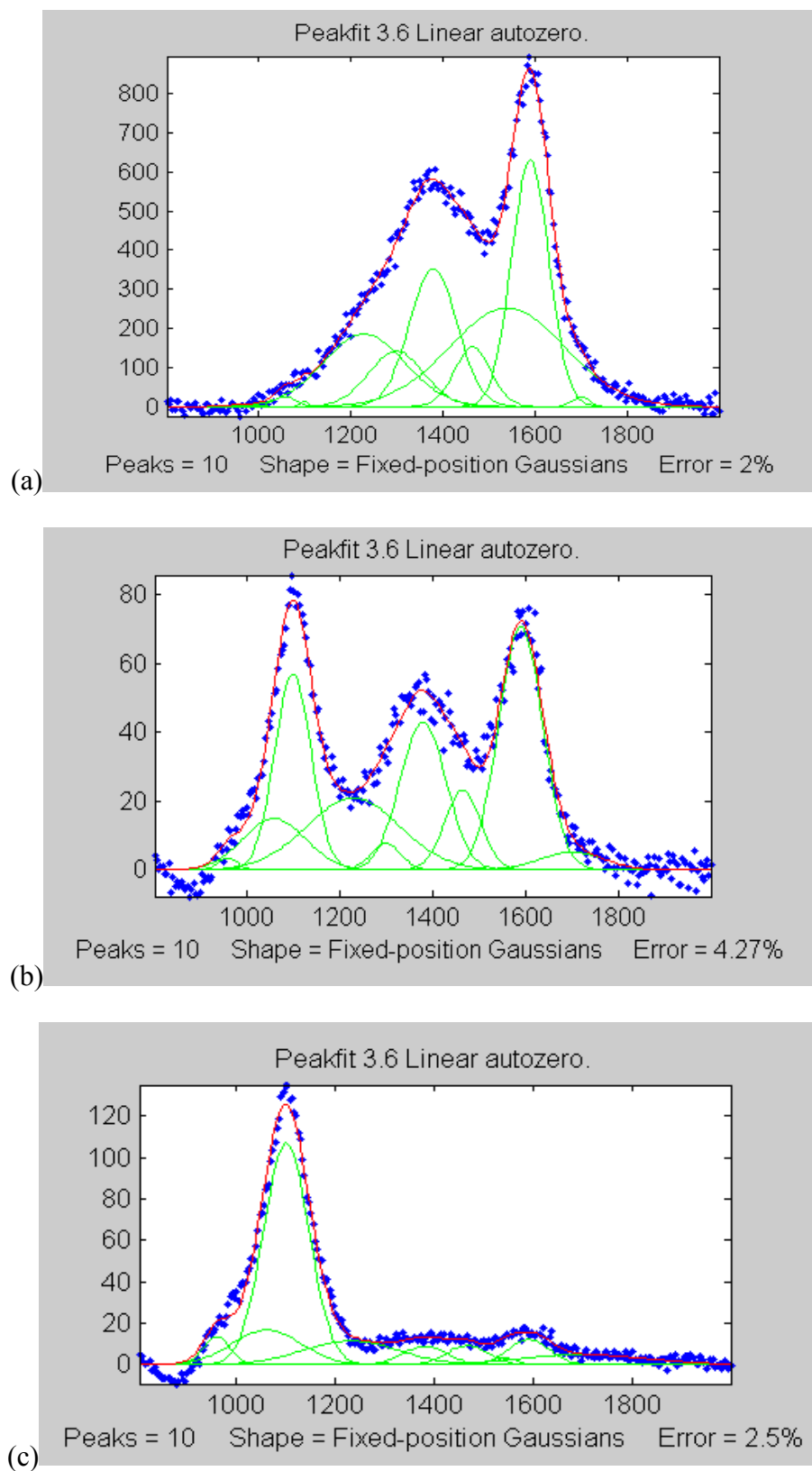


Figure 93: Raman spectra of solid obtained after 60 min (a) spectra of the core, (b) spectra of surface & core, (c) spectra of surface.

For the same sample, 3 spectra have been observed. Raman analysis is a surface analysis. Probably, some organic phases remained probably, on the surface of the particles and have been identified.

According to the observations, the core of the particle is an amorphous carbon, in agreement with literature. The spectra with 3 peaks and 1 peak refer to the organic phase, organic layer on the particles. This peak is noticed at  $1100\text{ cm}^{-1}$ , which corresponds to a shift of the peak at  $1185\text{ cm}^{-1}$  for  $C_{aromatics}-C_{alkyl}$ ; aromatics (aliphatic) ethers; C-C on hydroaromatic rings; hexagonal diamond carbon  $sp^3$ ; C-H on aromatics rings.

In the organic phase, aromatic carbons are linked to alkyl carbons, as expected in a carbonaceous particles generated by phenol-aldehyde polymerization. This demonstrates that the organic phase is a transition layer between aqueous phase and carbon spherules, with a degree of arrangements lower than the carbon spherules.

For Raman spectra constituted by only one peak, the G band does not exist, therefore the following ratio calculation is not possible. For the spectrum with 2 bands, the calculus of the ratio is  $ID / IG \approx 0.8$  as mentioned by Park et al. [137].

#### Limits of the method and interpretation:

However, a precaution has to be taken about deconvolution method. Because, deconvolution peaks are controversial, RAMAN measurement has to be considered as a qualitative technique. In addition, the laser beam of RAMAN analysis graphitizes a little the sample. Results obtained from this analysis are considered as elements helping to validate hypothesis for the solid formation.

#### Conclusion:

Carbonaceous particles are made thanks to an organic phase, using as transition and storage layer. The aromatization of the particles is higher than the aromaticity of the organic phase.

The rearrangement of aromatic molecules is accompanied by the creation of internal porosity.

#### IV.2.4. Density/Porosity:

Density and then porosity have been investigated. Table 11 shows the results for density values.

Table 11: Density of solid obtained after 30 min and 60 min of reaction time

Time (min)	CT (g/cm <sup>3</sup> )
30	1,52
60	1,47

Solid obtained for 30 min reaction time are denser than solid obtained for 60 min of reaction time. Furthermore, particles size increases over time (sections III and IV) so reaction time increases porosity. Particles porosity can be explained by the formation of gas or liquid bubbles due to the formation of volatile components during the hydrothermal carbonization such as decarboxylation, demethanation etc. Gas bubbles could also be due to the gas in the reactor which is trapped into viscous droplets when emulsion occurred, creating “pockets” in the solid. During the cooling, gases are either released creating open porosity or encapsulated in the particles (non-connected porosity), influencing the density. Higher non connected porosity, lower is the solid density. These values of densities are similar to the densities value of 1.66 g/cm<sup>3</sup> obtained from several hydrocarbons by Jin et al.[138]. However, the sensibility of the measurements does not allow concluding on the influence of operating parameters on the density.

BET measurements lead to a surface area of around 7 m<sup>2</sup>/g of particles. These values are similar to those obtained for carbon spherules made from mesitylene (8 m<sup>2</sup>/g) [133] and confirmed by Titirici et al. [38]. Moreover, she showed that the solid obtained directly after hydrothermal carbonization has a small surface area (compared to activated carbon) and a small number of micropores. BET results mean that particles are completely smooth with very small pores (~10 nm).

Given the composition of black liquor (e.g its high alkaline content) the determined surface area are in contradiction with literature. Titirici observed that hydrothermal material, obtained in the presence of KOH [37] or others alkali salts, has a surface area of 2200 m<sup>2</sup>/g, a pore volume of ~1 cm<sup>3</sup>.g<sup>-1</sup> and a microporosity (< 2µm).

Solids washed with demineralized water, after filtration have been observed by ESEM (Figure 94).

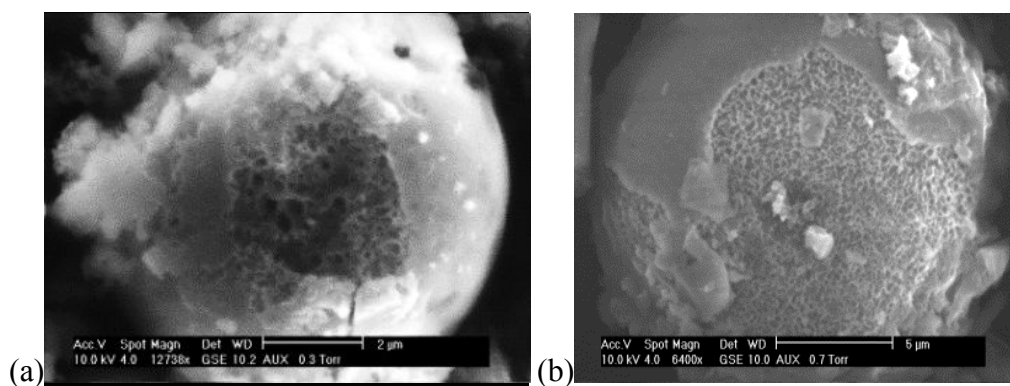


Figure 94: Particles obtained for different heating rate, after 60 min of reaction time and washed after filtration

This picture shows that particles are formed by a porous core and a non-porous shell.

The internal porosity is reaction time dependent and corresponds to the aromatization reactions created by dehydration and decarboxylation. During the cooling a non-porous shell is probably formed around, encapsulating the porosity and given, less dense porous particles with increasing reaction time. Further analysis such as tomography of the particles should confirm these observations.

### IV.3. Mechanism of solid formation - Discussions

Liquid and solid obtained after reaction are recovered at atmospheric pressure and temperature. Even if rapid heating and rapid cooling are used to have a better representation of the influence of reaction time, it is very difficult to know precisely what happened in the autoclave during the hydrothermal process.

#### IV.3.1. Analyses discussion

We summarize the information brought by the analysis on solid and liquid phase:

\*\*\*Three steps can be identified during the process of solid formation:

From 15 min to 90 min: isolated particles are formed corresponding to the polymerization of phenols and aldehyde, then they grow and start to coalesce.

Between 2 h and 4 h: carbonaceous blocks are identified. No spherical material is observed.

From 6 h: particles seem to emerge from a layer. This layer seems to be a continuous media; solid at atmospheric temperature and pressure, probably viscous during reaction.

\*\*\*Elemental composition shows that the degree of aromaticity increases with reaction time. This point is supported by TGA analysis which suggests that solids do not present the same chemical structure or organics functions regarding to the operating conditions e.g reaction time. Independently of change in their aromaticity, solids present a hydrophilic shell.

\*\*\*Solid formation is due to the polymerization of phenols with aldehyde.

\*\*\*After 90 min of reaction time, liquid composition is almost constant.

\*\*\*Regarding liquid composition, black liquor conversion in the liquid phase occurs mainly at short reaction time (~15 min). Morphological changes in the solid are thus mainly due to structural rearrangements with low kinetics in the phase's system maintained at constant temperature and pressure.

\*\*\* Solid formation is accompanied by a color change of liquid. Over reaction time, color solution change from black to red color showing the presence of lower molecules such as aromatic compounds and oligosaccharides.

#### IV.3.2. Showdown between literature and results

Two reactions pathway for hydrothermal carbonization are often proposed in the literature [76]. The first one considers liquid-solid conversion, from the raw material to “based unit molecules” then to solid; while the second one considers a solid-solid conversion. However, as the black liquor solution is a liquid phase without suspension inside, the reaction pathway considering solid-solid conversion is not an option, at least at the beginning of the process. The assumption is based on the decomposition of lignin into phenolic compounds and aldehydes as intermediate based-units, then from phenols-aldehyde as based units, to carbonaceous material.

From the literature, some authors, such as La Mer or Titirici et al., explain that firstly carbon microspheres are formed, then grow and coalesce to form a continuous media. The particles obtained for short reaction time in our experiments are similar to those obtained by Titirici.

On the contrary, some authors, such as Inagaki or Ayache et al. [126], [115], consider that carbonaceous particles are born from a continuous media by aromaticity changing. In the early stages of nucleation and growth, the mesophase appears as small “spherules<sup>6</sup>” emerging in the media [139]. As the reactions proceed, spherules grow, meet and coalesce into large

---

<sup>6</sup> = carbonaceous spherical particles, like mesophase describes earlier

anisotropic media. The coalescence process of microparticules considered as mesophase spherules results in the formation of continuous mesophase matrix. Furthermore, the spheres or agglomerated spheres of carbonaceous particles suggests that this material was liquid or plastic at operating conditions [127]. These latter suggestions could describe the solid formation in our experiments conducted for long reaction time.

Conclusion: both mechanisms seem to explain the evolution of solid morphology in our experiments. In fact, chemical and physical mechanisms involved in the hydrothermal conversion of the black liquor solution coexist and operate with different kinetics all along the reaction time. More, the cooling step, how fast it is, has in our experiments an unknown influence on the characteristics of the solids. A transition layer is formed, within the droplets of organic phase, between the organic phase and the carbonaceous particles.

#### IV.3.3. Mechanism proposition for the carbonaceous solid formation from black liquor solution in batch

Assuming the previous hypothesis, solid formation occurs according to the following mechanisms. However, the physical and chemical processes are not sequential but they are, more probably, simultaneous in time, even if their relative intensity is changing.

\*\*\*Decomposition of black liquor creates, inter alia, phenols and aldehyde which polymerize together and form an intermediate based-Unit similar to the based structural units describe by Inagaki in section I.2. Even if phenol and formaldehyde are miscible in aqueous phase, for a high concentration of “intermediate based unit” immiscibility begins, which creates an “oil in water” emulsion. This oily phase corresponds to the bio-oil formed by hydrothermal liquefaction concentrated in organic reactive compounds oxygenated such as hydroxy aldehyde, hydroxyketones, carboxylikes acid and polyphenolic compounds [140].

\*\*\*Oily phase is composed of different organics including phenols and aldehyde. When the concentration is over saturation, nucleation occurs locally and then maturation. Probably during this step the transition media (also called transition layer or transition phase) appears at the interface of carbon spherules as shown in the Figure 95.

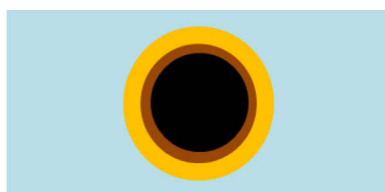


Figure 95: Scheme of the organic droplet organization in the subcritical water.

In the scheme different colors were used. The yellow circle represents the oily droplet, the brown circle the transition layer and the black circle the carbonaceous particle. The amount of transition phase is balanced between its production from the organic phase and its consumption by the carbon spherules. Therefore a radial gradient of phenols-aldehyde intermediate concentration exists from the surface of oily phase to the carbon spherule. As much as coalescence is observed, several particles could be generated within a same oily droplet.

\*\*\*For short reaction time (<90 min) the transition layer is extremely thin and strongly linked to the particle interface. After cooling transition layer and carbon spherules are indivisible and a remaining oily phase is recovered on the top of the aqueous phase.

At 90 min, coalescence begins due to Brownian movement (efficient collisions), such as drawn in Figure 96, dominates the mass agglomeration process. By consequent, bigger particles are created.

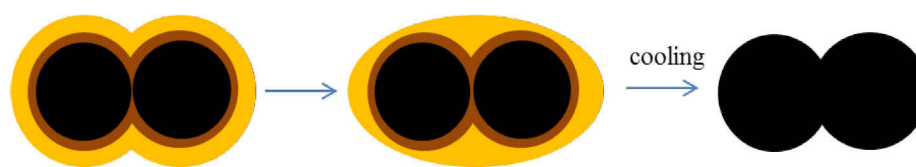


Figure 96: Coalescence of particles by solidification of particles and transition layer.

\*\*\*For reaction time between 2 h and 4 h, the amount of transition layer increases and oily droplets coalesce in the reactor. Transition layers coalesce also and carbon spherules are jailed in this media. Over time, all the spherules are trapped. After cooling patches of carbon are observed.

\*\*\*For long reaction time (> 6h), in addition to the previous carbon spherules formed and due to carbonization process, aromatization of some based-unit change and then nucleation occurs in the transition media. New carbon spherules are created and emerge from the continuous media. After cooling, a solid is formed with buds.

This suggested mechanism is based only on the organic content of both liquid and solid phase. However the mineral content in black liquor is high and would play an important role in the solid formation.

#### IV.3.4. Inorganic matter

At the operating conditions (350°C, 16.4 MPa), the salts are prone to precipitate, so their participation cannot be excluded as a carrier for the formation of solid, as shown by Rahmani et al. [127]. Indeed, ICP analysis made after hydrothermal conversion has shown that 10 % of minerals disappeared from liquid phase during batch process. Salts have been detected in the carbonaceous solid phase using EDX detector during TEM analyses. Microanalysis showed that sodium (Na) is included in solid particles. The content of calcium and potassium is very low. Sulfur is agglutinated around carbon particles as seen in the Figure 97.

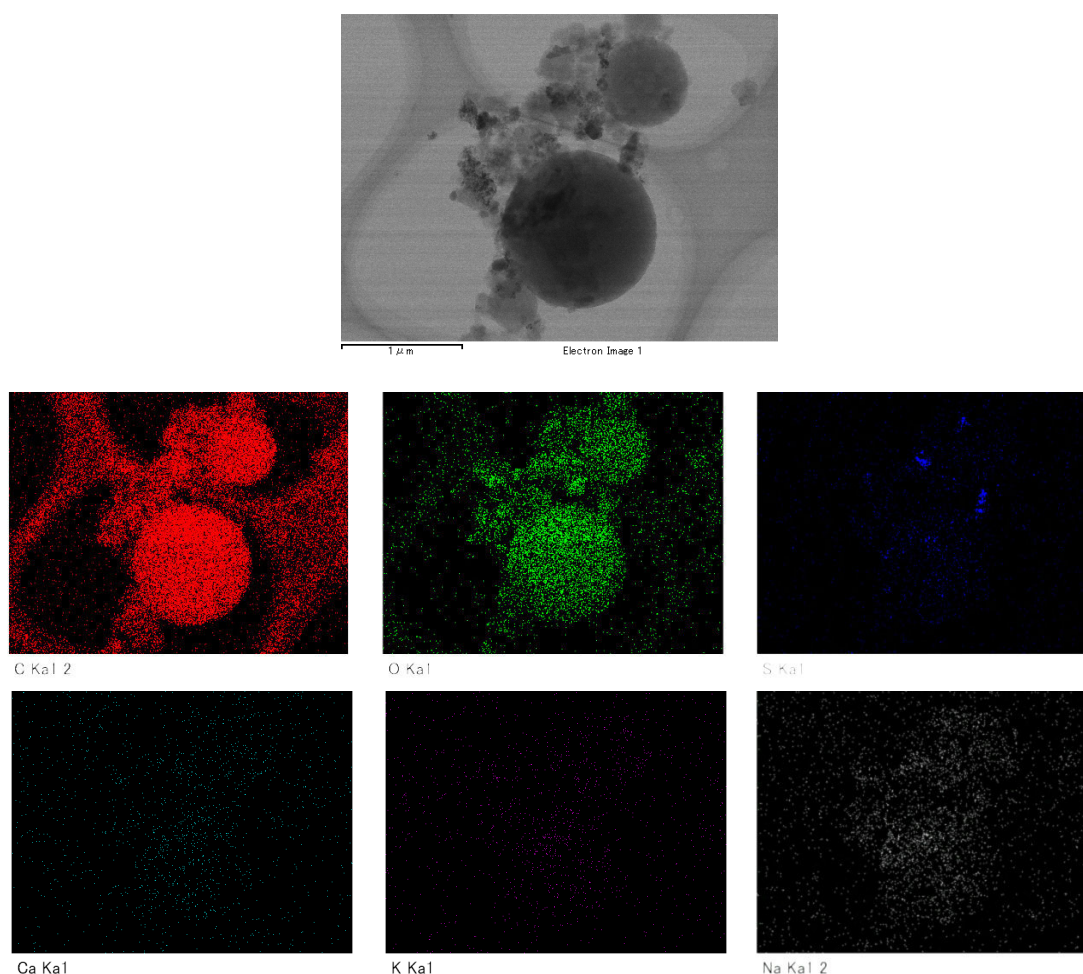


Figure 97: TEM observation of particles obtained at 350°C, 60 min and 10 wt%.

Mochida et al. [141] have studied sulfur behavior during hydrothermal carbonization and have shown that desulfurization of organic matter occurred firstly forming organic sulfur compounds in liquid phase or sulfured salts which precipitate. Then carbonaceous particles aromatization happened.



#### **IV.4. Conclusions**

By increasing reaction time, the morphology of the solid differs. Isolated microparticles are favored at short reaction times. chemical processes seems to control the process until 3 h of reaction time, then the rearrangement of the solid phases becomes dominant. The evolution of the structure is then more related to phase equilibria. This is summed up in the Figures 98 and 99.

Reaction was studied in this section; however the heating and cooling steps are of great importance regarding particle formation. The next section considers the effect of reaction time using 2 heating and cooling rates.

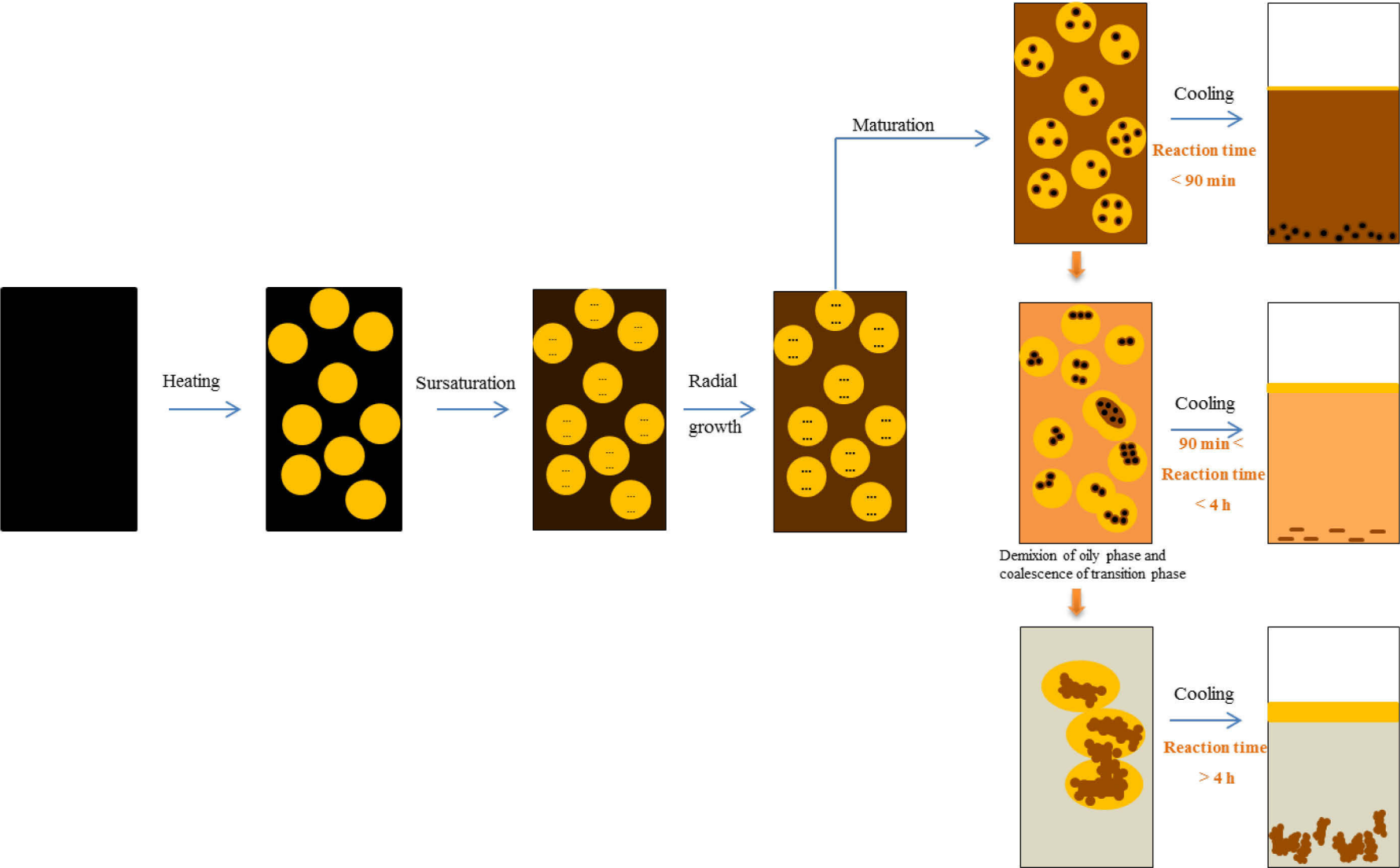
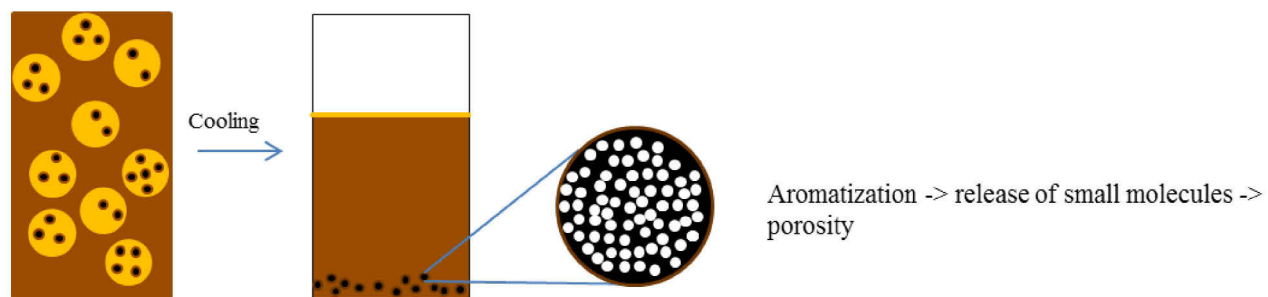


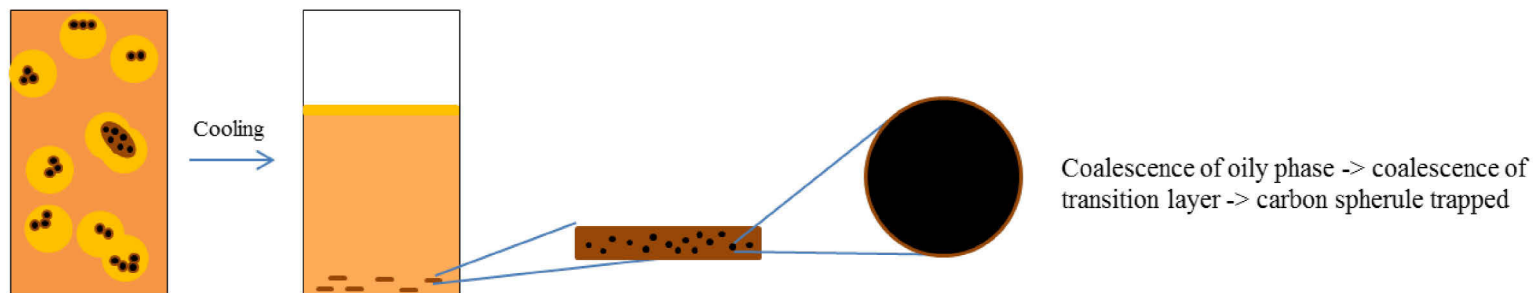
Figure 98: Scheme of particle generation

The specificities of each step is drawn Figure 99

Reaction time < 90 min



90 min < Reaction time < 4 h



Reaction time > 4 h

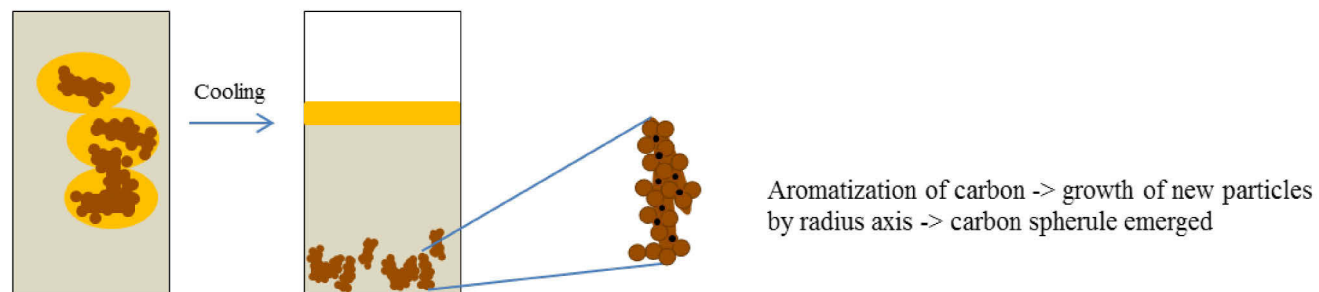


Figure 99: Zoom on the solid obtained after characteristic times

## V. Influence of heating and cooling rate

Heating and cooling rate influence the characteristics of the solid formed [123] and are key issues regarding the operation of batch and continuous processes.

### V.1. Influence of heating rate

This part describes the influence of heating rate (at same cooling rate) on the morphology and physico-chemical properties of the carbonaceous solid. To remember, the abbreviations are CT vs. NT with a quench cooling (iced water); CL vs. NL when a slow cooling is applied (ambient air), C and N referring to the type of ovens used.

#### V.1.1. Solid analysis

In both cases, and for each reaction time, the weight of solid obtained is higher with rapid than slow heating rate. As regards to the particles, Figure 100 shows the solids obtained after 30 min reaction time, with slow cooling.

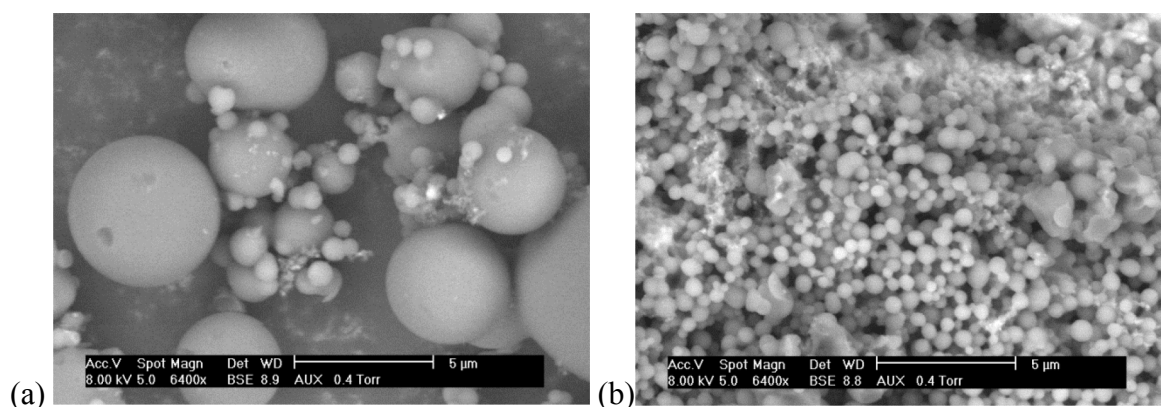


Figure 100: Morphology of particles obtained with rapid heating (a) and slow heating (b) after 30 min of reaction time, same magnification

The spherical particles obtained with a rapid heating have a large size distribution from 0.4 μm to 5 μm. On the contrary, when the heating is slower, the spherical particles have a finer distribution from 0.2 μm to 1.5 μm. At higher reaction time, the same difference in size and distribution of particles was observed. Moreover the particle size distribution obtained by laser granulometry reveals that sizes of particles increase with heating rate (Figure 101).

A fast heating rate in batch process (without stirring) leads to higher mass of solid generation, characterized by bigger particles with a larger size distribution due to a higher turbulence which favors the proximity between particles and therefore the maturation process.

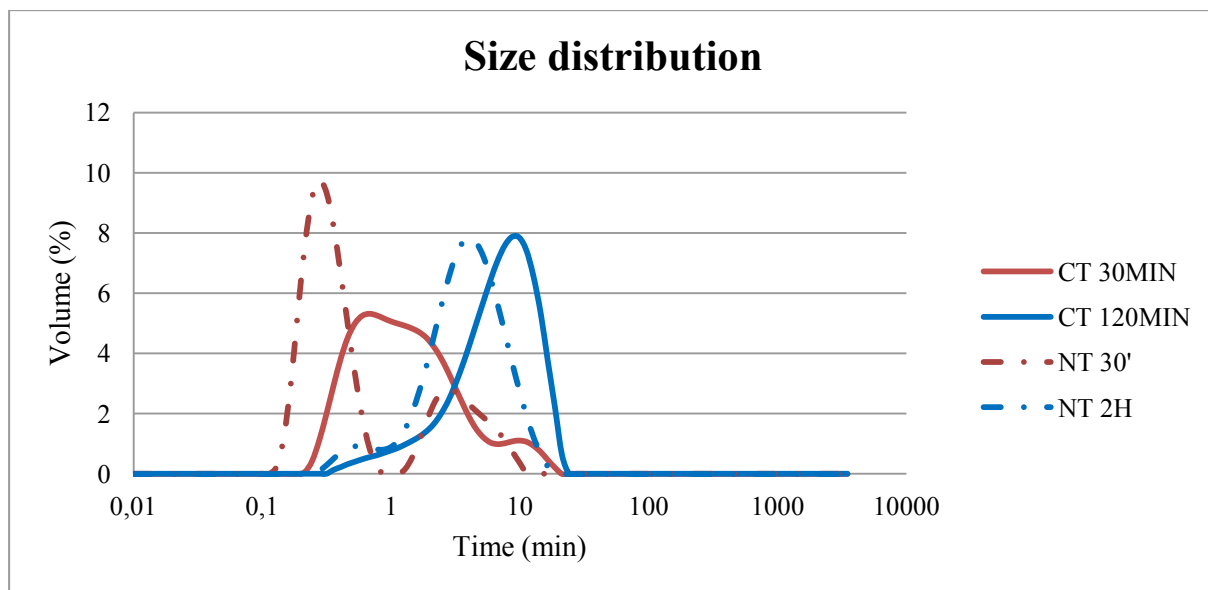


Figure 101: Influence of heating rate ( $20^{\circ}\text{C}\cdot\text{min}^{-1}$  vs.  $40^{\circ}\text{C}\cdot\text{min}^{-1}$ ) on the size distribution at  $350^{\circ}\text{C}$ , 30 min and 2 h with a quench cooling.

Other analyses such as TGA, C, H, N, O, S composition and Van Krevelen diagram have been realized and presented in annex 6. The TGA degradation profiles are similar to that in section IV.2.2, as well as Van Krevelen diagram in the section IV.2.1. In conclusion, the heating rate influences only the solid yield and size distribution in the unstirred batch hydrothermal conversion of black liquor solution.

The simultaneous obtained liquid phases have been also analyzed by COD, TOC, phenols and formaldehyde concentrations to compare rapid (CT) and slow heating rate (NT).

### V.1.2. Liquid analysis

Figure 102 shows that the values of TOC and COD are higher at slow heating rate (NT) up to 2 h of reaction time. Then the values are similar. This indicates that up to 2 h, oxidation reactions and organic carbon removal are faster at high heating rate (CT). In addition, the amount of phenols is significantly higher at high heating rate, especially for 15 min reaction time (annex 6). Therefore, the TOC disappearance of the liquid phase and the high phenols concentration explain an increase in the amount of solids recovered with rapid heating.

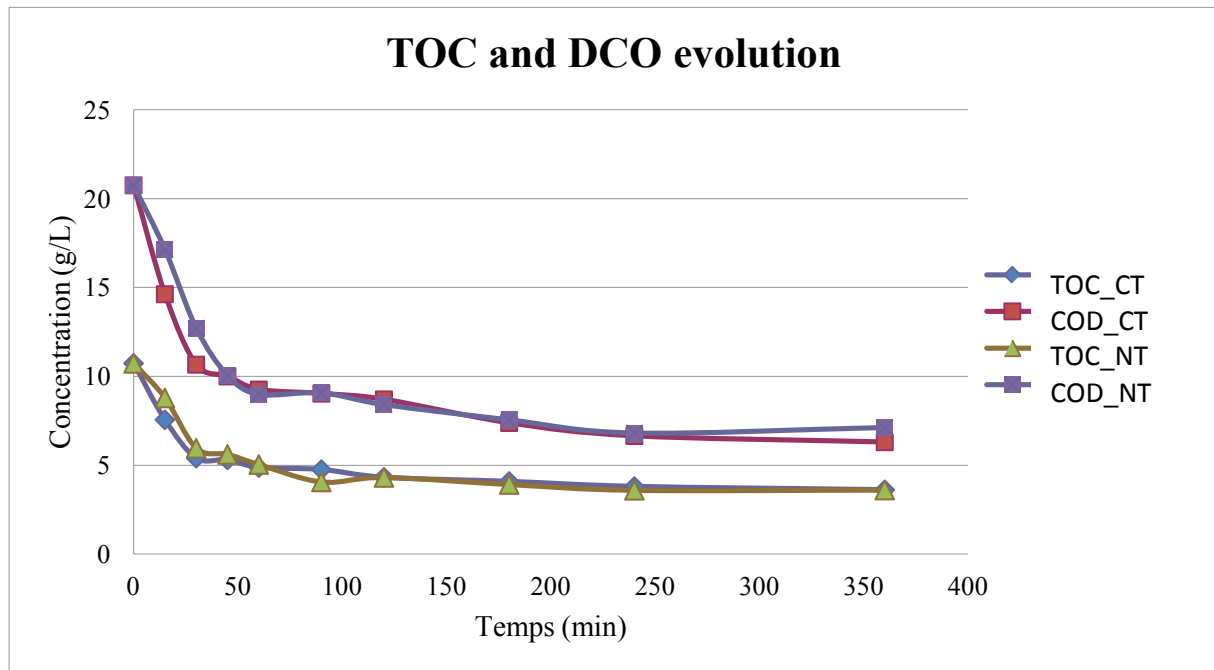


Figure 102: Evolution of TOC and COD of CT and NT liquids

To conclude: Considering the liquid analysis, for short reaction time, heating rate influences the transfer of based units molecules to the organic phase then to particles. The turbulence due to the rapid heating acts on the emulsion dispersion of the oily phase in the aqueous phase and improve the collision frequencies and efficiencies between particles, accelerating the maturation (coalescence or disappearance) process of oilydroplets.

## V.2. Influence of cooling rate

In this section two types of cooling have been studied (c.f chapter 2 II.2.3): cooling by quenching (rapid cooling  $\cong$  2 min) namely T or cooling at ambient temperature (slow heating  $\cong$  30 min), called L.

Pictures on the Figure 103 show that particles are bigger with a slow cooling. This observation is similar with the other oven, and is corroborated by particles size distribution in Figure 104.

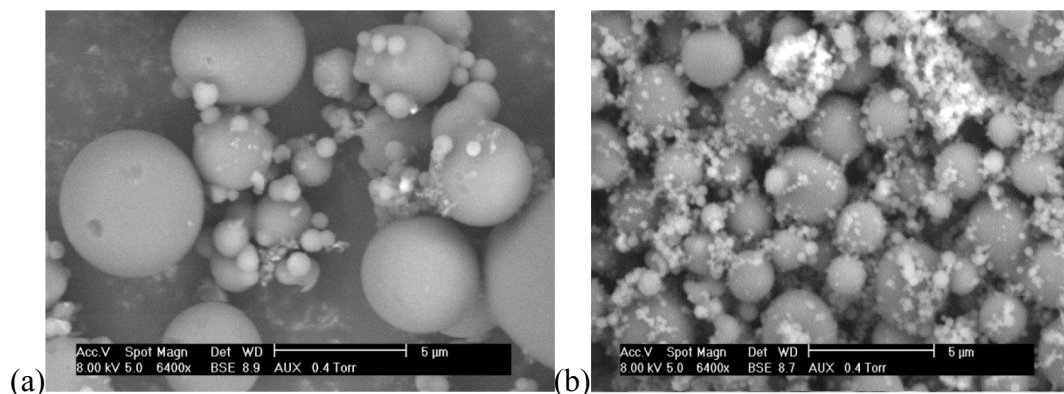


Figure 103: Morphology of solid obtained after a rapid heating and 30 min of reaction time: with slow cooling: CL (a) and by quenching: CT (b), same magnification.

Physical and chemical processes continue during the cooling with different relative intensities; whereas reaction media is “congealed” by quench cooling. Therefore, collisions required for coalescence are dramatically low. This result also explains that the weight of solid obtained is higher with slow cooling rate.

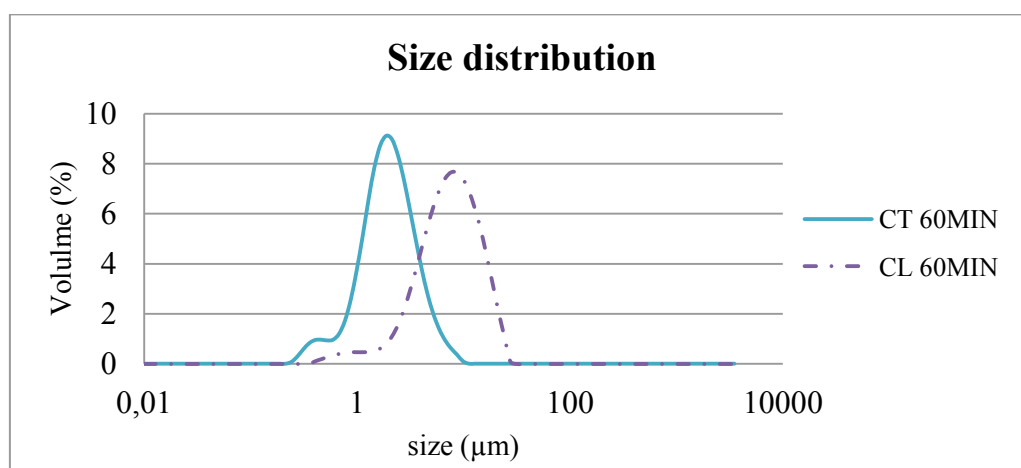


Figure 104: Size distribution considering cooling rate at 60 min reaction time

TOC, COD, phenols and formaldehydes concentrations curves are presented in annex (annex 7). The results are similar for the whole set of experiments, the cooling does not influence the global liquid composition. However particle sizes are different and a higher mass of solid is recovered for slow cooling. We expected a difference in the liquid composition, especially as regards to phenols and formaldehyde. The same liquid composition for both cooling experiments shows that the dominant mechanisms are physical (rearrangement of particles) for this set of experiments. The assumption would be the transfer of intermediate molecules (phenols-formaldehydes based units) in a transition phase used as a tank of “based-units” for the polymerization. The kinetics of lignin decomposition seems to be very fast (the maximum conversion reached into phenols and formaldehydes evolution). However as the liquid

composition after reaction is independent of the cooling, the transfer to the transition layer is supposed to be higher than the kinetics of polymerization. These results confirm also that carbonaceous particles are formed into the organic phase.

The thermogravimetric analysis shows quite similar curves comparing to the cooling methods (annex 7). Van Krevelen diagram suggests that during carbonization with rapid heating and slow cooling, the first reaction is dehydration, followed by decarboxylation.

The cooling affects particles size and to a lesser extent the elemental composition that suggest during the cooling physical rearrangements continue.

### **V.3. General conclusion on heating and cooling rates:**

#### **V.3.1. What the analysis bring as information?**

\*\*\* The turbulence created by a rapid heating rate in the non stirred fluid, acts on the oily phase dispersion in the aqueous phase that accelerate the maturation process by collision. With a chemical point of view, rapid heating produces molecules in liquid phase with higher degree of mineralization and oxidation. However, with both heating rates, elemental analyses of solids formed are similar.

\*\*\* The cooling rate acts only on the particles size.

#### **V.3.2. What the literature bring as other information?**

\*\*\*Chuntanapum et al. [142], observed the formation of carbonaceous microspheres under subcritical conditions (at 350°C) in continuous reactor. Emulsion and particles formation is not depending on the type of process, batch or continuous.

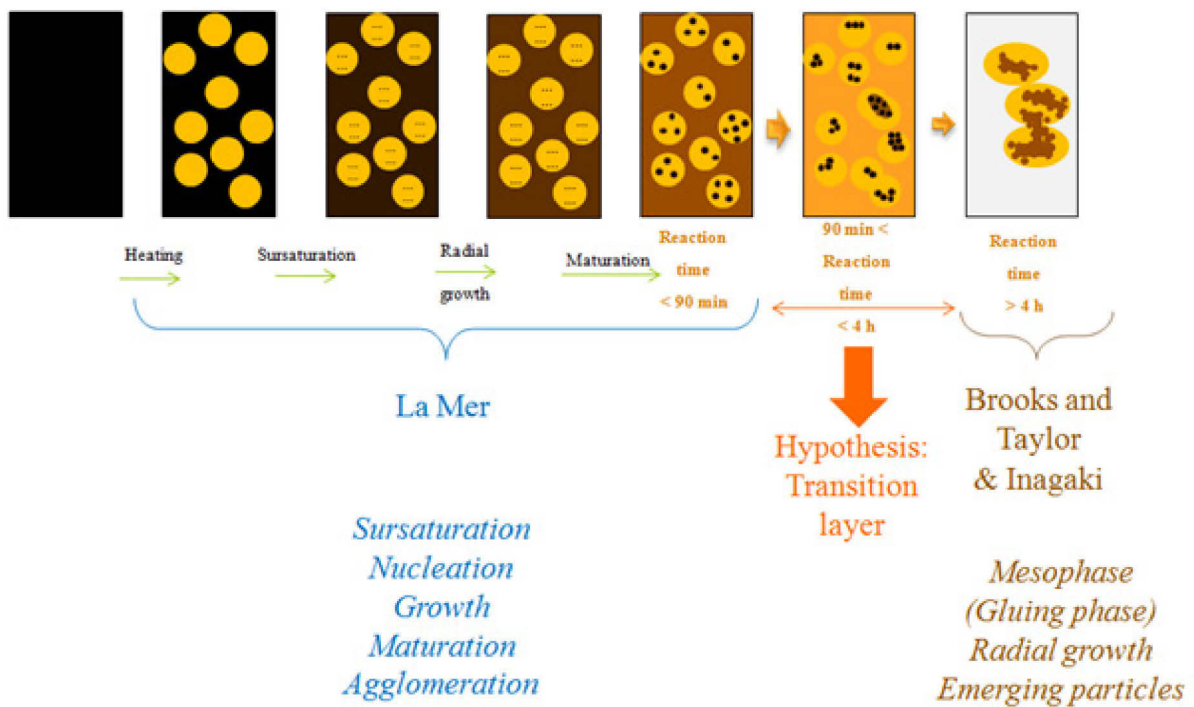
\*\*\*Kumar et al. [143].confirmed that the ultimate analysis are similar changing the heating rate and 60 min reaction time.



## VI. Summary of chapter

### VI.1. Phenomena involved during particles generation

To conclude, the mechanisms of solid formation described in (IV.3.3) are not dramatically influenced by the heating and cooling rate.



V.K. La Mer, *Ind. Eng. Chem.*, vol. 44, 1952

M. Inagaki, *et al.*, *New carbon matter*, 2010

Figure 105: Confrontation between carbonization theories and our solids evolution.

Hydrothermal carbonization is a physico-chemical phenomena. Morphology is guided by chemical reactions, phase equilibria and reorganizations (Figure 106).

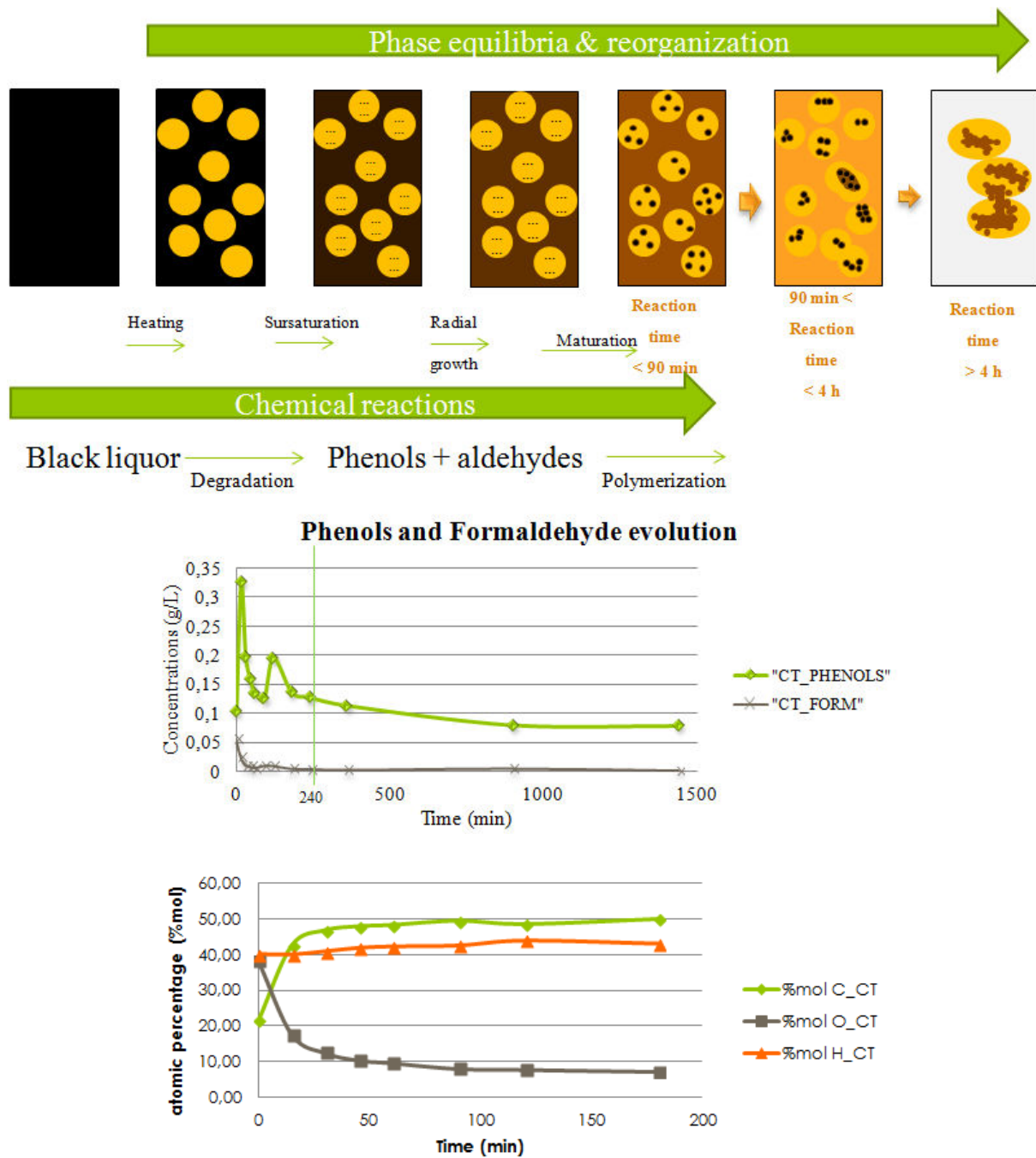


Figure 106: Morphology is due to a combination of chemical reaction and physical phenomena.

However, because we used unstirred batch reactors, during low heating and cooling processes, the physical mechanisms control the physical characteristics of the formed solids (granulometry, shape, etc), if the reaction is sufficient.

## VI.2. Applications of carbonaceous materials

In our society, many applications for carbon materials exist such as adsorbents, catalyst supports, batteries and energy storage, filters, drug delivery and so on. Thus, carbon spherules could be considered as matter or template. Depending on the materials properties, some applications are possible: conductivity leads to electronic applications; surface functionality leads to adsorption and acid/base lead to catalysis. Some applications are detailed thereafter.

Carbon as template is used in hollow spheres formation such as: CoO [144], TiO<sub>2</sub> [145], CeO<sub>2</sub> [146], MnO<sub>2</sub> [147], Cr<sub>2</sub>O<sub>3</sub> [144], WO<sub>3</sub> [148], ZnO [149]. Indeed, if microspheres particles are mixed with inorganics salts, hybrid carbon/metal material is formed by hydrothermal processes. Metal oxide hollow spheres are created by coating carbon particles. then carbon is removed by calcination. Hollow sphere become very attractive in several applications as catalysis, delivery and controlled release drugs microcapsule reactor and so on [150].

Carbon can also be considered as matter and can be linked to the energy storage as shown in Figure 107, serving as electrode in Li-ion batteries (LIBs) or Na-ion batteries (NIBs) for example.

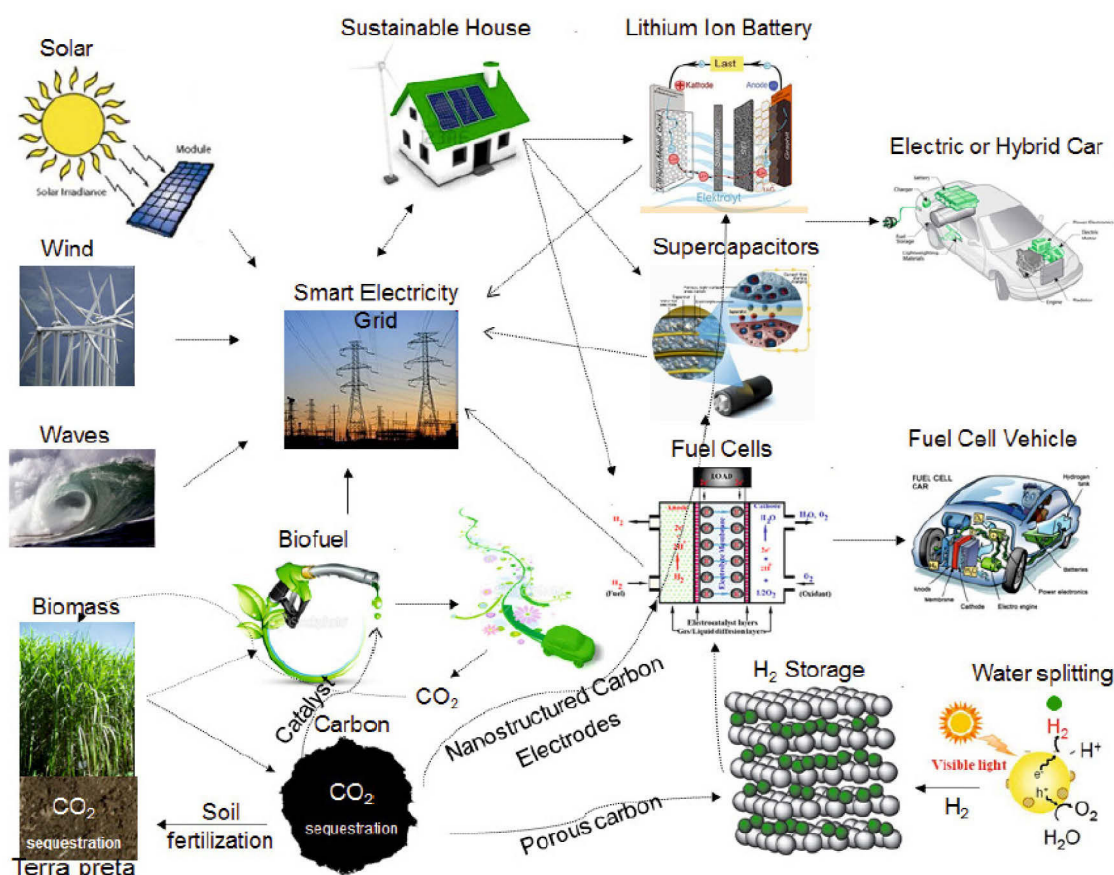


Figure 107: « Green » carbon materials used as basis of electrochemical devices for renewable energy generation, storage and utilization [103].

Carbon matter from hydrothermal conversion is also used as heterogeneous catalyst. They have the specificity to be synthesized at low temperature ( $<180^{\circ}\text{C}$ ) enabling them to have polar surface functionalities. Polar groups are hydrophilic so reactions taking place are selective.

Carbonaceous microspheres can be modified in situ by addition of heteroatoms (N, S ...), or after hydrothermal carbonization process by secondary chemical reaction as nucleophilic substitutions, cycloadditions... Thus, the study may enable to better fit the properties of the solid to the request.



Chapter 5: Catalytic hydrothermal  
conversion using CeO<sub>2</sub> nanocatalyst for  
H<sub>2</sub> production and coke suppression

---



**Résumé du chapitre 5 : conversion catalytique hydrothermale en utilisant le CeO<sub>2</sub> en tant que nano catalyseur pour la production d'hydrogène et la suppression de coke.**

Ce chapitre s'attache à l'étude de la conversion catalytique de la liqueur noire à basse température afin de s'affranchir de l'émission d'hydrogène sulfuré. L'ajout d'un catalyseur (CeO<sub>2</sub>) est étudié afin d'augmenter la production d'hydrogène et d'éviter la formation de solide lors de la réaction. Ainsi, la comparaison des résultats obtenus avec et sans catalyseur nous permet d'identifier les phénomènes complexes de la formation du solide et des autres molécules intéressantes et donc de mieux comprendre les phénomènes hydrothermaux.

La partie expérimentale a été faite au Japon dans les laboratoires du Professeur Adschiri, à l'université de Tohoku.

Ce chapitre se divise en 4 parties : la présentation du catalyseur utilisé, l'étude des phénomènes impliqués dans la conversion hydrothermale de la liqueur noire, une première étude de faisabilité énergétique pour une mise en place industrielle et enfin une étude préliminaire avec 2 molécules modèles de la liqueur noire afin d'établir les mécanismes réactionnels mis en jeu lors de la conversion hydrothermale avec et sans catalyseur.

Ce résumé sera également fait d'un seul tenant et non partie par partie.

Le catalyseur utilisé est de l'oxyde de cérium, ce catalyseur est synthétisé au sein du groupe du Professeur Adschiri. Sa taille moyenne est de 8 à 10 nm. L'activité catalytique de l'oxyde de cérium provient de son activité rédox via le cycle Ce<sup>4+</sup>/Ce<sup>3+</sup>, celui-ci est accompagné par la capture et le relargage de l'oxygène. L'oxyde de Cérium CeO<sub>2</sub> est connu pour avoir une capacité de stockage de l'oxygène très élevé (OSC). Celle de l'oxyde de cérium cubique est de 340 µg-O/g-cat, ce qui est 3,4 fois plus important que celle de l'oxyde de cérium octaédrique. Pour cette raison, l'oxyde de cérium cubique a été utilisé pour nos expériences.

Les expériences ont été faites en réacteurs batch de 5 mL, ce type de réacteur est décrit dans le chapitre 2, ils peuvent supporter une pression de 50 MPa et une température de 500°C. La liqueur noire diluée est introduite dans les réacteurs avec de l'oxyde de cérium, puis le réacteur est fermé. Après un ajout de N<sub>2</sub> dans le réacteur, celui-ci est chauffé dans un four électrique at 350°C et 450°C pendant 15 ou 60 min. Après le temps de réaction, le réacteur est refroidi par trempe dans de l'eau glacée pour arrêter la réaction immédiatement. Les produits sont collectés et séparés en 3 fractions : le gaz, le liquide et le solide.



Les principaux résultats sont les suivants :

En conditions supercritiques :

Après 60 min de réaction, en l'absence de CeO<sub>2</sub>, la conversion hydrothermale de la liqueur noire produit 22% de H<sub>2</sub> dans la phase gazeuse. En présence de CeO<sub>2</sub>, la conversion hydrothermale produit 24% de H<sub>2</sub>. Bien que la quantité de H<sub>2</sub> soit presque la même, la proportion de carbone transformé en phase gazeuse avec le catalyseur est supérieure de 5%; ce qui confirme une meilleure conversion au cours de la réaction avec catalyseur. Les espèces actives d'hydrogène créées par la division de la molécule d'eau, peuvent former directement H<sub>2</sub> ou réagir avec des molécules organiques pour former des molécules plus petites ou stabiliser également des espèces intermédiaires réactives en limitant leur réaction. Si c'est le cas, cela signifie que plus d'espèces d'H activées ou H<sub>2</sub> sont formées, mais simultanément l'hydrogène peut être utilisé pour stabiliser des molécules phénoliques et ainsi produire des molécules de plus faible poids moléculaire. Ce point est confirmé par l'analyse GPC des liquides. En parallèle, le rôle des espèces actives d'oxygène sont principalement impliqués dans des réactions d'oxydation. Plus l'oxydation est avancée, plus du CO<sub>2</sub> est produit. Cette meilleure conversion en présence de catalyseur est soutenue par la masse de solide formée. Après 60 min, la masse du solide obtenue est de 12 mg sans CeO<sub>2</sub> et 4,5 mg avec CeO<sub>2</sub>. Pendant le «cycle redox» du CeO<sub>2</sub>, les molécules d'eau sont libérées et capturées facilement. L'oxygène libéré promeut la conversion du carbone contenu dans la phase liquide initiale à la phase gazeuse finale. L'oxydation se produit jusqu'à ce que l'aldéhyde soit converti en CO<sub>2</sub> ce qui bloque la formation de coke, et inhibe la liaison entre les composés phénoliques.

En conditions subcritiques :

La quantité de H<sub>2</sub> produite est significativement accrue en présence de catalyseur.

Les espèces actives d'hydrogène, réagissent en continu pour former H<sub>2</sub> en phase gazeuse. En conditions subcritiques, H<sub>2</sub> est également produit par réaction de déshydrogénation des alcanes. Toutefois, la quantité d'H<sub>2</sub> est liée à la fois à la production et à la consommation des espèces actives d'hydrogène. En conditions sous-critiques, la diffusion interfaciale est limitée ce qui limite les réactions entre l'hydrogène (et toute la phase gazeuse) et la phase liquide ; ceci explique sa faible consommation. La quantité de carbone dans la phase gazeuse (~ 2 ou 3%) est plus faible dans des conditions sous-critiques que dans des conditions supercritiques. Cette tendance était en accord avec la plus faible quantité de produits gazeux. Une hypothèse pour expliquer la faible proportion de carbone en phase de gaz serait que l'oxydation des

molécules organiques est partielle et évite la production de CO<sub>2</sub>. Cette hypothèse est validée par l'analyse de la phase liquide.

Suite à ces principaux résultats, une première étude énergétique est faite et montre que les meilleures conditions opératoires pour obtenir un bilan positif sont : 450°C, 60 min de réaction au minimum et une concentration massique en liqueur noire de 100 %, avec catalyseur.

Ce dernier chapitre se termine par la proposition de mécanismes réactionnels de la conversion hydrothermale de 2 des molécules modèles de la liqueur noire : la lignine et la GGGE. Les mécanismes sont proposés avec et sans catalyseur. Ils permettent l'établissement en dernier lieu du mécanisme de conversion hydrothermale de la liqueur noire avec et sans catalyseur.

**\*\*\* Fin du résumé**



Hydrogen production from black liquor gasification is particularly efficient at high temperature close to 600°C, as demonstrated in section II.3 of chapter 3. However, this production is linked, above 500°C, with hydrogen sulphide which is an undesirable gas. Therefore a catalytic study has been considered at lower temperature to increase hydrogen production without hydrogen sulphide emission. Nevertheless, at these temperatures range, coke is still formed and useless. Given that, the choice of the catalyst is predominant to increase hydrogen production and decrease coke formation.

This work has been performed in Japan, in the Professor Adschiri's Laboratory at Tohoku University, where a previous PhD candidate studied the catalytic cracking of bitumen. CeO<sub>2</sub> nanocatalyst was used to increase hydrogen production and to limit coke formation.

The objectives of this study are to perform catalytic hydrothermal gasification of black liquor to improve hydrogen production at temperature lower than 500°C, as well as to reduce coke formation. The focus is made on the catalytic role of cerium oxide on the composition of liquid and gaseous phases, in view to figure out a simplified mechanism pathway. However the complex composition of black liquor is an obstacle to draw a clear route. Thus the study is completed by the use of model molecules to improve the knowledge on reactions involved. Lignin and Guaiacylglycerol- $\beta$ -guaiacyl ether, namely GGGE, have been used as model molecules. The work is completed by an energetic preliminary study that deals with the feasibility of a continuous process.

Results on the catalytic conversion of black liquor are already submitted in the *Journal of Supercritical Fluids*.

## **I. Catalyst characterization & its expected action**

CeO<sub>2</sub> nanocatalyst is homemade and synthesized in Professor Adschiri's Laboratory by hydrothermal process [105], [34]. CeO<sub>2</sub> has been chosen for its redox activities which facilitate the oxidation and hydrogenation reactions during hydrothermal conversion.

### **I.1. Characteristic of cubic CeO<sub>2</sub> nanocatalyst**

The catalytic activity of CeO<sub>2</sub> arises from its redox activity via Ce<sup>4+</sup>/Ce<sup>3+</sup> cycle, which is accompanied with the catch and release of oxygen. CeO<sub>2</sub> is available under two morphologies: cubic and octahedral. However oxygen storage capacity (OSC) is used to select the best morphology. The OSC analysis reflects the redox catalytic activity. The OSC of cubic CeO<sub>2</sub> is 340  $\mu\text{g-O/g-cat}$  that is 3.4 times higher than octahedral CeO<sub>2</sub> [105]. Moreover, the

study on bitumen cracking with CeO<sub>2</sub> [105] showed that cubic CeO<sub>2</sub> had a better efficiency on the catalytic conversion of bitumen. Therefore, cubic CeO<sub>2</sub> has been chosen for the study. The average size of Cubic CeO<sub>2</sub> nanoparticles was around 8 nm.

The ratio of catalyst to the reactants was defined (29):

$$R = \text{Mass of Catalyst} / \text{Mass of dry matter} \quad (29)$$

## I.2. Expected action of CeO<sub>2</sub>

During reaction CeO<sub>2</sub> acts as a catalyst and splits water into two active species: H and O [105]. These hydrogen active species can form directly H<sub>2</sub> or stabilize the reactive intermediate species which are then reacting with organic molecules to form smaller molecules following capping reaction. The amount of H<sub>2</sub> formed is also linked to hydrogenation / dehydrogenation reactions that occurred for big molecules from liquid phase. The role of active oxygen species were mainly involved in oxidation reactions. The more the oxidation is achieved, the more CO<sub>2</sub> is produced. The concentration of these active species is expected to increase in the presence of CeO<sub>2</sub> catalyst and thus the carbon conversion would be enhanced.

So the main reactions considered to interpret the results are:

- Hydrogenation: alkene + H<sub>2</sub> = alkane.
- Dehydrogenation: alkane = alkene + H<sub>2</sub> .
- Oxidation: partial to complete (CO<sub>2</sub>) by adding oxygen on molecules.
- Capping reaction: Hydrogen activated species react with organic active site and block other organic reactions.
- Water Gas Shift reaction (cf section I.3 of chapter 1).
- Aldolisation: condensation reaction.

Retro aldolisation: fragmentation reactions, breaking C-C bonds.

## **II. Understanding of the phenomena involved during the hydrothermal conversion of black liquor**

Hydrothermal conversion of black liquor was studied at sub (350°C, self generated pressure) and supercritical (450°C, 25 MPa) conditions based on the results from chapter 3. The catalytic effect will be evaluated as regards to hydrogen production and carbon conversion using either or not CeO<sub>2</sub> nanocatalyst. Liquid phase is also investigated to elucidate secondary reactions that occurred between gas phase and molecules formed in liquid phase. Then in a third part, catalytic effect of CeO<sub>2</sub> is discussed by comparing sub and supercritical media.

### **II.1. Catalytic conversion of black liquor under supercritical conditions**

Experiments at supercritical conditions were carried out in 5 mL batch autoclaves at 450°C, 25 MPa. Reaction time of 15 min and 60 min, as well as the amount of catalyst, were investigated. The catalytic effect was evaluated towards coke formation and hydrogen production. To highlight the reactions involved, the liquid is also analyzed and compared according to the operating conditions.

#### **II.1.1. Coke formation**

Black liquor is mainly composed of dissolved lignin. During hydrothermal conversion lignin is expected to be degraded into aromatics molecules [151] such as phenolic compounds and smaller molecules such as small aldehydes. Polymerization of the phenolic molecules takes place thanks to these smaller molecules, which connect aromatic components together. Coke formation was the result of this polymerization and was formed since the splitting of lignin molecule began [75].

TEM analysis reveals that a shapeless solid (Figure 108) has been recovered without catalyst. A microanalysis with EDX detector shows the presence of carbon, oxygen and minerals; particularly sulfur (darkest spots on Figure 108). According to literature [51], minerals recovered in the solid phase are not involved in the morphology of the carbonaceous material. So, the coke recovered after reaction is composed of organic compounds and to a less extent of minerals that influence the mass recovered. However as the proportion of minerals is low, the contribution of coke is assumed to be the overall weight.

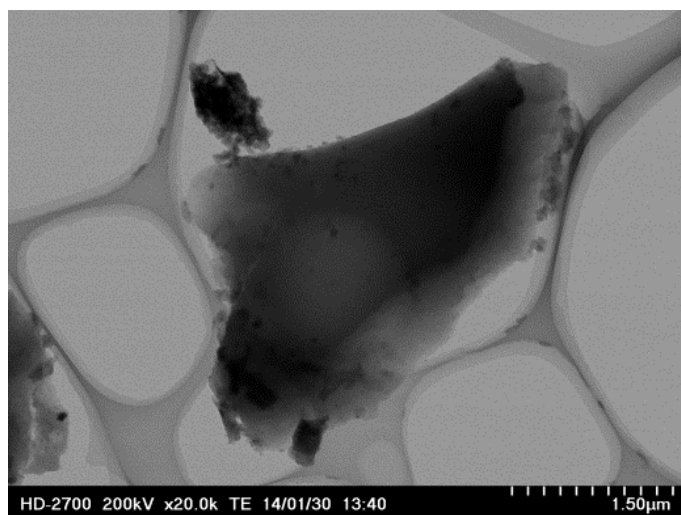


Figure 108: Solid obtained after 450°C, 15 min of reaction time, without catalyst.

The amount of coke was evaluated for the set of experiments and summarized in Table 12. The error related to mass of solids is 0.1 mg. The mass of coke produced during the reaction is about two times lower using CeO<sub>2</sub> catalyst. This result confirms that the use of catalyst reduces the coke formation. However, the amount of coke is ten times higher by increasing the reaction time. This same order of magnitude is observed using either or not the catalyst.

Using supercritical conditions, radical reactions are favored and result in the efficient degradation of lignin into phenolic compounds. So, several condensation reactions [73] are expected to take place and explain this non negligible amount of coke formed. Reaction time increased these phenomena as seen in Table 12.

Table 12: Proportion and weight of coke formed after reaction at 450°C, with /without catalyst.

	$m_{\text{coke} + \text{cat}} = (\text{g})$	% coke formed	$m_{\text{coke}} = (\text{mg})$
<b>60 min R = 5</b>	3,31E-02	13,87%	4.59
<b>60 min</b>	1,17E-02		11.7
<b>15 min R = 5</b>	1,00E-03	54,55%	0.50
<b>15 min</b>	1,00E-03		1.00

CeO<sub>2</sub> catalyst is able to oxidize organics more efficiently or rapidly than in supercritical water. Thus, the whole organics (aromatic and aliphatic molecules) are subjected to efficient oxidation reactions. Small molecules such as aldehyde, are known as promoter for polymerization of phenolic compounds [75]. In presence of catalyst, the kinetics of aldehyde oxidation is expected to be enhanced that results in a decrease of polymerization reactions and then a decrease of coke formation. Simultaneously, this complete oxidation of aliphatic compounds would increase the amount of CO<sub>2</sub> released in the gas phase.

### II.1.2. Gas formation

The gaseous phase analyzed directly after reaction is composed of H<sub>2</sub>, CO, CO<sub>2</sub>, and light hydrocarbons. However the proportion changes slightly regarding parameters studied (reaction time and catalyst). Indeed, reaction time, as well as the catalysts, played an important role in the carbon conversion and enhanced the gasification particularly towards H<sub>2</sub> production. Moreover a large amount of CO<sub>2</sub> is dissolved as carbonates due to the basic pH of the remaining solutions (pH = 10).

Figure 109 presents the proportion of carbon recovered in gas phase versus reaction time. The error related to percentage obtained from  $\mu$ -GC results is 1%. The main part of carbon in the gas phase was due to CO and CO<sub>2</sub>, produced from oxidation and water-gas shift reactions. Moreover the amount of carbon in gas phase increases with reaction time using or not the catalyst. At long reaction time, the compositions of both gaseous products are almost similar. The amounts of carbon dioxide, and to a lesser extent carbon monoxide and methane, are increasing the amount of carbon recovered in the gaseous phase at long reaction time.

As regards to the catalytic effect, Figure 109 shows that the amount of carbon converted to the gaseous phase is slightly higher at long reaction time (60 min) due to oxidation and water gas shift reactions. At short reaction time, carbon conversion to gas phase is surprisingly lower using catalyst. Indeed the gas produced using catalyst contains six times fewer methane and three times fewer CO<sub>2</sub> and light hydrocarbons. Moreover the amount of CO was under the detection limit and was not quantified using catalyst. As the volume of gas produced is almost the same in both experiments (15 min), it suggests that other gases are produced. Indeed the amount of oxygen in gas phase is tripled using catalyst and reaches 145  $\mu$ mol. Taking into account the role of catalyst on water splitting, these results would indicate that oxygen active species are recombined into O<sub>2</sub>, and the carbon gasification efficiency is affected by reactions involving these species. Kinetics of reaction between oxygen active species is expected to be higher than that of oxygen active species on organics, for short reaction time. This result underscores that the recombination of oxygen activated species could be a preliminary reaction in the global oxidation reaction of organics. Nevertheless, for a higher reaction time (450°C-60min), competition occurs between water gas shift reaction and extreme oxidation of organic molecules that released CO<sub>2</sub> also. This double production generates more CO<sub>2</sub>. After reaction an equilibrium between liquid and gas should occur and limit the capture of CO<sub>2</sub> in the liquid phase. Therefore it could explain the existence of CO<sub>2</sub> in gas phase and more amount of CO<sub>2</sub> in the presence of catalyst.



Considering the global action of CeO<sub>2</sub> on hydrothermal conversion, this catalyst increased the conversion of carbon into CO<sub>2</sub> by promoting oxidation and water gas-shift reactions.

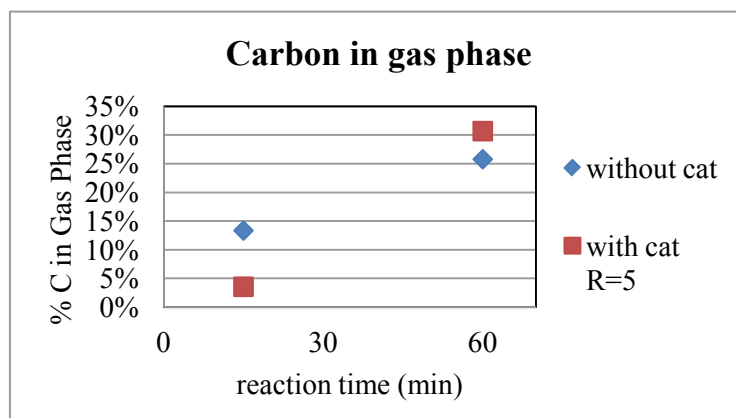


Figure 109: Proportion of carbon converted into gas phase at 450°C.

During the catalytic hydrothermal conversion of black liquor, hydrogen activated species are also expected. Figure 106 shows the amount of H<sub>2</sub> produced for the same operating conditions as previously. The error related to the calculation of produced H<sub>2</sub> is 0.02 mmol. For a long reaction time (60 min), the amounts of H<sub>2</sub> reached 345 μmol and 322 μmol using or not catalyst respectively. The amount of H<sub>2</sub> measured was related to its production and its consumption. Active hydrogen species that was produced from water splitting would easily and continuously react with another active hydrogen to form H<sub>2</sub>; as the amount of light hydrocarbons is lower using catalyst, the consumption of H<sub>2</sub> could be related to hydrogenation or/and capping reactions with organic molecules to form smaller molecules in liquid phase.

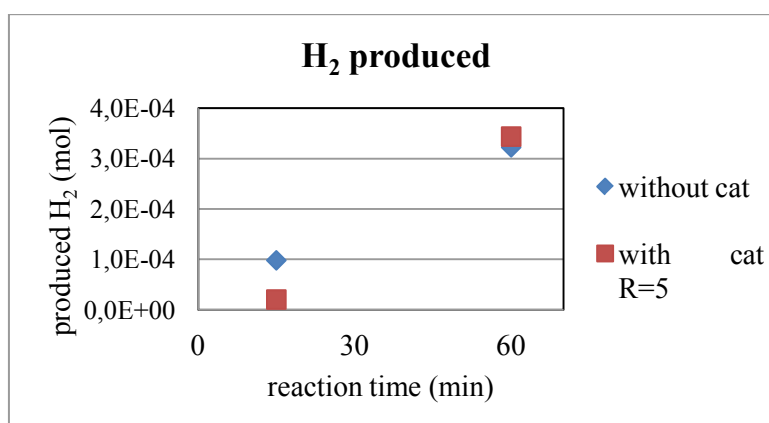


Figure 110: H<sub>2</sub> produced into gas phase after reaction at 450°C.

For short reaction time, the amount of H<sub>2</sub> is 5 times lesser using catalyst. This low amount of H<sub>2</sub>, while the amount of O<sub>2</sub> is high, indicated its consumption in other reactions. As described previously, the amount of light hydrocarbons is also lower using catalyst meaning that H<sub>2</sub> produced could be consumed in reactions such as hydrogenation in liquid phase.

To conclude, at long reaction time the catalyst improves gasification, mainly for CO<sub>2</sub>, and H<sub>2</sub> production. At short reaction time, the catalyst has a strong effect on O<sub>2</sub> production while H<sub>2</sub> and C amounts in gas phase are lower with catalyst than without catalyst. The proportion of carbon converted into gas phase suggested that exchange can occur between gaseous and liquid phases (high pH). In this case, hydrogenation reactions with liquid phase are supposed to play an important role.

### II.1.3. Liquid phase

Gel permeation chromatography (GPC) was used to separate molecules towards their molecular weight. The profiles of the curves are plotted in Figure 104, where the intensity is reported as function of the molecular weight. The profile obtained for black liquor indicates that molecules have mainly a molecular weight centered at  $\log M = 2.05$ . Moreover, a significant amount of molecules presents higher molecular weight up to  $\log M = 3.5$ . Firstly, the profiles of liquids recovered after reaction show the sharp decrease of the number of molecules between a  $\log M$  of 2.7 and 3.5. Simultaneously, the liquid was yellow (almost transparent) and the color became lighter by increasing reaction time. This is supposed to be due to the conversion of oligomer molecules to smaller colorless molecules (such as acids, aldehydes, alcohols...), polycyclic (2 or 3) aromatics molecules and/or to solid residues. Hydrothermal conversion, whatever the conditions used, is efficient to either convert organics into smaller structures (C removal) or hydrogenate molecules (O removal and H addition). Catalyst and reaction time are improving this phenomenon. Nevertheless this strong decrease could be also attributed to coke formation.

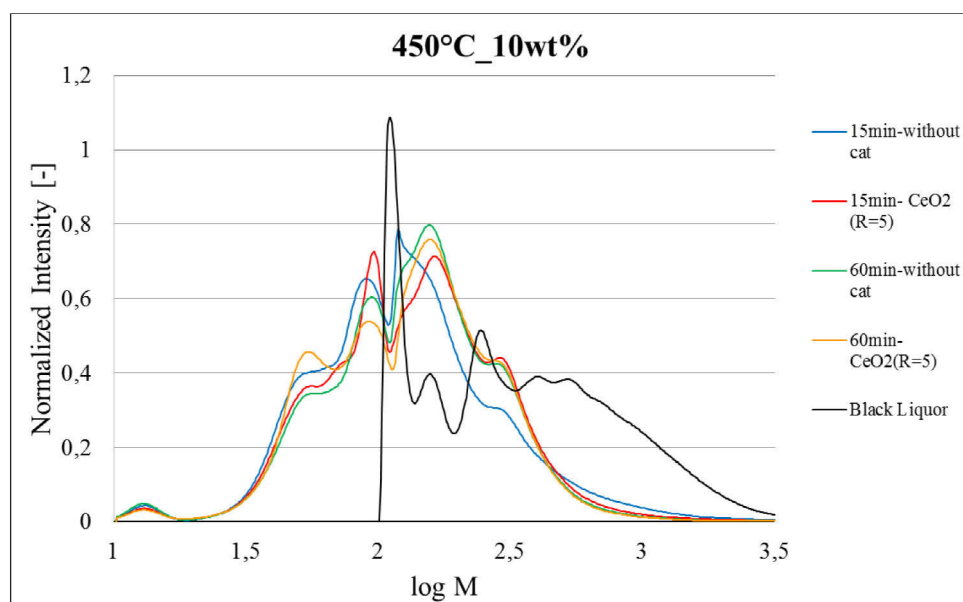


Figure 111: Catalyst influence on molecular weight at 450°C.

For experiments performed with catalyst, intensity at low molecular weight is higher, meaning that CeO<sub>2</sub> improved degradation of black liquor. At longer reaction time and using catalyst, the number of heavy molecules decreases while that of medium molecules increases with a molecular weight center at  $\log M = 1.77$ . Thus it explains the higher release of carbon to gaseous phase. Simultaneously, GC-MS analyses were carried out and confirmed that smaller molecules were detected in the presence of catalyst:

At 15min: 3- butanoic acid ; propane ; 3-methyl butanal ; phenol, etc.

At 60 min: acetone ; cyclopropane, 1-ethyl-2-methyl-, cis- ; butanal, 3-methyl ; phenol, etc.

The degradation of black liquor during reaction is confirmed by the presence of these smaller molecules. Moreover oxidation by CeO<sub>2</sub> on the black liquor is completed and leads to the release of CO<sub>2</sub> into gas phase.

The basicity of the liquid phase after reaction is preserved ( $\text{pH} > 10$ ), and CO<sub>2</sub> is captured by liquid phase until liquid and gas phase equilibrium. The saturation of the chains in liquid phase does not change suggesting rather capping reactions.

#### II.1.4. Conclusions about the catalytic effect of CeO<sub>2</sub> under supercritical conditions

CeO<sub>2</sub> nanocatalyst was selected to decrease coke formation and improve hydrogen production. The objectives have been achieved considering gas and liquid analysis. Under supercritical conditions splitting of water occurred efficiently, with the use of cubic CeO<sub>2</sub>; forming oxygen and hydrogen activated species. On the one hand, complete oxidation happened for smaller molecules to release CO<sub>2</sub>. A first step of oxygen activated species

recombination into O<sub>2</sub> has to be considered. On the other hand, the hydrogen actives species seemed to react into homolytic reaction to form H<sub>2</sub> and also into capping reaction to form smaller aromatics molecules. CeO<sub>2</sub> improved water-gas shift reaction that can explain also the higher amount of H<sub>2</sub> and CO<sub>2</sub>, and lower amount of CO.

Under subcritical conditions, most of the reactions occurred into liquid phase.

## II.2. Catalytic conversion of black liquor under subcritical conditions

Experiments at subcritical conditions were carried out in 5 mL batch autoclaves at 350°C, self generated pressure. Reaction time of 15 min and 60 min, as well as the amount of catalyst, were investigated. The catalytic effect was evaluated towards coke formation and hydrogen production as previously.

### II.2.1. Coke formation

At 350°C, under subcritical conditions, reaction media is made by the mixture of three phases: aqueous phase, oily phase and gaseous phase. Due to the pressure, it assumed that the gaseous phase is weak. During the conversion, polymerization of phenolic compounds occurred, and formed spherical micro particles (see chapter 4).

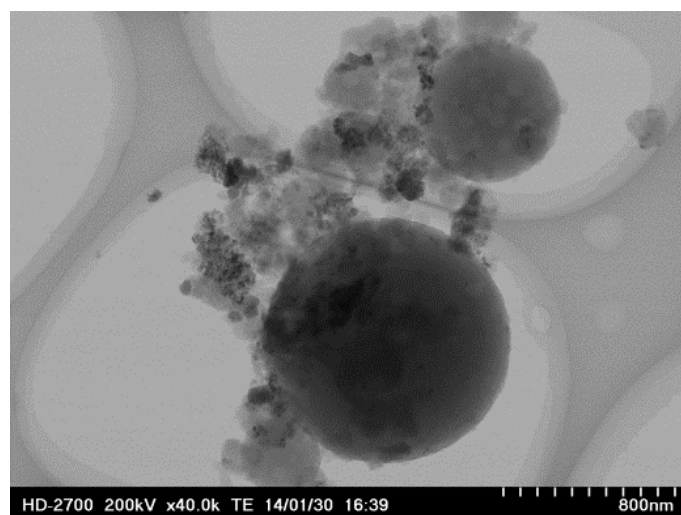


Figure 112: Solid obtained after 350°C, 60 min of reaction time, without catalyst.

Coke from black liquor at 350°C is still composed of carbon, oxygen and minerals. Sulfur (darkest spots on figure 112) is still detected. Minerals are observed as independent crystals to the coke.

However, in the presence of catalyst, spherical particles disappeared and the amount of coke formed is less. Coke is not visible by TEM observation, only the nanoparticles of catalyst as

shown in Figure 113. Thus the coke is not recovered as particles but as deposit on the catalyst surface. Simultaneously, the color of the virgin catalyst changed from yellow to dark brown after reaction.

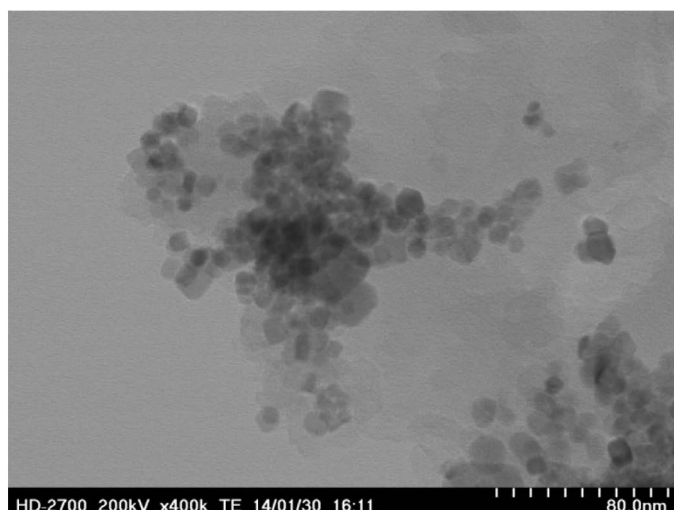


Figure 113: Solid obtained after 350°C, 60 min of reaction time, with catalyst.

The mass of coke was also evaluated after experiments and summarized in Table 13. The error related to mass of solids is 0.1 mg. At both reaction times, the amount of coke is almost halved using the catalyst.

Table 13: Proportion and weight of coke formed after reaction at 350°C (R=5).

	$m_{\text{coke} + \text{cat}} = (\text{g})$	% coke	$m_{\text{coke}} = (\text{mg})$
<b>60 min R = 20</b>	9,85E-01	1,56%	15.4
<b>60 min R = 5</b>	1,34E-01	3,81%	5.1
<b>60 min</b>	9,30E-03		9.3
<b>15 min R = 5</b>	2,51E-01	2,70%	6.8
<b>15 min</b>	1,01E-02		10.1

A second experiment was carried out using higher catalyst ratio (R=20) for 60 min reaction time. The total amount of coke formed was higher in mass (15.4 mg at R=20 compared to 5.1 mg at R=5) but lower in mass percentage in the solid (1.56 wt% compared to 3.81 wt% at R=20 and 5 respectively). A hypothesis was an antagonist effect of CeO<sub>2</sub> as catalyst and as carrier of coke formation. In addition, probably oxidation is not complete because catalyst efficiency is low under subcritical conditions and water properties are less optimal for reactivity.

Analyzes of gaseous phase can give first information on the level of oxidation made by CeO<sub>2</sub> on aromatic molecules regarding in particular carbon conversion.

### II.2.2. Gas formation

The volumes of the gaseous phases are not strongly affected by reaction time and catalyst. Gaseous phase is mainly composed of H<sub>2</sub>, CO, CO<sub>2</sub>, and light hydrocarbons. The carbon conversion to gas phase has been calculated and was found surprisingly low at long reaction time. The error related to percentage obtained from  $\mu$ -GC results is 1%. The analysis of CO<sub>2</sub> distribution shows that it is mainly recovered as carbonates. Therefore, the percentage of initial carbon recovered in the gaseous phase, as well as dissolved carbonates (inorganic carbon in liquid phase) was calculated and presented in Figure 114. For both reaction times, the amount of organic carbon converted increased slightly using the catalyst. The reactivity of CeO<sub>2</sub> is not significantly demonstrated with these conditions except with a ratio of 20 (not shown). The overall low conversion would be due to subcritical temperature which improves reactions in liquid phase rather than in gas phase. The compositions of the gaseous phases were also compared.

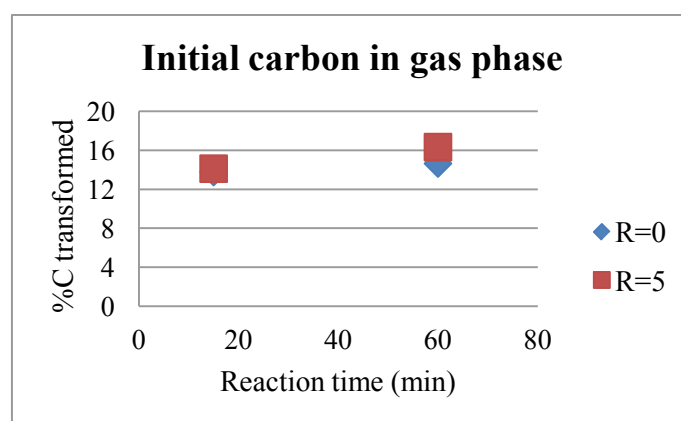


Figure 114: Distribution of initial organic carbon in gas phase and dissolved carbonates at 350°C.

Concerning the total amount of CO<sub>2</sub> (in gas phase and dissolved as carbonates), it is significantly higher using catalyst at higher reaction time. For short reaction time using the catalyst, the amounts of light hydrocarbons are 2 to 3 times higher while at higher reaction time, the amount of CH<sub>4</sub> increased significantly in presence of catalyst (10 times higher). For short reaction time, carbon monoxide was also detected. The proportion of organic carbon being higher (alkane and alkenes), the catalyst enhances the reactivity of the media.

Probably, the action of CeO<sub>2</sub> on water under subcritical conditions is the same as supercritical conditions with lower efficiency. Into subcritical conditions, in the same way as supercritical conditions, hydrogen active species can form directly H<sub>2</sub> or react with organic molecules. Simultaneously, other reactions occurred like dehydrogenation that release H<sub>2</sub> in gas phase from alkenes formation.

Figure 115 shows that the amount of produced H<sub>2</sub> is significantly increased in the presence of the catalysts at 350°C and 60 min. The error related to the calculation of produced H<sub>2</sub> is 0.02 mmol. The other experimental conditions demonstrate a moderate effect of the catalyst.

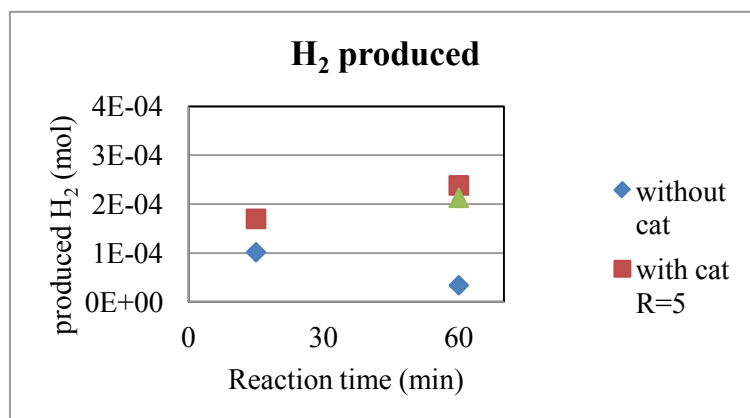


Figure 115: H<sub>2</sub> produced into gas phase after reaction at 350°C.

Active hydrogen species that was produced from water splitting would easily and continuously react in gas phase to form H<sub>2</sub>. H<sub>2</sub> was also produced by water-gas-shift reaction and by dehydrogenation reaction from alkane. However the increase in active hydrogen species would simultaneously increase reactions with organic molecules. Concerning the experiments carried out at 350°C and 60 min, the amount of H<sub>2</sub> was multiplied by 10 using CeO<sub>2</sub> as a catalyst. This means that H<sub>2</sub> consumption was higher at long reaction time without catalyst while H<sub>2</sub> production would be higher using catalyst. The amount of H<sub>2</sub> was not affected by the catalyst ratio (R= 5 or 20, 350°C and 60 min) even with a higher ratio of 20. As the amount of H<sub>2</sub> produced from water splitting would be higher especially for R = 20, H<sub>2</sub> produced would be used for capping reaction in liquid phase to produce smaller molecules; also committed into hydrogenation/dehydrogenation reactions.

Conversion of carbon into CO<sub>2</sub> is not high at long reaction time that can suggest oxidation is not complete to release CO<sub>2</sub> but to produce smaller molecules containing oxygen. H<sub>2</sub> seemed to be limited or used with faster kinetics into concurrent reactions. The analysis of liquid phase should help to better understand.

### II.2.3. Liquid composition

From gas phase analysis, black liquor conversion is expected to be less than under supercritical conditions. As the proportion of carbon converted into CO<sub>2</sub> is less, partial oxidation of liquid molecules is expected using catalyst. Regarding catalyst action, as previously, the focus is made on hydrogenation and oxidation reactions.

The oxidation of molecules is noticed; by GC-MS in the presence of catalyst, especially at 60 min; R=20 and R=5; with oxidized molecules like 1(3H)-Isobenzofuranone, 6,7-dimethoxy-3-[2-(2-methoxyphenyl)-2-oxoethyl]. Alkynes were also detected with 2-Methylphenylacetylene so reaction of dehydrogenation occurred in the same time as retroaldol reactions, favored in basic media. As a result, these reactions compete with capping reactions. Probably kinetics (at 350°C) for dehydrogenation reaction is higher than kinetics for capping reaction. This tendency can explain why the amount of H<sub>2</sub> remains the same. A high amount of aromatic compound was obtained into liquid and less coke was formed.

Some heavy molecules were remained into liquid phase (cf. GC-MS results). This result was supported by liquid color. The deep color is due to the presence of phenolic compounds [72]. The liquid was still brown and no color variation was observed within the reaction time. The color became lighter with increase of reaction time and for a high ratio (R=20). These results mean that degradation is slow under subcritical conditions and most of molecules were still polycyclic molecules. This observation was supported by gas permeation chromatography (Figure 116).

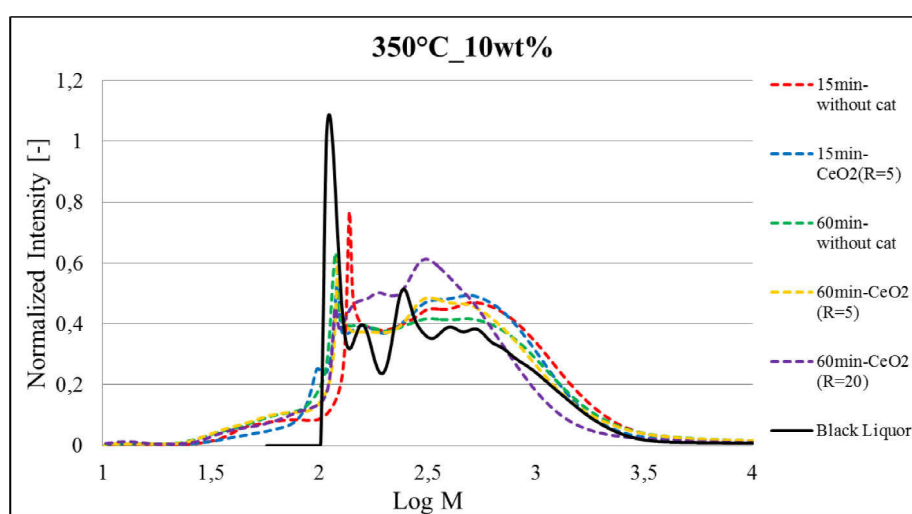


Figure 116: Catalyst influence on molecular weight at 450°C and 350°C.



The main peak of log M observed for original black liquor is slightly decreased using catalyst. The curve obtained after 15 min reaction time without catalyst presents a shift of the main peak to higher molecular weights. This significant increase of M would be due to O or C addition rather than H addition. For the whole set of conditions, the molecules in the region of log M comprised between 2.2 and 2.5 seem to be particularly reactive as the peaks of the original BL are smoothed. However the intensity of log M in the region of 2.5 to 3 suggests the recovery of polycyclic molecules.

The shift of the curve for R=20 means other populations of molecules were more represented. For this temperature, all curves are stackable to Log M = 2; so no smaller molecules are formed.

#### **II.2.4. Action of CeO<sub>2</sub> in the conversion under subcritical conditions**

Under subcritical conditions, splitting of water occurred by CeO<sub>2</sub> making water more reactive. From results obtained, most of reactions were in liquid phase. On the one hand, H reacts into hydrogenation / dehydrogenation reaction to form alkene and saturated cycle like indane. On the other hand, O is used to oxidize molecules but under these conditions oxidation is partial. That can explain the low percentage of carbon that was converted into gas phase and into coke. Under subcritical conditions retro-aldol reactions occurred also that decreased the availability of small aldehyde to connect phenolic compounds into coke.

Action of CeO<sub>2</sub> on water is the same under sub and supercritical reaction but main reactions differ between these both conditions

### **II.3. Comparison between the catalytic conversion of Black Liquor under sub and supercritical conditions.**

#### **II.3.1. Carbon conversion**

The quantity of coke was increased in the supercritical conditions; due to the efficiency of water under these conditions on the high degradation of lignin in phenolic compounds. Radical reactions were increased in supercritical conditions so a high level of condensation reactions is expected and they explain that no negligible weight of coke is formed. Reaction time increases this phenomenon.

The degradation of organic carbon to gas phase (or inorganic carbon) is higher at 450°C as expected. So gasification is favored under supercritical conditions. Indeed ~20 wt% of initial carbon is converted into gas phase at 450°C whereas only 5 wt% max is converted into gas

phase under subcritical conditions. This observation suggested that efficiency of catalyst is higher under supercritical conditions especially due to oxidation reactions. At the same time, the analyses of liquid phases (GPC, GC-MS and color) confirm the production of molecules with lower molecular weights at high temperature as reported in Figure 117 (GPC results). As a result, partial oxidation was obtained at subcritical conditions while the process is more achieved at high temperature.

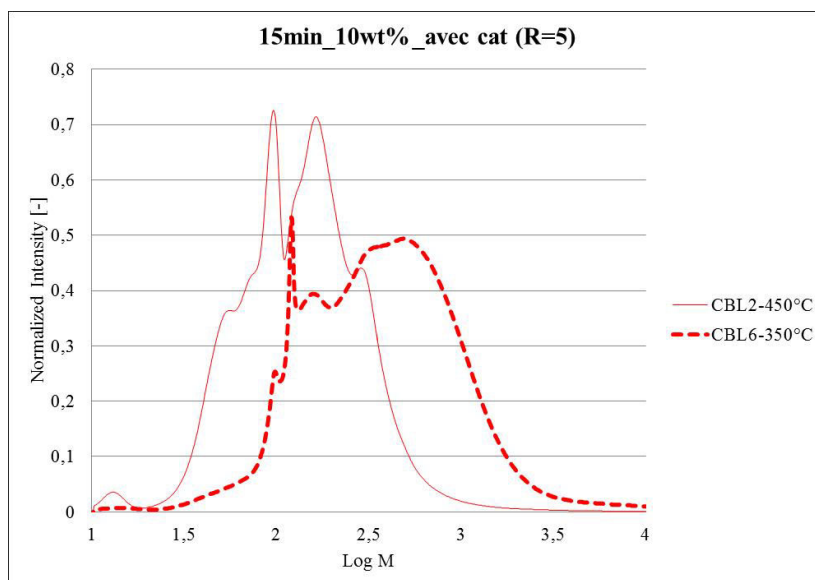


Figure 117: Comparison of GPC results at 350 and 450°C.  $t = 15$  min and  $R = 5$ .

As regards to coke formation, for both temperatures, coke was formed (Tables 12 and 13); its proportion was increased in the supercritical conditions. The proportion of coke formed decreased when the ratio of catalyst increases at 350°C. The efficiency of catalyst seems to be higher at low temperature (subcritical conditions). Under subcritical conditions, amount of coke would be lower due to a combined effect of catalyst and retro-aldol reaction. Thus the efficiency of the catalyst towards the reduction of coke formation seems to be higher at subcritical conditions. The analysis of the solid morphologies reveals some differences. Indeed, Figure 118 (a) presents TEM images of solid recovered at 450°C (60 min, using catalyst). A micro-analysis with EDX detector was performed and showed the presence of mineral content in the solid formation (Figure 118 b-f).

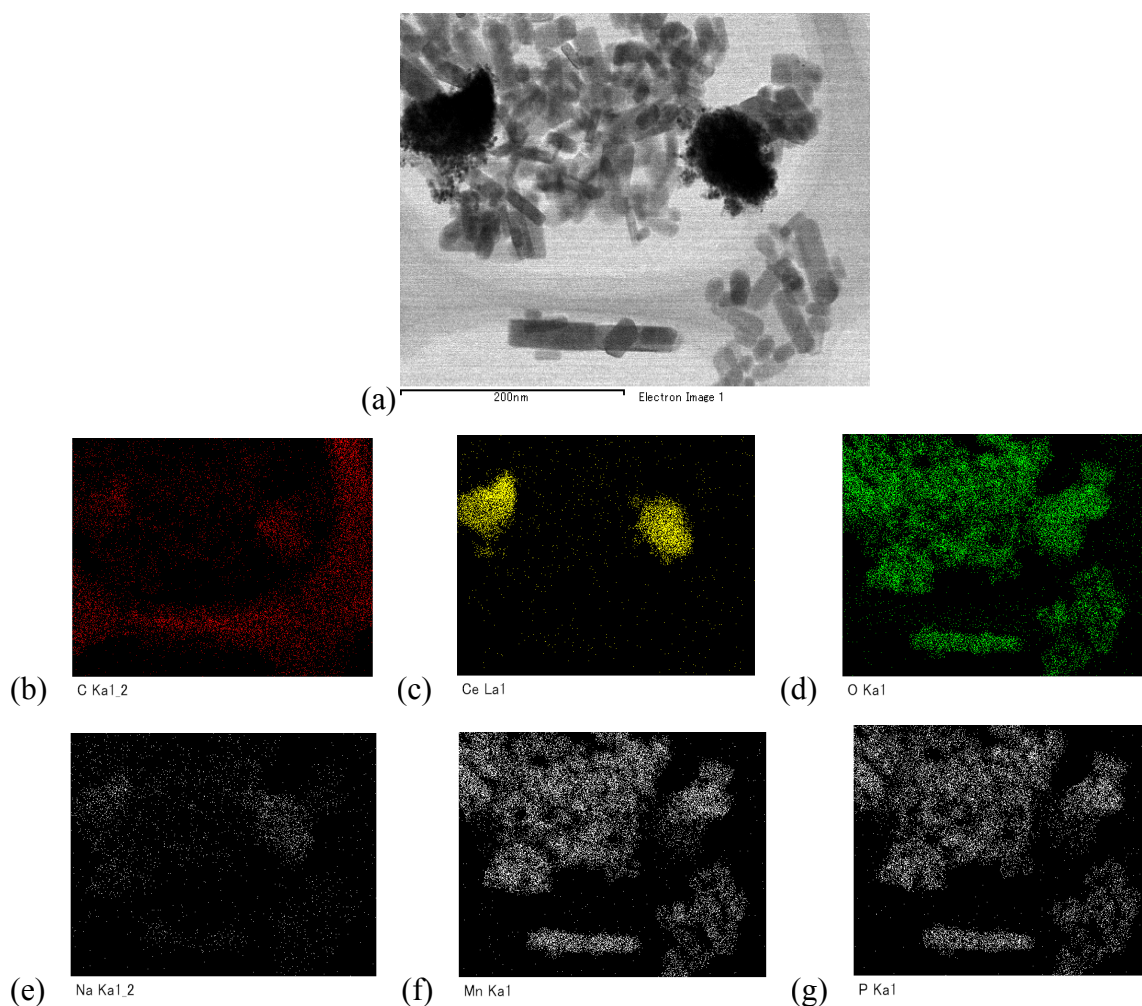


Figure 118: TEM image (a) and micro-analysis (b-g) of solid recovered after experiment (450°C,  $t = 60$  min,  $R = 5$ ).

The pictures from Figure 118 (a and b) shows a rod-shape solid. However this rod-shape is not attributed to the carbonaceous solid (i.e. coke) as regards to C distribution (Figure 118 a and b). Oxygen is a one of main element recovered in the solid formed (Figure 118 b and d). However this solid formed is not composed of carbon, but with minerals, such as Na, Mn, P (Figure 118 e-g) or Ca, S (not showed), are also recovered. These analyses highlight the high use of oxygen active species for oxidation or complexation reactions, either with organics or minerals. To conclude, the solid obtained from catalytic conversion at supercritical conditions seems to contain higher amounts of minerals compared to the solid obtained without catalyst. On the contrary, in the presence of cubic CeO<sub>2</sub> at 350°C, carbonaceous solid was not visible by TEM but the cartography was able to measure some carbon (Figure 119 a). Figure 119 presents the TEM pictures and micro-analysis of solid residue recovered at subcritical conditions (350°C,  $t = 60$  min,  $R = 5$ ). The shape of the solid recovered is different from that obtained at supercritical conditions. Figure 119 (b and c) shows that carbonaceous solid is dispersed on the catalyst. The amount of oxygen is still high but seems to be more distributed

between organic and mineral parts. The amount of minerals, especially oxygenated compounds, seems to be lower at subcritical conditions. Aside from the quenching that would lead to high amounts of precipitate salts at supercritical conditions, oxygen species from water splitting seem to be less available for mineral oxidation at subcritical conditions. Thus the effect of catalyst towards oxygen release seems to be higher at 450°C as regards to oxidation reactions in solid phase. In addition, the carbon conversion to solid phase requires an elemental analysis to be calculated.

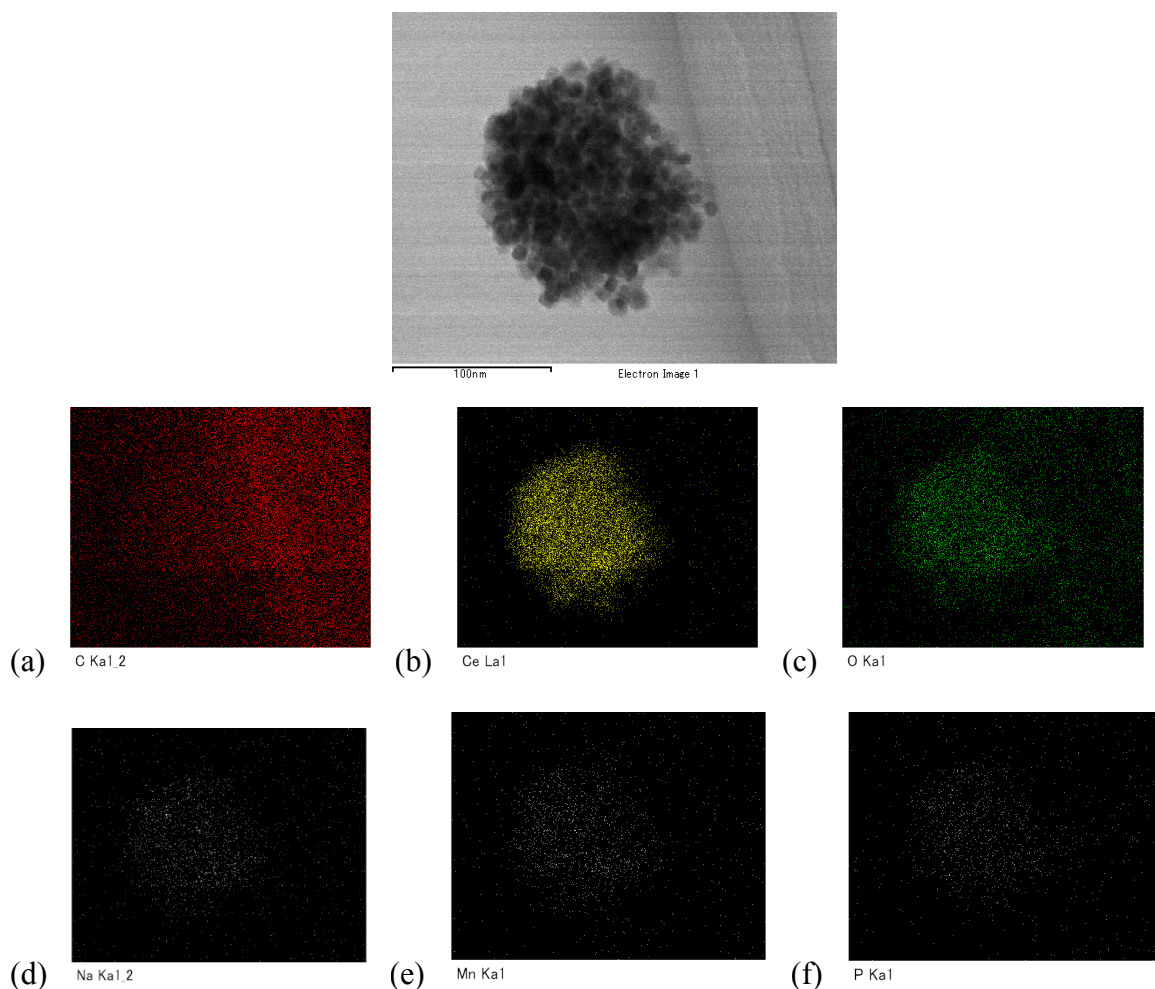


Figure 119: TEM image (a) and micro-analysis (b-g) of solid recovered after experiment (350°C,  $t = 60$  min,  $R = 5$ ).

### II.3.2. H<sub>2</sub> production

As mentioned previously the effect of catalyst has to be evaluated towards coke inhibition and hydrogen production. To compare the results, the amount of H<sub>2</sub> produced (in  $\mu\text{mol}$ ) was divided by the mass of organic content introduced (mg). The values obtained are close to 2 at subcritical conditions for both reaction time with catalyst; while this ratio reaches 10 to 40 at supercritical conditions respectively at 15 min and 60 min of reaction time with catalyst. So

the amount of hydrogen produced is clearly enhanced by temperature. Concerning the gaseous phase composition, light hydrocarbons with single bonds (C<sub>2</sub> and C<sub>3</sub>) are in higher concentration at supercritical conditions compared to C<sub>2</sub> and C<sub>3</sub> compounds with double bonds. On the contrary, concentrations of alkenes are higher than alkanes at 350°C. So these results indicate that hydrogenation is enhanced at 450°C. Hydrogenation reactions would be favored as the amount of hydrogen, such as hydrogen active species or dihydrogen, is higher at 450°C.

Hydrogen formed by water splitting is used to react with organic molecules. Reactions pathways are guides by operating conditions. Under subcritical conditions, hydrogenation/dehydrogenation is favored whereas, under supercritical conditions, capping reaction is predominant.

#### II.4. Conclusion

The goal of the study was to investigate the catalytic effect of cerium oxide nanocatalyst towards hydrothermal conversion of black liquor. The use of catalyst would lead to an increase of hydrogen production and an inhibition of the coke formation. First the analyses of gaseous phases reveal that catalyst seems to improve hydrogen production, as well as the temperature and the reaction time. Although this amount was lower using catalyst (450°C), the amount of hydrogenated products was increased. Concerning coke formation, the amount was lower using catalyst.

As expected, cerium oxide nanocatalyst is efficient to improve black liquor conversion.

As the trend observed for hydrogen concentration was not clearly defined, the mechanism or action of catalyst was also investigated. The hypothetic action was suggested through water splitting into hydrogen and oxygen active species. This active species are either able to react with organic and mineral compounds (i.e. hydrogenation, oxidation) or with other actives species. Indeed, H<sub>2</sub> molecules can be consumed by hydrogenation reaction from alkane or is released when dehydrogenation occurred. A part of these active species can react also with liquid molecules by capping to form smaller molecules (fewer complexes). GPC and color of liquid attested this degradation.

Active oxygen species are able to oxidize organic molecules that release CO<sub>2</sub> and CO at the final stages. The low amounts of CO suggested its consumption in water gas shift reaction; which was promoted by alkaline salts and CeO<sub>2</sub> catalyst. As the oxidation would be almost complete using catalyst, the amount of alcohols or aldehydes was limited compared to acids.

When oxidation was extreme, CO<sub>2</sub> was released to gas mixture. Thus polymerization of phenolic compounds and aldehydes is limited.

We also noticed that the amount of O<sub>2</sub> and H<sub>2</sub> at 450°C, short reaction time and using catalyst was significantly modified compared to the experiment without catalyst. Indeed, a higher O<sub>2</sub> content was measured and hydrogenated products (such as alkanes) were identified. By increasing reaction time, O<sub>2</sub> would be used for oxidation reaction that increases CO, CO<sub>2</sub> and intermediates of oxidation. In the same way the amount of mineral oxide in the solid phase seems to be favored by catalyst and temperature increase. Moreover the ratios between oxygen (or hydrogen) and initial organic content showed that the reaction were improved at high temperature where the splitting would be favored.

### III. Preliminary study for technical industrial feasibility

Considering the H<sub>2</sub> production from catalytic conversion of the black liquor, a preliminary feasibility study for energy balance can be done. It is based on experimental results and consists in heat and mass balances of the reaction. This study aims to determine the best operating conditions and the parameters in order to fit the industrial requirements of process implementation in industry. This first approach considers batch hydrothermal conversion of black liquor. The study highlights a list of routes to be explored and they are also exposed concerning continuous treatment.

#### III.1. Batch process

The fixed parameters for this study are:

- a 60 min reaction time,
- a 70% recovery of the heat used to perform the hydrothermal conversion,
- initial incoming reagent temperature and pressure (20°C, 0.1 MPa).

The other parameters for this study are:

- concentration of black liquor (10 wt. % of raw black liquor or raw black liquor),
- use of CeO<sub>2</sub> as catalyst (yes or not),
- final temperature (350°C or 450°C),
- final pressure (0.1 MPa or 25 MPa).

The global scheme of the process is drawn Figure 120.

The calculations are based on the hereafter assumptions:

- Black liquor enthalpy is treated as water enthalpy,
- H<sub>2</sub> production rate at 25 MPa and at 0.1 MPa are equals,
- Thermal efficiency of H<sub>2</sub> use is 100 %,
- H<sub>2</sub> production from raw black liquor is 10 times the H<sub>2</sub> production from 10 wt% black liquor solution,
- CeO<sub>2</sub> has no influence on the final pressure and on the heat required.

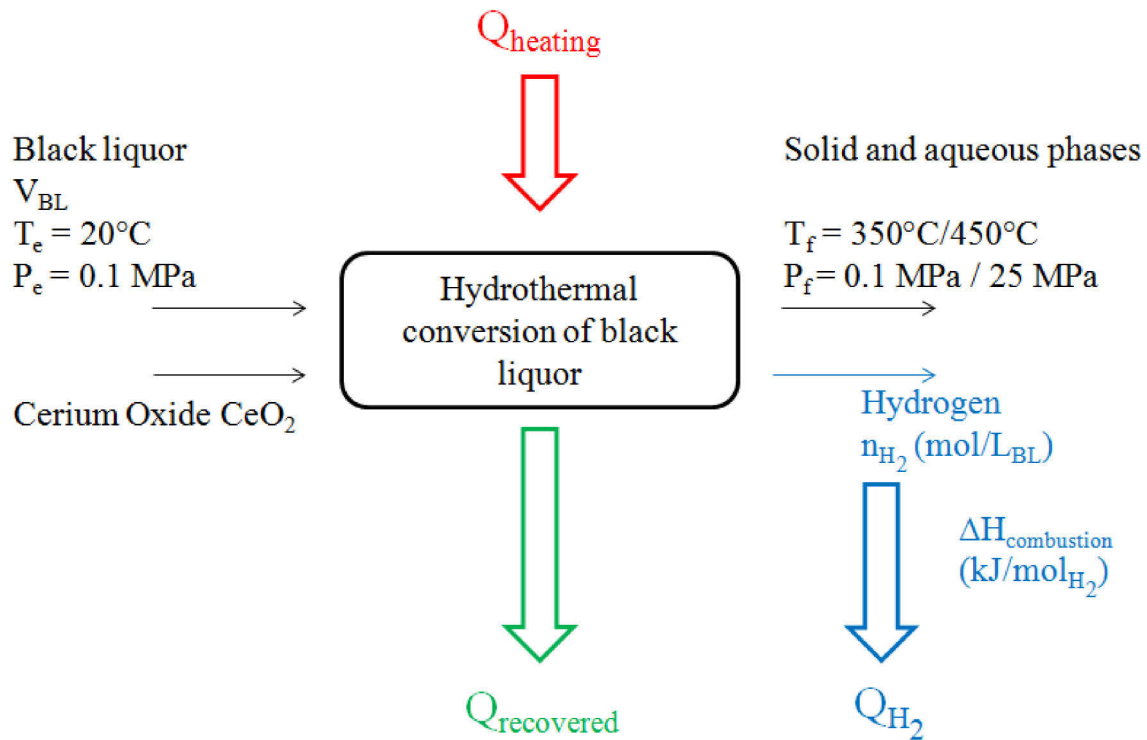


Figure 120: First approach for heat balance of hydrothermal conversion of black liquor.

The other parameters used for these calculations are:

- Molecular weight of water: 18 g/mol
- Molecular weight of hydrogen: 2 g/mol
- 10 wt. % black liquor density:  $d_{10\% \text{ wt}}^{BL} = 1.0112$
- Pure black liquor density:  $d_{\text{pure}}^{BL} = 1.12$
- Hydrogen heat of combustion:  $\Delta H_{H_2}^{\text{combustion}} = 241.83 \text{ kJ/mol}$
- Hydrogen production with 10 wt% black liquor are experimentally:

without CeO<sub>2</sub>:

- At 350°C  $V_{10\% \text{ wt BL}}^{\text{income}} = 3.12 \text{ mL} \Rightarrow n_{10\% \text{ wt BL}}^{H_2 \text{ produced}} = 3.40 * 10^{-5} \text{ mol}$
- At 450°C  $V_{10\% \text{ wt BL}}^{\text{income}} = 0.544 \text{ mL} \Rightarrow n_{10\% \text{ wt BL}}^{H_2 \text{ produced}} = 3.22 * 10^{-4} \text{ mol}$

with CeO<sub>2</sub>:

- At 350°C  $V_{10\% \text{ wt BL}}^{\text{income}} = 3.12 \text{ mL} \Rightarrow n_{10\% \text{ wt BL}}^{H_2 \text{ produced}} = 2.38 * 10^{-4} \text{ mol}$
- At 450°C  $V_{10\% \text{ wt BL}}^{\text{income}} = 0.544 \text{ mL} \Rightarrow n_{10\% \text{ wt BL}}^{H_2 \text{ produced}} = 3.43 * 10^{-4} \text{ mol}$



Regarding previous scheme nomenclature (Figure 120), the calculations can be lead following equations 1 to 5 as follow:

$$Q_{heating} = h_{pt(P_f, T_f)} - h_{pt(P_e, T_e)} \quad \text{kJ/kg income} \quad (1)$$

$$Q_{recovered} = 0.7 * Q_{heating} \quad \text{kJ/kg income} \quad (2)$$

$$Q_{10\% \text{ wt BL}}^{H_2} = \frac{n_{10\% \text{ wt BL}}^{H_2 \text{ produced}}}{V_{10\% \text{ wt BL}}^{income} * d_{10\% \text{ wt}}^{BL}} * \Delta H_{H_2}^{combustion} \quad \text{kJ/kg income} \quad (3)$$

$$Q_{pure \text{ BL}}^{H_2} = 10 * \frac{n_{10\% \text{ wt BL}}^{H_2 \text{ produced}}}{V_{10\% \text{ wt BL}}^{income} * d_{pure}^{BL}} * \Delta H_{H_2}^{combustion} \quad \text{kJ/kg income} \quad (4)$$

$$Q_{heat \text{ balance}}^{overall} = Q_{recovered} + Q_{BL}^{H_2} - Q_{heating} \quad \text{kJ/kg income} \quad (5)$$

The operating conditions corresponding to interesting heat balance are hydrothermal conversion of pure black liquor, with or without CeO<sub>2</sub> catalyst, at 25 MPa and 450°C. These results can be explained by the higher amount of hydrogen produced with pure black liquor on the one hand and by the lower heat required to heat black liquor up to 25 MPa on the other hand.

In order to achieve the energy balance, the minimum heat recovery rate has also been calculated regarding the chosen calculation. For a hydrothermal conversion of raw black liquor with CeO<sub>2</sub> catalyst, the minimum heat recovery must be 47%. It gives a direct indication of the energy amount available to fit other process thermal needs.

The calculations results are presented in the Table 14. Green blocks show positive heat balance: Raw black liquor, 60 min of reaction time at 450°C.

Table 14: Black liquor hydrothermal conversion preliminary feasibility study results

Income	T <sub>f</sub> (°C)	P <sub>f</sub> (MPa)	Overall energy needed (kJ/kg income) <i>Q<sub>heating</sub></i>	H <sub>2</sub> production rate (mol H <sub>2</sub> / kg income)	Heat production from H <sub>2</sub> combustion (kJ/kg income) <i>Q<sub>10% wt BL</sub><sup>H<sub>2</sub></sup></i>	Heat recovery (kJ/kg income) <i>Q<sub>recovered</sub></i>	Overall heat balance (kJ/kg income) <i>Q<sub>overall heat balance</sub></i>	Heat available in case of BL pre-heating at 0.1 MPa (kJ/kg income)
Diluted black liquor 10 wt%	350	0.1	3091.81	0.0108	2.60	2164.26	-924.94	-
		25	1539.85			1077.90	-461.96	-
	450	0.1	3298.80	0.5849	141.44	2309.16	-848.20	-
		25	2866.37			2006.46	-859.91	-
Pure black liquor 100 wt%	350	0.1	3091.81	0.1077	26.04	2164.26	-901.50	-1232.37
		25	1539.85			1077.90	-461.96	-792.83
	450	0.1	3298.80	5.8489	1414.45	2309.16	424.81	93.94
		25	2866.37			2006.46	554.54	223.67
Diluted black liquor 10 wt% + CeO <sub>2</sub>	350	0.1	3091.8	0.0754	18.23	2164.26	-909.31	-
		25	1539.85			1077.90	-443.73	-
	450	0.1	3298.80	0.6230	150.67	2309.16	-838.97	-
		25	2866.37			2006.46	-709.24	-
Pure black liquor 100 wt% + CeO <sub>2</sub>	350	0.1	3091.81	0.7538	182.29	2164.26	-745.26	-1076.13
		25	1539.85			1077.90	-461.96	-792.83
	450	0.1	3298.80	6.2304	1506.69	2309.16	517.05	186.18
		25	2866.37			2006.46	646.78	315.91

Considering that heat recovery is used for black liquor income pre-heating at 0.1 MPa to a limited temperature, chosen 6°C lower than boiling point (105°C – 6°C = 99°C), the heat transfer can be optimized as followed and changes the heats required and available for other process needs (respectively  $Q'_{heating}$  and  $Q'_{recovered}$ ).

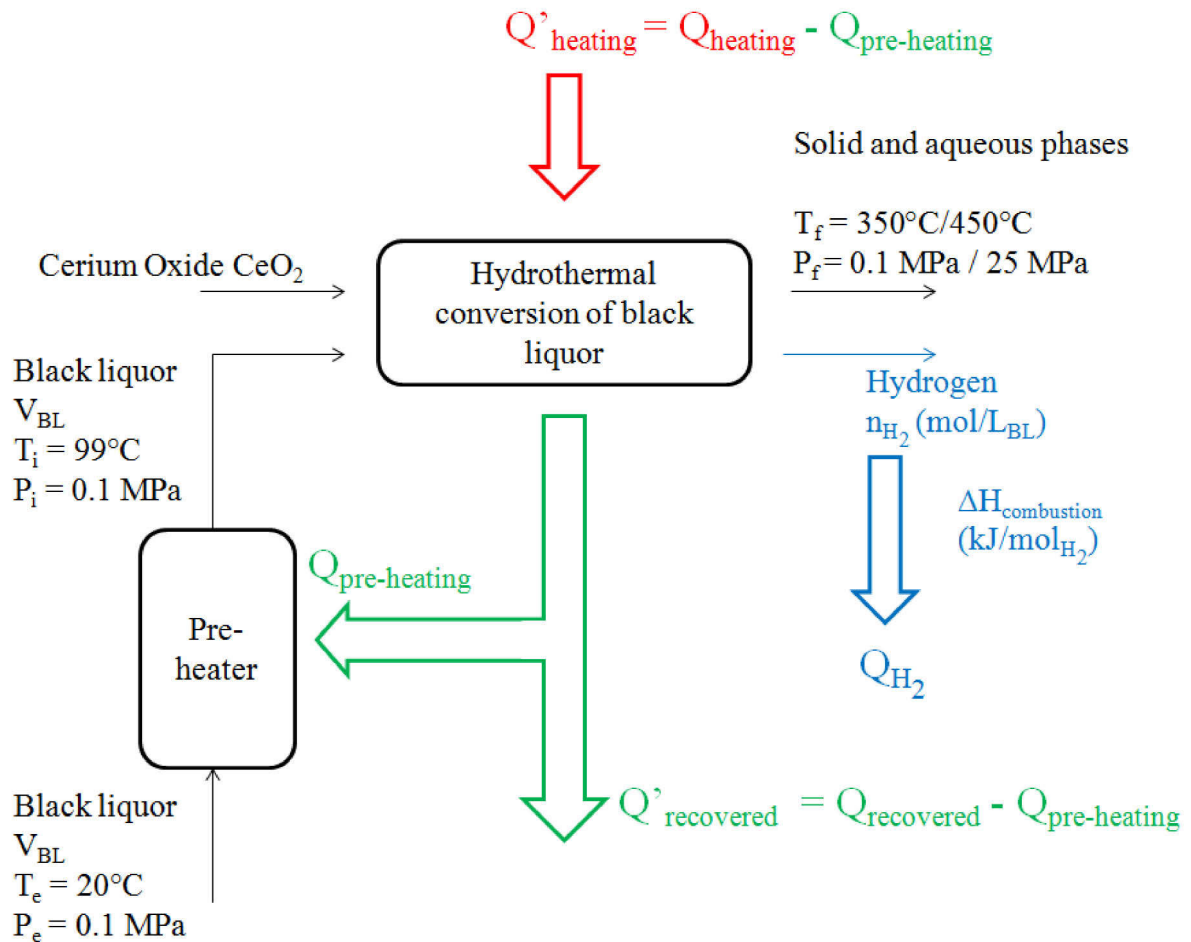


Figure 121: First approach for heat balance of hydrothermal conversion of black liquor with preheating heat recovery.

### III.2. Continuous process

Considering continuous hydrothermal conversion of black liquor, the energy recovery can be made directly using black liquor or using an intermediate heat transfer fluid. The use of intermediate fluid is most likely necessary because of products content (aqueous and solid phase) but also because of operating risks in case of fluid ingress for example.

With a view to reinstatement in the papermaking process, the temperature of products after heat recovery has been chosen very close to green liquor one before filtration and pre-treatment of causticizing, 80°C.

These two options are presented in the Figures 122 and 123; and the heat available for other needs, are presented in the Table 14.

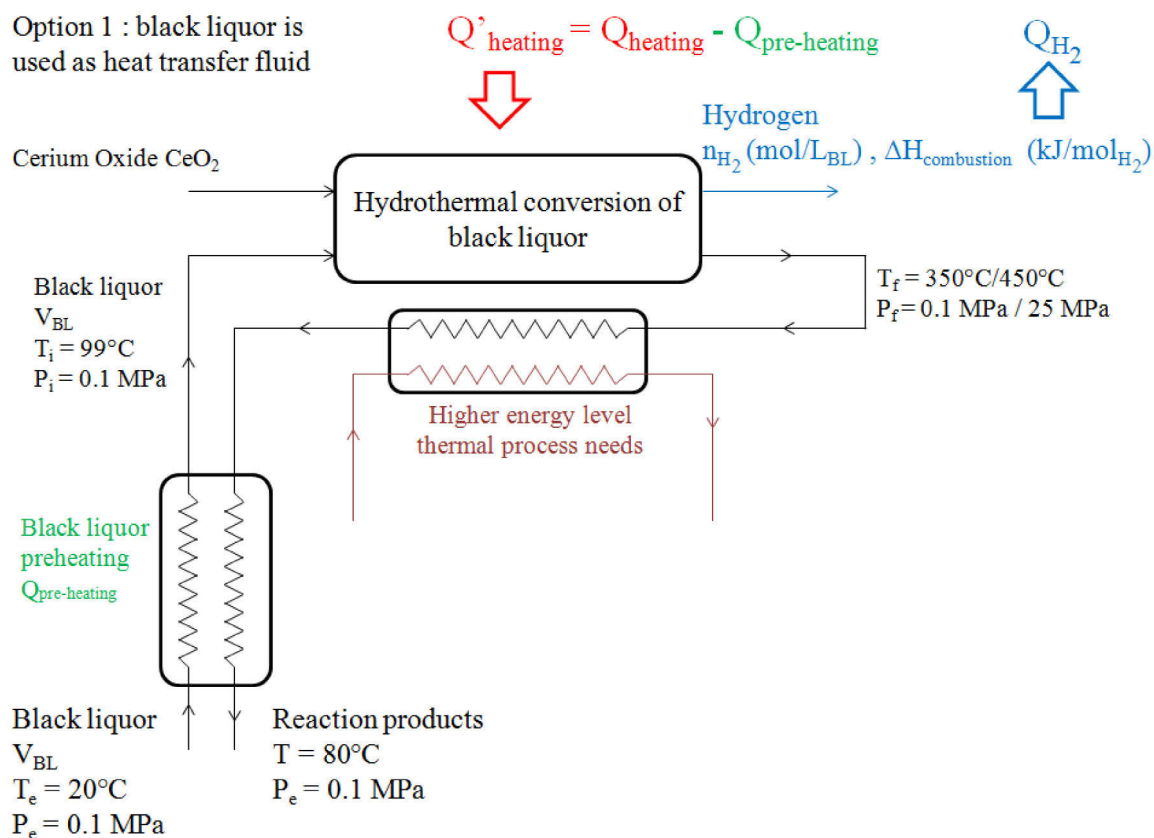


Figure 122: First approach for heat balance of continuous hydrothermal conversion of black liquor with preheating without intermediate heat transfer fluid.

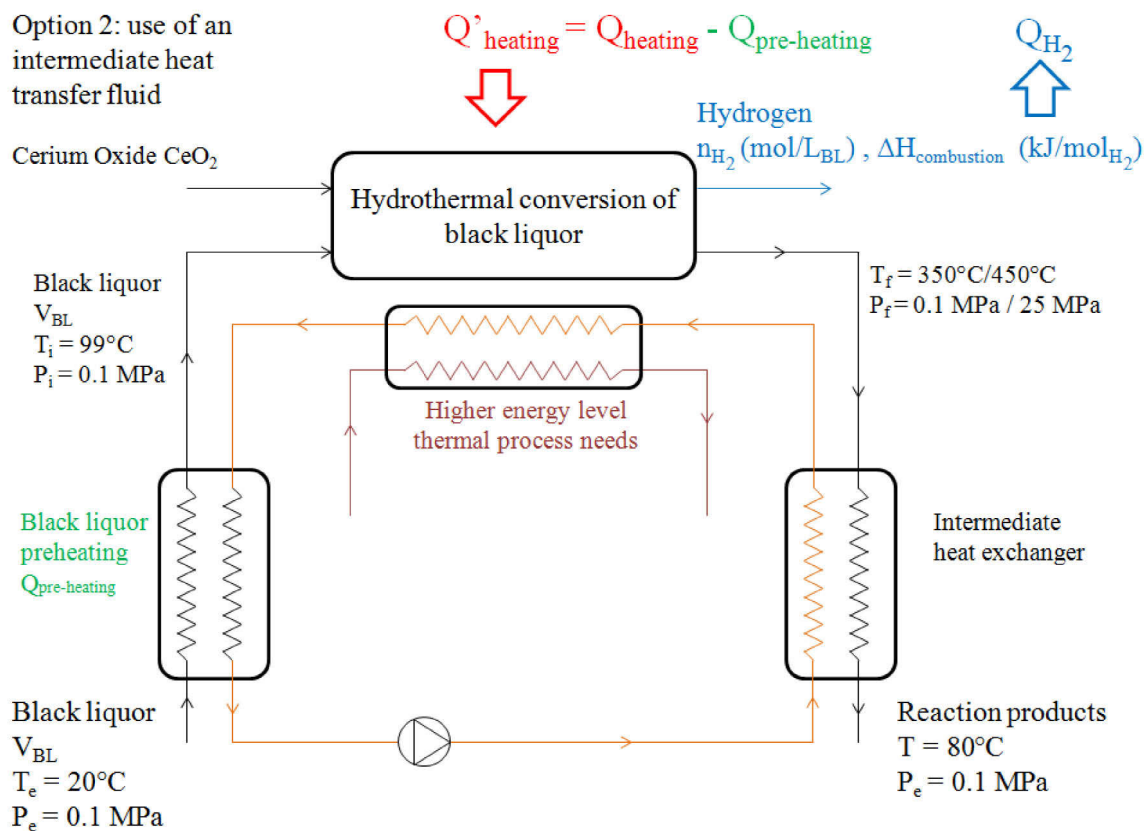


Figure 123: First approach for heat balance of continuous hydrothermal conversion of black liquor with preheating with intermediate heat transfer fluid.

Other possible optimizations for this process are:

- material and/or energy valorization of the solids obtained,
- oily phase energy valorization,
- material valorization in chemical products contained in the aqueous phase
- conversion operating conditions optimum (heat balance optimization with temperature and pressure and also reaction time)
- optimum use of recovered heat available to reach the highest energy level of black liquor (balance between auxiliary consumption for pressurizing for example and energy available after pre-heating)

Conditions for a positive energy balance are 450°C and 60 min of reaction time. To improve the balance, a continuous process with a counter current flow to preheat the black liquor could be investigated.

#### IV. Study of catalytic conversion of black liquor model molecules

Regarding the results from section II, black liquor is a very complex aqueous mixture and its complete composition is hard to analyze. To highlight its reactivity, studying its model molecules, such as lignin, and to a lesser extent GGGE, is essential. GGGE means Guaiacylglycerol- $\beta$ -guaiacyl ether; its formula is represented in Figure 124.

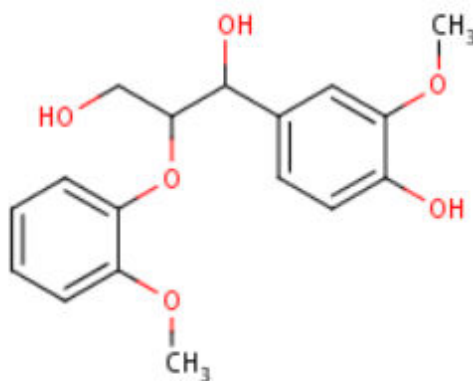


Figure 124: GGGE formula.

Among model molecules, lignin could come from different raw materials or different separation processes; and would be thus modified. Two kind of lignin were characterized to check their correspondence with black liquor and use one of them as model molecule: Alkali lignin and lignin. A GPC analysis (molecular weight) has been made and Figure 125 shows that lignin matches more with black liquor molecular weight profile than alkali lignin.

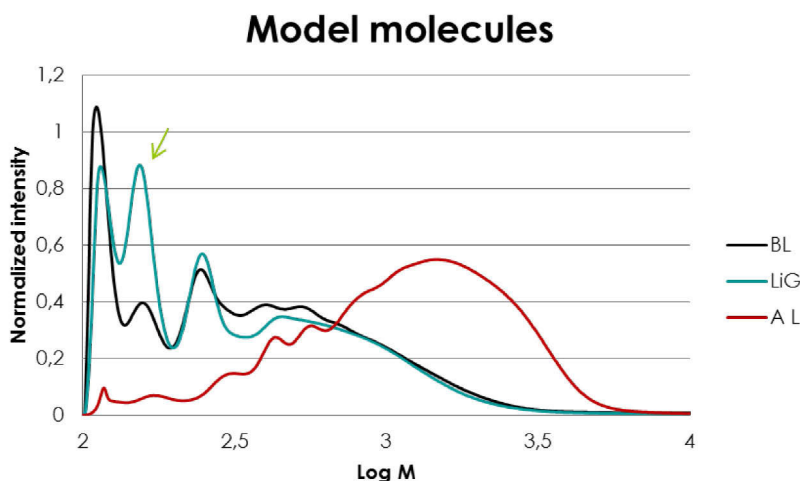


Figure 125: GPC results for the comparison between lignin, alkali lignin and black liquor.

Experiments made with black liquor have been reproduced with lignin under supercritical conditions and under subcritical conditions. The objective of this last section is a contribution to the comprehensive mechanism of catalytic decomposition of black liquor in sub and supercritical water

#### IV.1. Study of the conversion of lignin

To confirm the adequacy between black liquor and lignin, experiments with and without catalyst at 450°C and 350°C at 60 min of reaction time have been performed. Solutions of model molecules have been prepared in order to have the same ratio:  $Water/Dry\ matter$  as black liquor. As previously, liquid, solid and gas have been analyzed after hydrothermal process.

##### IV.1.1. Catalytic conversion under supercritical conditions

Figure 127 represents the profiles of GPC curves of liquid obtained after black liquor and lignin conversion. The profile of lignin is centered at  $\text{Log } M = 2.1$  whereas the profile of black liquor is centered at  $\text{Log } M = 2.2$ . Except for this predominant peak, curves have the same trend. So under supercritical conditions, lignin has the same behavior as black liquor.

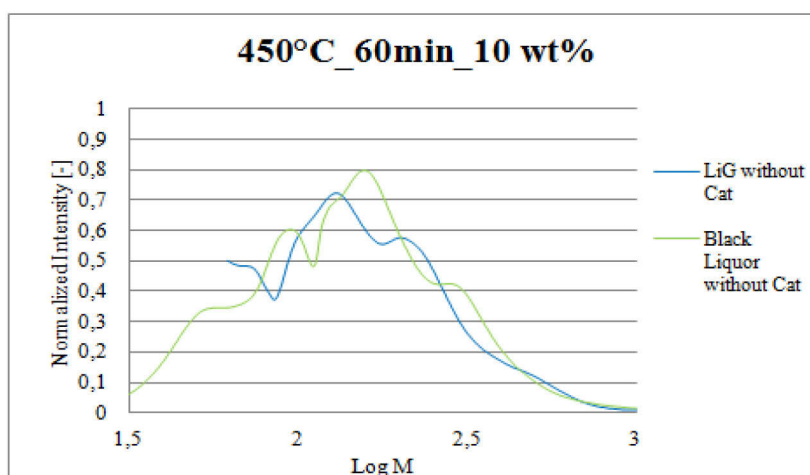


Figure 126: GPC results for liquid obtained from lignin conversion with and without catalyst ( $R=5$ ), under supercritical conditions.

Figure 127 shows the influence of the catalyst on lignin conversion. After reaction with catalyst, the curve is shifted to smaller molecular weight. For experiments performed with catalyst, intensity at low molecular weight is higher; meaning that CeO<sub>2</sub> improved degradation of lignin.

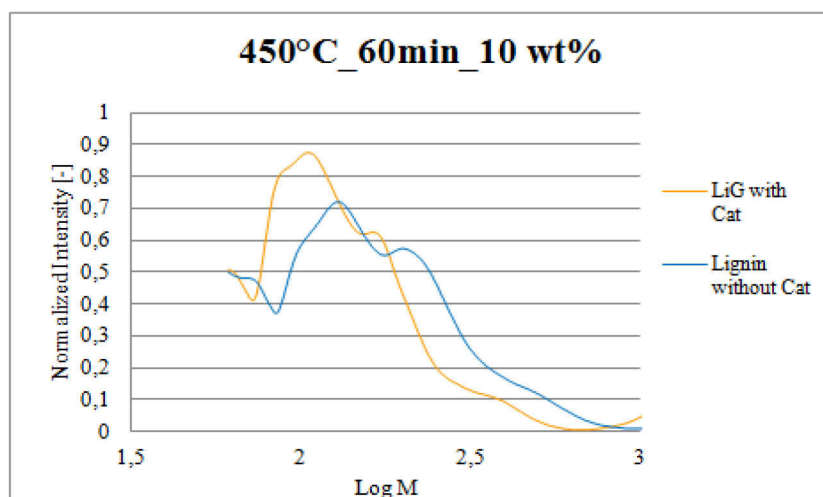


Figure 127: GPC results for liquid obtained after 60 min of reaction time without catalyst with lignin and black liquor under supercritical conditions.

The composition of the liquid is detailed Table 15.

Table 15: Molecules identified in liquid phase after hydrothermal conversion of lignin at 450°C during 60 min.

Without catalyst	With catalyst
Propane	Propane
(E)-2-Butenal,	Furan, 2,3-dihydro-
Toluene	Toluene
3-Buten-1-ol	Cyclohexane, ethyl-
Phenol	Ethylbenzene
2,5-Cyclohexadiene-1,4-dione, 2,6-bis(1,1-dimethylethyl)-	Benzene, (1-methylethyl)-
Butylated Hydroxytoluene	Benzene, propyl-
Retene	2,5-Cyclohexadiene-1,4-dione, 2,6-bis(1,1-dimethylethyl)-
Phenol, 2,2'-methylenebis[6-(1,1-dimethylethyl)-4-methyl-	Butylated Hydroxytoluene
	Benzene, (1-pentylheptyl)-
	Benzene, (1-butyloctyl)-
	Benzene, (1-propylnonyl)-
	Retene
	Phenol, 2,2'-methylenebis[6-(1,1-dimethylethyl)-4-methyl-

As exposed in Table 15 in the presence of catalyst, smaller molecules are identified with a plurality of monocyclic molecules with ramification such as 1-pentylheptyl-Benzene, 1-butyloctyl-Benzene, 1-methylethyl-Benzene, 1-propylnonyl-benzene, propyl Benzene, ethyl-Cyclohexane, Ethylbenzene. Substitutions are constituted by aliphatic group; these long carbonaceous chains are due to opening cycle (retroaldol reaction) of retene molecules (C<sub>18</sub>).



The degradation of lignin during reaction is confirmed by the presence of these ramified phenyl molecules. No more oxygenated molecules were detected meaning that oxidation by CeO<sub>2</sub> is a complete oxidation leading to the release of CO<sub>2</sub> into gas phase. The basicity of the liquid phase after reaction is preserved (pH>10) and CO<sub>2</sub> is captured by liquid. The saturation of aliphatic group in liquid phase suggested hydrogenation reactions while the presence of monocyclic mono benzene molecules suggested capping reactions.

Analyses of gaseous phases are exposed in Figure 128. The difference of the proportion of carbon converted in the gas phase (mostly CO<sub>2</sub>) between lignin and black liquor is probably due to alkali salts contained in black liquor which increase the water gas shift reaction. Moreover, lignin in black liquor is a lignin degraded by white liquor and so more easily oxidable than chemical lignin. CeO<sub>2</sub> does not seem to affect the conversion of carbon during lignin conversion. Considering GPC and GC-MS results, a part of carbon corresponds to CO<sub>2</sub> dissolving.

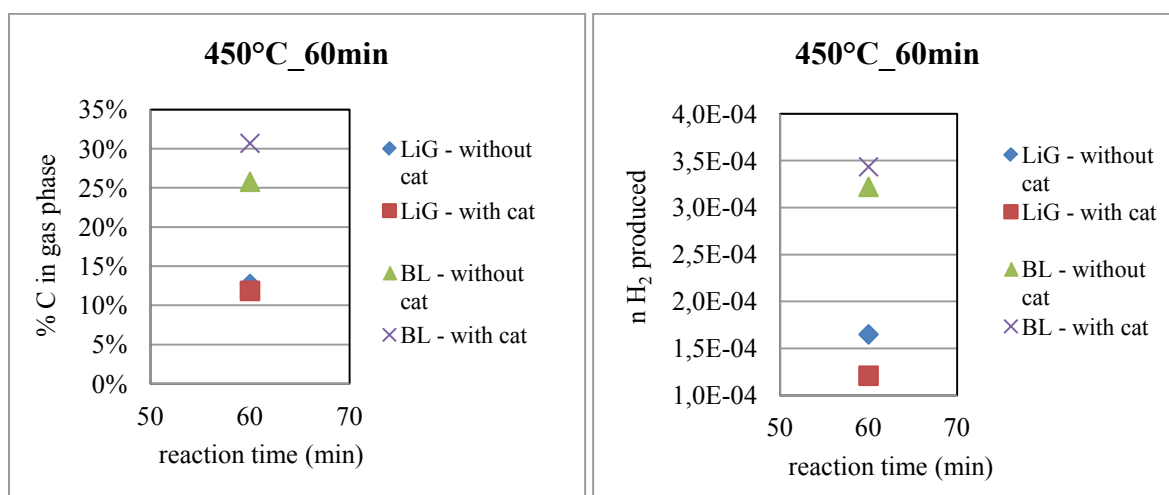


Figure 128: Gas analysis - Comparison between lignin and black liquor, with and without catalyst ( $R=20$ ). Errors are 1% for the percentage of carbon in gas phase, 0.02 mmol for H<sub>2</sub> produced.

Hydrogen production from lignin conversion is lower with catalyst. The catalyst promotes formation of more activated hydrogen that reacts in hydrogenation reactions. Indeed, as exposed in the GC-MS results saturated aliphatic groups are formed that consumes hydrogen.

Differences observed are due to alkalinity of the black liquor which improves water-gas shift reaction. During catalytic conversion, CO<sub>2</sub> formed by oxidation reaction is dissolved in liquid phase and H<sub>2</sub> produced is used in hydrogenation reactions. Alkali salts interfere with CeO<sub>2</sub> catalyst and seem to improve the effect of the catalyst.

#### IV.1.2. Catalytic conversion under subcritical conditions

Under subcritical conditions, Figure 129 shows that the molecular weight profiles, after reaction, are similar for black liquor and lignin. Thus without catalyst, bond breaking leads to molecules with similar molecular weight. It is assumed that these two molecules have the same reactivity.

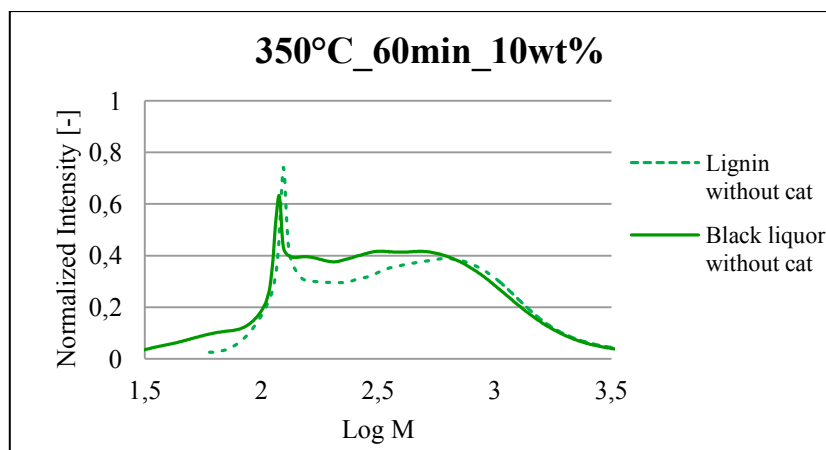


Figure 129: GPC results for liquid obtained after 60 min of reaction time without catalyst with lignin and black liquor under subcritical conditions.

As shown in Figure 129, catalyst has the same effect on lignin as on black liquor (Figure 116). The curve shifts to lower molecular weight with the formation of two populations (Log M = 2.2 and Log M = 2.5). Degradation is enhanced in the presence of CeO<sub>2</sub> catalyst as expected and observed during black liquor hydrothermal conversion in the same conditions.

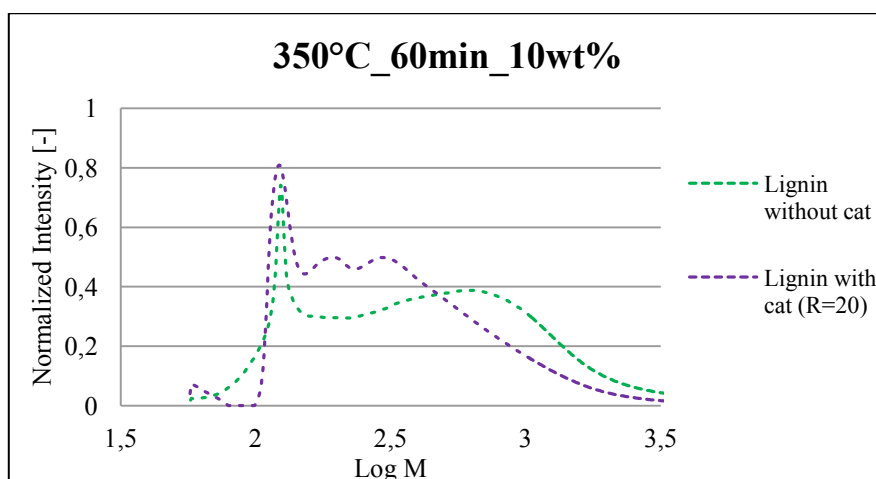


Figure 130: GPC results for liquid obtained from lignin conversion with and without catalyst (R=20), under supercritical conditions.

The results from GC-MS analysis are exposed in Table 16.

Table 16: Molecules identified in liquid phase after hydrothermal conversion of lignin at 350°C during 60 min.

Without catalyst	With catalyst (R = 20)
Furan, 2,3-dihydro-	Propane
2-Furanol, tetrahydro-	Butanal, 3-methyl-
Butyrolactone	Toluene
Phenol	Butyrolactone
p-Cymene	Phenol, 2-methoxy-
Phenol, 2-methoxy-	2,5-Cyclohexadiene-1,4-dione, 2,6-bis(1,1-dimethylethyl)-
2-Methoxy-6-methylphenol	Butylated Hydroxytoluene
Creosol	Phenol, 2,2'-methylenebis[6-(1,1-dimethylethyl)-4-methyl
Phenol, 4-ethyl-2-methoxy-	
Phenol, 2-methoxy-4-propyl-	
Homovanillic acid	

Catalyst opens the cycles creating molecules such as propane or 3-methyl-butanal by retroaldol reactions. In the same time, molecules identified in the presence of catalyst are polycyclic and highly substituted such as 2,5-Cyclohexadiene-1,4-dione, 2,6-bis(1,1-dimethylethyl)- and Phenol, 2,2'-methylenebis[6-(1,1-dimethylethyl)-4-methyl. Molecules with a higher oxidation degree are formed such as 2,5-Cyclohexadiene-1,4-dione, 2,6-bis(1,1-dimethylethyl)-. These results suggest a more complex conversion of the initial carbon but hydrogen generation was not enhanced by the presence of catalyst, as shown in Figure 131. Figure 131 compares the percentage of initial carbon converted in gas phase and the amount of hydrogen produced, from black liquor and lignin with and without catalyst.

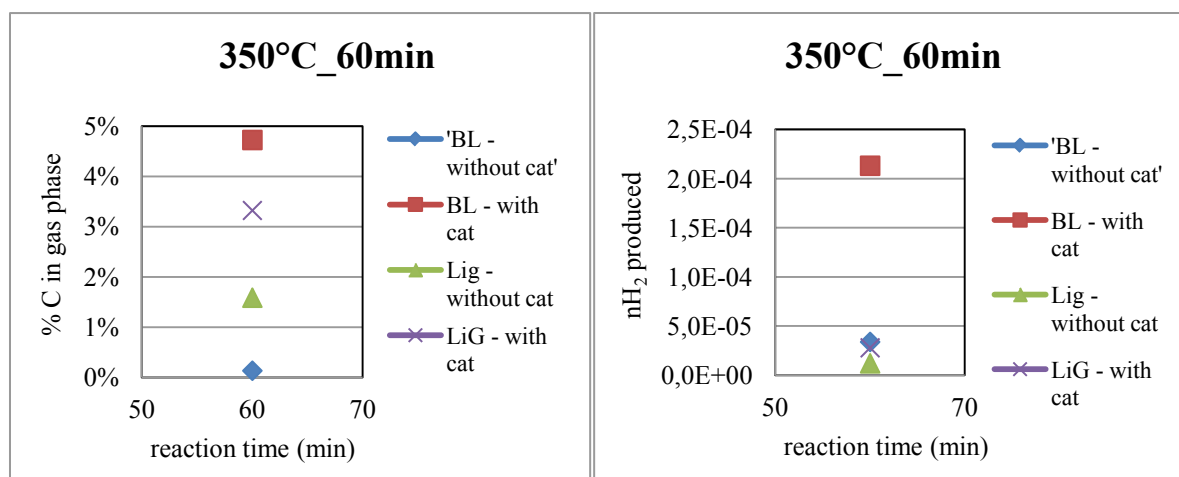


Figure 131: Gas analysis - Comparison between lignin and black liquor, with and without catalyst ( $R=20$ ). Errors are 1% for the percentage of carbon in gas phase, 0.02 mmol for H<sub>2</sub> produced.

The proportion of carbon converted in the gas phase is higher in the presence of catalyst for both materials. However, the amount of hydrogen from lignin conversion is not significantly affected by the catalyst either because of its utilization by hydrogenation reaction in liquid phase or because the amount produced is low.

Furthermore, alkali components in black liquor play an important role that explains differences observed between results from lignin and black liquor. The alkaline media in black liquor improves water gas-shift reaction producing hydrogen that increases the conversion of carbon to the gaseous phase. Differences observed in the composition of gas can be linked to the presence of alkali salts in black liquor.

In both conditions, sub and supercritical conditions, coke is formed during reaction. In the presence of catalyst, these amounts are less.

To conclude: even if no main similar molecules are highlighted, lignin and black liquor conversions lead to the same trends of phase evolutions. Similar mechanisms would occur. Due to the presence of alkali salts in black liquor, water gas shift reaction is improved that shifts chemical equilibrium.

### IV.1.3. Main mechanism pathway for lignin conversion

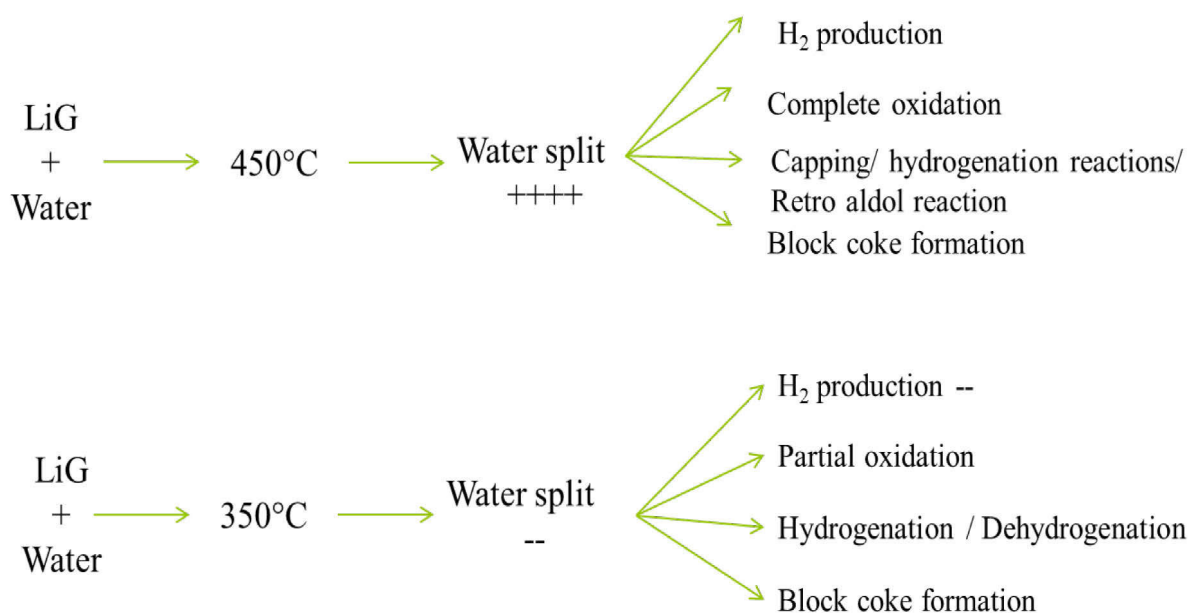


Figure 132: Summary of reactions during catalytic conversion of lignin

To understand more precisely the mechanism of the catalytic conversion, a smaller model molecule is required. A good model molecule for lignin is considered pure Guaiacylglycerol- $\beta$ -guaiacyl ether (GGGE). GGGE molecules present similar bonds and functional groups like lignin: ether, hydroxy, etoxy, phenols ... (Figure 124). Thus as the molecular structure of GGGE is well known, analyses of liquid phase after its hydrothermal conversion will let us to determine which reactions occur.

## IV.2. Study of the conversion of GGGE

GGGE is known to be a good model molecule for lignin as well as lignin is a good model molecule for black liquor. The elucidation of reaction pathway during hydrothermal conversion of GGGE will help to understand that of lignin and so of black liquor. The following analysis is exclusively devoted to the liquid phase.

### IV.2.1. Catalytic conversion under supercritical conditions

The catalytic conversion of GGGE has been studied under supercritical conditions with and without catalyst at 15 min, 30 min, 45 min and 60 min.

*Without catalyst*

Profiles of GPC plotted Figure 129 present same peaks, only intensities change. As expected, reaction time enhances degradation creating both smaller molecules (peak at Log M = 2.1 increase with reaction time) and polymerized molecules (Log M >2.4).

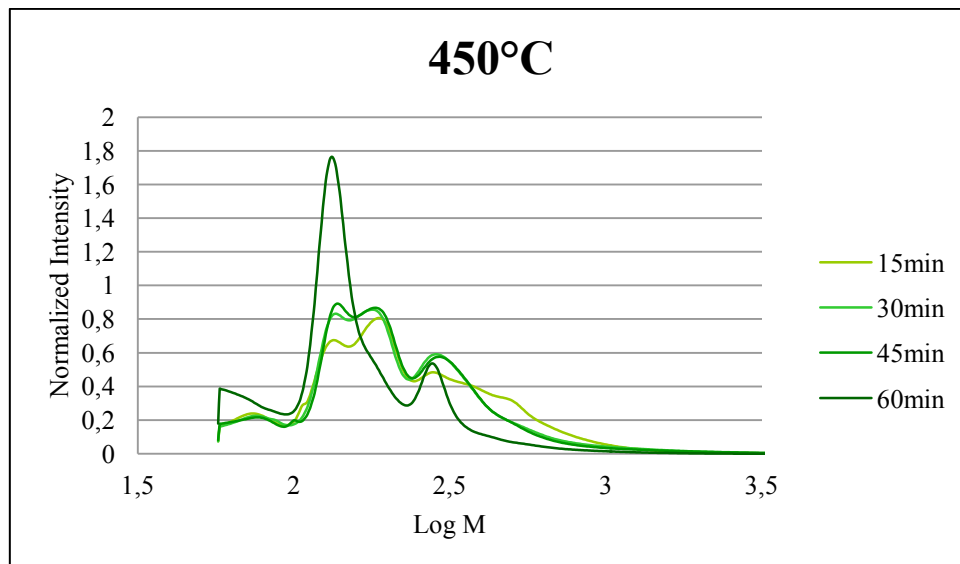


Figure 133: GPC results for liquid obtained after hydrothermal conversion of GGGE under supercritical conditions, without catalyst.

GC-MS results are presented in table 6. GGGE is degraded under supercritical water by the cleavage of the  $\beta$ -O-4 linkage to form guaiacol and guaiacylglycerol then each of these molecules react to form the molecules identified and detailed in Table 17. Phenol is obtained by retroene elimination. C-C bonds in glycerol are broken under supercritical condition; and generate formaldehyde and acetaldehyde. Under supercritical conditions formaldehyde is known to react with phenolic compounds to form molecules such as Phenol, 2,2'-methylenebis [6-(1,1-dimethylethyl)-4-methyl-]. Ramified phenolic compounds such as 2-methyl phenol, 3-methylphenol, or bi-substituted such as 2,3-dimethyl phenol and 2,4 dimethylphenol and so on are coming from alkylation reaction on phenol. Aldolisation reaction is able to formed alkanes identified such as tetracosane, hexadecane, and so on.

Table 17: GC-MS results for the liquid obtained after hydrothermal conversion of GGGE under supercritical conditions with catalyst

15 min	30 min	45 min	60 min
Phenol	Cyclohexane, ethyl-	Propane	Cyclohexane, ethyl-
Phenol, 2-methyl-	Phenol	Cyclohexane, ethyl-	Phenol
Phenol, 3-methyl-	Phenol, 2-methyl-	Phenol	p-Cresol
Guaiacol	p-Cresol	Phenol, 2-methyl-	Phenol, 2-methoxy-
Phenol, 2-(1,1-dimethylethyl)-4-methyl-	Guaiacol	p-Cresol	Phenol, 2,6-dimethyl-
Butylated Hydroxytoluene	Phenol, 2,3-dimethyl-	2,5-Cyclohexadiene-1,4-dione, 2,6-bis(1,1-dimethylethyl)-	Phenol, 2,4-dimethyl-
3,5-di-tert-Butyl-4-hydroxybenzyl alcohol	Phenol, 2,4-dimethyl-	Butylated Hydroxytoluene	Phenol, 3-ethyl-
Phenol, 2,2'-methylenebis[6-(1,1-dimethylethyl)-4-methyl-	Phenol, 2-(1,1-dimethylethyl)-4-methyl-		Phenol, 2-(1,1-dimethylethyl)-4-methyl-
	Butylated Hydroxytoluene		Butylated Hydroxytoluene
	E-15-Heptadecenal		1,2-Benzenediol, 3,5-bis(1,1-dimethylethyl)-
	Tetracosane		3,5-di-tert-Butyl-4-hydroxybenzyl alcohol
	Phenol, 2,2'-methylenebis[6-(1,1-dimethylethyl)-4-methyl-		Octadecanoic acid, ethyl ester
	Hexadecane		1-Acetynonadecane
	Tetracosane		Tetracosane
	Eicosane		Cyclohexadecane, 1,2-diethyl-

*With CeO<sub>2</sub> catalyst*

GPC curves are plotted Figure 134. Profiles are similar versus reaction time, only intensities change. GPC results suggest that catalyst improve the degradation to form higher quantity of small molecules. Curves look like the profile obtained for black liquor conversion at 450°C and 60 min reaction time without catalyst.

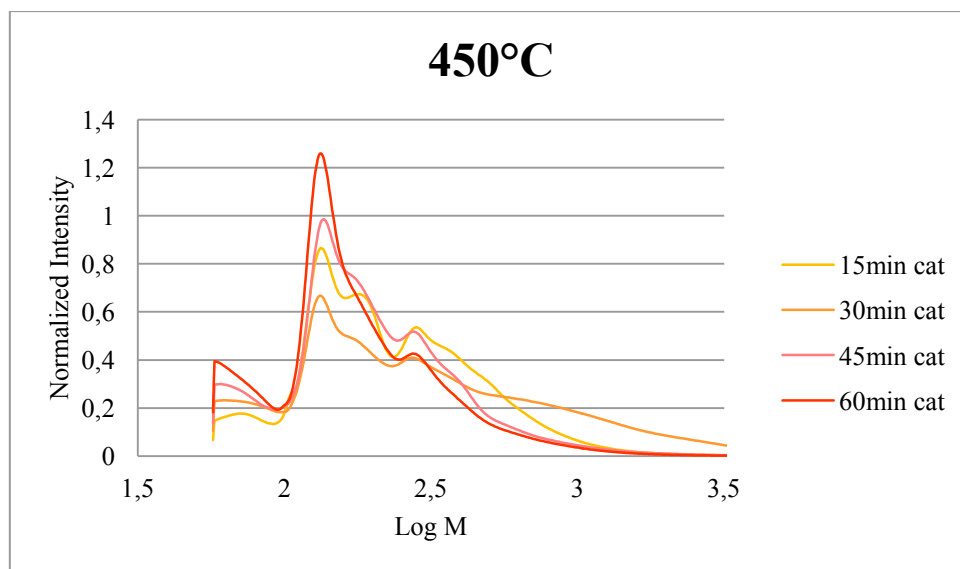


Figure 134: GPC results for liquid obtained after hydrothermal conversion of GGGE, without catalyst.

Table 18 presents GC-MS results. Similar types of molecules, as previous section, are observed. Previous mechanisms are completed by the reactions due to cerium oxide. Looking at the molecules identified, differences are due to the degree of substitution of the phenols such as 2,3- dimethyl-phenol. Similar condensed molecules are observed over reaction time, only their concentration decrease regarding GPC results. It is due to the oxygen activated species which oxidizes aldehyde and limits polymerization. Oxygen activated species also improve radical reaction of acetaldehyde splitting allowing alkylation of phenol [74]. (cf mechanism).

Considering GPC results, small molecules are more concentrated than big molecules and so capping reaction would also take place.



Table 18: GC-MS results for the liquid obtained after hydrothermal conversion of GGGE under supercritical conditions with catalyst

15 min	30 min	45 min	60 min
Phenol	Propane	Propane	Toluene
Phenol, 2-methyl-	Cyclohexane, ethyl-	Phenol	Phenol
Phenol, 3-methyl- p-Cresol	Phenol Phenol, 2-methyl-	Phenol, 2-methyl- p-Cresol	Phenol, 2-methyl- p-Cresol
Guaiacol	p-Cresol	Guaiacol	Guaiacol
Phenol, 2-(1,1-dimethylethyl)-5-methyl-	Guaiacol	Butylated Hydroxytoluene	Phenol, 2,3-dimethyl-
Butylated Hydroxytoluene	2,5-Cyclohexadiene-1,4-dione, 2,6-bis(1,1-dimethylethyl)-		Phenol, 3-ethyl-
	Butylated Hydroxytoluene		Phenol, 3,5-dimethyl-
			Phenol, 3,4-dimethyl-
			Phenol, 2-(1,1-dimethylethyl)-4-methyl-
			Butylated Hydroxytoluene
			3,5-di-tert-Butyl-4-hydroxybenzyl alcohol
			E-15-Heptadecenal
			Phenol, 2,2'-methylenebis[6-(1,1-dimethylethyl)-4-methyl-

#### IV.2.2. Catalytic conversion under subcritical conditions

Similar experiments have been performed at subcritical conditions.

##### *Without catalyst*

Profiles of molecular weight of the component in the liquid are almost similar from 15 min to 45 min of reaction time (Figure 135), only intensities change. For 60 min of reaction time small molecules disappear and bigger one are in majority.

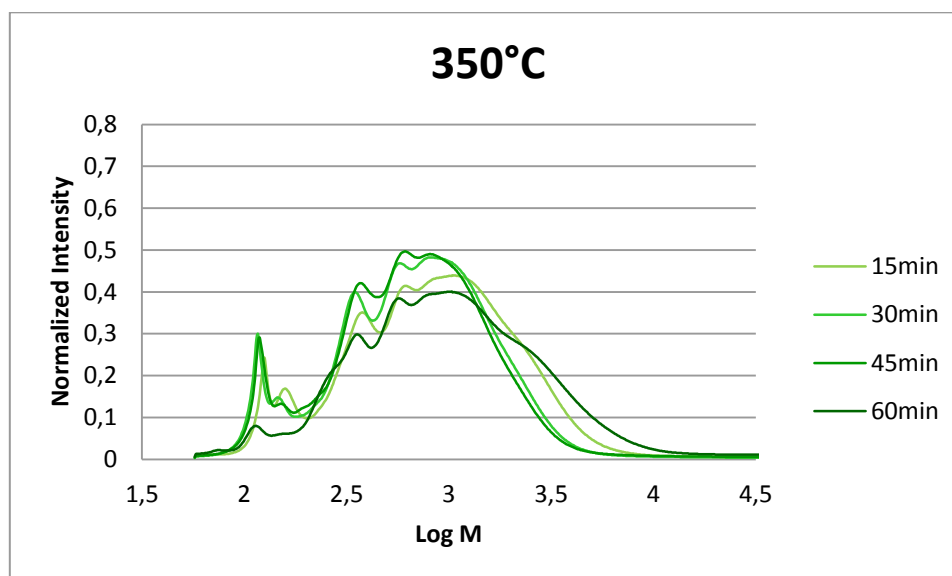


Figure 135: GPC results for liquid obtained after hydrothermal conversion of GGGE under subcritical conditions, without catalyst

GC-MS results are presented in the Table 19. GGGE is degraded under subcritical water by the cleavage of the  $\beta$ -O-4 linkage to form guaiacol (phenol, 2-methoxy) and guaiacylglycerol then each of them react to form the molecules identified in Table 19.

A plurality of substituted phenolic compounds is identified over reaction time in addition to polycyclic molecules. These polycyclic molecules are oxygenated and formed by condensation reactions between phenolic molecules and cyclization of unsaturated aldehyde molecules. The mechanisms to obtain these molecules are not detailed.

Substituted phenolic compounds such as Phenol, 2-methoxy-3-methyl-, Phenol, 4-ethyl-2-methoxy-, Phenol, 2-methoxy-3-methyl-, Phenol, 2-methoxy-4-propyl-, Phenol, 2-methoxy-4-(1-propenyl)- and so on are obtained by alkylation reactions on guaiacol. On the contrary to the conversion under supercritical conditions, phenol is not identified and does not seem to be a stable intermediate. Polymerization of phenolic compounds is allowed by the reaction between phenolic compounds and aldehyde which is formed by the cleavage of glycerol.

Molecule such as 2,2'-methylenebis[6-(1,1-dimethylethyl)-4-methyl-Phenol], has been identified. Condensation reactions between aldehydes in the media would explain the formation of linear ether such as heneicosyl acetate, linoleic acid ethyl ester, octadecanoic acid, ethyl ester. Conjugated alkenes such as Phenol, 2-methoxy-4-(1-propenyl)- and alkene such as linoleic acid ethyl ester are produced.

Table 19: GC-MS results for the liquid obtained after hydrothermal conversion of GGGE under subcritical conditions without catalyst

15 min	30 min	45 min	60 min
Furan, 2,3-dihydro-	Phenol, 2-methoxy-	Phenol, 2-methyl-	Cyclohexane, ethyl-
Phenol, 2-methoxy-	Phenol, 2-methoxy-3-methyl-	Phenol, 2-methoxy-	Phenol, 2-methoxy-
Benzene, 1,2-dimethoxy-	Creosol	Phenol, 2-methoxy-3-methyl-	Phenol, 2-methoxy-3-methyl-
Phenol, 2-methoxy-3-methyl-	Benzofuran, 7-methoxy-	Creosol	2-Methoxy-5-methylphenol
Creosol	Phenol, 4-ethyl-2-methoxy-	Benzofuran, 7-methoxy-	Creosol
Benzofuran, 7-methoxy-	Butylated Hydroxytoluene	Phenol, 4-ethyl-2-methoxy-	3,4-Dimethoxytoluene
Phenol, 4-ethyl-2-methoxy-	Heneicosyl acetate	Phenol, 2-methoxy-4-propyl-	Phenol, 4-ethyl-2-methoxy-
Phenol, 2-methoxy-4-(1-propenyl)-	Phenol, 2,2'-methylenebis[6-(1,1-dimethylethyl)-4-methyl-	Phenol, 2-methoxy-4-(1-propenyl)-	Phenol, 2-(1,1-dimethylethyl)-5-methyl-
Butylated Hydroxytoluene	Cyclopenta[d]anthracene-6,8,11-trione, 1,2,3,3a,4,5,6,6a,7,8,11,12-dodecahydro-3-(1-methylethyl)	Butylated Hydroxytoluene	1,4-Dimethoxy-2,3-dimethylbenzene
Dibenz[a,c]cycloheptane, 2,3,7-trimethoxy-		E-15-Heptadecenal	Phenol, 2-methoxy-4-propyl-
4H-1-Benzopyran-4-one, 2-(3,4-dimethoxyphenyl)-7-hydroxy-		Phenol, 2,2'-methylenebis[6-(1,1-dimethylethyl)-4-methyl-	Butylated Hydroxytoluene
		Methyl 3-(1-formyl-3,4-methylenedioxy)benzoate	Linoleic acid ethyl ester
		Cyclopenta[d]anthracene-6,8,11-trione, 1,2,3,3a,4,5,6,6a,7,8,11,12-dodecahydro-3-(1-methylethyl)	Octadecanoic acid, ethyl ester
			1-Acetoxynonadecane
			Cyclohexadecane, 1,2-diethyl-
			Phenol, 2,2'-methylenebis[6-(1,1-dimethylethyl)-4-methyl-

Methyl 3-(1-formyl-3,4-methylenedioxy)benzoate
4H-1-Benzopyran-4-one, 2-(3,4-dimethoxyphenyl)-7-hydroxy-
Cyclopenta[d]anthracene-6,8,11-trione,1,2,3,3a,4,5,6,6a,7,8,11,12-dodecahydro-3-(1-methylethyl)
Tetracosane

### With CeO<sub>2</sub> catalyst

Profiles obtained from 15 min to 60 min with catalyst are quite similar (Figure 136), excepted for the profile obtain with R = 20 where the main peak is observed for Log M = 2 and other peaks are shifted to the lower molecular weight. Furthermore, profiles obtained with catalyst are quite similar with profiles obtained without catalyst, only intensities change. Indeed, for each reaction time the intensity of the peak at Log M = 2 are higher with catalyst. This suggests that more small molecules are formed.

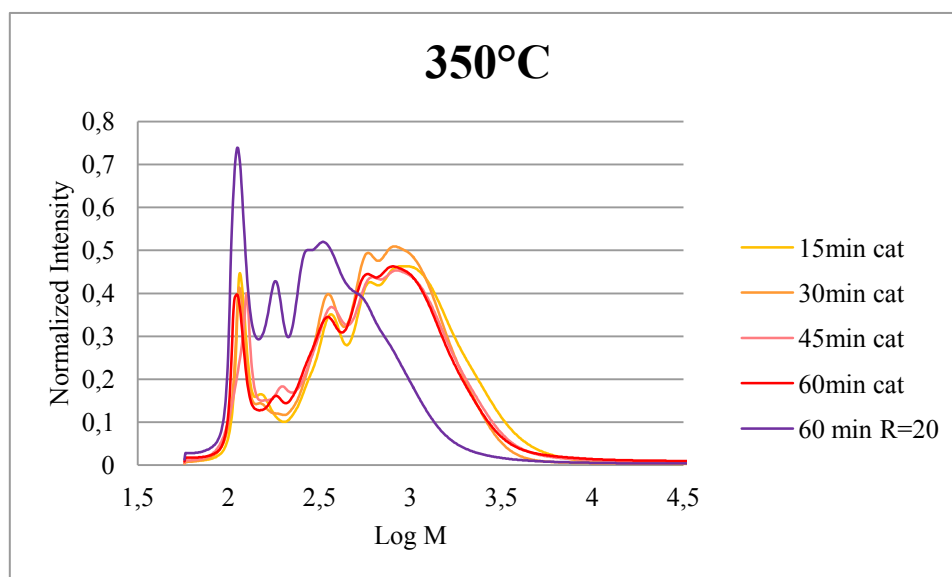


Figure 136: GPC results for liquid obtained after hydrothermal conversion of GGGE under subcritical conditions, without catalyst.

These results are confirmed with the identification of the molecules obtained by GC-MS and summarize in Table 20. With catalyst same substituted phenols molecules are identified and from 45 min, phenol is noticed. However, no oxygenated condensed molecules are identified, especially with a ratio of catalyst R = 20. This suggests oxidation reactions took place,

increasing the degree of oxidation of the molecules and leading to the degradation of the condensed molecules or to their inhibition.

Table 20: GC-MS results for the liquid obtained after hydrothermal conversion of GGGE under subcritical conditions with catalyst

15 min	30 min	45 min	60 min	60 min R=20
Phenol, 2-methoxy-	Phenol, 2-methoxy-	Phenol	Phenol	Phenol
Creosol	Benzene, 1,2-dimethoxy-	Phenol, 2-methyl-	Phenol, 2-methyl-	Phenol, 2-methyl-
Phenol, 4-ethyl-2-methoxy-	Phenol, 2-methoxy-3-methyl-	Phenol, 2-methoxy-	Phenol, 2-methoxy-	Phenol, 2-methoxy-
Butylated Hydroxytoluene	Creosol	Benzene, 1,2-dimethoxy-	Phenol, 2-methoxy-3-methyl-	Benzene, 1,2-dimethoxy-
Phenol, 2,2'-methylenebis[6-(1,1-dimethylethyl)-4-methyl-	Phenol, 4-ethyl-2-methoxy-	Phenol, 2-methoxy-3-methyl-	Creosol	2-Methoxy-5-methylphenol
	Butylated Hydroxytoluene	Creosol	Phenol, 4-ethyl-2-methoxy-	Phenol, 4-ethyl-2-methoxy-
	Phenol, 2,2'-methylenebis[6-(1,1-dimethylethyl)-4-methyl-	Benzofuran, 7-methoxy-	Phenol, 2-methoxy-4-(1-propenyl)-	Butylated Hydroxytoluene
	Dibenz[a,c]cycloheptane, 1,2,9-trimethoxy-	Phenol, 4-ethyl-2-methoxy-	Butylated Hydroxytoluene	Phenol, 2,2'-methylenebis[6-(1,1-dimethylethyl)-4-methyl-
		Butylated Hydroxytoluene	3,5-di-tert-Butyl-4-hydroxybenzyl alcohol	
		Phenol, 2,2'-methylenebis[6-(1,1-dimethylethyl)-4-methyl-	1-Hexadecanol, acetate	
		Dibenz[a,c]cycloheptane, 2,3,7-trimethoxy-	E-15-Heptadecenal	
			Phenol, 2,2'-methylenebis[6-(1,1-dimethylethyl)-4-methyl-	
			Dibenz[a,c]cycloheptane, 2,3,7-trimethoxy-	

#### IV.2.3. Mechanism under sub and supercritical conditions with and without catalyst

GGGE is first degraded in guaiacol then to phenol. The other part of the GGGE molecule gives formaldehyde and acetaldehyde molecules.

Under supercritical conditions without catalyst, polymerization, alkylation and aldolisation reaction occurred. Under supercritical conditions with CeO<sub>2</sub> catalyst, in addition to the previous reactions, capping reaction occurred to limit phenols reactivity as confirmed by GPC results: small molecules are more concentrated than big molecules. Big molecules are less present due to the oxidation of formaldehyde and other small aldehyde which used to favor the polymerization and the condensation between phenolic molecules. In addition, CeO<sub>2</sub> shifts probably the equilibrium of radical decomposition of acetaldehyde by oxidation that increases the number of alkyl group available to react.

Under subcritical conditions, phenol was not observed suggesting either this intermediate is rapidly consumes or not produced. Moreover, guaiacol seems to be also an important intermediate of reaction. Without catalyst, alkylation, aldolisation and condensation reactions lead to oxygenated molecules. With CeO<sub>2</sub> catalyst, oxidation of the molecules is more achieved as smallest molecules are recovered.

Mechanisms of GGGE with and without catalyst under super and subcritical conditions are exposed as follows (Figure 137 and 138). From these mechanisms, probable reaction pathways for lignin (Figure 140 and 141) and black liquor (Figure 142 and 143) have been drawn. All that is green in mechanisms relates to the catalyst. All of the green labels in the mechanism figures are related to the catalyst action. These mechanisms are proposal of reaction pathways from initial material to the products obtained; ways exposed do not take into account of intermediates reaction

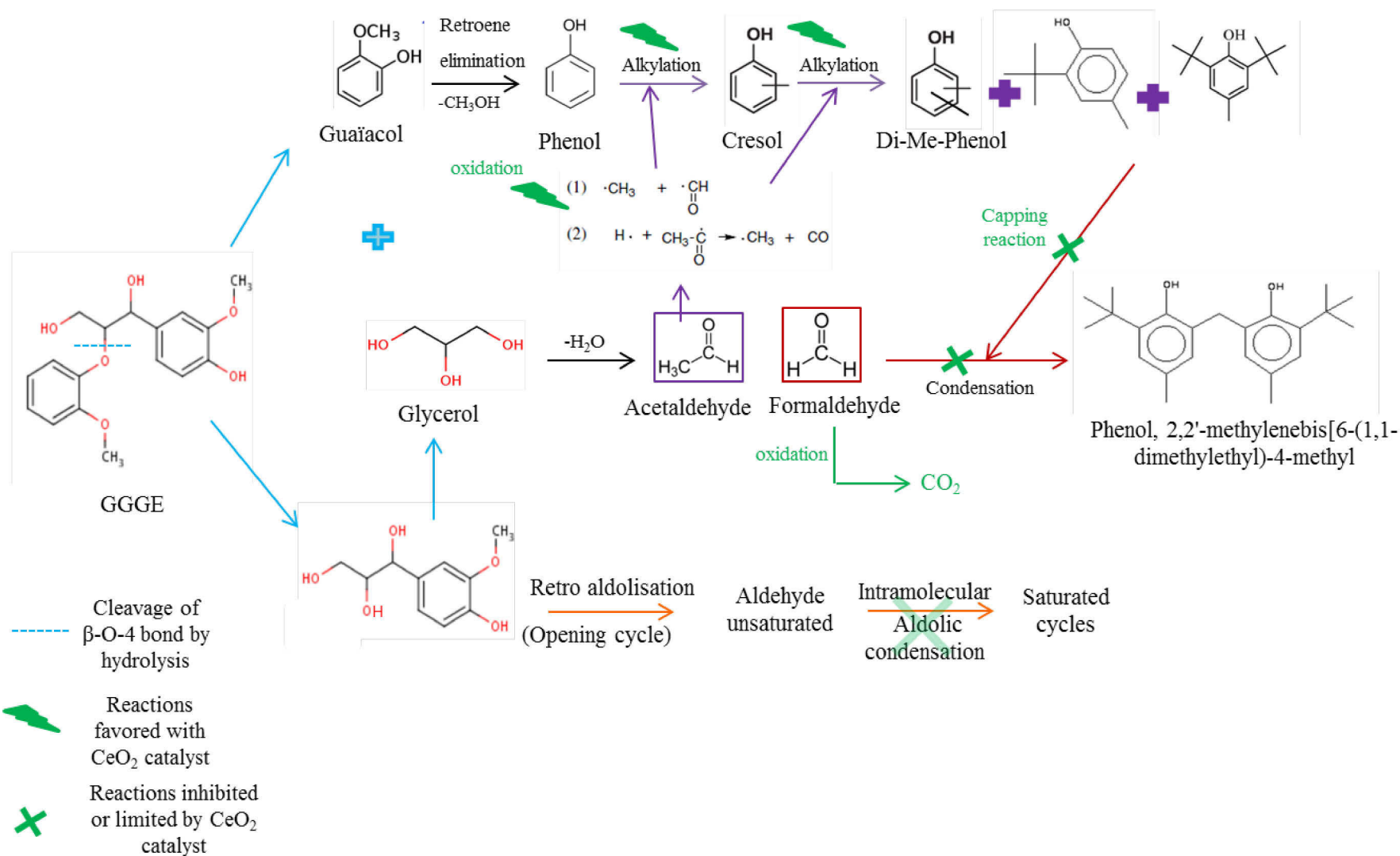


Figure 137: Mechanism of GGGE hydrothermal conversion with and without catalyst under supercritical conditions

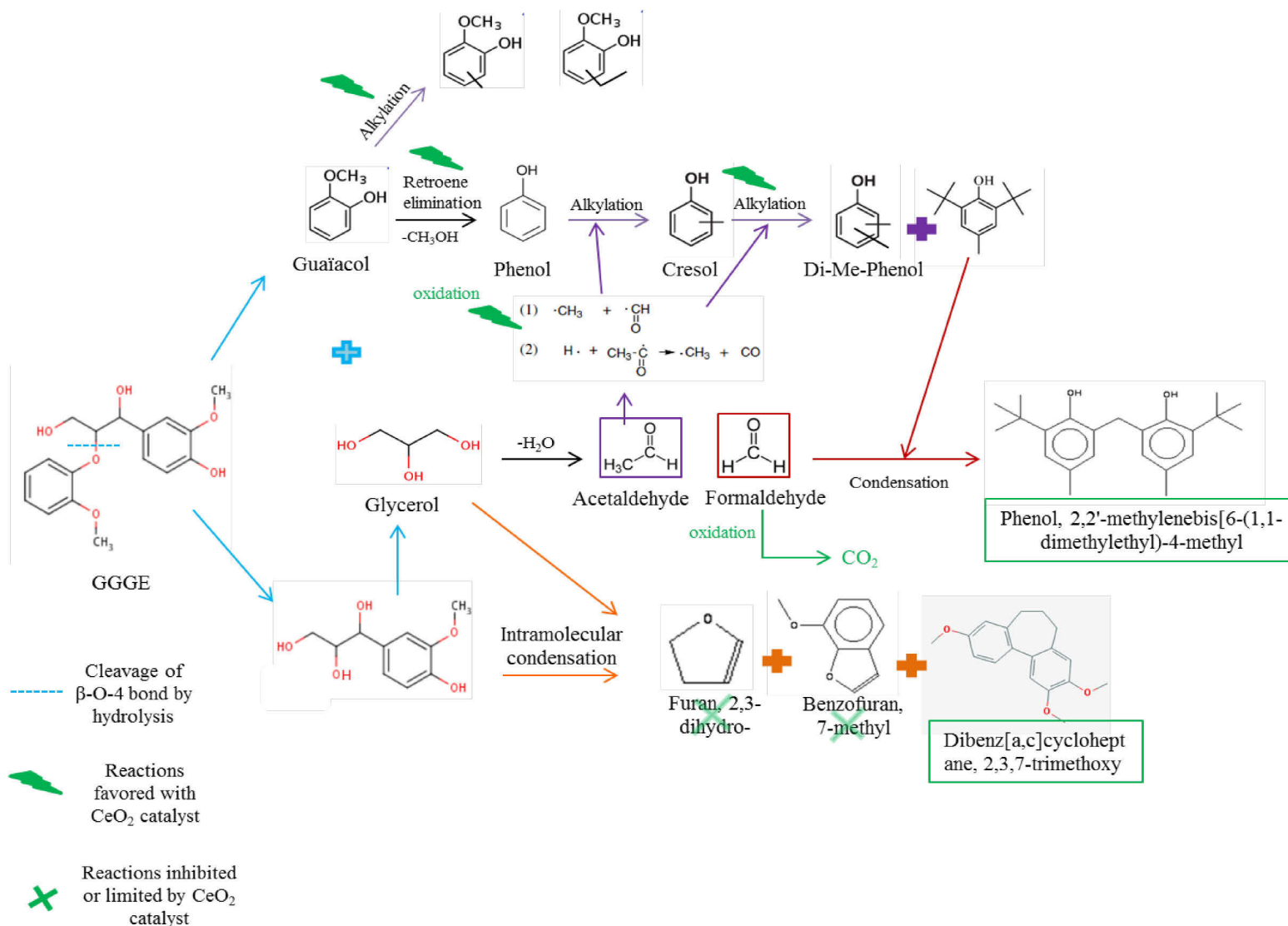


Figure 138: Mechanism of GGGE hydrothermal conversion with and without catalyst under subcritical conditions



These mechanisms can be linked to supercritical water reactivity as suggested in chapter 1:

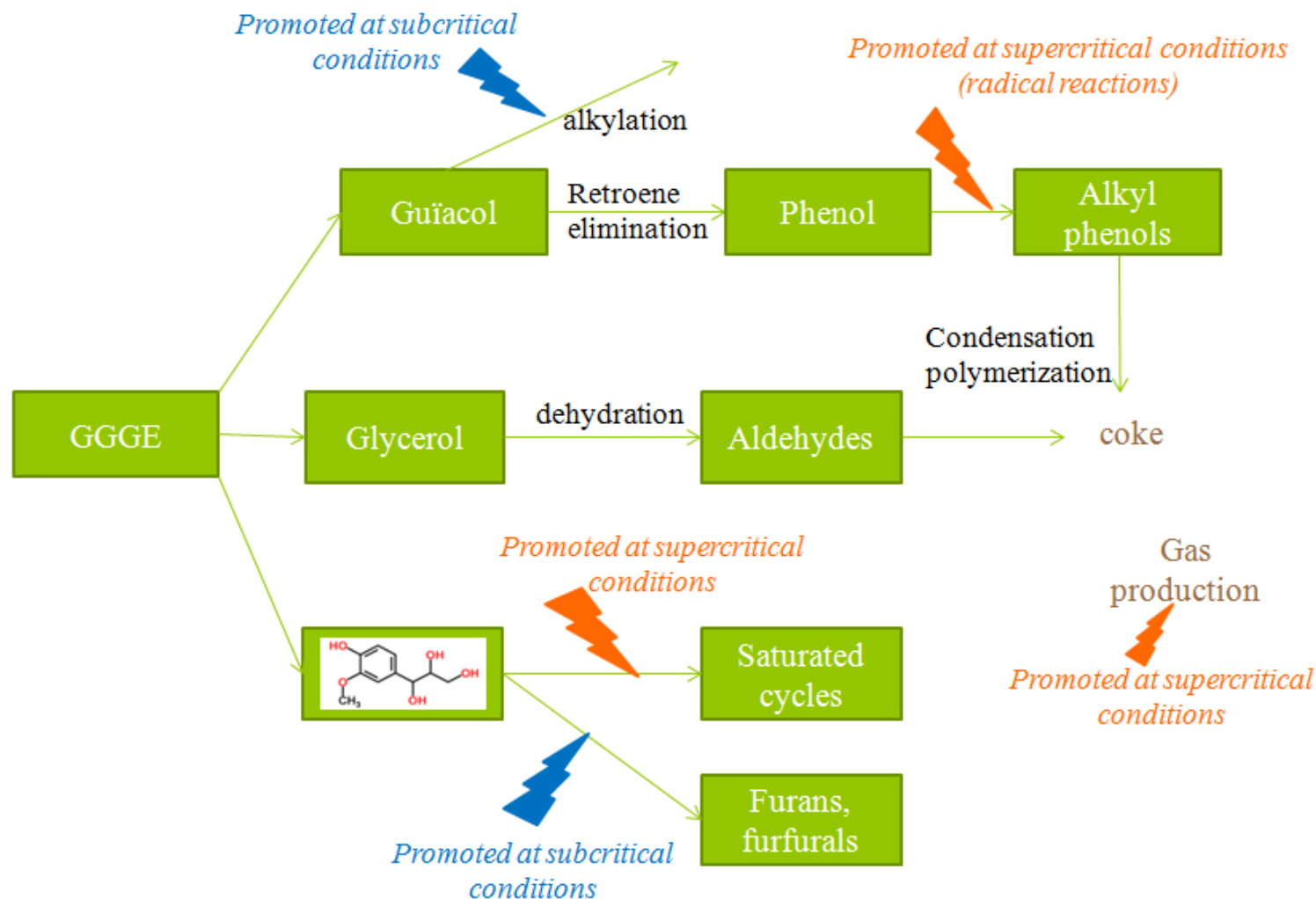


Figure 139: Reactions promoted under sub and supercritical conditions without catalyst

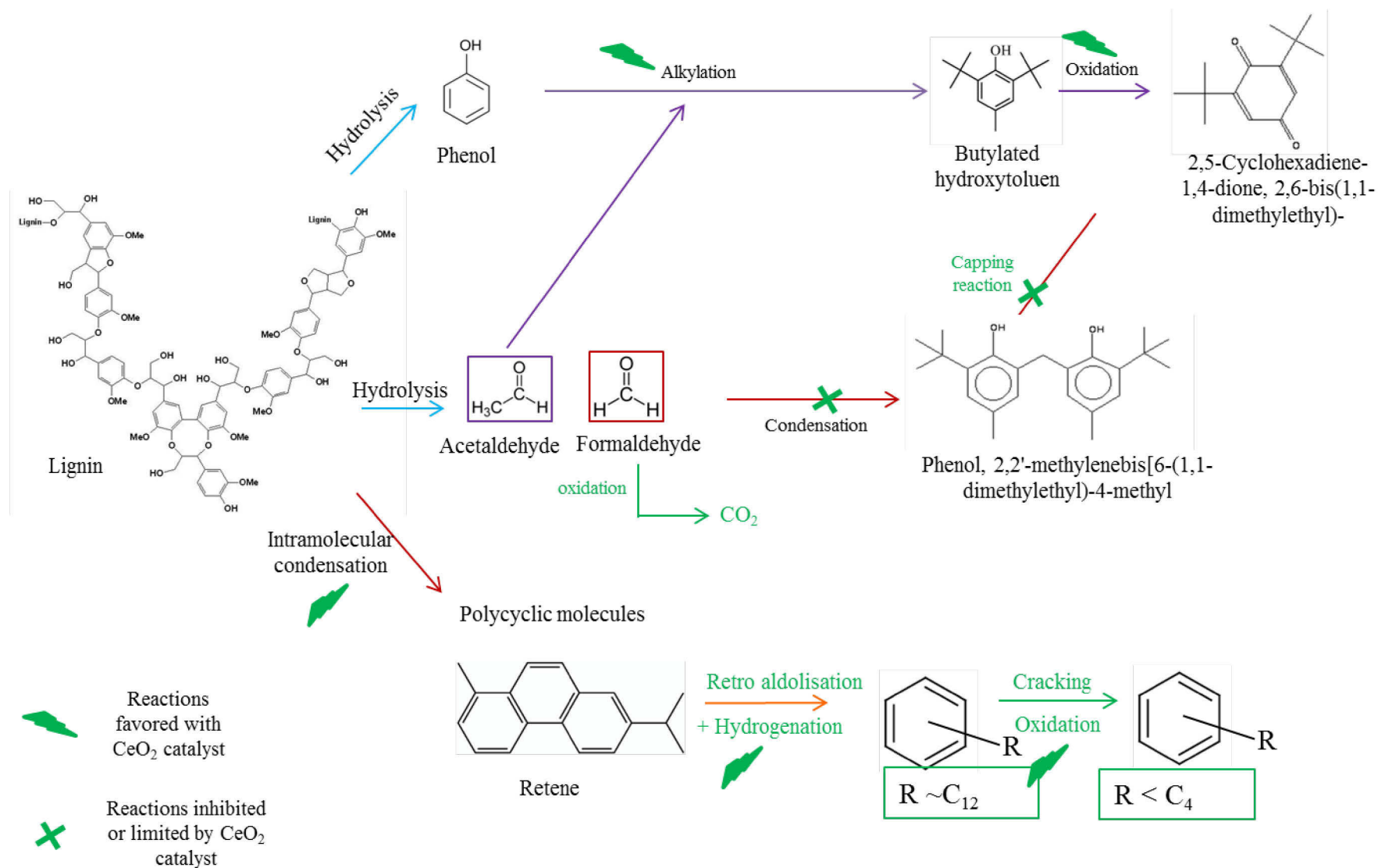


Figure 140: Mechanism of lignin hydrothermal conversion with and without catalyst under supercritical conditions

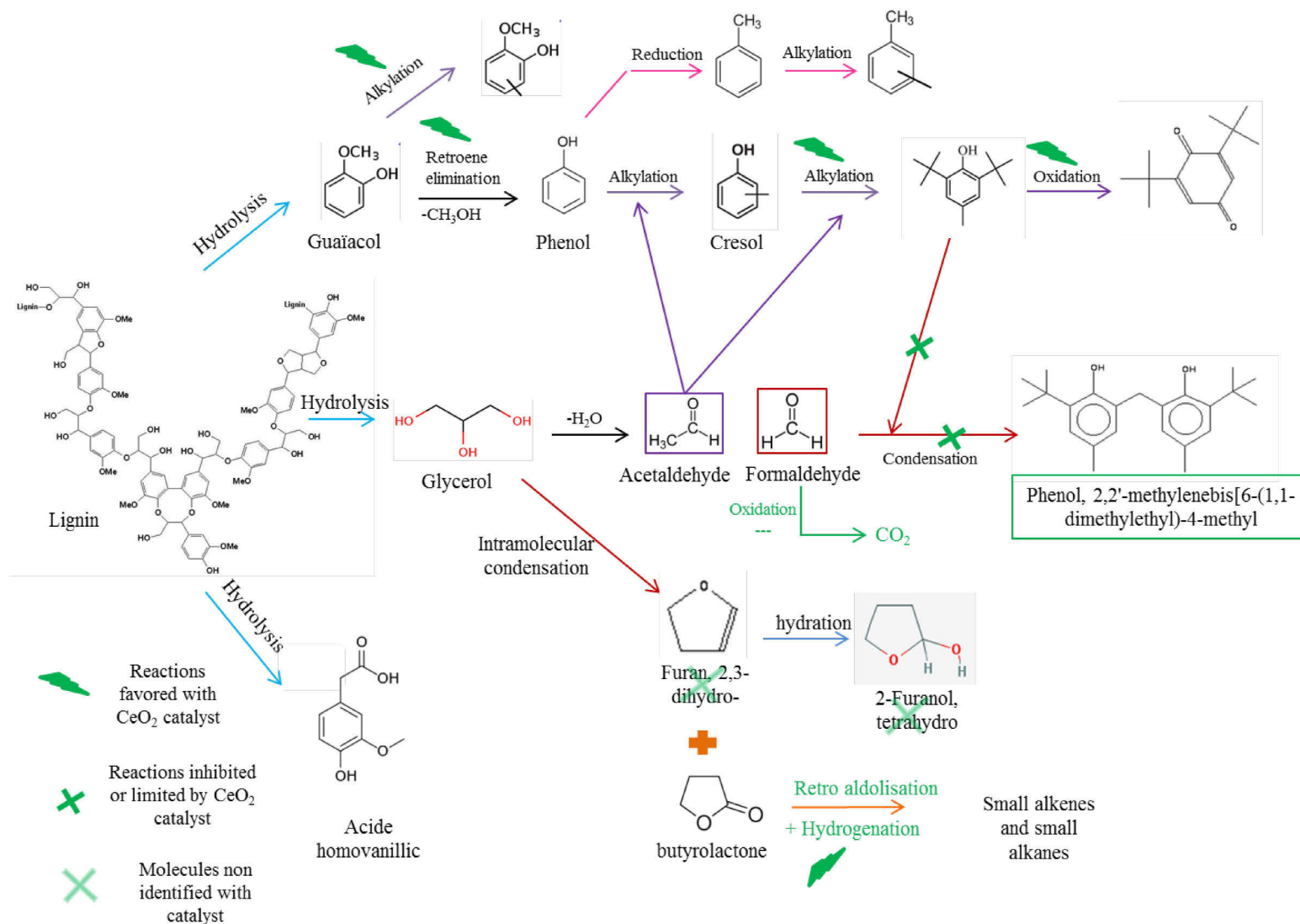


Figure 141: Mechanism of GGGE hydrothermal conversion with and without catalyst under subcritical conditions

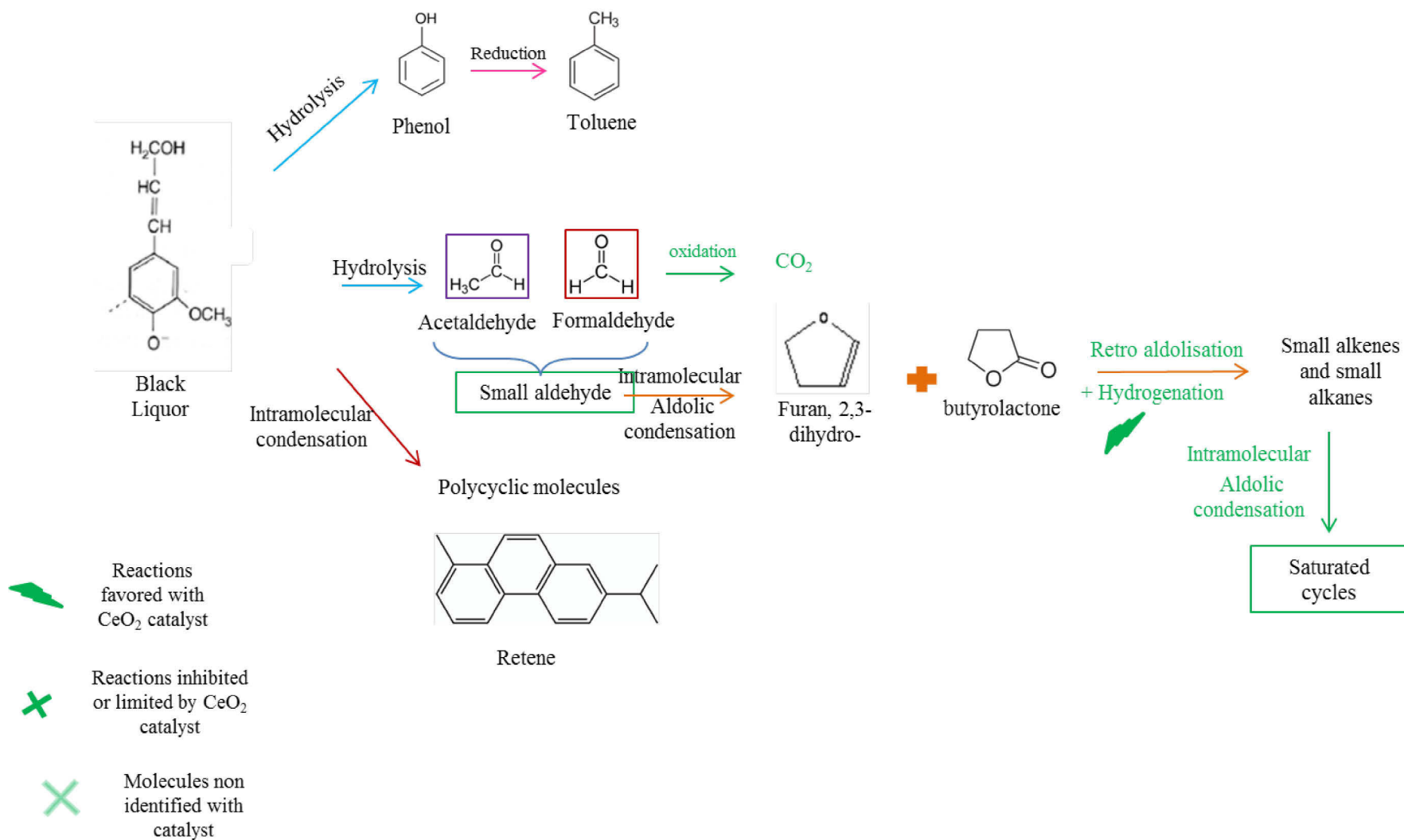


Figure 142: Mechanism of Black liquor hydrothermal conversion with and without catalyst under supercritical conditions

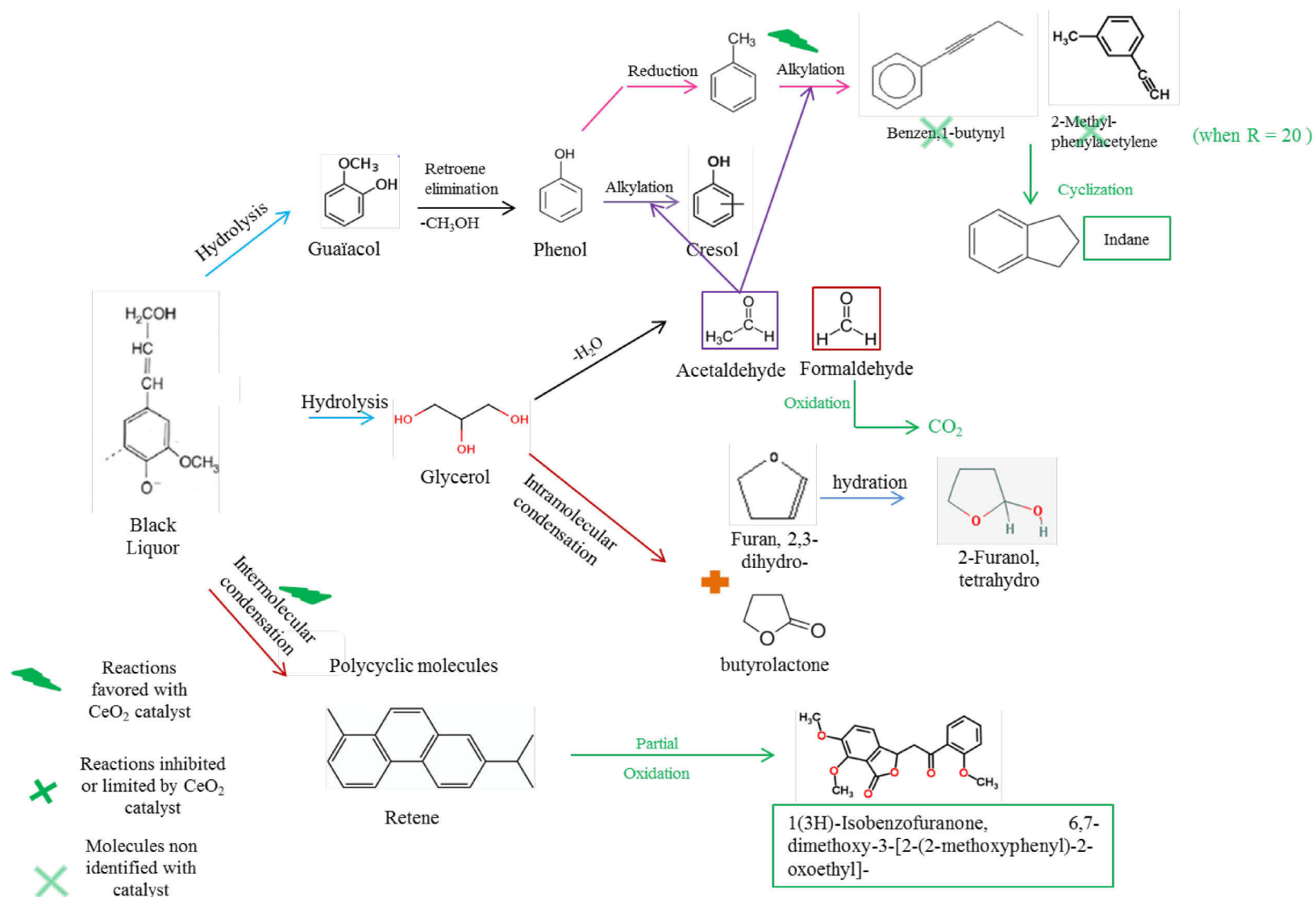


Figure 143: Mechanism of black liquor hydrothermal conversion with and without catalyst under subcritical conditions

## V. Summary of chapter

The goal of the study was to investigate the effect of cerium oxide nanocatalyst towards hydrothermal conversion of black liquor. The use of catalyst would lead to an increase of hydrogen production and an inhibition of the coke formation.

As expected, cerium oxide nanocatalyst is efficient to improve black liquor conversion.

The hypothetic action was suggested through water splitting into hydrogen and oxygen active species. These activated species are either able to react with organic and mineral compounds (i.e. hydrogenation, oxidation) or with other activated species. Indeed, H<sub>2</sub> molecules can be formed by recombination of active species or during dehydrogenation of alkanes. A part of these activated species can also react with liquid molecules by capping reaction to form smaller molecules (fewer complexes). GPC and color of liquid attested this degradation. Thus, activated hydrogen species lead to H<sub>2</sub> molecules, which could be involved in hydrogenation reaction to form alkane at high temperature or in the liquid at subcritical conditions. H<sub>2</sub> could be also released from dehydrogenation.

Active oxygen species are able to oxidize organic molecules that release CO<sub>2</sub> and CO at the final stages. The low amounts of CO suggest its consumption in water gas shift reaction; which was promoted by alkaline salts and CeO<sub>2</sub> catalyst. When oxidation was extreme, CO<sub>2</sub> is released to gas mixture; CO<sub>2</sub> was also due to the consumption of CO by the water gas shift reaction which was promoted by alkaline salts and CeO<sub>2</sub> catalyst. Thus, polymerization of phenolic compounds and aldehydes is limited.

We also noticed that the amount of O<sub>2</sub> and H<sub>2</sub> at 450°C, short reaction time and using catalyst was significantly modified compared to the experiment without catalyst. Indeed, a high oxygen content was measured and hydrogenated products (such as alkanes) were identified. By increasing reaction time, oxygen activated species would be used for oxidation reaction that increases CO, CO<sub>2</sub> and intermediates of oxidation. In the same way the amount of mineral oxide in the solid phase seems to be favored by catalyst and temperature increase. Moreover the ratios between oxygen (or hydrogen) and initial organic content showed that the reaction were improved at high temperature where the splitting was favored. So the water splitting into activated species would be suitable to describe the system.

To elucidate more precisely the mechanism of black liquor conversion, model molecules have been used. Lignin represents correctly the behavior of black liquor. However lignin structure is also too complex therefore GGGE (Guaiacylglycerol- $\beta$ -guaiacyl ether) was used. In addition to the reactions highlighted by CeO<sub>2</sub> catalyst, condensation, aldolisation and

alkylation (Friedel-Craft reaction) occurred leading to polycyclic molecules, aldehyde and substituted phenolic compounds.

The evaluation of the energy balance, regarding to the amount of hydrogen produced, suggests that the best operating conditions are 450°C 60 min of reaction time.

## General conclusion & Prospects

---





## I. Conclusion

Hydrothermal processes are gaining attention the last decades in order to convert biomass, by-products or wastes into valuable compounds. This wet thermo-chemical treatment is based on the physico-chemical properties of water at high temperature and pressure. Gasification, liquefaction, as well as carbonization, are applied for energy or useful materials recovery. The main issues limiting the industrial development of these processes are solid formation which block the pipes and initiate corrosion, while expensive building materials are required at high temperatures ( $>400^{\circ}\text{C}$ ) and high pressure ( $P > 20 \text{ MPa}$ ). The goals of the work were to improve knowledge about these issues. In this context, black liquor was selected as raw material regarding its high water, organic and mineral content. Black liquor is an alkaline by-product of paper industry, coming from the step of wood cooking.

The first results presented the influence of operating conditions on carbon conversion during hydrothermal treatment of black liquor. It was concluded that initial concentration modifies mainly the amount of resulting organics, reaction time promotes degradation and the temperature drives the type of process, favoring one phase among others. At high temperature ( $600^{\circ}\text{C}$ ), the gaseous phase revealed a high proportion of  $\text{H}_2$  and a low proportion of  $\text{CO}_2$ . Hydrothermal gasification of black liquor is therefore an interesting and efficient process. However, this high temperature imposes expensive building materials and a pollutant toxic gas,  $\text{H}_2\text{S}$ , was unfortunately recovered. In fact,  $\text{H}_2\text{S}$  is not a problem for paper industry (recycling into white liquor) but at laboratory scale  $\text{H}_2\text{S}$  avoid gas analysis because it is very corrosive. At the same time, solid formation was not avoided although its yield is low. At medium temperature ( $450^{\circ}\text{C}$ ), organic carbon conversion indicates that liquefaction was predominant, and resulted in a bouquet of valuable phenolic compounds such as phenol, guaiacol, p-cresol and so on. In addition, gasification is less efficient but  $\text{H}_2\text{S}$  formation was avoided, and carbonaceous solid was still recovered. At low temperature ( $350^{\circ}\text{C}$ ), 15 to 20 wt% of initial organic mass was recovered in the solid phase while no gas was detected. Black liquor began to be degraded into phenolic compounds partially incorporated in solid. Carbon-based microspheres were recovered at short reaction time. The first results let to conclude that:

- Solid, mainly carbonaceous, is recovered over the range of reaction temperature and its generation versus reaction temperature is not suitable at high temperature. The solid formation was studied at  $350^{\circ}\text{C}$ , as the microparticles have spherical and well-defined shape at this temperature.

- Hydrogen production is efficient at 600°C but H<sub>2</sub>S is simultaneously produced that is an important at laboratory scale for gas analysis. Thus catalytic gasification is proposed at lower temperature (450°C), where H<sub>2</sub>S is not produced, and at subcritical conditions.
- Liquefaction process conducts to a very complex mixture of organic molecules more or less interesting as building blocks. Their separation is considered as a technological challenge.

A focus has been made on solid formation at 350°C as function of reaction time and at different heating and cooling rates. Literature considers that solid formation during hydrothermal carbonization mimics coalification. However, although multiple authors are interested in phenomena leading to spherical particles during hydrothermal processes, no one has elucidated completely the mechanisms involved in their formation. Fixing temperature and pressure, reaction time with heating and cooling rate appear as mostly influencing parameters. Among them, reaction time is the most significant one on solid morphology while heating and cooling rate act principally on particles size distribution. Data collected from the analysis of liquid and solid phases allow us to propose a mechanism of solid formation during hydrothermal conversion. Solid is formed by the polymerization of phenolic compounds with smaller linear molecules such as aldehyde. The mechanism of particle generation resonates on the one hand, for short reaction time, with La Mer theory and on the other hand with Brooks's and Taylor's one for long reaction time. Considering continuity between them, the hypothesis of a transition layer around the particle, in organic phase, has been made; providing a radial concentration gradient (polymerizing units) between the structural organic phase and the particles. Then for short reaction time, its increasing leads to a gluing-type phase trapping particles. Then, this phase becomes the seat of a new small particles generation by aromatization of the polymerizing units. Demixing gives the appearance of budding. In addition to these physical considerations, chemical analysis informs on an uniform hydrophilic shell (transition layer) and a porous core due to gas released by aromatization reactions leading to a lower solid density. Solid formation is a complex balance between physical and chemical phenomena, and cannot be totally avoided. In order to avoid/limit solid formation during hydrothermal conversion, the addition of a CeO<sub>2</sub> nanocatalyst was experimented.

Finally, a focus is made on the catalytic hydrothermal conversion of black liquor using CeO<sub>2</sub> nanocatalyst under sub and supercritical conditions. CeO<sub>2</sub> allows to generate hydrogen without H<sub>2</sub>S and to avoid solid formation during the process. CeO<sub>2</sub> nanocatalyst has the ability to split water molecules into hydrogen and oxygen activated species. H<sub>2</sub> molecules are also obtained by dehydrogenation from alkane and consumed by hydrogenation of no saturated molecules or react with phenolic compounds by capping to form smaller aromatic molecules. Oxygen activated species are able to oxidize organic molecules to CO<sub>2</sub>, if oxidation is complete. CO<sub>2</sub> is also produced from CO by the water gas shift reaction; which was promoted by alkaline salts and CeO<sub>2</sub> catalyst. Oxidative action of CeO<sub>2</sub> allows the oxidation of small molecules such as aldehyde that limits solid formation by polymerization.

In addition to the reactions highlighted by CeO<sub>2</sub> catalyst, model molecules (GGGE, Lignin...) have been used to understand the mechanism of black liquor hydrothermal gasification/conversion with and without CeO<sub>2</sub> catalyst. Even for these simple molecules, the reactive processes developed are very complex. Accompanying the mentioned oxidation, hydro/dehydrogenation reactions, others have been identified, like condensation, aldolisation and alkylation (Friedel-Craft reaction), leading to polycyclic molecules, linear aldehydes and substituted phenolic compounds. The evaluation of the energy balance in view to industrial applications, regarding the amount of hydrogen produced, suggests that the best operating conditions are 450°C and 60 min of reaction time.

The study on hydrothermal conversion of black liquor allows an overview on the valorization options of this raw material by hydrothermal process such as useful carbon-based solids with spherical microparticles or as energy through hydrogen production.

## II. Prospects

Based on the main conclusions of our work, some prospects could be drawn in academic or industrial points of view.

Following the results obtained on the solid formation, the mechanism proposed would be confirmed by using a reactor equipped with a window. However to see the solution evolution, the initial solution has to be light color. That means the initial solution should be very diluted if black liquor solution is considered or should be made with model molecules, which are transparent at the beginning of the reaction. Solid formation mechanisms are mainly based on phase equilibrium, the observation of the phases will be of great interest. In addition, the batch reactor, even with quenching, was not suitable to observe salts precipitation. As the

amount of salts is particularly high in black liquor, a reactor with window will help to highlight the potential role of salts on solid formation and or morphology. This work could be also considered as a scientific basis for further developments on hydrothermal carbonization mechanisms. The carbon-based solid obtained at 350°C and short reaction time is composed of spherical microparticles and the specific surface area equals  $7 \text{ m}^2 \text{ g}^{-1}$ . This solid, namely hydrochar, is supposed to be used in various applications (support for catalyst or for hollow sphere formation) but this aspect has to be checked. To better measure the impact of temperature on the morphology of the solid phase, it could be interesting to conduct the study using a reactor equipped with a temperature monitoring. It may be possible to estimate the pressure by state equations. To better understand the transfer of material during the hydrothermal conversion, a comparative study between the reactor 5 mL and 500 mL could be conducted. The use of software, such as Prosim, with the use of data on model molecules helps to understand the phase's behavior.

Concerning the catalytic gasification, the mechanism of black liquor conversion might be generalized as this work stated about a model molecule GGGE. Further studies may move to continuous reactors to evaluate the hydrogen production efficiency. Industrial application requires treatment of high volumes that is more in accordance with continuous processes.

In this study, black liquor was used as reagent for two main purposes. However, salts recovery from black liquor using alternative process is an actual industrial challenge. Batch hydrothermal process showed that salts are dissolved in the recovered final solution rather than precipitated. If the conversion to gas or solid phase is achieved, inorganics remain in liquid phase which can be re-injected in white liquor recovery process. In these conditions, it is possible to imagine a process as followed (Figure 144):

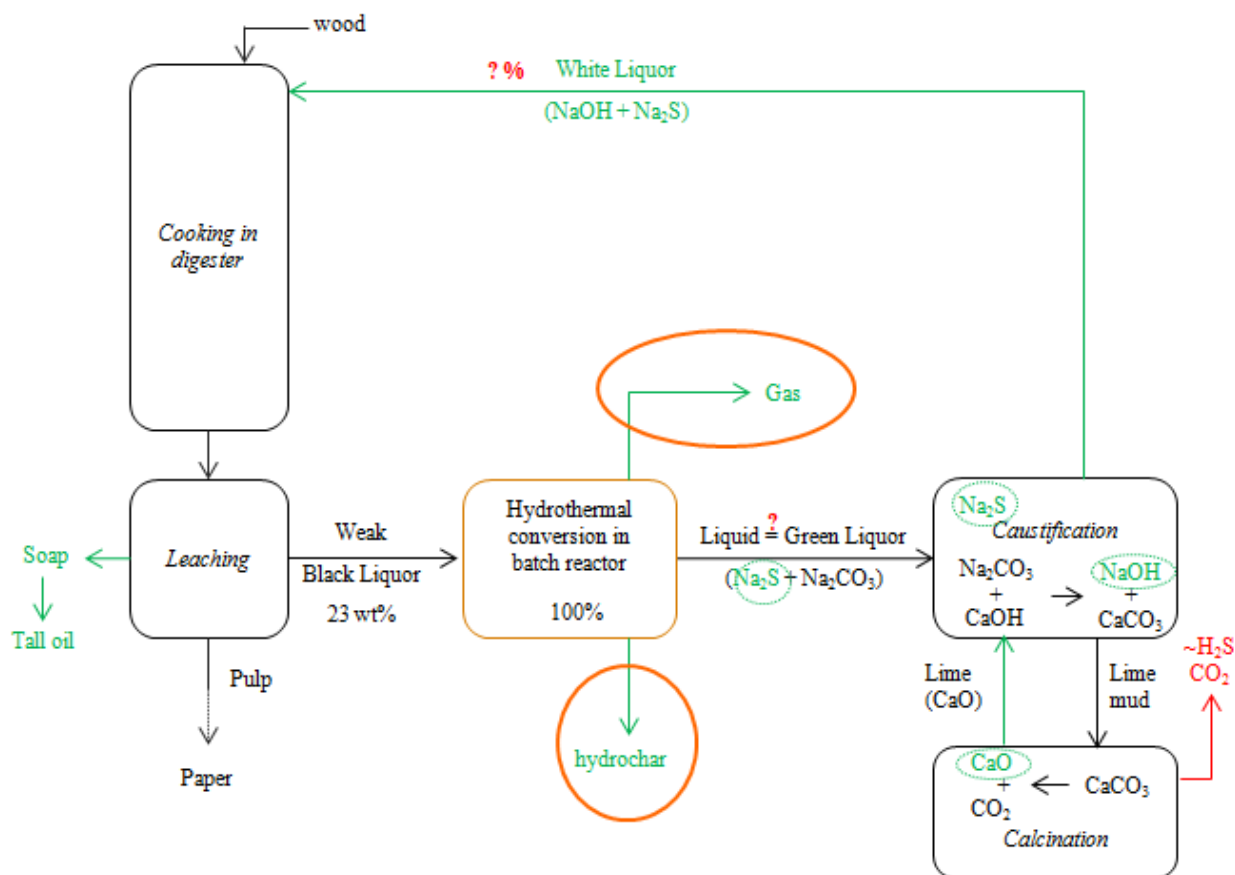


Figure 144: Integration of hydrothermal conversion of black liquor in Kraft process.

In this option, an exhaustive identification of inorganic compounds would be done. To decrease the cost of this kind of process, catalytic conversion would be considered in continuous reactors at moderate temperatures. It could be interesting to investigate the catalytic activity of inorganics contained in black liquor to optimize the process with catalyst, and the real efficacy of other catalysts.

In a way to recover building block molecules in liquid phase, a catalytic study, longer than 1h at 350°C, should be considered taking into account the energy gain to work under subcritical conditions. The study of hydrothermal liquefaction with bigger volumes of black liquor would allow the study of bio-oil formed during reaction.



## Conclusion générale et perspectives

---





## I. Conclusions

Ces dernières décennies, les procédés hydrothermaux ont émergé notamment pour la conversion de biomasse, sous-produits et de résidus en composés valorisables. Ce traitement thermo-chimique en voie humide est basé sur les propriétés physico-chimiques de l'eau à haute température et haute pression. Les procédés hydrothermaux, qui regroupent les opérations de gazéification, liquéfaction, ainsi que carbonisation, permettent d'atteindre une valorisation sous forme d'énergie ou de matière. Les principaux verrous limitant leur développement industriel concernent la formation de solide (obstruction des tubes et corrosion entre autres) et l'utilisation de matériaux techniques de haute résistance aux conditions sévères (alliages onéreux). Les objectifs de ce travail sont d'améliorer la connaissance scientifique en regard de ces principaux verrous. Pour cela, la liqueur noire a été sélectionnée comme matière d'étude, de par ses quantités élevées en eau et en matières organiques et minérales. Ce déchet industriel aqueux et très alcalin provient de l'étape de cuisson du bois d'un procédé Kraft.

Les premiers résultats présentent l'influence des conditions opératoires sur la conversion du carbone au cours de la conversion hydrothermale de la liqueur noire. La concentration initiale n'impacte que la quantité de matière organique récupérée et le temps de réaction augmente le taux de dégradation, alors que la température oriente le procédé en favorisant la composition d'une phase. A hautes températures (600°C), la phase gazeuse est enrichie en H<sub>2</sub> tandis que la proportion de CO<sub>2</sub> est faible. La gazéification en conditions hydrothermale de la liqueur noire est donc un procédé intéressant et efficace. Cependant, ces conditions opératoires imposent d'une part l'utilisation de matériaux onéreux pour la construction des réacteurs et d'autre part s'accompagne de la production de H<sub>2</sub>S, un gaz toxique et indésirable nécessitant ainsi le traitement du flux gazeux. Simultanément, la production de solide, même si elle est faible, n'a pas pu être évitée. A températures modérées (450°C), le procédé de liquéfaction domine, donnant lieu à des molécules phénoliques telles que le phénol, le guaiacol ou encore le p-crésol, molécules plateforme de la chimie. Dans le même temps, le gaz produit, en plus faibles quantités, est dépourvu d'H<sub>2</sub>S et la formation de solide carboné est à nouveau observée. A basses températures (350°C), la phase solide récupérée représente 15 à 20% de la masse initiale de composés organiques. La dégradation de la liqueur noire conduit aussi à la formation de composés phénoliques incorporés partiellement dans le solide, tandis que la proportion de la phase gazeuse n'est pas significative. Le matériau carboné récupéré est composé de microsphères pour des temps de réaction courts. La première partie de ce travail a permis de conclure que :

- La phase solide, principalement carbonée, est obtenue pour l'ensemble des conditions de température de réaction étudiées. A hautes températures, la géométrie du solide formé est difficilement étudiable alors qu'à 350°C des microsphères sont obtenues. De ce fait, le mécanisme de formation du solide a été approfondi à température fixe (350°C) et pour des temps de réaction différents.
- H<sub>2</sub> est produit efficacement à 600°C, mais s'accompagne de la production d'H<sub>2</sub>S. la gazéification catalytique est donc étudiée en vue de réduire la température de réaction, mais aussi de limiter la production de ce gaz indésirable. Par exemple ce gaz toxique n'est pas formé à 450°C en l'absence de catalyseur, donc la gazéification catalytique a été développée à cette température et aussi en conditions sous critiques.
- Le procédé de liquéfaction conduit à un mélange complexe de molécules organiques plus ou moins assimilables à des molécules plateforme. Leur isolation apparaît comme un véritable challenge technologique.

La formation de solide à 350°C en fonction du temps de réaction et des vitesses de chauffe et de refroidissement a fait l'objet d'une étude approfondie. La carbonisation hydrothermale est un procédé de plus en plus convoité et de nombreux auteurs s'attachent à comprendre les phénomènes mis en jeu lors de la formation de ces particules sphériques. Le mécanisme complet de formation n'a pas encore été élucidé et de nombreuses contributions sont encore nécessaires. Dans ce travail, l'impact des vitesses de chauffe et de refroidissement ainsi que du temps de réaction a été développé. Le temps de réaction apparaît comme un paramètre plus significatif envers la morphologie tandis que les vitesses de chauffe et de refroidissement impactent la taille des particules. Une analyse détaillée des phases solides et liquides ont permis de proposer un mécanisme de formation du solide au cours de la conversion hydrothermale. Le solide provient de la copolymérisation des composés phénoliques avec des molécules plus petites telles que des aldéhydes. Le mécanisme proposé est en accord avec les deux théories de formation du solide qui prédominent la littérature, cependant la théorie de La Mer convient aux temps de réaction courts tandis que la théorie de Brooks s'adapte mieux aux temps de réaction plus longs. Une continuité a été apportée entre ces deux théories au travers de l'hypothèse de formation d'une couche de transition autour des particules dans la phase organique. Cette couche de transition génère alors un gradient de concentration radial (unités de polymérisation) entre la phase organique structurante et les particules. Aux courts temps de réaction, cette phase est fine. Lorsque son épaisseur augmente, cette phase visqueuse agit

comme un isolant et conduit à encapsuler les particules. Alors ces unités isolées de polymérisation contenues dans cette couche de transition peuvent devenir le siège de la génération de nouvelles particules indépendamment des premières particules encapsulées. De ce fait, de fines particules se forment et se déposent sur les premières particules de taille plus importante générées précédemment. En plus de ces considérations physiques, des analyses chimiques ont montré que les particules sont constituées d'une couche extérieure hydrophile (couche de transition) renfermant un cœur poreux. Cette porosité au sein de la particule est certainement due à la production de gaz au cours des réactions d'aromatization, et abaisse la densité du solide obtenu. La formation du solide est un équilibre complexe entre les phénomènes physiques et chimiques et ne semble pas pouvoir être totalement évitée. Une solution envisagée et expérimentée pour réduire la formation de ce solide dans les procédés de conversion hydrothermale est l'ajout de nanocatalyseur d'oxyde de cérium ( $\text{CeO}_2$ ).

Dans une dernière partie, la conversion catalytique de la liqueur noire, en présence de nanocatalyseur de  $\text{CeO}_2$ , a été étudiée aux conditions sous et super critiques. La présence de l'oxyde de cérium a permis de mener la production d' $\text{H}_2$  sans polluant toxique,  $\text{H}_2\text{S}$  notamment, et de limiter la quantité de solide formé. Ce nanocatalyseur est utilisé essentiellement car il permet de rompre les molécules d'eau et de générer des espèces actives de l'oxygène et de l'hydrogène. Les molécules d' $\text{H}_2$  sont donc obtenues soit par recombinaison de ces espèces actives soit par déshydrogénation des alcanes. Cependant  $\text{H}_2$  est aussi potentiellement consommé lors de l'hydrogénation des alcènes ou la réaction de « capping » pour former des molécules aromatiques plus petites. Les espèces actives de l'oxygène agissent principalement sur les réactions d'oxydation, de manière plus ou moins avancée, pour former du  $\text{CO}_2$ . Le  $\text{CO}_2$  est aussi issu de la consommation du  $\text{CO}$  par la réaction du « water-gas-shift », laquelle est généralement catalysée en présence de sels alcalins. D'un autre côté le pouvoir oxydant des espèces actives de l'oxygène a pour avantage d'oxyder jusqu'à l'état ultime de  $\text{CO}_2$  les molécules de faible poids moléculaire comme les aldéhydes, ce qui réduit la concentration de précurseurs de la polymérisation.

En plus des réactions mettant en évidence l'action du catalyseur d'oxyde de cérium, l'étude du mécanisme réactionnel catalytique a été approfondie au travers de l'utilisation de molécules modèles (GGGE, Lignine...). Même pour ces molécules plus simples, le mécanisme développé reste très complexe. En plus des réactions d'oxydation et d'hydrogénation/déshydrogénation, des réactions telles que la condensation, l'aldolisation et l'alkylation (Friedel-Craft) ont été identifiées et donnent lieu à des molécules polycycliques,

des aldéhydes linéaires des composés phénoliques substitués. L'évaluation du bilan énergétique, en tenant compte de la quantité d'hydrogène produite, suggère que la gazéification catalytique serait industriellement favorisée à 450°C et pour 60 minutes de temps de réaction.

L'étude de la conversion hydrothermale de la liqueur noire a permis de mettre aussi en évidence quelques options de valorisation de ce déchet comme des solides carbonés constitués de microsphères ou la production d'hydrogène comme vecteur énergétique.

## II. Perspectives

À partir des conclusions principales de ce travail, les perspectives suivantes peuvent être énoncées, que ce soit d'un point de vue académique ou industriel.

Le mécanisme de formation du solide proposé pourrait être amélioré et confirmé par l'utilisation de réacteur équipé de fenêtres transparentes. Les équilibres de phase ont été les principales forces motrices de ce mécanisme et leur observation permettrait d'améliorer la connaissance sur le mécanisme proposé. Le réacteur batch, malgré le refroidissement par trempe, n'a pas permis d'observer la précipitation des sels. Alors un réacteur permettant la visualisation directe in-situ permettrait d'accéder au rôle des sels, et leur précipitation, vis-à-vis de la formation et de la morphologie du solide. Ce travail peut aussi constituer une base scientifique pour de nouveaux développements concernant la carbonisation hydrothermale. Les solides carbonés obtenus à 350°C et pour des temps de réaction courts sont composés des microparticules sphériques et présentent une surface spécifique de l'ordre de  $7 \text{ m}^2 \text{ g}^{-1}$ . Ce type de solide peut être envisagé dans des applications multiples telles que support de catalyseur ou pour la formation de sphères creuses, mais ces investigations doivent être menées. Afin de mieux mesurer l'impact de la température sur la morphologie du solide obtenu, il serait intéressant de mener une étude similaire avec un réacteur équipé d'un dispositif permettant le suivi de température en temps réel. La pression serait estimable par des équations d'états. Afin de mieux comprendre le transfert de matière lors de la conversion hydrothermale, une étude comparative doit être menée en utilisant les réacteurs de 5 mL et 500 mL en parallèle. L'utilisation de logiciel type Prosim, avec des molécules modèles permettrait également de mieux comprendre le comportement des phases.

Concernant la gazéification catalytique, le mécanisme de la conversion de la liqueur noire pourrait éventuellement être généralisé du fait de l'utilisation de molécules modèles (GGGE) comme support de ce travail. Des études complémentaires pourraient initier le passage vers le

procédé continu pour évaluer l'efficacité de production de l'hydrogène puisque le fonctionnement continu est plus à même de répondre à une problématique industrielle.

Dans cette étude, la liqueur noire a été choisie comme matière première pour satisfaire deux objectifs académiques principaux. Cependant, la récupération des sels dans la phase aqueuse peut constituer un procédé de recyclage alternatif du fait que le recyclage des sels est un réel challenge des industries papetières. En effet, le procédé hydrothermal en mode discontinu a démontré que les sels étaient dissous plutôt que précipités. Alors si la conversion de la matière organique est quasi complète, la récupération et le recyclage des sels directement dans le procédé seront immédiats. Dans ces conditions, il serait possible d'imaginer une intégration du procédé hydrothermal dans le procédé Kraft comme suit (figure 145) :

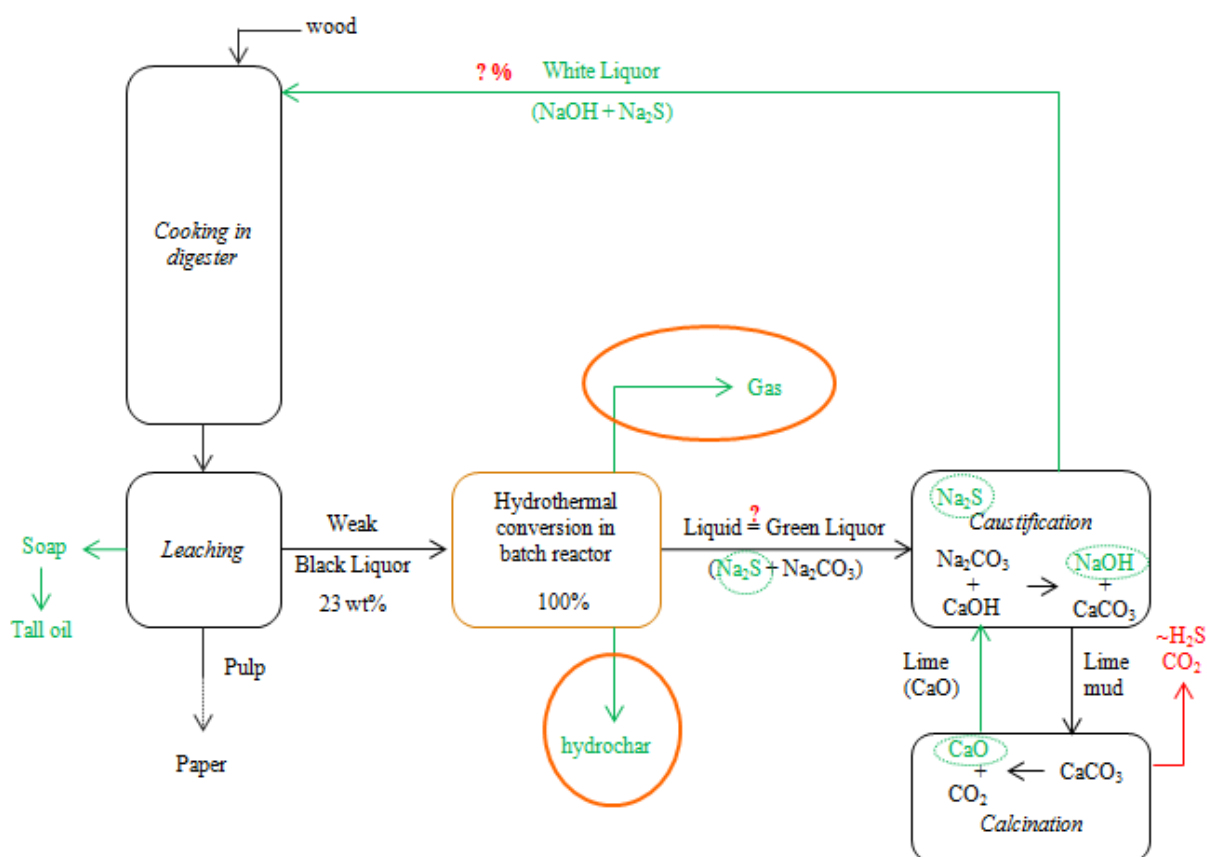


Figure 145: Intégration du procédé de conversion hydrothermale de la liqueur noire dans le procédé Kraft.

Dans cette éventualité, une identification plus approfondie des composés inorganiques est nécessaire. Les réacteurs batchs ne sont pas parfaitement adaptés aux débits élevés alors un procédé continu de récupération des sels doit être plutôt envisagé. L'option permettant d'abaisser le coût de ce traitement serait d'envisager une conversion catalytique à température modérée. Il serait intéressant d'étudier l'activité catalytique des inorganiques contenus dans la

liqueur noire afin d'optimiser le procédé avec catalyseur, et la véritable efficacité des catalyseurs en général sur sa conversion hydrothermale.

Dans une optique de récupération de molécules plateformes en phase liquid, une étude catalytique de plus d'une heure à 350°C, devrait être menée. En effet, la voie subcritique permet un gain d'énergie non négligeable par rapport à la voie supercritique. L'étude de liquéfaction hydrothermale avec des volumes plus importants de liqueur noire permettrait l'étude de la bio-oil formée lors de la réaction

## Annexes

---





## I. Annex 1: Industrial issues in Kraft process

### **Technical and technological issues**

*Multi-effect evaporators:* Fouling, tube corrosion, foaming are the main issues that occur as the black liquor is concentrated. Leakage may also occur, that dissipates steam and requires a supply of water. Sometime a low amount of solid is also formed in liquid and foul pipes.

*Boiler:* fouling of heat transfer tubes and flue gas passage, tube corrosion and cracking, floor tube damage, poor water circulation, low steam production, air emissions and so on can appear in the boiler that reduces process efficiency and causes environmental problems. The boiler represents a high initial investment and its operation and maintain are important operation cost of the plant.

The boiler is the main bottleneck of the black liquor treatment. Its capacity could limit paper production.

*Causticizing plant:* problems often encountered are overliming, poor washing efficiency, high sodium and low solids contents in the lime mud, low liquor causticizing efficiency, and liquor-line corrosion in storage tanks.

*Lime kiln:* faced to following kinds of degraded modes: low thermal efficiency, high fuel consumption, chain damage, poor lime quality and also emissions going to calcination step.

*Recycling chain:* some problems are found with the accumulation of inorganics like non process element such as chloride (Cl), potassium (K),  $\text{Na}_2\text{CO}_3$  and  $\text{Na}_2\text{SO}_4$ .

These operational problems result in an increase of mill energy consumption and a poor recycling of black liquor; which lead to a decrease of the capacity and the availability of the plant to produce paper.

## **Environmental issue**

Environmental issues come firstly from emissions throughout the process:

Sulfur emissions:

### *Digester and evaporator:*

In the digester, sulfur compounds (methyl mercaptan, hydrogen sulfide, dimethyl disulfide) are emitted and are responsible for Kraft odor. To limit them, incinerators of gases are installed.

### *Boiler:*

During sulfur reduction to sulfide in the reducing zone (figure 21), a low amount of H<sub>2</sub>S is produced. If its oxidation into SO<sub>2</sub> is not achieved, some H<sub>2</sub>S would be carried by combustion gases. H<sub>2</sub>S is toxic.

Sulfur emissions from the boiler depend on several parameters:

- In the oxidizing zone sulfur is transformed into sulfur dioxide which combines with Na in the gaseous phase producing sodium sulphate. So the ratio S/Na is important. If S/Na is too high, the amount of Na is not enough to link sulfur and consequently SO<sub>2</sub> is emitted instead of producing Na<sub>2</sub>SO<sub>4</sub>. It's necessary to connect the boiler to wet scrubbers, which treat vapors before discharging them.

- Air supply and air distribution inside the boiler are important to oxidize correctly sulphur and others elements and to control the temperature.

### *Lime kiln:*

Some sulfur dioxide is noticed in the lime kiln. Usually it is capted by sodium carbonate (Na<sub>2</sub>CO<sub>3</sub>) but when sodium carbonate is saturated SO<sub>2</sub> is emitted.

Hydrogen sulfide (H<sub>2</sub>S) can also be produced if sodium sulfide (Na<sub>2</sub>S) comes in the cold drying zone of the lime kiln where CO<sub>2</sub> and water are present as follows:



NOx issues:

Boiler:

NOx emissions, with a maximum value of 2 kg/ton of produced pulp, are due to the initial amount of nitrogen in the black liquor and the excess of O<sub>2</sub> from the combustion.

Particles emissions:

Boiler:

To prevent particulate emissions outlet, boilers are equipped with dry bottom electrostatic precipitators.

Lime kiln:

Lime kiln is equipped also with either wet scrubbers or precipitators for lime and sodium dust.

Others emissions:

From lime kiln, CO<sub>2</sub> is also emitted.



## II. Annex 2: Phases characterization

### Gas analysis

Gaseous phases were exclusively analyzed by gas chromatography. This technique is used to separate, identify and quantify the components.

The principle is based on the equilibrium of compounds concentrations between stationary phase and mobile phase. Compounds are transported by mobile phase and more or less retained by the stationary phase. This difference of affinity separates molecules. At the end of the column, molecules are detected and quantified if possible. In France and Japan, the same  $\mu$ -GC was used: Micro-GC – Agilent 3000.

### Liquid analysis

#### Total Organic Carbon (TOC):

This analysis is made in two stages with the measurement of total carbon and inorganic carbon. To measure the total carbon (TC) sample is injected with a syringe in a packed bed at 720°C. The sample is evaporated under an air flow and oxidized to CO<sub>2</sub> thanks to a platinum catalyst. Then CO<sub>2</sub> is measured by infrared spectroscopy at the output of the oven. To measure inorganic carbon (IC) a new sample of the solution is taking again and injected in phosphoric acid (30%) where a neutralization reaction (equation 2) occurs. Solution is subjected to bubbling with air to release, the inorganic carbon of the solution (CO<sub>3</sub><sup>2-</sup>, HCO<sub>3</sub><sup>-</sup>, H<sub>2</sub>CO<sub>3</sub>) as CO<sub>2</sub>. CO<sub>2</sub> is then measured by infrared spectroscopy.



TOC is suitable to evaluate the mineralization of the solution.

$$TOC = x \times M_c \times [C_xH_yO_z] \quad (3)$$

With

$M_c$  Atomic mass of carbon (g.mol<sup>-1</sup>),

$[C_xH_yO_z]$  The concentration (mol.L<sup>-1</sup>) and,

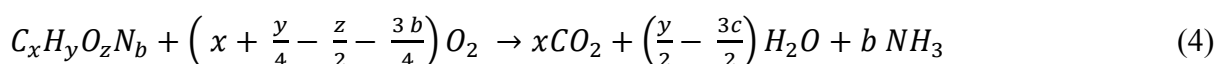
$TOC$  (g.C.L<sub>solution</sub><sup>-1</sup>),

x is the number of carbon atom in the molecule.

Chemical oxygen demand: COD (Hach Lange):

The sample is introduced in a tube (cuvette test Hach Lange) containing the oxidizing agent together with a catalyst. Tubes are then placed in a heating device (HT 200 S, Hach Lange) to perform reaction (170°C during 15 min). During oxidation, chrome ions change their oxidation degree which is accompanied by a change of color. When the tube is cooled, the intensity of this color change is measured using a spectrometer (Hach Lange DR 6000).

The equation for oxidation is:



NH<sub>3</sub> is then oxidized as follow:



The analysis wavelength is 605 nm for the ranges 100-2000 mg.L<sup>-1</sup> (LCK514) and 1000-10000 mg.L<sup>-1</sup> (LCK014).

Phenols and formaldehydes measurement:

Phenols react with 4-aminoantipyrine (AAP) and formed a colored complex in the presence of oxidizing agent. This reaction can occur if the pH sample is between 2 and 11 at ambient temperature. Ranges of concentration measured are 5 to 50 mg/L and 20 to 200 mg/L with LCK346 cuvettes. For these latest tubes, phenols react with 4-nitroaniline to form a yellow color complex, the color is measured by photometer at 510 nm (Hach Lange DR 6000).

Formaldehyde reacts with ammonium ions and acetylacetone to give a yellow dye. The pH sample has to be between 3 and 10 and temperature from 15 to 25°C. Reaction needs heat so tube is placed in thermostat at 40°C during 10 min (Hach Lange, HT 200 S). The measurement is made by spectrometer (Hach Lange DR 6000) after cooling at 413 nm.

Inductively Couple Plasma Optical Emission-spectrometry (ICP-OES):

The solution is nebulized and sprayed in the argon plasma flame (at a temperature of 6000-8000°C). Compounds are decomposed into atoms and ions. Plasma flame drives atoms and

ions into an excited state. During the transition to the non-excited state, elements emit light. The elements are then detected by a photomultiplier tube according to the specific wavelength of emitted light. Thanks to calibration, light intensities are converted into compounds concentration.

*Gel Permeation chromatography (GPC): (HP1100).*

The stationary phase is made by porous beads packed in a column. The mobile phase is constituted by a solvent (Tetrahydrofuran was used for analysis presented in this work). Smaller molecules are retained into pores while bigger are not stopped. Molecules with high molecular weight are eluted before molecules with low one.

*Gas chromatography coupled with mass spectroscopy (GC-MS): (GC: Agilent 7890A; MS:Agilent 5975C)*

This analysis combined features of gas chromatography and mass spectrometry. It is particularly advantageous to identify compounds separated after chromatography. Indeed, first GC allows separating and then MS allows identifying compounds in a mixture with a percentage of identification.

**Solid analysis**

Solid obtained from hydrothermal carbonization and presented in chapter 3 is characterized using particle size distribution, elemental analysis, microscopy (transmission electron microscopy and environmental scanning electron microscopy), total surface and specific surface measurements with BET, density (helium pycnometer), thermogravimetric analysis, Fourier Transform infrared spectroscopy, RAMAN spectroscopy, X-ray diffraction.

*Particle size distribution:* Mastersizer 3000 Malvern

Laser granulometry is a technique which allows observing the size distribution of a set of particles using optical properties resulting from the interaction between this and set an incident laser wavelength. The measurement can be made on a dispersed gas (smoke) solid or a liquid (suspension) but also dispersed in another liquid fluid (emulsion).

The optical bench is composed by the red laser source (633 nm), the blue one (470 nm) and detectors. The blue laser allows a better resolution on the finest particles (<0.1 microns) after



running red laser. A measuring cell is filled by the wet sample. The liquid is dispersed by ultrasound.

CHNOS: elemental analysis (Thermo NA 2100).

Analyses of C, H, N, and S are first made of a combustion oven where the solid phase is burnt by combustion at 1050°C under helium and oxygen flows. Then, combustion gases go through a tube reduction filled with copper where oxygen is retained and nitrogen oxides are transformed in nitrogen. The reduction step is made at 450°C. At the end of the reduction step, emitted gases (CO<sub>2</sub>, H<sub>2</sub>O, SO<sub>2</sub> and N<sub>2</sub>) are routed through the detector by helium. After that, C, H, N and S are quantified based on mass balance calculations.

The oxygen is calculated by difference or analyses separately. Combustion is made at 1800°C, CO is formed and goes through an oxidation tube where it is transformed in CO<sub>2</sub>. Then CO<sub>2</sub> is detected and O is quantified.

Electronic microscopy:

ESEM: environmental scanning electron microscopy (ESEM, Philips XL 30 FEG).

The basic principle of this microscope is the differential vacuum maintained in different parts of the electron column between the barrel and chamber object [152]. The observation is possible thanks to the detection of secondary electrons emerging from the sample. It is possible to use different voltages of direct electrons that allow observing sample at different depths. The different contrasts (Like topographic contrast, chemical contrast) available provide numerous features about the compounds in the sample. In addition, a local elementary microanalysis using X-ray spectrometry is possible. Analyses made using ESEM are surface analysis. It allows us to observe non-conductive samples in different atmospheres (wet, dry, oxidizing or reducing atmospheres). With ESEM, it is possible to observe distinctly with magnification of 50 000 or 100 000; it means that a 100 nm sample can be observed. Depending on the type of contrast, the beam depth is not the same: for a topographic contrast, the detector captures secondary electrons with a depth of 10 nm; for a chemical contrast, the detector captures back-scattering electrons (the depths for analysis is 100 to 200 nm); and finally for an analysis of the chemical composition, detector captures X-rays, the depth of this elementary analysis is ~1 µm. The depths of these observations have to be known to understand results given by the ESEM. When the size of the interesting element is 1 µm, it is impossible to differentiate if the surface and the core have different compositions. On the

contrary it is impossible to make a chemical analysis on a big sample if the sample is heterogeneous. In this last case, the analysis is not representative.

Transmission Electron Microscopy TEM: (TEM, Hitachi H7650)

Measures have been made with an acceleration voltage of 100 kV. The principle of the measurement is the same as SEM or ESEM, the resolution is higher with just few nm observed distinctly, that allows to examine also fine details of bigger structure. TEM sample are prepared on a 3 mm support called “grid” in copper.

BET: Tristar II 3020.

This technique has been invented by Stephen Brunauer, Paul Hugh Emmett and Edward Teller. This theory is an extension of the Langmuir one which is based on the adsorption of a gas as multilayer on a solid surface. This adsorption allows measuring the surface area of the material. The technique is also based on several assumptions [153]:

- 1 - As it is a physical adsorption, it is guided by Van der Waals forces.
- 2 - When the equilibrium pressure tends to vapor saturation pressure, the number of layer tends to infinity.
- 3 - The first layer is adsorbed according to the Langmuir model, i.e. each adsorption site is energetically identical and without lateral interactions between adsorbed molecules. The Langmuir theory can be applied to each layer.
- 4 - The layer of adsorbed molecules is considered as sites of adsorption for the next layer

The BET equation is:

$$\frac{P/P_0}{V(1-P/P_0)} = \frac{C-1}{V_m C} \times \frac{P}{P_0} + \frac{1}{V_m C} = A \times \frac{P}{P_0} + B \quad (6)$$

With: P: equilibrium pressure; P<sub>0</sub>: saturation pressure; V: adsorbed volume at P pressure, V<sub>m</sub>: monolayer adsorbed gas quantity; C is the BET constant:

$$C = \exp\left(\frac{E_1 - E_L}{RT}\right) \quad (7)$$

With E<sub>1</sub>: heat of adsorption for the first layer and E<sub>L</sub>: heat of adsorption for the second and higher layers. These energies correspond to heat of liquefaction.

BET relation is the equation of an adsorption isotherm and can be plotted as a straight line with y-axis as  $\frac{P/P_0}{V(1-P/P_0)}$  and with x-axis as  $\frac{P}{P_0}$ . A is the slope and B the y-intercept.

From this plot it is possible to obtain the following parameters:  $V_m = \frac{1}{A+B}$  and  $C = 1 + \frac{A}{B}$ .

Then it is possible to calculate the total surface area and the specific surface area as:

$$S_{total} = \frac{(V_m N S)}{V} \text{ and } S_{BET} = \frac{S_{total}}{m} \text{ with m: mass of solid sample.}$$

#### Pycnometer:

Pycnometer determines density and volume of solid sample by measuring the pressure change of helium in a calibrated volume. Analysis measures sample volume, from which density can be derived automatically if sample weight has been entered. Calibration is used to determine the size of the cell and expansion chambers within the instrument. After calibration, the cell and expansion chamber volumes are automatically stored in the set-up parameters. Density is automatically given by the software installed on computer and linked to the device.

#### Thermogravimetric analysis (TGA): TG-ATD 92, Setaram

This technique measures the mass loss of a sample depending on the temperature.

It consists of a thermostated sealed chamber to control the atmosphere of the sample, a furnace for temperature control, a weighing module, thermocouple for temperature measurement and a computer to monitor and record all the data. Analyses are conducted under inert atmosphere (nitrogen). Thermocouples record the variation of heating flow.

#### Fourier Transform Infrared: FTIR (PERKIN ELMER 200 FTIR).

Principle: the device used the Mickelson interferometer. A source generates lights across the spectrum of interest. <sup>7</sup>The light passes through a beam splitter, which sends the light in two directions at right angles. One beam goes to a stationary mirror then back to the beam splitter. The other goes to a moving mirror. The motion of the mirror makes the total path length variable versus the stationary-mirror beam one. When the two meet up again at the beam splitter, they recombine, but the difference in path lengths creates constructive and destructive interference: an interferogram. Then the recombined beam passes through the sample. The difference between spectrum of molecule and original spectrum is sent to the detector. The obtained interferogram is converted to spectrum thanks to Fourier transform. The spectrum obtained is transmittance as a function of wavenumbers. The wavenumbers are between 400 and 4000  $\text{cm}^{-1}$ .

#### RAMAN spectrometry: RAMAN – AFM: Alpha 300R, WITec

The ample is illuminated with a laser beam. Electromagnetic radiation from the illuminated spot is collected with a lens and sent through a monochromator. The elastic scattered radiation

---

<sup>7</sup> <http://chemistry.oregonstate.edu/courses/ch361-464/ch362/irinstrs.htm>  
(30 Aug 2014)

at the laser line wavelength is called elastic Rayleigh scattering. It is filtered out while the rest of the collected light is dispersed onto a detector by either a notch filter or a band pass filter.

*X-ray diffraction (XRD): (PANalytical X'Pert MPD diffractometer)*

An X-ray diffractometer is used to identify the crystallinity/amorphism of a compound and the evolution of the amorphism. Indeed, each crystalline phase has a single diffractometer with specific fine peaks. On the contrary if the structure is amorphous, this indicates that it is composed by not organized atoms. X-rays are then diffracted in all directions, pattern are then obtained with large peaks.



### III. Annex 3: Carbon and texture characterizations obtained by carbonization from Inagaki

Table 21: Carbon and texture characterizations obtained by carbonization from Inagaki

Carbon	Formation conditions	Interface	Texture
carbon blacks	thermal decomposition of hydrocarbon gases	liquid/gas	concentric
Fluid cokes	decomposition of oil onto carbon nucleus	solid/liquid & liquid/gas	concentric
graphite nodules	precipitation of molten cast iron	solid/liquid	concentric
mesophase sphere	segregation in molten pitches	liquid/liquid	radial
Carbon spherule	decomposition & carbonization under pressure	liquid/liquid	radial
Glass-like carbon spheres	solid carbonization of organic precursors	solid/gas	random



**IV. Annex 4: Preliminary study on hydrothermal carbonization of black liquor (Proceeding for SFGP congress)**

**Generation of Carbon Microparticules by Hydrothermal Conversion of Black Liquor**

H.Boucard<sup>1</sup><sup>8</sup>, E. Weiss-Hortala<sup>1</sup>, R. Barna<sup>1</sup>

<sup>1</sup>Université de Toulouse; Mines Albi; CNRS; Centre RAPSODEE, Campus Jarlard, F-81013 Albi Cedex 09, France

**ABSTRACT**

Black liquor is a waste of paper industry containing important concentration of organic compounds (140 g.L<sup>-1</sup>) and quantity of water (77 wt%). A preliminary study was focused on the scanning of the operating conditions for the conversion of black liquor by supercritical water. The results obtained lead us to explore the solid phase more in detail. Indeed, the carbonaceous solid produced at low temperature presents microscopic spherical particles which can be used, for example, to form hollow sphere.

This paper focuses on the characterization of the solid phase recovered as regards to the operating conditions involved in the batch hydrothermal conversion of 10 wt% black liquor solutions. The structure of the solid obtained is complex, varying from aggregates of micrometric spherical particles (0.4-1 µm or 1-11 µm) to more massif structure showing an external porosity. Under certain operating conditions, an internal porosity was also highlighted for long reaction time. DVS analysis suggests a modification of the surface.

**INTRODUCTION**

As papers only contain cellulose, lignin and hemicellulose has to be separated from cellulose. Paper industry operates the delignification of wood through the wood cooking with white liquor (Na<sub>2</sub>S and NaOH mixture of Kraft process). Kraft lignin is then recovered in the cooking juice (black liquor) [1]. As white liquor is a basic mixture, black liquor is also a basic aqueous solution (pH ~13), containing dissolved lignin, fragments of cellulose and hemicellulose and several minerals and salts (Na, K, Ca, S.... carbonates, sulfates, sulfides...). Although black liquor serves an auto-energetic supply of industrial Kraft process facilities [2],

---

<sup>8</sup> Corresponding author : helene.boucard@mines-albi.fr



extra volumes of black liquor are produced. Thus this part of black liquor would be valorized as useful materials. As a result, thanks to its high water content, black liquor is an interesting candidate to be converted using sub and supercritical water properties.

Supercritical water has been firstly used to achieve total oxidation of waste and more recently is used to recycle waste by generating energetic gas, building block molecules or added-value solids. Indeed, above its critical point ( $T > 374^{\circ}\text{C}$  and  $P > 22.1 \text{ MPa}$ ) water is a reactant and a solvent. In subcritical condition ( $T < 374^{\circ}\text{C}$  and  $P < 22.1 \text{ MPa}$ ), water is a polar solvent in which salts are partially miscible while organic molecules are immiscible. In supercritical state, the properties of water change drastically. The water molecules form clusters [3] that results in a nonpolar solvent and thus free radical reactions are favored. As black liquor is a wet biomass (~80 wt%) composed of long aliphatic and aromatic chains, hydrothermal process is suitable to use its high water content to convert its significant organic content (~ 140 g.C.L<sup>-1</sup>). Therefore some studies are devoted to the supercritical water gasification [4, 5] and revealed the efficiency and the interest of the process in batch and continuous process. As the black liquor is a very complex mixture of organics, containing aliphatic together with aromatic fractions, the gasification process requires a complete cut-down of the long molecules to form hydrogen that increases the energetic cost of the treatment. Another point of view is to use BL to produced materials with relatively long carbon chains that will decrease the cost.

Thus the present work is focused on solid generation with sub or supercritical water, namely hydrothermal carbonization (HTC).

The solid residue from HTC is mainly composed of carbon and oxygen and comes from phenolic compounds polymerization [6, 7]. HTC experiments realized with lignin, glucose or other carbohydrates as raw materials produces carbon particles [7-12].

The microspheres obtained by hydrothermal conversion could be used as hollow sphere containing inorganic compounds [6], sorbent [8], highly functionalized carbon materials or hybrid materials [9, 10] and spherical activated carbons [12]. As the main studies used model feedstock, this paper focuses on the operating conditions impact on the generation of carbon particles from the real feedstock: black liquor.

## **MATERIALS AND METHODS**

### **1- Reagents**

Black liquor was supplied by a paper industry: Smurfit Kappa Cellulose du Pin in Factice, France. It comes from the digester after recovery of tall oil in Kraft process. The dry matter is of 23 wt% (organic and mineral) while the other part is water (77 wt%). Moreover, the organic compounds represent 65 wt% of the dry mass that equals to 140 gC.L<sup>-1</sup>.

### **2- Experimental protocol**

Experiments are performed at 350°C in a pressure-resistant batch reactor with an inner volume of 5mL. The black liquor is introduced into reactor which is capped tightly. 5 autoclaves are placed together in an oven. The reaction time starts when oven has reached target temperature. The reactor is filled at atmospheric temperature and pressure, with the amount of black liquor required to reach reaction temperature and pressure. After reaction time (15, 30 or 60 min), reactor is cooled by quench into frozen water to stop immediately the reaction (rapid cooling) or cooled by ambient air (slow cooling). After reaction liquid and solid are collected. Both fractions are separated by filtration.

### **3- Analysis of gas, liquid and solid phases**

Liquid and solid phases were analyzed and characterized after reaction.

#### Liquid phase:

Total Organic Carbon was quantified with a TOC-analyzer (Shimadzu 5050A) and the pH was measured after reaction.

#### Solid phase:

Carbonaceous solid residues were analyzed by environmental scanning electron microscopy (ESEM, Philips XL 30 FEG), optical microscopy and FTIR (PERKIN ELMER 200 FTIR).

## RESULTS

### 1- Solid morphology related to reaction temperature

Black liquor is an aqueous liquid which can be turned to hydrochar under certain conditions. However, the goal is to obtain carbon particles. Thus, hydrothermal experiments were carried at various temperatures and the morphologies of remaining carbonaceous solids were compared. Figure 146 shows ESEM pictures of solid residues obtained by hydrothermal conversion of a solution of 10wt% black liquor, after 15 min of reaction and under 25 MPa of pressure for supercritical temperatures or self-generated pressure for subcritical temperatures.

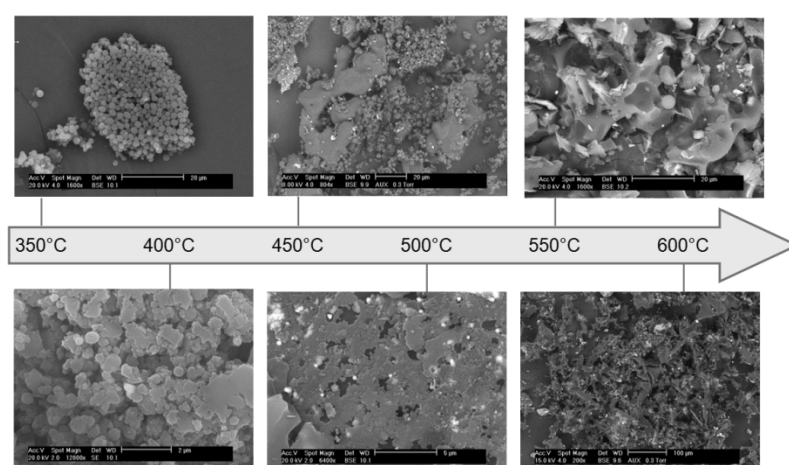


Figure 146: ESEM pictures of solid residue at various reaction temperatures. Black liquor concentration = 10 wt%,  $P = 25$  MPa or self generated pressure,  $t = 15$  min.

The solid phase represents ~ 20 wt. % of the total initial carbon. Its composition remains quite the same: carbon, oxygen and minerals. However, minerals do not play a role on the surface morphology. The morphology evolves from microparticles at 350°C to shapeless structure under severe conditions. Thus, carbon-based microparticles are only obtained at subcritical conditions as regards to the range of reaction temperature. At the end of experiments at 350°C, 2 liquid phases are observed: an oily and an aqueous phase. Although the amount of oily phase is low, it would contain high concentrations of organics such as phenolic compounds, furfurals and so on, which are widely precursors of polymerization reactions [7]. At subcritical, the oily phase would be dispersed into the aqueous phase that can form the microparticles of solid due to interfacial energies [7].

Figure 146 shows that the structure becomes denser at higher temperatures, probably due to by sintering or agglomeration of particles. It could be also due to the interfaces between the carbon residue and the reactor, salts, liquid/gas or supercritical phase.

Solids obtained at various temperatures demonstrate various morphologies. The properties of these carbon-based solids would favor a valorization either as energy [7] or useful materials [8-12]. Indeed, energy recovery should be considered for a solid with high LHV in substitution of coal. Material recovery will be justified if the solid is porous (catalyst support, adsorbent ...), if it is filled with minerals or metals (new catalyst, hollow spheres), if it has structural or crystalline qualities (electrochemical applications, nanotubes carbon ....). All current challenge is to develop future materials from waste and / or renewable resources with specific textures.

Others operating conditions act also on the particles morphology but only a few parameters are summarized in the following sections.

## 2- Influencing parameters

### Influence of reaction time with slow cooling

Size and porosity are influenced by reaction time as showed in Figure 2.

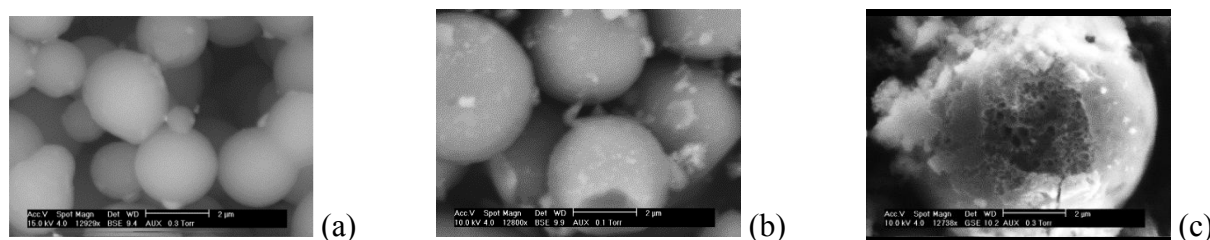


Figure 147: Particles obtained after 15 min (a), 30 min (b) and 60 min (c) of reaction.

The increase of reaction time indicates an increase of particle diameter. After 60 min of reaction, particles become porous and fragile/ friable inside. One hypothesis is that the precipitation was carried out in several stages to create a core and a shell. Thus the properties of the different “layers” could be different in composition and in terms of physico-chemical properties. A second hypothesis is to assume that liquid or gaseous phases are trapped inside the particles during their maturation, and then are degraded prior to go back to ambient conditions. The influence of cooling rate has been studied.

### Influence of heating rate and cooling rate

For experiments performed with rapid heating and pure black liquor, the solid is built in contact with the walls of the reactor as a continuous phase (Figure 148 a). This phase is a porous network as shown in Figure 148 b. In contrast to slow heating rate ( $20^{\circ}\text{C}\cdot\text{min}^{-1}$ ), the

solid phase is concentrated at the bottom of the reactor (Figure 148 c), suggesting that a small interface (or an exchange surface) between solid and liquid phases occurs during the reaction. This can also suggest a higher solid density. The carbon conversion to the solid phase is reduced by more than half at slow heating rate, and the solid (Figure 148 c) is denser and remains less porous. Thus high heating would promote the formation of solid or polymerization of species present initially in pure black liquor. Another hypothesis is that a rapid heating increases the agitation of molecules and thus polymerization reactions by increasing the number of successful collisions.

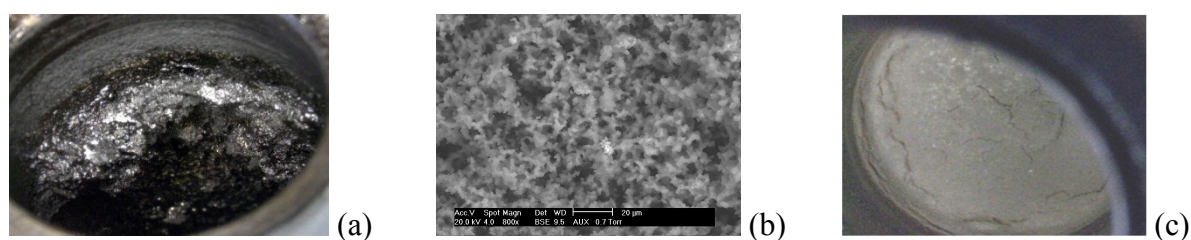


Figure 148: Solid formation inside the reactor for a pure black liquor solution.

Thereafter, experiments were carried out with diluted black liquor (10wt%) from 20°C to 350°C with controlled temperature ramp: 7°C.min<sup>-1</sup>, 20°C.min<sup>-1</sup> and 40°C.min<sup>-1</sup> and a slow cooling rate (duration ~40 min). It appears that rapid heating favors the formation of microparticles and a slow heating leads to the formation of larger particles (~ 20 μm). These latter have a brittle and porous core (Figure 149).

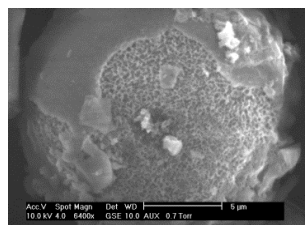


Figure 149: 350°C, 60 min temperature rate 7°C.min<sup>-1</sup>, black liquor 10 wt%, batch reactor (500 mL).

For rapid heating and a slow cooling, the size distribution of particles is from 1 μm to 5 μm, and particles are bigger than with slow heating.

The study about cooling rate showed that quench cooling homogenized particle size and decreased their size favoring nanoparticles. This means that either the growth of particles occurs during cooling step or the reaction continues during cooling, and therefore the maturation step is not achieved after 15 min of reaction time. The reaction nuclei supersaturation evolves with time, to a growth or a complete disappearance of the particle. A study about particle size distribution is under progress.

Organic functions in solid phase

FTIR analysis was applied to the solid recovered. All the spectrums were similar (Figure 150). The ordinate axis represents the transmittance (%) and the abscissa the wave number ( $\text{cm}^{-1}$ ).

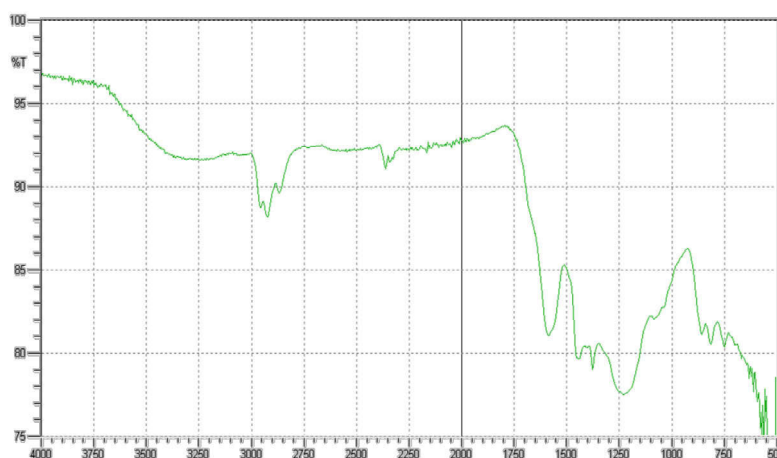


Figure 150: FTIR spectrum of solid residue obtained after reaction.

The profile obtained was similar to that obtained by Liu et al. [13] in their study on the hydrothermal conversion of solid biomass (coconut fiber and Eucalyptus leaves). The large peak around  $3300 \text{ cm}^{-1}$  corresponds to the free -OH function and/or -OH intermolecular bonds (hydrogen bonding). The peaks observed close to  $3000 \text{ cm}^{-1}$  correspond to CH stretching (in -CH<sub>3</sub> and -CH<sub>2</sub>-) of saturated (under) and unsaturated molecules (above). The peaks around  $1600 \text{ cm}^{-1}$  and  $1450 \text{ cm}^{-1}$  correspond to the C=C bonds of the aromatic rings. So these peaks reveal the presence of alcohol function and aromatic rings which derived from phenolic compounds obtained by cleavage of the lignin; and their repolymerization. The other peaks are difficult to identify precisely: one at  $1350 \text{ cm}^{-1}$  may correspond to a double bond S=O. that is in accordance with microanalysis realized with EDS detector that highlighted the presence of sulfur. The broad peak at  $1250 \text{ cm}^{-1}$  may correspond to the vibration of the CO bond of acetate. These organic functions are observed on all the solids obtained and confirm that the solids would have quite similar chemical compositions.

## CONCLUSION

Black liquor contains a high concentration of lignin that was converted into carbonaceous material, using sub-/supercritical water in batch reactor. The focus was the study of operating conditions that provide microparticulate solid. The results show that microparticles are only obtained at sub critical conditions, in a short reaction time, from a dispersed oily phase. The heating and cooling rate are key steps influencing the morphology of these particles, especially for a short reaction time. High heating and cooling rate are clearly favoring the smallest size of microparticles together with a short reaction time. Thus kinetics of particle formation is currently in progress as regards to the liquid composition. As phenolic compounds and formaldehyde are assumed to initiate the polymerization, their concentrations will be followed in the liquid phase

## REFERENCES

- [1] LEASK, R.A. ; Pulp and papermanufacture, Joint Textbook Committee of the Paper Industry, **1987**
- [2] DEMIRBAS, A., Energy Conversion Management, Vol 43, **2002**, p.877
- [3] KRUSE, A., DINJUS, E, Journal of supercritical fluids, vol.39, **2007**, p.362
- [4] CAO, C et al. ; International Journal of Hydrogen Energy, Vol.36, **2011**,p.13528
- [5] SRICHAROENCHAIKUL, V., Bioresource Technology, 100, **2009**, p. 638
- [6] KANG, S., LI X., FAN J. et CHANG J., , Bioresource Technology, **2012**
- [7] DINJUS, E., KRUSE, A., TROGER, N., Chemical Engineering Technology, 34, **2011**, p. 2037
- [8] DEMIR-CAKAN, R., BACCILE, N., ANTONIETTI, M., TITIRICI, M.M., Chem. Mater., 21, **2009**, p. 484
- [9] TITIRICI, M.M., ANTONIETTI, M. Chemical Society Reviews, 39, **2010**, p. 103
- [10] FALCO, C., BACCILE, N., TITIRICI, M.M., Green Chemistry, 13, **2011**, p. 3273
- [11] SEVILLA, M., MACIA-AGULLO, J.A., FUERTES, A.B., Biomass and Bioenergy, 35, **2011**, p. 3152
- [12] ROMERO-ANAYA, A.J., OUZZINE, M., LILLO-RODENAS, M.A., LINARES-SOLANO, A., Carbon, 68, **2014**, p. 296
- [13] LIU, Z., A. QUEK, S. KENT HOEKMAN, R. BALASUBRAMANIAN, Fuel, **2012**

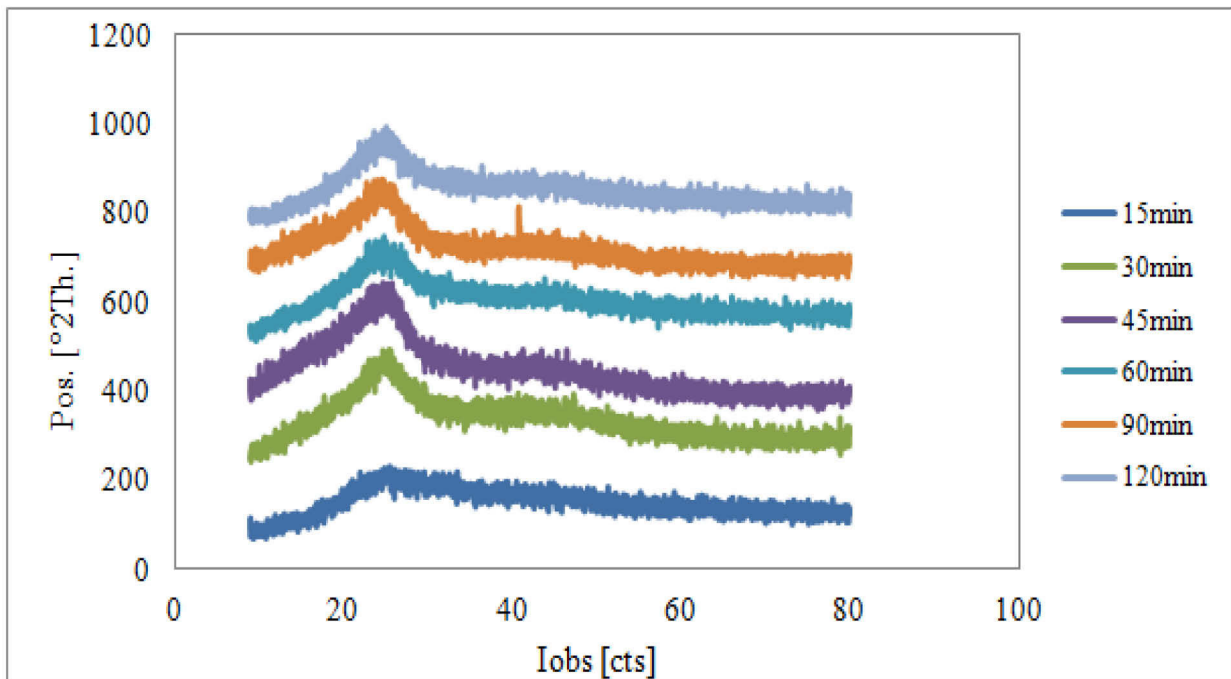
**V. Annex 5: XRD of CT series – carbonization study.**

Figure 151: XRD of CT series – carbonization study.





## VI. Annex 6: Influence of heating rate NT/CT.

### TGA analysis to compare CT and NT series at 60 min reaction time:

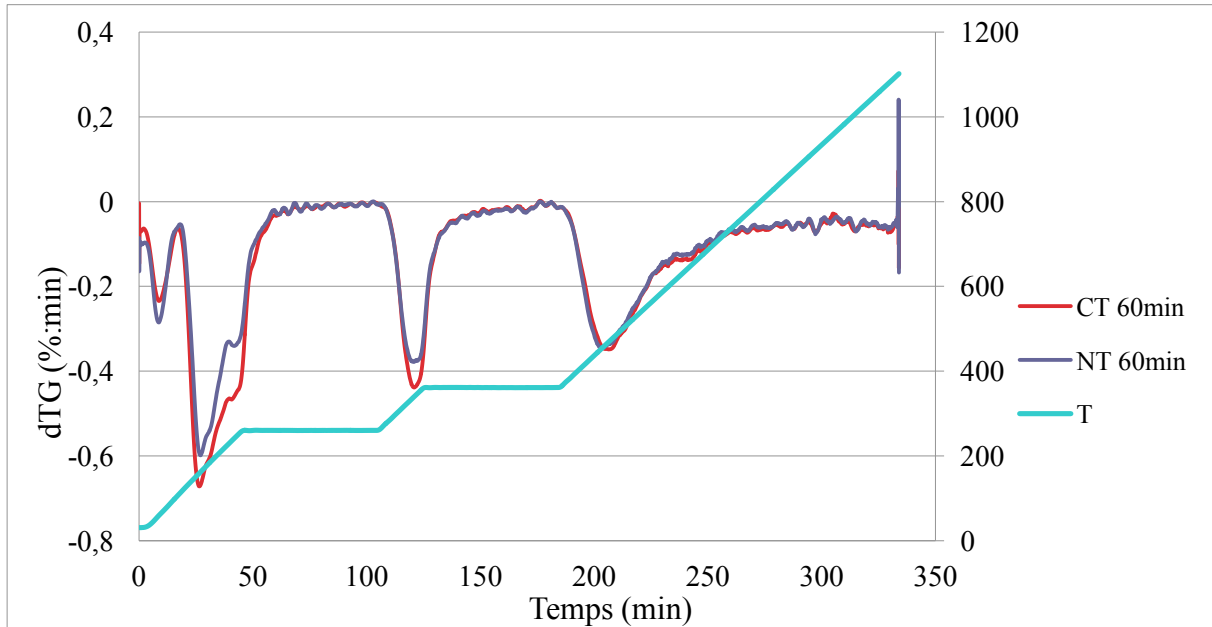


Figure 152: TGA analysis to compare CT and NT series at 60 min reaction time.

### Van Krevelen diagram for NT series:

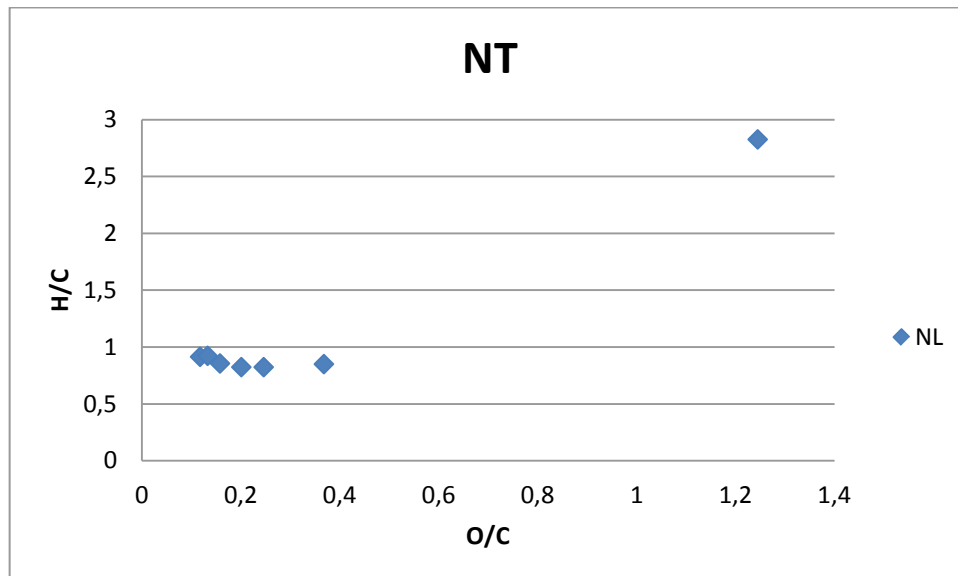


Figure 153: Van Krevelen diagram for NT series.

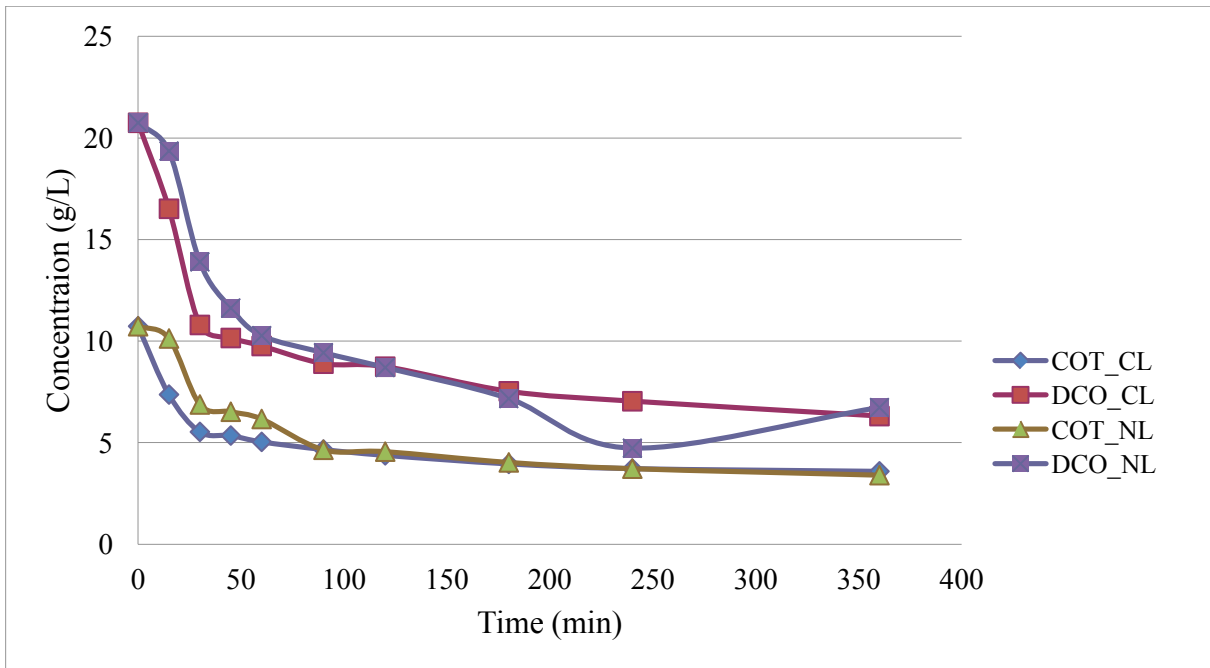
**Monitoring of TOC, COD phenols and formaldehyde to compare CL and NL series over reaction time,**

Figure 154: TOC and COD monitoring over reaction time.

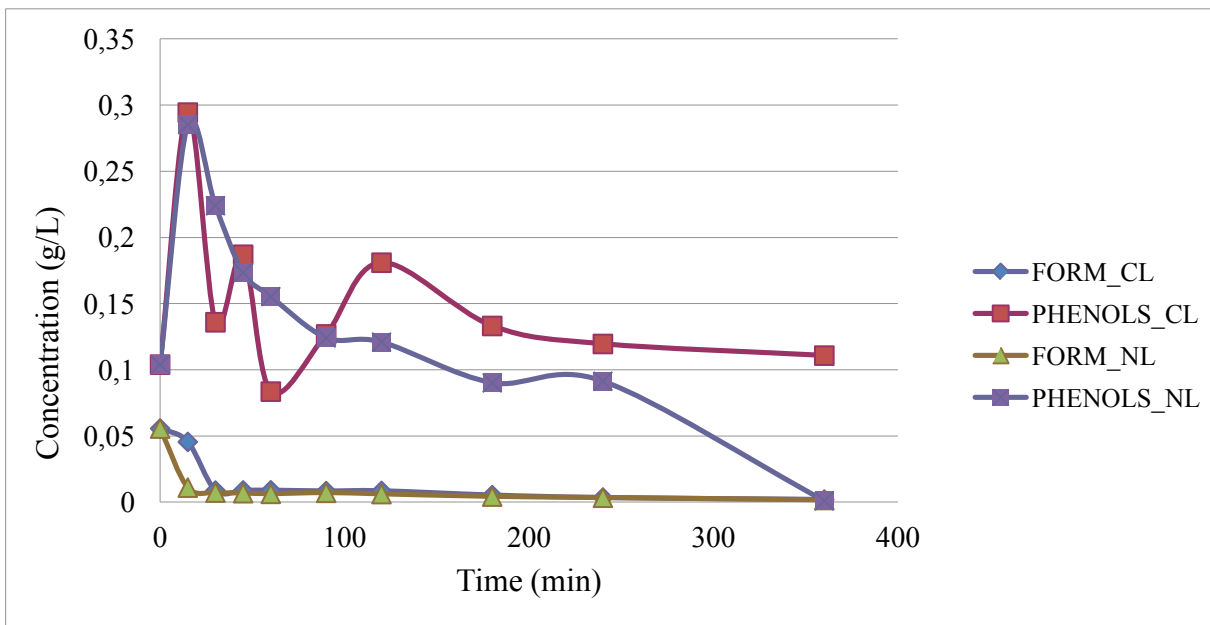


Figure 155: Formaldehyde and phenols monitoring over reaction time.

## VII. Annex 7: Influence of cooling rate – CL/CT.

### TGA analysis to compare CL and CT series at 60 min reaction time.:

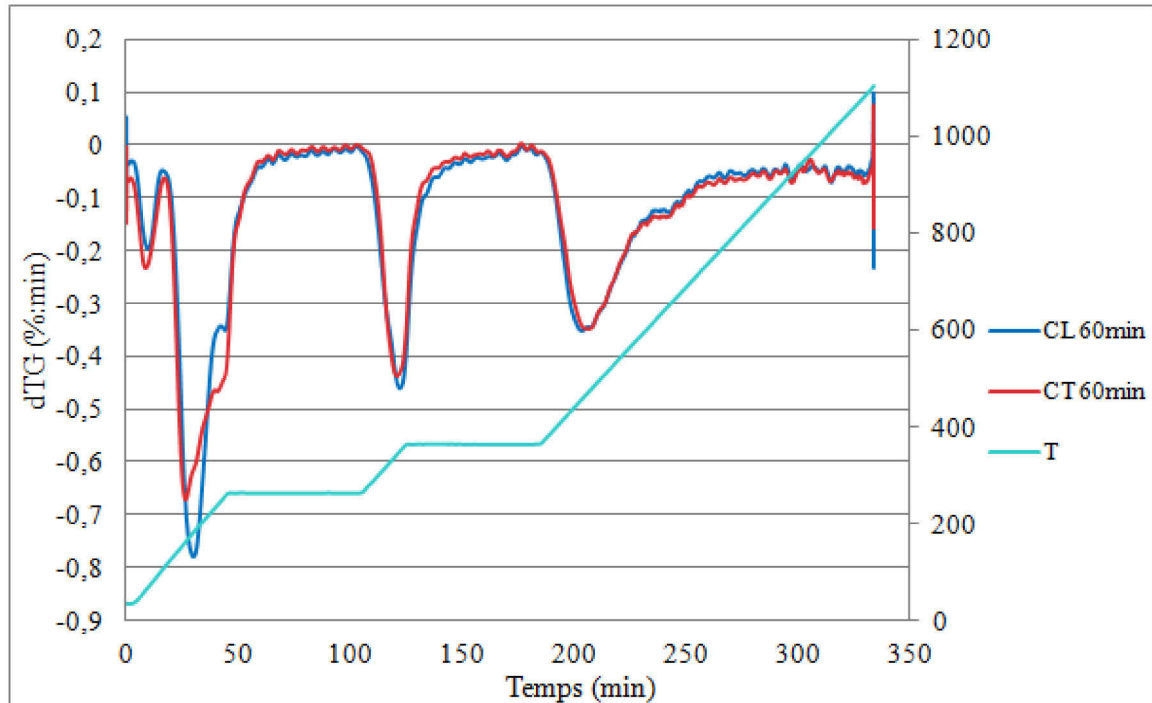


Figure 156: TGA analysis to compare CT and NT series at 60 min reaction time.

### Van Krevelen diagram of CL series:

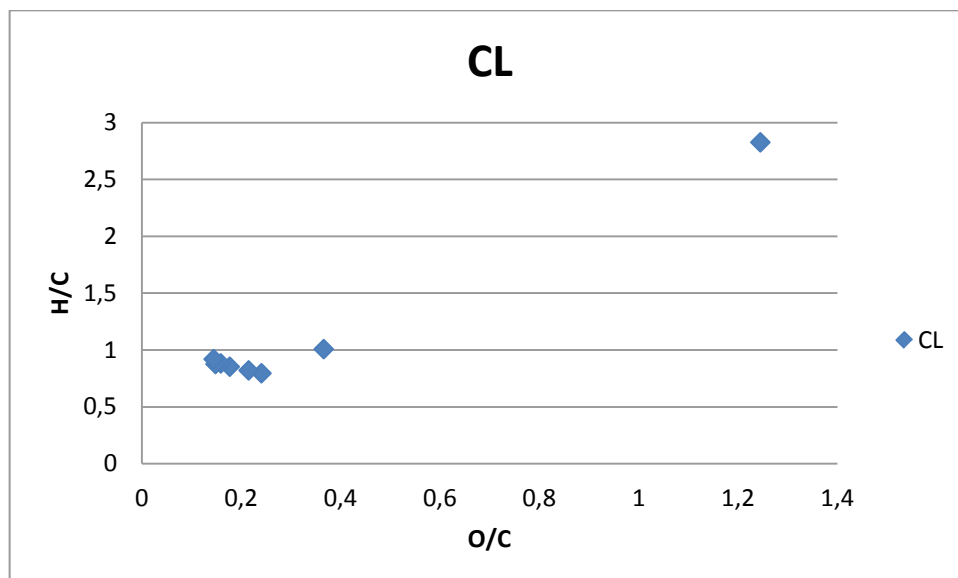


Figure 157: Van Krevelen diagram for NT series.

**Monitoring of TOC, COD, phenols and formaldehyde to compare CL and CT series over reaction time**

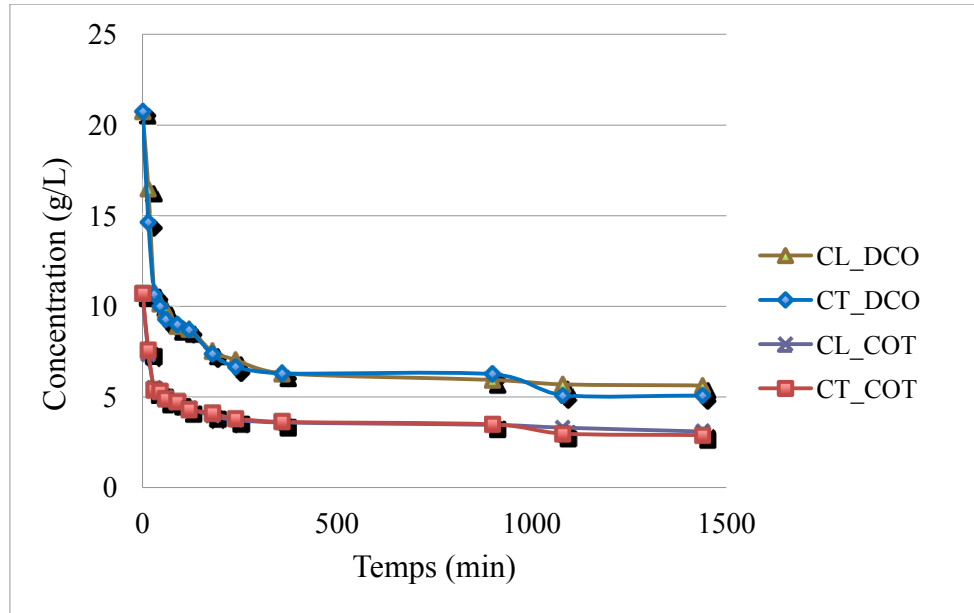


Figure 158: TOC and COD monitoring over reaction time.

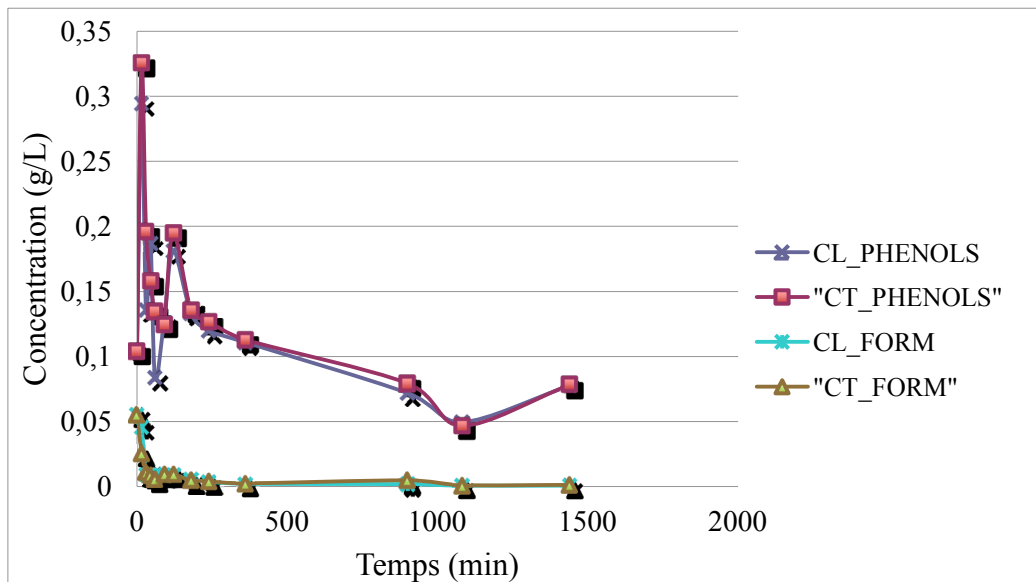


Figure 159: TOC and COD monitoring over reaction time.

**VIII. Annex 8: GC-MS results for liquid recovered after black liquor conversion under sub (350°C) and supercritical (450°C) conditions with and without CeO<sub>2</sub> catalyst.**

Under supercritical conditions at 450°C for 15 min and 60 min reaction time with and without catalyst.

Table 22: GC-MS results for liquid recovered after black liquor conversion under supercritical (450°C) conditions with and without CeO<sub>2</sub> catalyst for 15 min and 60 min of reaction time.

15 min without catalyst	15 min with catalyst (R = 5)	60 min with catalyst (R = 5)
Toluene	Propane	Acetone
2-Furanol, tetrahydro-	3-Butenoic acid	Cyclopropane, 1-ethyl-2-methyl-, cis-
Butyrolactone	Butanal, 3-methyl-	Butanal, 3-methyl-
Butanoic acid, anhydride	Toluene	Toluene
Retene	Butyrolactone	Butyrolactone
	Butanoic acid, anhydride	Butanoic acid, anhydride
	Phenol	Phenol
	Retene	Retene

Under subcritical conditions at 350°C for 15 min and 60 min reaction time with and without catalyst

Table 23: GC-MS results for liquid recovered after black liquor conversion under subcritical (350°C) conditions with and without CeO<sub>2</sub> catalyst for 15 min and 60 min of reaction time.

<b>15 min without catalyst</b>	<b>15 min with catalyst (R = 5)</b>	<b>60 min without catalyst</b>	<b>60 min with catalyst (R = 5)</b>	<b>60 min with catalyst (R = 20)</b>
Acetone	Toluene	Toluene	Furan, 2,3-dihydro-	Furan, 2,3-dihydro-
Toluene	2-Furanol, tetrahydro-	2-Furanol, tetrahydro-	Toluene	Toluene
2-Furanol, tetrahydro-	Butyrolactone	Butanoic acid, 4-hydroxy-	3-Buten-1-ol	2(3H)-Furanone, dihydro-3,5-dimethyl-
Butyrolactone	Phenol, 2-methoxy-	Butyrolactone	2-Furanol, tetrahydro-	2-Furanol, tetrahydro-
2-Butenal, 2-ethenyl-		Benzene, 1-butynyl-	Butyrolactone	Butyrolactone
Phenol			Phenol	Indane
Phenol, 2-methoxy-			2-Methyl phenylacetylene	1(3H)-Isobenzofuranone, 6,7-dimethoxy-3-[2-(2-methoxyphenyl)-2-oxoethyl]-
-			2-Cyclopenten-1-one, 3,4,5-trimethyl-	
			(E)-1-Phenyl-1-butene	
			Benzene, 1-butynyl-	
			Benzene, (2-cyclopropylethenyl)-	
			10,18-Bisnorabieta-8,11,13-triene	
			1(3H)-Isobenzofuranone, 6,7-dimethoxy-3-[2-(2-methoxyphenyl)-2-oxoethyl]-	

## Bibliography

---





- [1] M. Svanström, M. Fröling, M. Modell, W. a Peters, and J. Tester, "Environmental assessment of supercritical water oxidation of sewage sludge," *Resour. Conserv. Recycl.*, vol. 41, no. 4, pp. 321–338, Jul. 2004.
- [2] M. Svanstrom, M. Froling, M. Modell, W. Peters, and J. Tester, "Environmental assessment of supercritical water oxidation of sewage sludge," *Resour. Conserv. Recycl.*, vol. 41, no. 4, pp. 321–338, 2004.
- [3] M. D. Bermejo and M. J. Cocero, "Supercritical Water Oxidation: A Technical Review," vol. 52, no. 11, 2006.
- [4] A. Kruse, "Biomass gasification in supercritical water: Key compounds as a tool to understand the influence of biomass components .," pp. 1–10, 2005.
- [5] a. Kruse and E. Dinjus, "Hot compressed water as reaction medium and reactant," *J. Supercrit. Fluids*, vol. 39, no. 3, pp. 362–380, Jan. 2007.
- [6] Y. G. Bushuev and S. V. Davletbaeva, "New intermolecular interaction potential for simulation of water and aqueous solutions in a wide range of state parameters," *Russ. Chem. Bull.*, vol. 53, pp. 742–750, 2004.
- [7] M. Boero, K. Terakura, T. Ikeshoji, C. Liew, and M. Parrinello, "Water at supercritical conditions: a first principales study," *J. Chem. Phys.*, vol. 115, p. 2219, 2001.
- [8] M. Nakahara, N. Matubayasi, C. Wakai, and Y. Tsujino, "Structure and dynamics of water: from ambient to supercritical," *J. Mol. Liq.*, vol. 90, 2001.
- [9] V. Marques Leite dos Santos, F. G. Brady Moreira, and R. L. Longo, "Topology of the hydrogen bond networks in liquid water at room and supercritical conditions: a small-world structure," *Chem. Phys. Lett.*, vol. 390, 2004.
- [10] M. Boero, T. Ikeshoji, C. C. Liew, K. Terakura, and M. Parrinello, "Hydrogen Bond Driven Chemical Reactions: Beckmann Rearrangement of Cyclohexanone Oxime into  $\epsilon$ -Caprolactam in Supercritical Water," *J. Am. Chem. Soc.*, vol. 126, 2004.
- [11] A. A. Chialvo, P. T. Cummings, H. D. Cochran, J. M. Simonson, and R. E. Mesmer, "Na<sup>+</sup>-Cl<sup>-</sup> ion pair association in supercritical water," *J. Chem. Phys.*, vol. 103, 1995.
- [12] Z. Zhang and Z. Duan, "Lithium chloride ionic association in dilute aqueous solution: a constrained molecular dynamics study," *Chem. Phys.*, vol. 297, 2004.
- [13] V. Simonet, Y. Calzavara, J. L. Hazemann, R. Argoud, O. Geaymond, and D. Raoux, "X-ray absorption spectroscopy studies of ionic association in aqueous solutions of zinc bromide from normal to critical conditions," *J. Chem. Phys.*, vol. 117, 2002.
- [14] T. Yagasaki, K. Iwahashi, S. Saito, and I. Ohmine, "A theoretical study on anomalous temperature dependence of pK<sub>w</sub> of water," *J. Chem. Phys.*, vol. 122, 2005.

- [15] H. Takahashi, W. Satou, T. Hori, and T. Nitta, "An application of the novel quantum mechanical/molecular mechanical method combined with the theory of energy representation: An ionic dissociation of a water molecule in the supercritical water," *J. Chem. Phys.*, vol. 122, 2005.
- [16] R. Van Eldik and F.-G. Klärner, "High Pressure Chemistry: Synthetic, Mechanistic, and Supercritical Applications.," *Wiley-VCH Verlag GmbH*, 2002.
- [17] L. J. Sealock, D. C. Elliott, E. G. Baker, and R. S. Butner, "Chemical processing in high-pressure aqueous environments. 1. Historical perspective and continuing developments," *Ind. Eng. Chem. Res.*, 1993.
- [18] P. E. Savage, S. Gopalan, T. I. Mizan, C. J. Martino, and E. E. Brock, "Reactions at supercritical conditions: Applications and fundamentals," [Online]. Available: <http://deepblue.lib.umich.edu/handle/2027.42/37432>.
- [19] T. Miyazawa and T. Funazukuri, "Hydrothermal Production of Mono(galacturonic acid) and the Oligomers from Poly(galacturonic acid) with Water under Pressures," *Ind. Eng. Chem. Res.*, 2004.
- [20] R. R. Davda, J. W. Shabaker, G. W. Huber, R. D. Cortright, and J. A. Dumesic, "A review of catalytic issues and process conditions for renewable hydrogen and alkanes by aqueous-phase reforming of oxygenated hydrocarbons over supported metal catalysts," *Appl. Catal. B Environ.*, 2005.
- [21] A. Sinag, A. Kruse, and V. Schwarzkopf, "Key Compounds of the Hydrolysis of Glucose in Supercritical Water in the Presence of  $K_2CO_3$ ," *Ind. Eng. Chem. Res.*, 2003.
- [22] M. T. Reza, W. Yan, M. H. Uddin, J. G. Lynam, S. K. Hoekman, C. J. Coronella, and V. R. Vásquez, "Reaction kinetics of hydrothermal carbonization of loblolly pine.," *Bioresour. Technol.*, vol. 139, pp. 161–9, Jul. 2013.
- [23] Z. Fang, T. Sato, R. L. Smith, H. Inomata, K. Arai, and J. a Kozinski, "Reaction chemistry and phase behavior of lignin in high-temperature and supercritical water.," *Bioresour. Technol.*, vol. 99, no. 9, pp. 3424–30, Jun. 2008.
- [24] H. Schmieder, J. Abeln, N. Boukis, E. Dinjus, a. Kruse, M. Kluth, G. Petrich, E. Sadri, and M. Schacht, "Hydrothermal gasification of biomass and organic wastes," *J. Supercrit. Fluids*, vol. 17, no. 2, pp. 145–153, Apr. 2000.
- [25] R. L. Smith, P. Atmaji, Y. Hakuta, M. Kawaguchi, T. Adschiri, and K. Arai, "Recovery of metals from simulated high-level liquid waste with hydrothermal crystallization," *J. Supercrit. Fluids*, 1997.
- [26] M. Svanstrom, M. Modell, and J. Tester, "International Conference on Wastewater Sludge as a Resource (BIOSOLIDS 2003)," in *Direct energy recovery from primary and secondary Sludges by supercritical water oxidation*, 2003.

- [27] A. Yamaguchi, N. Hiyoshi, O. Sato, K. K. Bando, M. Osada, and M. Shirai, "Hydrogen production from woody biomass over supported metal catalysts in supercritical water," *Catal. Today*, 2008.
- [28] S. R. A. Kersten, B. Potic, W. Prins, and W. P. M. Van Swaaij, "Gasification of Model Compounds and Wood in Hot Compressed Water," *Ind. Eng. Chem. Res.*, 2006.
- [29] A. Kruse, "Hydrothermal biomass gasification," *J. Supercrit. Fluids*, vol. 47, no. 3, pp. 391–399, Jan. 2009.
- [30] M. Watanabe, H. Inomata, M. Osada, T. Sato, T. Adschiri, and K. Arai, "Catalytic effects of NaOH and ZrO<sub>2</sub> for partial oxidative gasification of n-hexadecane and lignin in supercritical water," *Fuel*, 2003.
- [31] M. Watanabe, H. Inomata, and K. Arai, "Catalytic hydrogen generation from biomass (glucose and cellulose) with ZrO<sub>2</sub> in supercritical water," *Biomass and Bioenergy*, 2002.
- [32] C. Xu and J. Lancaster, "Conversion of secondary pulp/paper sludge powder to liquid oil products for energy recovery by direct liquefaction in hot-compressed water," *Water Res.*, vol. 42, no. 6–7, pp. 1571–82, Mar. 2008.
- [33] K. Sue, "One-Pot Synthesis of Nickel Particles in Supercritical Water," *Ind. Eng. Chem. Res.*, 2006.
- [34] K. Byrappa, S. Ohara, and T. Adschiri, "Nanoparticles synthesis using supercritical fluid technology - towards biomedical applications," *Adv. Drug Deliv. Rev.*, vol. 60, no. 3, pp. 299–327, Feb. 2008.
- [35] A. Sahraneshin, S. Takami, D. Hojo, K. Minami, T. Arita, and T. Adschiri, "Synthesis of shape-controlled and organic-hybridized hafnium oxide nanoparticles under sub- and supercritical hydrothermal conditions," *J. Supercrit. Fluids*, vol. 62, pp. 190–196, Feb. 2012.
- [36] G. Seong, S. Takami, T. Arita, K. Minami, D. Hojo, A. R. Yavari, and T. Adschiri, "Supercritical hydrothermal synthesis of metallic cobalt nanoparticles and its thermodynamic analysis," *J. Supercrit. Fluids*, vol. 60, pp. 113–120, Dec. 2011.
- [37] M.-M. Titirici, R. J. White, C. Falco, and M. Sevilla, "Black perspectives for a green future: hydrothermal carbons for environment protection and energy storage," *Energy Environ. Sci.*, vol. 5, no. 5, p. 6796, 2012.
- [38] M.-M. Titirici and M. Antonietti, "Chemistry and materials options of sustainable carbon materials made by hydrothermal carbonization," *Chem. Soc. Rev.*, vol. 39, no. 1, pp. 103–16, Jan. 2010.
- [39] N. Brun, L. Edembe, S. Gounel, N. Mano, and M. M. Titirici, "Emulsion-templated macroporous carbons synthesized by hydrothermal carbonization and their application for the enzymatic oxidation of glucose," *ChemSusChem*, vol. 6, no. 4, pp. 701–10, Apr. 2013.

- [40] K. Chandler, C. L. Liotta, C. A. Eckert, and D. Schiraldi, "Tuning alkylation reactions with temperature in near-critical water," *AIChE*, vol. 44, pp. 2080–2087, 1998.
- [41] A. R. Katritzky, S. M. Allin, and M. Siskin, "Aquathermolysis: reactions of organic compounds with superheated water," *Acc. Chem. Res.*, vol. 29, pp. 399–406, 1996.
- [42] C. M. Comissar and P. E. Savage, "Kinetics of crossed aldol condensations in high-temperature water," *Green Chem.*, vol. 4, pp. 227–287, 2005.
- [43] R. L. Holliday, Y. M. Jong, and J. W. Kolis, "Organic synthesis in subcritical water: oxidation of alkyl aromatics," *J. Supercrit. Fluids*, vol. 12, pp. 255–260, 1998.
- [44] E. Garcia-Verdugo, J. Fraga-Dubreuil, P. A. Hamley, W. B. Thomas, K. Whiston, and M. Poliakoff, "Simultaneous continuous partial oxidation of mixed xylenes in supercritical water," *Green Chem.*, vol. 7, pp. 294–300, 2005.
- [45] J. M. Jennings, T. A. Bryson, and J. M. Gibson, "Catalytic reduction in subcritical water," *Green Chem.*, vol. 2, 2000.
- [46] T. Adschiri, R. Shibata, T. Sato, M. Watanabe, and K. Arai, "Catalytic hydrodesulfurization of dibenzothiophene through partial oxidation and a water-gas shift reaction in supercritical water," *Ind. Eng. Chem. Res.*, vol. 37, pp. 2634–2638, 1998.
- [47] K. Arai, T. Adschiri, and M. Watanabe, "Hydrogenation of hydrocarbons through partial oxidation in supercritical water," *Ind. Eng. Chem. Res.*, vol. 39, pp. 4697–4701, 2000.
- [48] T. Adschiri, S. Okazaki, M. Mochiduki, S. Kurosawa, and K. Arai, "Hydrogenation through partial oxidation of hydrocarbons in supercritical water," *Int. J. Soc. Mater. Eng. Resour.*, vol. 7, pp. 273–281, 1999.
- [49] H. Borwieck, O. Walter, E. Dinjus, and J. Rebizant, "Organometallic chemistry in supercritical water: metallorganic products of the CpCo-catalyzed cyclotrimerization of acetylenes," *J. Organomet. Chem.*, pp. 121–127, 1998.
- [50] P. H. Li, J. C. Yan, M. Wang, and L. Wang, "Glaser coupling reaction without organic solvents and bases under near-critical water conditions," *Chin. J. Chem.*, vol. 22, pp. 219–221, 2004.
- [51] M. Wu, "Etude de procédés de conversion de biomasse en eau supercritique pour l'obtention d'hydrogène. Application au glucose, glycérol et bio-glycérol," 2012.
- [52] P. Zhao, Y. Shen, S. Ge, Z. Chen, and K. Yoshikawa, "Clean solid biofuel production from high moisture content waste biomass employing hydrothermal treatment," *Appl. Energy*, vol. 131, pp. 345–367, 2014.
- [53] C. Cao, L. Guo, Y. Chen, S. Guo, and Y. Lu, "Hydrogen production from supercritical water gasification of alkaline wheat straw pulping black liquor in continuous flow system," *Int. J. Hydrogen Energy*, vol. 36, no. 21, pp. 13528–13535, Oct. 2011.

- [54] D. C. Elliott, "Catalytic hydrothermal gasification of biomass," *Biofuels, Bioprod. Biorefining*, vol. 2, pp. 254–265, 2008.
- [55] Y. J. Lu, L. J. Guo, C. M. Ji, X. M. Zhang, X. H. Hao, and Q. H. Yan, "Hydrogen production by biomass gasification in supercritical water: A parametric study," *Int. J. Hydrogen Energy*, vol. 31, pp. 822–831, 2006.
- [56] J. S. Luterbacher, M. Fröling, F. Vogel, F. Maréchal, and J. W. Tester, "Hydrothermal Gasification of Waste Biomass: Process Design and Life Cycle Assessment," *Environ. Sci. Technol.*, vol. 43, pp. 1578–1583, 2009.
- [57] P. Azadi, O. R. Inderwildi, R. Farnood, and D. a. King, "Liquid fuels, hydrogen and chemicals from lignin: A critical review," *Renew. Sustain. Energy Rev.*, vol. 21, pp. 506–523, May 2013.
- [58] K. Okuda, M. Umetsu, S. Takami, and T. Adschiri, "Disassembly of lignin and chemical recovery—rapid depolymerization of lignin without char formation in water–phenol mixtures," *Fuel Process. Technol.*, vol. 85, no. 8–10, pp. 803–813, Jul. 2004.
- [59] C. Häggström, O. Öhrman, A. a. Rownaghi, J. Hedlund, and R. Gebart, "Catalytic methanol synthesis via black liquor gasification," *Fuel Process. Technol.*, vol. 94, no. 1, pp. 10–15, Feb. 2012.
- [60] N. Brun, K. Sakaushi, L. Yu, L. Giebeler, J. Eckert, and M. M. Titirici, "Hydrothermal carbon-based nanostructured hollow spheres as electrode materials for high-power lithium-sulfur batteries.," *Phys. Chem. Chem. Phys.*, vol. 15, no. 16, pp. 6080–7, Apr. 2013.
- [61] M.-M. Titirici and M. Antonietti, "Chemistry and materials options of sustainable carbon materials made by hydrothermal carbonization.," *Chem. Soc. Rev.*, vol. 39, no. 1, pp. 103–16, Jan. 2010.
- [62] X. Lu, B. Jordan, and N. D. Berge, "Thermal conversion of municipal solid waste via hydrothermal carbonization: comparison of carbonization products to products from current waste management techniques.," *Waste Manag.*, vol. 32, no. 7, pp. 1353–65, Jul. 2012.
- [63] Z. Liu, A. Quek, S. Kent Hoekman, and R. Balasubramanian, "Production of solid biochar fuel from waste biomass by hydrothermal carbonization," *Fuel*, vol. 103, pp. 943–949, Jan. 2013.
- [64] D. Tsingakis, "Modélisation de propriétés de liqueurs Kraft," 1996.
- [65] Ministère de l'économie de l'industrie et de l'emploi, "Chiffres clés L 'industrie papetière chiffres," 2008.
- [66] C. Lapiere, "Les lignines, des polymères uniques au monde" *AgroParisTech*, 2010.
- [67] J. L. Wertz, "La lignine-Note de synthèse," *ValBiom*, 2010.

- [68] C. Forgacz, "Elaboration de matériaux poreux à partir de sous-produits de la biomasse par polymérisation d'émulsions concentrées," 2011.
- [69] R. Grant and C. Grant, "Tall oil production and processing," *Grant Hockh's Chem. Dictionnary*, pp. 1–11, 1987.
- [70] H. Tran and E. K. Vakkilainen, "the Kraft chemical recovery process."
- [71] M. Gustavsson, "The Significance of Liquor-to-Wood Ratio on the Reaction Kinetics of Spruce Sulphate Pulping," 2007.
- [72] I. Rönnlund, L. Myréen, K. Lundqvist, J. Ahlbeck, and T. Westerlund, "Waste to energy by industrially integrated supercritical water gasification – Effects of alkali salts in residual by-products from the pulp and paper industry," *Energy*, vol. 36, no. 4, pp. 2151–2163, Apr. 2011.
- [73] S. Kang, X. Li, J. Fan, and J. Chang, "Solid fuel production by hydrothermal carbonization of black liquor.," *Bioresour. Technol.*, vol. 110, pp. 715–8, Apr. 2012.
- [74] K. Okuda, S. Ohara, M. Umetsu, S. Takami, and T. Adschiri, "Disassembly of lignin and chemical recovery in supercritical water and p-cresol mixture. Studies on lignin model compounds.," *Bioresour. Technol.*, vol. 99, no. 6, pp. 1846–52, Apr. 2008.
- [75] M. Saisu, T. Sato, M. Watanabe, T. Adschiri, and K. Arai, "Conversion of Lignin with Supercritical Water - Phenol Mixtures," *ENERGY & FUELS*, no. 17, pp. 922–928, 2003.
- [76] S. Kang, X. Li, J. Fan, and J. Chang, "Hydrothermal conversion of lignin: A review," *Renew. Sustain. Energy Rev.*, vol. 27, pp. 546–558, Nov. 2013.
- [77] C. Peng, G. Zhang, J. Yue, and G. Xu, "Pyrolysis of lignin for phenols with alkaline additive," *Fuel Process. Technol.*, vol. 124, pp. 212–221, 2014.
- [78] R. J. a Gosselink, W. Teunissen, J. E. G. van Dam, E. de Jong, G. Gellerstedt, E. L. Scott, and J. P. M. Sanders, "Lignin depolymerisation in supercritical carbon dioxide/acetone/water fluid for the production of aromatic chemicals.," *Bioresour. Technol.*, vol. 106, pp. 173–7, Feb. 2012.
- [79] H. Pińkowska, P. Wolak, and A. Złocińska, "Hydrothermal decomposition of alkali lignin in sub- and supercritical water," *Chem. Eng. J.*, vol. 187, pp. 410–414, Apr. 2012.
- [80] D. Guo, S. Wu, B. Liu, X. Yin, and Q. Yang, "Catalytic effects of NaOH and Na<sub>2</sub>CO<sub>3</sub> additives on alkali lignin pyrolysis and gasification," *Appl. Energy*, vol. 95, pp. 22–30, Jul. 2012.
- [81] D. Guo, S. Wu, Y. Zhao, T. Dai, and X. Yin, "CATALYTIC EFFECTS OF EXISTING FORM OF Na ATOM ON ALKALI LIGNIN PYROLYSIS," in *4TH INTERNATIONAL CONFERENCE ON PULPING, PAPERMAKING AND BIOTECHNOLOGY*, 2012.

- [82] V. Sricharoenchaikul, "Assessment of black liquor gasification in supercritical water.," *Bioresour. Technol.*, vol. 100, no. 2, pp. 638–43, Jan. 2009.
- [83] M. Naqvi, J. Yan, and E. Dahlquist, "System analysis of dry black liquor gasification based synthetic gas production comparing oxygen and air blown gasification systems," *Appl. Energy*, vol. 112, pp. 1275–1282, 2013.
- [84] G. Nong, S. Wang, J. Mu, and X. Zhang, "Kinetics of Reaction between Dimethyl Sulfide and Hydrogen in Black Liquor Gasification Gas with ZnO Catalyst," *ASIAN J. Chem.*, vol. 24, pp. 3118–3122, 2012.
- [85] H. Wiinikka, P. Carlsson, M. Marklund, C. Grönberg, E. Pettersson, M. Lidman, and R. Gebart, "Experimental investigation of an industrial scale black liquor gasifier. Part 2: Influence of quench operation on product gas composition," *Fuel*, vol. 93, pp. 117–129, Mar. 2012.
- [86] C. Häggström, O. Öhrman, A. a. Rownaghi, J. Hedlund, and R. Gebart, "Catalytic methanol synthesis via black liquor gasification," *Fuel Process. Technol.*, vol. 94, no. 1, pp. 10–15, Feb. 2012.
- [87] L. Xiao, G. Nong, B. Lu, L. Huang, S. Li, and S. Wang, "Determination of Gaseous Sulphides in the Black Liquor Pyrolysis Gas," *ASIAN J. Chem.*, vol. 25, no. 13, pp. 7247–7250, 2013.
- [88] X.-Y. Zhao, J.-P. Cao, K. Morishita, J. Ozaki, and T. Takarada, "Electric Double-Layer Capacitors from Activated Carbon Derived from Black Liquor," *ENERGY & FUELS*, vol. 24, pp. 1889–1893, 2010.
- [89] A. Demirbas, "Biorefineries - For biomass upgrading facilities," in *Green Energy and Technology*, 2010.
- [90] R. Beauchet, F. Monteil-Rivera, and J. M. Lavoie, "Conversion of lignin to aromatic-based chemicals (L-chems) and biofuels (L-fuels).," *Bioresour. Technol.*, vol. 121, pp. 328–34, Oct. 2012.
- [91] K. Okuda, X. Man, M. Umetsu, S. Takami, and T. Adshiri, "Efficient conversion of lignin into single chemical species by solvothermal reaction in water-p-cresol solvent," *J. Phys. Condens. Matter*, vol. 16, pp. S1325–S1330, 2004.
- [92] X. Man, K. Okuda, S. Ohara, M. Umetsu, S. Takami, and T. Adshiri, "disassembly of Organosolv Lignin in supercritical Fluid-Phenol as a suppressor for repolymerization," *J. Japan Inst. Enrgy*, vol. 84, pp. 486–490, 2005.
- [93] P. Trambouze, "Réacteurs chimiques - technologie," *Tech.*, 2014.
- [94] service public de Wallonie, "Reacteurs chimiques," *Cah. Tech. n°8*.
- [95] Y. Lu, L. Guo, X. Zhang, and Q. Yan, "Thermodynamic modeling and analysis of biomass gasification for hydrogen production in supercritical water," *Chem. Eng. J.*, vol. 131, pp. 233–244, 2007.



- [96] H. Faustino, N. Gil, C. Baptista, and A. P. Duarte, "Antioxidant activity of lignin phenolic compounds extracted from kraft and sulphite black liquors.," *Molecules*, vol. 15, no. 12, pp. 9308–22, Jan. 2010.
- [97] A. Kruse, A. Funke, and M. Titirici, "Hydrothermal conversion of biomass to fuels and energetic materials," *Curr. Opin. Chem. Biol.*, vol. 17, no. 3, pp. 515–521, 2013.
- [98] C. Amen-Chen, H. Pakdel, and C. Roy, "Production of monomeric phenols by thermochemical conversion of biomass: a review.," *Bioresour. Technol.*, vol. 79, no. 3, pp. 277–99, Sep. 2001.
- [99] H. Wiinikka, P. Carlsson, M. Marklund, C. Gronberg, E. Pettersson, M. Lidman, and R. Gebart, "Experimental investigation of an industrial scale black liquor gasifier. Part 2: Influence of quench operation on product gas composition," *Fuel*, vol. 93, pp. 117–129, 2011.
- [100] M. Sugano, H. Takagi, K. Hirano, and K. Mashimo, "Hydrothermal liquefaction of plantation biomass with two kinds of wastewater from paper industry," *J. Mater. Sci.*, vol. 43, no. 7, pp. 2476–2486, Nov. 2007.
- [101] H. Boucard, M. Watanabe, S. Takami, R. Barna, and T. Adschiri, "Catalytic Conversion of Black Liquor under Sub- / Supercritical Conditions," *Proceeding 14h Eur. Meet. Supercrit. fluids*, 2014.
- [102] K. Tang, R. J. White, X. Mu, M.-M. Titirici, P. a van Aken, and J. Maier, "Hollow carbon nanospheres with a high rate capability for lithium-based batteries.," *ChemSusChem*, vol. 5, no. 2, pp. 400–3, Feb. 2012.
- [103] M. Titirici, "Hydrothermal Carbonisation: A Sustainable Alternative to Versatile Carbon Materials," 2012.
- [104] M. W. Haenel, "recent progress in coal structure research," *Fuel*, vol. 71, pp. 1211–1223, 1992.
- [105] M. Dejhosseini, T. Aida, M. Watanabe, S. Takami, D. Hojo, N. Aoki, T. Arita, A. Kishita, and T. Adschiri, "Catalytic cracking reaction of heavy oil in the presence of cerium oxide nanoparticles in supercritical water," *ENERGY & FUELS*, vol. 27, pp. 4624–4631, 2013.
- [106] M. Inagaki, "hugh temperature high pressure H-NMR study on formation of carbon spherules," *Carbon N. Y.*, pp. 771–772, 1986.
- [107] F. Bergius, " *Zeitschrift fur Komprim. und Fluss. Gase*, vol. 17, 1915.
- [108] Q. Wang, H. Li, L. Chen, and X. Huang, "Monodispersed hard carbon spherules with uniform nanopores," vol. 39, no. February, pp. 2211–2214, 2001.
- [109] E. Dinjus, a. Kruse, and N. Tröger, "Hydrothermal Carbonization - 1. Influence of Lignin in Lignocelluloses," *Chem. Eng. Technol.*, vol. 34, no. 12, pp. 2037–2043, Dec. 2011.

- [110] P. L. Walker, "carbon: an old but new material revisited," *Carbon N. Y.*, vol. 28, pp. 261–279, 1990.
- [111] L. Khezami, a. Chetouani, B. Taouk, and R. Capart, "Production and characterisation of activated carbon from wood components in powder: Cellulose, lignin, xylan," *Powder Technol.*, vol. 157, no. 1–3, pp. 48–56, Sep. 2005.
- [112] V. Fierro, V. Torné-Fernández, and A. Celzard, "highly microporous carbons prepared by activation of kraft lignin with KOH," *Stud. Surf. Sci. Catal.*, vol. 160, pp. 607–614, 2006.
- [113] M. Sevilla and a. B. Fuertes, "The production of carbon materials by hydrothermal carbonization of cellulose," *Carbon N. Y.*, vol. 47, no. 9, pp. 2281–2289, Aug. 2009.
- [114] M. Washiyama, M. Sakai, and M. Inagakib, "FORMATION OF CARBON SPHERULES BY pressure carbonization - relation to molecular structure of precursor," *Carbon N. Y.*, vol. 26, no. 3, pp. 303–307, 1988.
- [115] J. Ayache and A. Oberlin, "mechanism of carbonization under pressure Part II: influence of impurities," *Carbon N. Y.*, vol. 28, pp. 353–362, 1990.
- [116] M. Inagaki, "Carbon materials- structure, texture and intercalation," *Solid State ionics*, vol. 88, pp. 833–839, 1996.
- [117] M. Inagaki, K. C. Park, and M. Endo, "Carbonization under pressure," *New Carbon Mater.*, vol. 25, no. 6, pp. 409–420, Dec. 2010.
- [118] M. Inagaki, "Discussion of the formation of nanometric texture in spherical carbon bodies," *Carbon N. Y.*, pp. 771–713, 1997.
- [119] K. Azami, S. Yamamoto, and Y. Sanada, "Kinetics of mesophase formation of petroleum pitch," *Carbon N. Y.*, vol. 32, no. 5, pp. 947–951.
- [120] V. K. La Mer, "Nucleation in Phase Transitions," *Ind. Eng. Chem.*, vol. 44, no. 6., 1952
- [121] Z. Fang, R. L. Smith, J. A. Kozinski, T. Minowa, and K. Arai, "Reaction of d-glucose in water at high temperatures (410°C) and pressures (180MPa) for the production of dyes and nano-particles," *J. Supercrit. Fluids*, vol. 56, pp. 41–47, 2011.
- [122] M. Modell, R. P. Overend, T. A. Milne, and L. K. Mudge, *Gasification and liquefaction of forest products in supercritical water in Fundamentals of thermochemical biomass conversion*. 1985, pp. 95–120.
- [123] H. Boucard, "14 th european meeting on Supercritical Fluids," in *Generation of Carbon Microparticules by Hydrothermal Conversion of Black Liquor*, 2014.
- [124] Y. Qian, C. Zuo, J. Tan, and J. He, "Structural analysis of bio-oils from sub-and supercritical water liquefaction of woody biomass," *Energy*, vol. 32, no. 3, pp. 196–202, 2007.

- [125] M.-M. Titirici, M. Antonietti, and N. Baccile, "hydrothermal carbon from biomass- a comparison of the local structure from poly- to monosaccharides and pentoses-hexoses," *Green Chem.*, vol. 10, pp. 1204–1212, 2008.
- [126] J. Ayache and A. Oberlin, "mechanism of carbonization under pressure. part I: influence of aromaticity," *Carbon N. Y.*, vol. 28, pp. 337–351, 1990.
- [127] S. Rahmani, W. McCaffrey, J. A. W. Elliott, and M. R. Gray, "liquid-phase behavior during the cracking of asphaltenes," *Ind. Eng. Chem. Res.*, vol. 42, no. 17, pp. 4101–4108, 2003.
- [128] M. Sevilla and A. B. Fuertes, "Chemical and structural properties of carbonaceous products obtained by hydrothermal carbonization of saccharides.," *Chemistry*, vol. 15, no. 16, pp. 4195–203, Jan. 2009.
- [129] Z. Liu, A. Quek, S. Kent Hoekman, and R. Balasubramanian, "Production of solid biochar fuel from waste biomass by hydrothermal carbonization," *Fuel*, Aug. 2012.
- [130] R. Demir-Cakan, N. Baccile, M. Antonietti, and M.-M. Titirici, "Carboxylate-Rich Carbonaceous Materials via One-Step Hydrothermal Carbonization of Glucose in the Presence of Acrylic Acid," *Chem. Mater.*, vol. 21, no. 3, pp. 484–490, Feb. 2009.
- [131] S. Folestad and J. Johansson, "Raman Spectroscopy: A Technique for the Process Analytical Technology Toolbox," *Am. Pharm. Rev.*
- [132] A. Sadezky, H. Muckenhuber, H. Grothe, R. Niessner, and U. Pöschl, "Raman microspectroscopy of soot and related carbonaceous materials: Spectral analysis and structural information," *Carbon N. Y.*, vol. 43, pp. 1731–1742, 2005.
- [133] V. G. Pol, M. Motiei, A. Gedanken, J. Calderon-Moreno, and M. Yoshimura, "Carbon spherules: synthesis, properties and mechanistic elucidation," *Carbon N. Y.*, vol. 42, no. 1, pp. 111–116, Jan. 2004.
- [134] D. M. Keown, X. Li, J. Hayashi, and C. Li, "evolution of biomass char structure during oxidation in O<sub>2</sub> as revealed with FT-Raman spectroscopy," *Fuel Process. Technol.*, vol. 89, pp. 1429–1435, 2008.
- [135] P. Mahanty, S. Nanda, K. K. Pant, S. Naik, J. A. Kozinski, and A. K. Dalai, "Evaluation of the physicochemical development of biochars obtained from pyrolysis of wheat straw, timothy grass and pinewood\_Effects of heating rate," *J. Anal. Appl. Pyrolysis*, vol. article in , 2013.
- [136] C. Guizani, "Effects of CO<sub>2</sub> on the biomass pyro-gasification in high heating rate and low heating rate conditions," 2014.
- [137] K. C. Park, H. Tomiyasu, S. Morimoto, K. Takeuchi, Y. J. Kim, and M. Endo, "Carbon formation promoted by hydrogen peroxide in supercritical water," *Carbon N. Y.*, vol. 46, no. 13, pp. 1804–1808, Nov. 2008.

- [138] Y. Z. Jin, C. Gao, W. K. Hsu, Y. Zhu, A. Huczko, M. Bystrzejewski, M. Roe, C. Y. Lee, S. Acquah, H. Kroto, and D. R. M. Walton, "Large-scale synthesis and characterization of carbon spheres prepared by direct pyrolysis of hydrocarbons," *Carbon N. Y.*, vol. 43, no. 9, pp. 1944–1953, Aug. 2005.
- [139] Y. A. Lebedev, A. P. Krekhov, A. N. Chuvyrov, and N. K. Gil'manova, "Declinaison structure of carbonaceous mesophase spherule," *Carbon N. Y.*, vol. 24, no. 6, pp. 719–724, 1986.
- [140] J.-L. Wertz, "Bioraffineries de deuxième génération utilisant la voie thermo-chimique," 2013.
- [141] I. Mocida, T. Ando, K. Maeda, H. Fujitsu, and K. Takeshita, "catalytic carbonization of aromatic hydrocarbons - carbonization mechanism of heterocyclic sulfur compounds leading to the anisotropic coke," *Carbon N. Y.*, vol. 18, pp. 131–136, 1980.
- [142] A. Chuntanapum and Y. Matsumura, "Formation of tarry Materials from 5-HMF in subcritical and supercritical water," *Ind. Eng. Chem. Res.*, vol. 48, pp. 9837–9846, 2009.
- [143] M. Kumar, R. C. Gupta, and T. Sharma, "Effets of carbonisation conditions on the yield and chemical composition of acacia and eucalyptus wood chars," *Biomass and Bioenergy*, vol. 3, no. 6, pp. 411–417, 1992.
- [144] X. M. Sun, J. F. Liu, and Y. D. Li, "No Title," *Chem. Eur. J.*, vol. 12, pp. 2039–2047, 2006.
- [145] Y. H. Ao, J. J. Xu, D. G. Fu, and C. W. Yuan, "No Title," *Electrochem. Commun.*, vol. 10, pp. 1812–1814, 2008.
- [146] M. M. Titirici, M. Antonietti, and A. Thomas, "No Title," *Chem. Mater.*, vol. 18, pp. 3808–3812, 2006.
- [147] N. Wang, Y. Gao, J. Gong, X. Y. Ma, X. L. Zhang, Y. H. Guo, and L. Y. Qu, "No Title," *Eur. J. Ino. Chem.*, pp. 3827–3832, 2008.
- [148] X. L. Li, T. J. Lou, X. M. Sun, and Y. D. Li, "No Title," *Inorg. Chem.*, vol. 43, pp. 5442–5449, 2004.
- [149] X. Wang, P. Hu, F. L. Yuan, and L. J. Yu, "No Title," *J Phys Chem C*, vol. 111, pp. 6706–6712, 2007.
- [150] M. Titirici, M. Antonietti, and A. Thomas, "A Generalized Synthesis of Metal Oxide Hollow Spheres Using a Hydrothermal Approach," vol. 43, no. 21, pp. 3808–3812, 2006.
- [151] M. Sasaki and M. Goto, "Recovery of phenolic compounds through the decomposition of lignin in near and supercritical water," *Chem. Eng. Process. Process Intensif.*, vol. 47, no. 9–10, pp. 1609–1619, Sep. 2008.

- [152] H. Paqueton and J. Ruste, “Microscopie électronique à balayage Images , applications et développements,” vol. 33, no. 0, 2012.
- [153] Moulay-Rachid BABAA, “Contribution à l’étude de l’adsorption physique de gaz sur les nanotubes de carbone mono- et multiparois,” 2004.

## Figures list

---



Figure 1: Phase diagram of water.....	34
Figure 2: Supercritical water observation in DECLIC (from CNES). .....	34
Figure 3: Density evolution with temperature (100°C to 700°C) and pressure (15 MPa to 40 MPa). .....	35
Figure 4: Dielectric constant evolution with temperature (200°C to 700°C) and pressure (15 MPa to 40 MPa). .....	36
Figure 5: Water dimers: in bifurcated form (a) and reverse form (b) (from [6]). .....	37
Figure 6: Evolution of ionic product as a function of temperature (from 20°C to 600°C) and pressure (15 MPa to 40 MPa). .....	38
Figure 7: Evolution of dynamic viscosity as a function of temperature (100°C to 700°C) and pressure (15 MPa to 40 MPa). .....	40
Figure 8: Evolution of enthalpy as a function of temperature (100°C to 700°C) and pressure (15 MPa to 40 MPa). .....	41
Figure 9: Evolution of heat capacity as a function of temperature (100°C to 700°C) and pressure (15 MPa to 40 MPa). .....	41
Figure 10: Evolution of thermal conductivity as a function of temperature (100°C to 700°C) and pressure (15 MPa to 40 MPa). .....	42
Figure 11: Preferred reaction pathway following process temperature [4]. .....	43
Figure 12: Applications of supercritical water properties. ....	44
Figure 13: Synthesis reactions considering water properties [5]. .....	44
Figure 14: Hydrolysis of esters from [5]. .....	45
Figure 15: Friedel-Craft alkylation ([5]) .....	45
Figure 16: Friedel- Craft acylation ([5]). .....	45
Figure 17: Aldol condensation ([5]). .....	46
Figure 18: Cannizzaro reaction. ....	46
Figure 19: Diels-alder reaction. ....	46
Figure 20: Reactions occurring during hydrothermal conversion of biomass. ....	47
Figure 21: Products obtained by SCW and their applications. ....	48
Figure 22: Kraft process. ....	50
Figure 23: Cooking step. ....	51
Figure 24: Process of Kraft pulping (adapted from [64]). .....	51
Figure 25: (a) p-coumarylic Alcohol, (b) coniferylic alcohol and (c) sinapylic alcohol. ....	52



---

Figure 26: Possible structure of lignin [67].....	52
Figure 27: Labile bond of lignin: liaisons $\beta$ -O-4.....	53
Figure 28: Strong bond of lignin. ....	53
Figure 29: Lignin degradation mechanism during Kraft process (adapted from [68]). ....	54
Figure 30: Tall oil process (extracted from [69]). ....	56
Figure 31: Reactions into black liquor boiler. ....	58
Figure 32: Causticizing step. ....	59
Figure 33: Synthesis of black liquor treatment in paper industry. ....	62
Figure 34: Guaiacol formula. ....	63
Figure 35: Catechol formula. ....	63
Figure 36: GGGE formula.....	64
Figure 37: Mechanisms suggested by Kang et al. for the hydrothermal liquefaction of lignin [76]. ....	64
Figure 38: Reactions pathways suggested by Kang et al. for the hydrothermal gasification of lignin [76]. ....	65
Figure 39: Reactions paths for hydrothermal conversion of lignin suggested by Fang et al. ([23]). ....	65
Figure 40: Experimental procedures for hydrothermal conversion of black liquor. ....	75
Figure 41: Reagents in hydrothermal process. ....	75
Figure 42: Black liquor composition given by Smurfit Kappa cellulose du Pin, Factice.....	76
Figure 43: 5 mL batch reactor: mini-autoclave. ....	78
Figure 44: Opening / closing apparatus.....	78
Figure 45: Sampling for collect gas for 5 mL batch reactor. ....	79
Figure 46: 5 mL batch reactor (Adschiri Laboratory).....	81
Figure 47: 500 mL batch reactor. ....	82
Figure 48: Temperature profiles.....	84
Figure 49: Scheme of characterizations tools. ....	85
Figure 50: Procedures for solid thermogravimetric analysis. ....	88
<i>Figure 51: Normalized TOC concentration at 350°C depending on reaction time. ....</i>	<i>102</i>
Figure 52: Collected liquids after treatment versus reaction time (black liquor solution is 10 wt%, self generated pressure, 350°C, batch reactor 5 mL).....	103

Figure 53: Influence of reaction time at 350°C (Black liquor, 0 min, 8 min, 15 min, 30 min)	103
Figure 54: Carbon distribution at 350°C as a function of reaction time	104
Figure 55: Normalized TOC concentration at 500°C depending on reaction time	105
Figure 56: Collected liquids after treatment versus reaction time (black liquor solution is 10 wt%, 25 MPa, 500°C, batch reactor 5 mL)	106
Figure 57: Influence of reaction time at 500°C (black liquor, 0 min, 8 min, 15 min, 30 min)	106
Figure 58: Carbon distribution at 500°C as a function of reaction time	107
Figure 59: pH of the liquid obtained at 350°C and 500°C in term of reaction time	107
Figure 60: Normalized TOC concentration at 500°C depending on black liquor concentrations	108
Figure 61: Liquid obtained after 15 min of reaction time at 500°C, for four different concentrations of raw black liquor: 5 wt%, 10 wt%, 20 wt% and 30 wt%	109
Figure 62: pH of the liquid obtained at 500°C, 15 min of reaction time, various initial concentrations	109
Figure 63: Influence of the concentration (Black liquor, 10 wt%, 20 wt%, 30 wt%) at 500°C	110
Figure 64: Carbon distribution at 500°C as a function of concentration	110
Figure 65: Normalized TOC concentration in liquids obtained after 15 min of reaction time, with initial black liquor at 10 wt%, for temperatures range from 350°C to 600°C	111
Figure 66: Liquid obtained after hydrothermal conversion conducted at temperature from 350°C to 600°C, at 15 min of reaction time with black liquor at 10 wt%	112
Figure 67: Carbon distribution after 15 min reaction time as a function of temperature	112
Figure 68: Summary of expected products from hydrothermal conversion of biomass	113
Figure 69: GC-MS of the liquid obtained at 600°C and 15 min of reaction time	116
Figure 70: Solid obtained after 600°C 15 min of reaction time, 10 wt% of black liquor	117
Figure 71: GC-MS analysis of the liquid obtained at 450°C, 15 min of reaction time	118
Figure 72: ICP measurements of the liquid obtained after hydrothermal conversion, 15 min of reaction time. The error related to ICP measurement is around 5 %	119
Figure 73: ESEM pictures for solid obtained at 450°C and 15 min of reaction time	120
Figure 74: ESEM pictures for solid obtained at 500°C and 15 min of reaction time	120

Figure 75: GC-MS analysis of liquid obtained at 350°C, 15 min of reaction time.....	121
Figure 76: ESEM pictures for solid obtained at 350°C and 15 min of reaction time, 10 wt% of black liquor solution.....	122
Figure 77: ESEM pictures for solid obtained at 400°C and 15 min of reaction time with a 10 wt% black liquor solution .....	122
Figure 78: Summary on the presence of the phases .....	123
Figure 79: ESEM pictures of solid residue obtained after filtration of reaction media .....	124
Figure 80: Temperature profile .....	139
Figure 81: ESEM pictures of solids obtained by CT experiments, same magnification. ....	140
Figure 82: Confrontation between carbonization theories and our solids evolution.....	141
Figure 83: Size distribution for the solids obtained by CT experiments.....	141
Figure 84: Evolution of TOC and COD removal with reaction time.....	144
Figure 85: Evolution of phenols and formaldehyde concentrations over time .....	145
Figure 86: Liquids color evolution over time.....	145
Figure 87: Evolution of C, H, and O in CT solids over reaction time .....	146
Figure 88: Reactions evolution on Van Krevelen diagram. ....	147
Figure 89: Biomass Van Krevelen diagram. ....	147
Figure 90: Van Krevelen diagram for CT solids compared to black liquor (atomic ratios). .	148
Figure 91: FTIR spectrum of solid residue obtained after reaction. ....	149
Figure 92: TGA of CT solids .....	150
Figure 93: Raman spectra of solid obtained after 60 min (a) spectra of the core, (b) spectra of surface & core, (c) spectra of surface.....	152
Figure 94: Particles obtained for different heating rate, after 60 min of reaction time and washed after filtration.....	155
Figure 95: Scheme of the organic droplet organization in the subcritical water.....	157
Figure 96: Coalescence of particles by solidification of particles and transition layer.....	158
Figure 97: TEM observation of particles obtained at 350°C, 60 min and 10 wt%. ....	159
Figure 98: Scheme of particle generation .....	161
<i>Figure 99: Zoom on the solid obtained after characteristic times.....</i>	<i>162</i>
Figure 100: Morphology of particles obtained with rapid heating (a) and slow heating (b) after 30 min of reaction time, same magnificance.....	163

Figure 101: Influence of heating rate ( $20^{\circ}\text{C}\cdot\text{min}^{-1}$ vs. $40^{\circ}\text{C}\cdot\text{min}^{-1}$ ) on the size distribution at $350^{\circ}\text{C}$ , 30 min and 2 h with a quench cooling. ....	164
Figure 102: Evolution of TOC and COD of CT and NT liquids.....	165
Figure 103: Morphology of solid obtained after a rapid heating and 30 min of reaction time: with slow cooling: CL (a) and by quenching: CT (b), same magnification. ....	166
Figure 104: Size distribution considering cooling rate at 60 min reaction time .....	166
Figure 105: Confrontation between carbonization theories and our solids evolution.....	168
Figure 106: Morphology is due to a combination of chemical reaction and physical phenomena. ....	169
Figure 107: « Green » carbon materials used as basis of electrochemical devices for renewable energy generation, storage and utilization [103]. ....	170
Figure 108: Solid obtained after $450^{\circ}\text{C}$ , 15 min of reaction time, without catalyst.....	182
Figure 109: Proportion of carbon converted into gas phase at $450^{\circ}\text{C}$ . ....	184
Figure 110: $\text{H}_2$ produced into gas phase after reaction at $450^{\circ}\text{C}$ . ....	184
Figure 111: Catalyst influence on molecular weight at $450^{\circ}\text{C}$ . ....	186
Figure 112: Solid obtained after $350^{\circ}\text{C}$ , 60 min of reaction time, without catalyst.....	187
Figure 113: Solid obtained after $350^{\circ}\text{C}$ , 60 min of reaction time, with catalyst.....	188
Figure 114: Distribution of initial organic carbon in gas phase and dissolved carbonates at $350^{\circ}\text{C}$ .....	189
Figure 115: $\text{H}_2$ produced into gas phase after reaction at $350^{\circ}\text{C}$ . ....	190
Figure 116: Catalyst influence on molecular weight at $450^{\circ}\text{C}$ and $350^{\circ}\text{C}$ . ....	191
Figure 117: Comparison of GPC results at 350 and $450^{\circ}\text{C}$ . $t = 15$ min and $R = 5$ . ....	193
Figure 118: TEM image (a) and micro-analysis (b-g) of solid recovered after experiment ( $450^{\circ}\text{C}$ , $t = 60$ min, $R = 5$ ). ....	194
Figure 119: TEM image (a) and micro-analysis (b-g) of solid recovered after experiment ( $350^{\circ}\text{C}$ , $t = 60$ min, $R = 5$ ). ....	195
Figure 120: First approach for heat balance of hydrothermal conversion of black liquor. ....	199
Figure 121: First approach for heat balance of hydrothermal conversion of black liquor with preheating heat recovery. ....	202
Figure 122: First approach for heat balance of continuous hydrothermal conversion of black liquor with preheating without intermediate heat transfer fluid.....	203

Figure 123: First approach for heat balance of continuous hydrothermal conversion of black liquor with preheating with intermediate heat transfer fluid.....	204
Figure 124: GGGE formula.....	205
Figure 125: GPC results for the comparison between lignin, alkali lignin and black liquor.	205
Figure 126: GPC results for liquid obtained from lignin conversion with and without catalyst (R=5), under supercritical conditions.....	206
Figure 127: GPC results for liquid obtained after 60 min of reaction time without catalyst with lignin and black liquor under supercritical conditions.....	207
Figure 128: Gas analysis - Comparison between lignin and black liquor, with and without catalyst (R=20). Errors are 1% for the percentage of carbon in gas phase, 0.02 mmol for H <sub>2</sub> produced.....	208
Figure 129: GPC results for liquid obtained after 60 min of reaction time without catalyst with lignin and black liquor under subcritical conditions.....	209
Figure 130: GPC results for liquid obtained from lignin conversion with and without catalyst (R=20), under supercritical conditions.....	209
Figure 131: Gas analysis - Comparison between lignin and black liquor, with and without catalyst (R=20). Errors are 1% for the percentage of carbon in gas phase, 0.02 mmol for H <sub>2</sub> produced.....	211
Figure 132: Summary of reactions during catalytic conversion of lignin.....	212
Figure 133: GPC results for liquid obtained after hydrothermal conversion of GGGE under supercritical conditions, without catalyst.....	213
Figure 134: GPC results for liquid obtained after hydrothermal conversion of GGGE, without catalyst.....	215
Figure 135: GPC results for liquid obtained after hydrothermal conversion of GGGE under subcritical conditions, without catalyst.....	217
Figure 136: GPC results for liquid obtained after hydrothermal conversion of GGGE under subcritical conditions, without catalyst.....	219
Figure 137: Mechanism of GGGE hydrothermal conversion with and without catalyst under supercritical conditions.....	222
Figure 138: Mechanism of GGGE hydrothermal conversion with and without catalyst under subcritical conditions.....	223
Figure 139: Reactions promoted under sub and supercritical conditions without catalyst....	224

Figure 140: Mechanism of lignin hydrothermal conversion with and without catalyst under supercritical conditions .....	225
Figure 141: Mechanism of GGGE hydrothermal conversion with and without catalyst under subcritical conditions.....	226
Figure 142: Mechanism of Black liquor hydrothermal conversion with and without catalyst under supercritical conditions .....	227
Figure 143: Mechanism of black liquor hydrothermal conversion with and without catalyst under subcritical conditions .....	228
Figure 144: Integration of hydrothermal conversion of black liquor in Kraft process. ....	237
Figure 145: Integration du procédé de conversion hydrothermale de la liqueur noire dans le procédé Kraft.....	245
Figure 146: ESEM pictures of solid residue at various reaction temperatures. Black liquor concentration = 10 wt%, P = 25 MPa or self generated pressure, t = 15 min.....	266
Figure 147: Particles obtained after 15 min (a), 30 min (b) and 60 min (c) of reaction. ....	267
Figure 148: Solid formation inside the reactor for a pure black liquor solution.....	268
Figure 149: 350°C, 60 min temperature rate 7°C.min <sup>-1</sup> , black liquor 10 wt%, batch reactor (500 mL).....	268
Figure 150: FTIR spectrum of solid residue obtained after reaction. ....	269
Figure 151: XRD of CT series – carbonization study.....	271
Figure 152: TGA analysis to compare CT and NT series at 60 min reaction time.....	273
Figure 153: Van Krevelen diagram for NT series.....	273
Figure 154: TOC and COD monitoring over reaction time. ....	274
Figure 155: Formaldehyde and phenols monitoring over reaction time. ....	274
Figure 156: TGA analysis to compare CT and NT series at 60 min reaction time.....	275
Figure 157: Van Krevelen diagram for NT series.....	275
Figure 158: TOC and COD monitoring over reaction time. ....	276
Figure 159: TOC and COD monitoring over reaction time. ....	276



## Table list

---





---

Table 1: Synthesis of water properties at subcritical and supercritical conditions. ....	42
Table 2: Main products expected by conversion of black liquor model compounds.....	67
Table 3: Principal products expected by black liquor (BL) conversion.....	68
Table 4: Comparison of reactor conditions. ....	82
Table 5: Advantages and drawbacks of batch reactor.....	98
Table 6: Range of operating conditions studied under constant reaction pressure of 25 MPa under supercritical conditions and under self generated pressure for subcritical conditions. ....	101
Table 7: Composition of gas obtained after 15 min reaction time, 25 MPa and a 10 wt% initial solution of black liquor. ....	114
Table 8: Comparative molar composition of gas obtained for black liquor at 10 wt%, 25 MPa, 600°C, batch autoclave.....	115
Table 9: Summarize of operating conditions .....	138
Table 10: Masses introduced in 6 reactors, weight of solid recovered by filtration and overpressure measured during opening of reactors. The errors related to mass is 0.1 mg. ...	139
Table 11: Density of solid obtained after 30 min and 60 min of reaction time .....	154
Table 12: Proportion and weight of coke formed after reaction at 450°C, with /without catalyst.....	182
Table 13: Proportion and weight of coke formed after reaction at 350°C (R=5). ....	188
Table 14: Black liquor hydrothermal conversion preliminary feasibility study results.....	201
Table 15: Molecules identified in liquid phase after hydrothermal conversion of lignin at 450°C during 60 min. ....	207
Table 16: Molecules identified in liquid phase after hydrothermal conversion of lignin at 350°C during 60 min. ....	210
Table 17: GC-MS results for the liquid obtained after hydrothermal conversion of GGGE under supercritical conditions with catalyst.....	214
Table 18: GC-MS results for the liquid obtained after hydrothermal conversion of GGGE under supercritical conditions with catalyst.....	216
Table 19: GC-MS results for the liquid obtained after hydrothermal conversion of GGGE under subcritical conditions without catalyst.....	218
Table 20: GC-MS results for the liquid obtained after hydrothermal conversion of GGGE under subcritical conditions with catalyst.....	220
Table 21: Carbon and texture characterizations obtained by carbonization from Inagaki.....	261

Table 22: GC-MS results for liquid recovered after black liquor conversion under supercritical (450°C) conditions with and without CeO<sub>2</sub> catalyst for 15 min and 60 min of reaction time.

..... 277

Table 23: GC-MS results for liquid recovered after black liquor conversion under subcritical (350°C) conditions with and without CeO<sub>2</sub> catalyst for 15 min and 60 min of reaction time.

..... 278

Doctorat de l'Université de Toulouse  
Délivré par l'École des Mines d'Albi-Carmaux, conjointement avec l'INP Toulouse  
École doctorale MEGeP  
Spécialité Génie des procédés et environnement  
Laboratoire RAPSODEE  
Soutenue le 12 décembre 2014  
Hélène BOUCARD

**Contributions à la compréhension des procédés hydrothermaux :  
application à la liqueur noire**

**Résumé :**

La liqueur noire, sous-produit de l'industrie papetière, est convertie par un processus hydrothermal. Elle a été choisie pour son contenu élevé en eau (80 wt%), matière organique (14 wt%) et minéraux (6 wt%) qui font d'elle une biomasse à haute valeur ajoutée bien qu'encore peu exploitée. L'étude en batch, balayant une large gamme de température (350°C-600°C), permet d'identifier deux flux sortant : une proportion d'hydrogène élevée dans la phase gazeuse (600°C), ainsi qu'une phase solide, appelée coke, générée quel que soient les conditions opératoires utilisées. La génération de solide modifie la composition du milieu réactionnel en procédé batch et peut poser problème en cas de transposition en réacteur continu. Il est donc important de comprendre sa formation pour pallier ces verrous. L'analyse du résidu montre qu'à 350°C, pour des temps de réaction courts (<2h), de micro-particules carbonées se forment. Leur taille est influencée par les vitesses de montée et descente en température. Pour des températures plus hautes, le solide ne présente pas d'intérêt morphologique et sa proportion massique augmente avec la température. Ainsi, une production d'hydrogène significative s'accompagnera d'un dépôt solide dans le réacteur. Une étude catalytique a donc été menée en vue d'augmenter la quantité d'hydrogène et de diminuer la formation de coke tout en travaillant à plus basse température. Cette étude, menée à 350°C et 450°C, montre que les réactions d'hydrogénation et d'oxydation mises en jeu par le catalyseur conduisent aux résultats escomptés. La conversion de molécules modèles de la liqueur noire, menée dans les mêmes conditions d'expériences, a permis d'appréhender les mécanismes majeurs mis en jeu lors de la conversion hydrothermale. Les micro-particules à 350°C peuvent être valorisées. Cependant, le changement de taille et de morphologie au cours du temps interroge sur la possibilité de passer en réacteur continu. La formation de solide peut être évitée à partir de 450°C en présence de catalyseur, favorisant en parallèle la production d'hydrogène. De ce fait, ce travail de thèse aborde les verrous scientifiques, techniques et technologiques liés à la conversion hydrothermale de la liqueur noire et notamment de la formation du solide, en présence ou non de catalyseur.

**Mots clés :** Biomasse humide, Liqueur noire, Procédés hydrothermaux, Réacteur batch, Production d'H<sub>2</sub>, Génération de microparticules, Mécanismes de conversion hydrothermale.

Doctorat de l'Université de Toulouse  
Délivré par l'École des Mines d'Albi-Carmaux, conjointement avec l'INP Toulouse  
École doctorale MEGeP  
Spécialité Génie des procédés et environnement  
Laboratoire RAPSODEE  
Soutenue le 12 décembre 2014  
Hélène BOUCARD

**Contributions to the understanding of hydrothermal processes:  
application to black liquor**

**Abstract :**

Black liquor, a by-product of paper industry, is converted by hydrothermal process. It was chosen for its high water content (80 wt%), organic material (14 wt%) and minerals (6 wt%) that make it a high-value biomass while still untapped. The study in batch, screening a wide temperature range (350°C-600°C), used to identify two outgoing flows: a high proportion of hydrogen in the gas phase (600°C) and a solid phase, called coke, generated regardless the operating conditions used. The generation of solid changes the composition of the reaction medium in batch process and can be problematic in case of transposition in continuous reactor. Thus it is important to understand its formation to overcome these obstacles. Analysis of the residue shows that at 350°C, for short reaction times (< 2h), carbonaceous micro-particles are formed. Their size is influenced by the temperature rates of rise and fall. For higher temperatures, the solid is of no morphological interest and its weight proportion increased with temperature. Thus, a significant production of hydrogen will be associated with a solid deposit in the reactor. A catalytic study was conducted to increase the amount of hydrogen and reduce the formation of coke while working at lower temperature. This study, conducted at 350°C and 450°C, shows that hydrogenation and oxidation reactions involved with the catalyst, lead to the expected results. Converting models molecules of black liquor, conducted with the same experimental conditions, helped to understand the major mechanisms involved during the hydrothermal conversion. The micro-particles at 350°C can be valorized. However, the change in size and morphology over time wondered about the possibility of implement in continuous reactor. The solid formation can be prevented from 450°C in the presence of catalyst, favoring in parallel hydrogen production. Therefore, this thesis deals with scientific, technical and technological locks related to hydrothermal conversion of black liquor and especially the solid formation, with or without catalyst.

**Keywords:** Wet biomass, Black liquor, Hydrothermal processes, Batch reactor, H<sub>2</sub> production, Microparticles generation, Mechanism of hydrothermal conversion.